Imperial College London
Department of Physics
Abdus Salam Centre for Theoretical Physics

Gauging Global Symmetries with Magnetic Quivers

Guhesh Kumaran

Under the Supervision of Prof. Amihay Hanany

Submitted in part fulfilment of the requirements for the degree of
Doctor of Philosophy in Physics of the Diploma of Imperial College, May 2026

Abstract

In this thesis four techniques which gauge Coulomb branch global symmetry subgroups of $3d$ $\mathcal{N} = 4$ quiver gauge theories are introduced. This is a challenging problem due to the quantum corrections of the Coulomb branch, nevertheless each technique developed here is combinatorial in nature which avoids this issue. Three of the methods are a type of *quotient quiver subtraction*, involving a subtraction of quiver diagrams, and the fourth is a *quiver polymerisation*, which involves combining two quivers or forming a loop in one quiver. These methods are derived from either $3d$ mirror symmetry, or through the analysis of Higgs branches of $6d$ $\mathcal{N} = (1, 0)$ or class $\mathcal{S}$ theories using magnetic quivers. Mathematically, Coulomb branches of $3d$ $\mathcal{N} = 4$ theories and Higgs branches of theories with eight supercharges are a type of hyper-Kähler variety called a *symplectic singularity*. The act of gauging a global symmetry subgroup corresponds to performing a hyper-Kähler quotient on the moduli space which results in constructions for new symplectic singularities. After going through some physics and mathematics background for the computations involved, the thesis proceeds by developing each of the four techniques in turn and applying them to a range of physics and mathematical contexts including: moduli spaces of instantons, dualities in $4d$ $\mathcal{N} = 2$ theories, the $6d$ $\mathcal{N} = (1, 0)$ (E_6, E_6) conformal matter theory, and nilpotent orbit closures. These results are supported with computation of Hilbert series.

Statement of Originality

This thesis is based primarily on the following original works of the author and his collaborators

1. A. Hanany, R. Kalveks and G. Kumaran, *Quotient quiver subtraction*, *Nucl. Phys. B* **1009** (2024) 116731 [2308.05853]
2. A. Hanany, R. Kalveks and G. Kumaran, *Quiver polymerisation*, *JHEP* **11** (2024) 168 [2406.11561]
3. S. Bennett, A. Hanany and G. Kumaran, *Orthosymplectic quotient quiver subtraction*, *JHEP* **12** (2024) 063 [2409.15419]
4. S. Bennett, A. Hanany and G. Kumaran, *Quotient Quiver Subtraction – Classical Groups*, 2603.08774

whereas the following works will not form large parts of the discussion

5. A. Hanany, G. Kumaran, C. Li, D. Liu and M. Sperling, *Actions on the quiver: discrete quotients on the Coulomb branch*, *JHEP* **05** (2024) 318 [2311.02773]
6. S. Bennett, A. Hanany, G. Kumaran, C. Li, D. Liu and M. Sperling, *Quiver subtraction on the Higgs branch*, *Nucl. Phys. B* **1016** (2025) 116917 [2409.16356]
7. S. Bennett, A. Hanany and G. Kumaran, *Orthosymplectic quotient quiver subtraction. Part II. Framed quivers*, *JHEP* **12** (2025) 046 [2503.19954]
8. S. Bennett, A. Hanany, G. Kumaran and L. Mansi, *Symmetry Mitosis and Hasse Diagram Diamonds: A Note on Brane Configurations with* ON^0 *Planes*, 2601.10826

All works used in this thesis have been cited properly to the best of the author's knowledge.

Acknowledgements

The groundwork for the past four years of research effort for this PhD thesis was laid years in advance, when I met Prof Amihay Hanany. Ami was my Comprehensives tutor when I was in the third year of my undergraduate degree at Imperial. As an aspiring theoretical physicist, I asked for one of his infamous projects during that year, to which he agreed, and I never looked back since! Ami's wealth of knowledge of all things stringy, supersymmetric, symplectic, and singular has been a great treasure for me, and I feel extremely privileged to have been mentored by him. Over the years, I have grown to appreciate the respect he has for individuality and self-expression in research contexts. This has helped me to develop confidence and my own voice when discussing physics, particularly early on when I was in periods of self-doubt.

This work could not have been done without the close collaboration and discussions with the members of the "quiver group" at Imperial in my time. It has been a great pleasure intersecting ideas and learning from: Rudolph (for demystifying Hilbert series computations), Chunhao (for his enthusiasm for mathematics), Deshuo (for insights into discrete groups), Sam (for his passion for brane systems), and Elias (for unravelling brane webs).

I would like to thank the "alumni of the school of Ami": Antoine, Zhenghao, Julius, and Kirsty for patiently answering the numerous stupid questions I had when I was starting out in this field. These first steps were also taken with Lucas back in our undergraduate years, who I'd like to thank from across the pond. Cheers also go to Guillermo and Mohammad for widening my horizons with discussions. And a special thanks to Julius for advising me at the start of the PhD that gauging Coulomb branch global symmetries, the central topic of the thesis, is too difficult and to investigate other research questions (this is a joke).

I learnt a great deal about F-theory, six dimensional theories, and their brane constructions from Marcus, Noppadol, and Lorenzo. Thank you all for being fantastic colleagues!

This thesis would not come to light, from an administrative point of view, if it were not for Loli.

I'd also like to thank Travis, Tiziano, Mykola, and Richard for sharing their insights from across the corridor.

The drab atmosphere of the Huxley building has been partially fixed by the amazing assortment

of people who currently and have previously occupied H606. In addition to those already mentioned, I'd like to thank: Max, Kinga, Carlos, Stefan K, Stephanie, Pulkit, Torben, and Calvin for the cherished memories we've made and for the strong sense of community we've built over the years.

I'd also like to give a nod to the "downstairs people": Jan, Yusheng, Ray, Théo, Jae, Daniele (who is now an "upstairs person"), Anubha, Stefan K, Nicky, Jieming, and Zihan.

Although it might be difficult to imagine a life outside of the confines of Imperial, I do have one, and I'd like to thank my friends since our school days who knew that I wanted to do a PhD in theoretical physics and wanted to be a professor by 26 years old (which I will turn this year). Cheers to: Dharshan, Mayank, Rohit, Farhad, Luke, and Pothie.

In Haresh, I found my brother with whom I was always able to be open about life, our shared interests, and the similar paths we wish to walk in the future.

To Sivakami, your companionship, unwavering support, and encouragement means so much to me. You know exactly how to put a smile on my face which never fails to motivate me to persevere.

To my twin Lahasthaa (who is paradoxically three years younger than me), you always seem to know how I feel. I am so blessed to have your constant support, your advice, and love. On a separate note, I am eagerly waiting for your next sweet treat! You truly are the right-handed fermion to my left-handed.

To my parents I want to extend my deepest gratitude for all of the love and support you have given me throughout my life. Appa, you are my rock and provide me the balance and wisdom that I need. Amma, you are the spark to my pursuit of knowledge, the source of my strength and your warm embrace always lifts my spirits. Nothing I do can ever repay you both for all you have done for me, but I would still like to dedicate this thesis to the family you have built as a small token.

And finally, there are many individuals that I may have inevitably missed out but have nonetheless played a part in supporting me in the years gone by. Thank you to you all too!

Creative Commons License

The copyright of this thesis rests with the author. Unless otherwise indicated, its contents are licensed under a Creative Commons Attribution-Non Commercial 4.0 International Licence (CC BY-NC).

Under this licence, you may copy and redistribute the material in any medium or format. You may also create and distribute modified versions of the work. This is on the condition that: you credit the author and do not use it, or any derivative works, for a commercial purpose.

When reusing or sharing this work, ensure you make the licence terms clear to others by naming the licence and linking to the licence text. Where a work has been adapted, you should indicate that the work has been changed and describe those changes.

Please seek permission from the copyright holder for uses of this work that are not included in this licence or permitted under UK Copyright Law.

To my family.

Contents

Abstract i

Statement of Originality i

Acknowledgements v

1 Introduction 1

2 Physics Background 10

2.1 Introduction 10

2.2 Supermultiplets 10

2.3 Quivers 11

2.4 Moduli Spaces of Vacua 12

2.5 $3d\ \mathcal{N} = 4$ Quiver Gauge Theories 13

2.5.1 Moduli Space of Vacua 14

2.5.2 Higgs Branch 15

2.5.3 Higgs Branch Hilbert Series – Weyl Integration 17

2.5.4 Coulomb Branch 21

2.5.5 Coulomb Branch Hilbert Series – The Monopole Formula 22

2.5.6 Non-simply laced edges . . . 24
2.5.7 "Good", "Bad", and "Ugly" Theories . . . 25
2.5.8 Alternative methods to computing Hilbert series . . . 26
2.5.9 Highest Weight Generating Function . . . 26
2.5.10 $3d$ Mirror Symmetry . . . 28
2.5.11 Framed and Unframed Quivers . . . 28
2.6 $6d$ $\mathcal{N} = (1,0)$ Theories . . . 30
2.6.1 Tensor Branch . . . 31
2.6.2 Higgs Branch . . . 32
2.7 Type IIB Brane Constructions for $3d$ $\mathcal{N} = 4$ Theories . . . 33
2.7.1 Brane Creation and Annihilation . . . 36
2.7.2 Orientifold Planes . . . 38
2.8 Type IIA Brane Construction for $6d$ $\mathcal{N} = (1,0)$ Theories . . . 40
2.8.1 Magnetic Quivers . . . 42

3 Background on Symplectic Singularities 54

3.1 Introduction . . . 54
3.2 Symplectic Singularities . . . 54
3.3 Poisson Brackets . . . 55
3.3.1 Example: $\mathbb{C}^2/\mathbb{Z}_n$ . . . 57
3.4 Hilbert Series . . . 58
3.4.1 Example: $\mathbb{C}^2$ . . . 58
3.4.2 Example: $\mathbb{C}^2/\mathbb{Z}_n$ . . . 59

3.4.3 Hilbert Series Divination . . . 59

3.5 Nilpotent Orbits . . . 60

3.6 Slodowy Slices and Intersections . . . 63

3.7 Affine Grassmannian . . . 64

4 Quotient Quiver Subtraction 66

4.1 Introduction . . . 66

4.2 Method of quotient quiver subtraction for SU(n) hyper-Kähler quotients . . . 68

4.2.1 Rules for SU(n) hyper-Kähler quotient by quotient quiver subtraction . . . 68

4.2.2 A physical interpretation of the SU(n) quotient quiver . . . 73

4.3 Moduli Space of Free Fields . . . 74

4.3.1 Moduli Space of Free Fields SU(2) hyper-Kähler quotient . . . 74

4.4 Exceptional Orbits . . . 76

4.4.1 Exceptional Orbit SU(2) hyper-Kähler quotient . . . 77

4.4.2 Exceptional Orbit SU(3) hyper-Kähler quotient . . . 82

4.4.3 Exceptional Orbit SU(4) hyper-Kähler quotient . . . 84

5 Quotient Quiver Subtraction – Classical Groups 87

5.1 Introduction . . . 87

5.2 **Sp(n)** Quotient Quivers . . . 88

5.2.1 $\overline{min.E_8}///\mathrm{Sp}(2)$ . . . 91

5.2.2 $(\overline{min.E_6} \times \mathbb{H}^{12})///\mathrm{Sp}(2)$ . . . 94

5.3 **SO($2n$)** Quotient Quivers . . . 98

5.3.1 $\overline{min.F_4}///\mathrm{SO}(2)$ . . . 101

5.3.2 $\overline{min.E_7}///\mathrm{SO}(4)$ . . . 102

5.3.3 $\overline{min.E_8}///\mathrm{SO}(4)$ . . . 103

5.4 **SO(2n + 1)** Quotient Quivers . . . 104

5.4.1 $\overline{min.E_6}///\mathrm{SO}(3)$ . . . 107

5.4.2 $\overline{min.F_4}///\mathrm{SO}(3)$ . . . 108

5.5 **Sp(n) + $\frac{1}{2}$F** Quotient Quivers . . . 110

5.5.1 $\left(\overline{min.E_6} \times \mathbb{H}\right)///\mathrm{Sp}(1)$ . . . 112

6 Quiver Polymerisation **115**

6.1 Introduction . . . 115

6.2 Chain and Cyclic Polymerisation . . . 118

6.2.1 Diagrammatic methods . . . 118

6.3 Chain Polymerisation Examples . . . 121

6.3.1 Affine $D^{(1)}_{k+p}$ . . . 122

6.3.2 Affine $B^{(1)}_{k+p-1}$ . . . 123

6.3.3 Twisted affine $D^{(2)}_{k+p-1}$ . . . 124

6.3.4 Additive $\frac{1}{2}D^{(1)}_{2k+2p-1}$ . . . 125

6.3.5 Additive $\frac{1}{2}A^{(1)}_{2k+2p-3}$ . . . 127

6.3.6 Additive $\frac{1}{2}D^{(2)}_{2k+2p-1}$ . . . 128

6.3.7 Two $\frac{1}{2}$ M5 branes probing E_6 Klein Singularity . . . 129

6.4 Cyclic Polymerisation for SU(N) instanton Moduli Spaces on $\mathbb{C}^2/\mathbb{Z}_l$ . . . 131

6.4.1 1 SU(N) instanton on $\mathbb{C}^2$ . . . 132

6.4.2 2 SU(N) instantons on $\mathbb{C}^2$ . . . 133

6.4.3 2 SU(N) instantons on $\mathbb{C}^2/\mathbb{Z}_2$ . . . 134

6.4.4 k SU(N) instantons on $\mathbb{C}^2/\mathbb{Z}_l$ . . . 135

6.4.5 Generic Kronheimer-Nakajima Quivers . . . 137

6.5 Cyclic polymerisation of ADE-shaped Quivers . . . 139

6.5.1 U(1) cyclic polymerisation of A_N for $N \geq 2$ . . . 139

6.5.2 U(1) cyclic polymerisation of $E_6^{(1)}$ . . . 141

6.5.3 U(2) cyclic polymerisation of $E_6^{(1)}$ . . . 142

6.5.4 U(1) cyclic polymerisation of $E_7^{(1)}$ . . . 144

6.5.5 U(3) cyclic polymerisation of $E_7^{(1)}$ . . . 145

7 Unframed Orthosymplectic Quotient Quiver Subtraction 147

7.1 Introduction . . . 147

7.2 Derivation of Orthosymplectic Quotient Quivers . . . 150

7.2.1 Gauging SU(3) . . . 151

7.2.2 Gauging G_2 . . . 154

7.2.3 Gauging SO(7) . . . 157

7.2.4 Gauging SU(2) . . . 159

7.2.5 A comment on other groups . . . 160

7.3 Method of Orthosymplectic Quotient Quiver Subtraction . . . 161

7.4 Examples of SU(2) Orthosymplectic Quotient Quiver Subtraction . . . 163

7.4.1 $\overline{min.E_7}///\mathrm{SU}(2)$ . . . 163

7.4.2 $\overline{min.E_6}///\mathrm{SU}(2)$ . . . 165

7.4.3 $\overline{n.min.A_5}///\mathrm{SU}(2)$ . . . 166

7.4.4 $\overline{min.E_8}///\mathrm{SU}(2)$ . . . 170

7.4.5 $\overline{min.E_8}///(\mathrm{SU}(2)\times\mathrm{SU}(2))$ . . . 172

7.5 Examples of SU(3) Orthosymplectic Quotient Quiver Subtraction . . . 175

7.5.1 $\overline{min.E_7}///\mathrm{SU}(3)$ . . . 175

7.5.2 $\overline{min.E_8}///\mathrm{SU}(3)$ and $\overline{min.E_8}///(\mathrm{SU}(3)\times\mathrm{SU}(3))$ . . . 178

7.6 Examples of G_2 Orthosymplectic Quotient Quiver Subtraction . . . 181

7.6.1 $\overline{min.E_8}///G_2$ . . . 181

7.6.2 $(\overline{min.E_7}\times\overline{min.E_7})///G_2$ . . . 184

7.7 Example of SO(7) Orthosymplectic Quotient Quiver Subtraction . . . 186

7.7.1 $(\overline{min.E_7}\times\overline{min.E_7})///\mathrm{SO}(7)$ . . . 186

7.8 Magnetic Quivers for one M5-brane on E_6 Klein Singularity . . . 189

7.8.1 Two $\frac{1}{2}$M5-branes on E_6 Klein singularity . . . 190

7.8.2 One M5 brane on E_6 Klein Singularity – $6d$ $\mathcal{N}=(1,0)$ (E_6,E_6) Conformal Matter . . . 193

8 Conclusion **196**

Bibliography **208**

A Violation of Quotient Quiver Subtraction Rules **231**

A.1 Violation of the Junction Rule . . . 231

A.2 Violation of the External Leg Rule . . . 233

B Star-shaped Quivers and Connections to Class $\mathcal{S}$ **236**

C Gluing Hilbert Series and Hall-Littlewood Polynomials **241**

D Justification of Quiver Polymerisation **244**

D.1 Justifying Chain Polymerisation – Unitary Case 244

D.2 Justifying Cyclic Polymerisation – Unitary Case 246

E Kronheimer-Nakajima Quivers and Moduli Spaces of Instantons **248**

E.1 Brane Realisations 249

E.2 Special Cases 250

List of Tables

2.1 Representations that the chiral multiplets of $\mathcal{Q}_{2.3}$ transform in. 16

2.2 Occupation of NS5, D5, and D3 branes in spacetime for Hanany-Witten setup. . 33

2.3 Gauge algebra for electric and magnetic BPS states with orientifold planes. . . . 38

2.4 Occupation of NS5, D8, and D6 branes in spacetime for Hanany-Witten setup. . 41

3.1 Action of SU(2) and $SU(2)_R$ on the holomorphic and anti-holomorphic coordinates of $\mathbb{C}^2$. 56

6.1 Some quivers which take the form of affine, twisted affine, or generalised Dynkin diagrams. The gauge nodes are specified by the dual Coxeter labels, except for $\frac{1}{2}A^{(1)}_{2n-1}$ where twice the dual Coxeter labels are used. The Coulomb branch and Higgs branch are identified where possible. 122

7.1 The orthosymplectic fixtures of SO(6) alongside the corresponding fixture for SU(4). 164

8.1 The moduli spaces $\mathbb{H}^n$ and their SU(2) hyper-Kähler quotients. These fall into two families for even and odd n. These families are labelled by an integer k, with the appropriate limits on k shown. 198

8.2 Some classical and exceptional nilpotent orbits and their SU(2) hyper-Kähler quotients. For families of orbits, labelled by their rank k, the limits on k are shown. 198

8.3 Some classical and exceptional nilpotent orbits and their SU(3) hyper-Kähler quotients. For families of orbits, labelled by their rank k, the limits on k are shown. 198

8.4 Exceptional nilpotent orbits and their SU(4) hyper-Kähler quotients. 198

8.5 SU(2) chain polymerisation of finite D and B type and related quivers. Initial and chained Coulomb and Higgs branches are shown if known. 200

8.6 Table of cyclic polymerisations to produce Kronheimer-Nakajima quivers. 201

8.7 Table of cyclic polymerisations of finite A_N and D_{N+4} quivers. 201

8.8 Table of cyclic polymerisations of affine $D^{(1)}_{N+4}$, $E^{(1)}_6$, and $E^{(1)}_7$ quivers. 201

8.9 The set of orthosymplectic quotient quivers introduced in Chapter 7. 202

8.10 Some unitary quivers and their orthosymplectic doppelgängers. 204

8.11 Table 8.10 continued. 205

8.12 The $E_6 \times E_6$ representations Higgs branch generators transform in, of the $6d$ $\mathcal{N} = (1,0)$ worldvolume theory of two $\frac{1}{2}$M5 branes (finite coupling) and one M5 brane (infinite coupling) on Klein E_6 singularity. 206

List of Figures

1.1 Left: Gauging a G subgroup of the Coulomb branch global symmetry of a $3d$ $\mathcal{N} = 4$ theory $\mathcal{Q}$ producing $\mathcal{Q}_G$ and the effect on the Higgs and Coulomb branches. Right: Image in the "3d mirror" showing that the $3d$ mirrors of $\mathcal{Q}$ and $\mathcal{Q}_G$, $\mathcal{Q}^\vee$ and $\mathcal{Q}_G^\vee$ respectively are also related by gauging a G subgroup of the flavour symmetry. The corresponding actions on the moduli space are also shown. . . . 7

1.2 Left: Gauging a G subgroup of the Coulomb branch global symmetry of a magnetic quiver $\mathcal{Q}^M$ producing $\mathcal{Q}_G^M$ and the effect on the Coulomb branch. Right: Gauging a G subgroup of the flavour symmetry of an electric $d = 4, 5, 6$ theory $\mathcal{Q}^E$ producing $\mathcal{Q}_G^E$. 7

2.1 Quiver for U(n) gauge theory with k flavours and one adjoint hypermultiplet. . . 12

2.2 D3 brane ending on either an NS5 or D5. 34

2.3 D3 brane ending between five branes. 35

2.4 Simple Type IIB Hanany-Witten brane setup and the corresponding electric quiver theory that lives on the D3 worldvolume 36

2.5 Depiction of the brane creation/annihilation effect. 37

2.6 Summary of brane creation effect in the presence of Op planes. The circle with a cross indicates an NS5 brane and vertical lines indicate a D($p + 2$) brane. . . . 40

4.1 Schematic drawing of a valid target quiver (top) having a junction and an external leg. The target quiver for the quotient quiver subtraction must have a leg that starts as $(1)-\cdots-(n)$. If the quotient quiver (bottom) overlaps a junction node of rank j on the target quiver, this must align with a node of rank $2 \leq j$ on the quotient quiver. The remainder of the target quiver, denoted Q, can take any "good" or "ugly" form. 68

4.2 Type IIB brane system for the SU(n) quotient quiver. There are $2n$ NS5 branes with $2n-1$ intervals on which D3 branes are suspended. 73

4.3 One subtraction of the SU(2) quotient quiver from the magnetic quiver $\mathcal{Q}_{4.3}$ for $\mathbb{H}^{2k}$ to produce the magnetic affine $D_k^{(1)}$ quiver for $\overline{min.D_k}$. 74

4.4 Subtraction of the SU(2) quotient quiver from the magnetic quiver $\mathcal{Q}_{4.4}$ for $\mathbb{H}^{2k+1}$ to produce the magnetic affine $B_k^{(1)}$ quiver for $\overline{min.B_k}$. 75

4.5 Quiver subtraction of the SU(2) quotient quiver from an unframed magnetic quiver for $\overline{min.F_4}$ to produce quiver $\mathcal{Q}_{4.5}$. 77

4.6 Quiver subtraction of the SU(2) quotient quiver from an unframed magnetic quiver for $\overline{min.E_6}$ to produce quiver $\mathcal{Q}_{4.6}$. 78

4.7 Magnetic quiver $\mathcal{Q}_{4.7}$ for $\overline{min.E_6} \times \mathbb{H}^2$. 79

4.8 Subtraction of the SU(2) quotient quiver from the unframed magnetic quiver $\mathcal{Q}_{4.7}$ for $\overline{min.E_6} \times \mathbb{H}^2$ to produce the magnetic quiver $\mathcal{Q}_{4.8}$. 79

4.9 Quiver subtraction of the SU(2) quotient quiver from an unframed magnetic quiver for $\overline{min.E_7}$ to produce quiver $\mathcal{Q}_{4.9}$. 81

4.10 Quiver subtraction of the SU(2) quotient quiver from an unframed magnetic quiver for $\overline{min.E_8}$ to produce quiver $\mathcal{Q}_{4.10}$. 81

4.11 Both alignments of the SU(3) quotient quiver against $\overline{min.E_7}$ to produce quivers $\mathcal{Q}_{4.11a}$ and $\mathcal{Q}_{4.11b}$. Their intersection, reached via A_1 Kraft-Procesi transitions, is $\mathcal{Q}_{4.11c}$. 83

4.12 Quiver subtraction of the SU(3) quotient quiver from an unframed magnetic quiver for $\overline{min.E_8}$ to produce quiver $\mathcal{Q}_{4.12}$. 84

4.13 Both alignments of the SU(4) quotient quiver against $\overline{min.E_8}$ to produce quivers $\mathcal{Q}_{4.13a}$ and $\mathcal{Q}_{4.13b}$. Their intersection, reached via A_1 KP transitions, is $\mathcal{Q}_{4.13c}$. . . 85

5.1 Gauging an Sp(n) flavour subgroup of U(N) SQCD with $2N + k$ flavours gives the theory drawn in Figure 5.1a with the corresponding Type IIB brane system drawn in the electric phase in Figure 5.1b. The 3d mirror theory is drawn in $\mathcal{Q}_{5.1c}$ with its corresponding Type IIB brane system in electric phase drawn in Figure 5.1d. 89

5.2 Sp(2) quotient quiver subtraction on the affine $E_8^{(1)}$ quiver which occurs in two steps. The first step is shown in 5.2a and involves the subtraction of the Sp(2) quotient quiver from the maximal leg. The second step, shown 5.2b, is the splitting of the U(5) node into a U(2) and U(3), producing the resulting quiver $\mathcal{Q}_{5.2}$. Note the emergence of an S_2 outer automorphism between the two U(3) gauge nodes. 92

5.3 Sp(2) quotient quiver subtraction on the extended affine $E_6^{(1)}$ quiver $\mathcal{Q}_{5.15}$ which occurs in two steps. The first step is shown in 5.3a and involves the subtraction of the Sp(2) quotient quiver from the maximal leg. The second step, shown 5.3b, is the splitting of the U(4) node into two U(2) nodes producing the resulting quiver $\mathcal{Q}_{5.3}$. 96

5.4 Sp(k) quotient quiver subtraction on $\mathcal{Q}_{5.18}$ which occurs in two steps. The first step is shown in 5.4a and involves the subtraction of the Sp(k) quotient quiver from the maximal leg. The second step, shown 5.4b, is the splitting of the U($2k$) node into two U(k) nodes producing the resulting quiver $\mathcal{Q}_{5.4}$. 98

5.5 Gauging an SO($2n$) flavour subgroup of U(N) SQCD with $2N+k$ flavours returns the theory in Figure 5.5a, realised from the brane system in Figure 5.5b. The magnetic theory is conjectured to be Figure 5.5c, associated to the brane system in Figure 5.5d, related to that of Figure 5.5b by brane-creation and S-duality. Comparison to the mirror of the SQCD in (5.1) leads to the conjectural quotient quiver (5.19). 99

5.6 SO(2) quotient quiver subtraction on the affine $F_4^{(1)}$ quiver occurs in two steps. The first is shown in 5.6a and involves the subtraction of the SO(2) quotient quiver from the maximal leg. The second step, given in 5.6b, is the non-simple lacing of the edge connecting the left U(2) node to the U(3), producing the resulting quiver $\mathcal{Q}_{5.6}$. 101

5.7 SO(4) quotient quiver subtraction on the affine $E_7^{(1)}$ quiver occurs in two steps. The first step, shown in 5.7a, involves the subtraction of the SO(4) quotient quiver from one maximal leg. The second step, in 5.7b, is the non-simple lacing of the two edges emerging from the U(4) node. 102

5.8 SO(4) quotient quiver subtraction on the affine $E_8^{(1)}$ quiver occurs in two steps. The first step is shown in 5.8a and involves the subtraction of the SO(4) quotient quiver from the maximal leg. The second step, shown 5.8b, is the non-simple lacing of the two edges going from the U(4) node producing $\mathcal{Q}_{5.8}$. 104

5.9 Gauging an SO($2n+1$) flavour subgroup of U(N) SQCD with $2N+k$ flavours returns the theory in Figure 5.9a, realised from the brane system in Figure 5.9b. The magnetic theory is conjectured to be Figure 5.9c, associated to the brane system in Figure 5.9d, related to that of Figure 5.9b by brane-creation and S-duality. Comparison to the mirror of the SQCD in (5.1) leads to the conjectural quotient quiver (5.31). 105

5.10 SO(3) quotient quiver subtraction on the affine $E_6^{(1)}$ quiver which occurs in two steps. The first step is shown in Figure 5.10a and involves the subtraction of the SO(3) quotient quiver from one maximal leg. The second step, shown in Figure 5.10b, is the non-simple lacing of the two edges going from the U(3) node producing $\mathcal{Q}_{5.10}$. 107

5.11 SO(3) quotient quiver subtraction on the affine $F_4^{(1)}$ quiver occurs in two steps. The first step is shown in Figure 5.11a and involves the subtraction of the SO(3) quotient quiver from one maximal leg. The second step, shown in Figure 5.11b, is the non-simple lacing of the two edges going from the U(3) node producing $\mathcal{Q}_{5.11}$. Note that the non-simply laced-ness of this edge goes from two to four. . 109

5.12 Gauging an $\mathrm{Sp}(n) + \frac{1}{2}$ flavour subgroup of $\mathrm{U}(N)$ SQCD with $2N + k$ flavours returns the theory in Figure 5.12a, realised from the brane system in Figure 5.12b. The magnetic theory is conjectured to be Figure 5.12c, associated to the brane system in Figure 5.12d, related to that of Figure 5.12b by brane-creation and S-duality. Comparison to the mirror of the SQCD in (5.1) leads to the conjectural quotient quiver (5.43). 110

5.13 $\mathrm{Sp}(1) + \frac{1}{2}\mathsf{F}$ quotient quiver subtraction on the affine $E_6^{(1)}$ quiver which occurs in two steps. The first step is shown in Figure 5.13a and involves the subtraction of the $\mathrm{Sp}(1) + \frac{1}{2}\mathsf{F}$ quotient quiver from one maximal leg. The second step, shown in Figure 5.13b, is the non-simple lacing of the U(2) gauge node producing $\mathcal{Q}_{5.13}$. 113

6.1 Schematic showing the chain polymerisation of two unframed quivers (assumed to be computable) with a node of $\mathrm{U}(n)$ on a leg to give a single unframed quiver. 119

6.2 Schematic showing the cyclic polymerisation of some generic quiver (assumed good or ugly) with two external legs of $(1) - \cdots - (n) -$. 120

6.3 SU(2) chain polymerisation of the finite D_{k+2} and D_{p+2} quivers to produce the affine $D_{k+p}^{(1)}$ quiver. 123

6.4 SU(2) chain polymerisation of the finite D_{k+2} and B_{p+1} quivers to produce the affine $B_{k+p-1}^{(1)}$ quiver. 124

6.5 SU(2) chain polymerisation of the finite B_{k+1} and B_{p+1} quivers to produce the twisted affine $D_{k+p-1}^{(2)}$ quiver. 124

6.6 Unframed magnetic quiver $\mathcal{Q}_{6.6}$ for $\mathbb{C}^2/\mathbb{Z}_2 \times \mathbb{H}^{2k-1}$. 125

6.7 SU(2) chain polymerisation of $\mathcal{Q}_{6.6}$ with the finite D_{p+2} quiver to give the additive $\frac{1}{2}D_{2k+2p-1}^{(1)}$ quiver, $\mathcal{Q}_{6.7}$. 125

6.8 SU(2) chain polymerisation of $\mathcal{Q}_{6.6}$ with itself to give the additive $\frac{1}{2}A_{2k+2p-3}^{(1)}$ quiver, $\mathcal{Q}_{6.8}$. 127

6.9 SU(2) chain polymerisation of $\mathcal{Q}_{6.6}$ with the finite B_{p+1} quiver to give the additive $\frac{1}{2}D_{2k+2p-1}^{(2)}$ quiver, $\mathcal{Q}_{6.9}$. 128

6.10 Two $\frac{1}{2}$ M5 branes probing an E_6 Klein singularity. The directions $x^{0,1,2,3,4,5}$ are suppressed. The corresponding electric quiver $\mathcal{Q}_{6.10b}$ comes from the F-theory dual description. 130

6.11 SU(3) chain polymerisation of two $E_8^{(1)}$ quivers to produce $\mathcal{Q}_{6.11}$. This quiver is a magnetic quiver for $6d$ $\mathcal{N} = (1,0)$ theory for two separated $\frac{1}{2}$ M5 branes probing Klein E_6 singularity. 130

6.12 Naïve Type IIA brane system for $\mathcal{Q}_{6.11}$. The two O8$^-$ planes are indicative of a Type I′ brane system with 16 D8 branes in the interval, this brane system only has 10. 131

6.13 U(1) cyclic polymerisation of the finite A_{N+2} quiver to produce the CFHM quiver $\mathcal{Q}_{6.13}$. 132

6.14 U(2) cyclic polymerisation of the finite D_{N+4} quiver to produce $\mathcal{Q}_{6.14}$ for $N \geq 1$. 133

6.15 U(2) cyclic polymerisation of the unframed magnetic quiver $\mathcal{Q}_M\left(\overline{n.min.A_{N+3}}\right)$ for $N \geq 1$ to produce $\mathcal{Q}_{6.15}$. 134

6.16 Magnetic quiver $\mathcal{Q}_{6.16}$ for $\overline{\left[\mathcal{W}_{A_{2k+N-1}}\right]}^{[0^{k-1},l-l',0^{N-1},l',0^{k-1}]}_{[0^{k-1},l-l'-1,0^{N-1},l'-1,0^{k-1}]}$ for $N \geq 1$ and $l > l' \geq 1$. 135

6.17 Magnetic quiver $\mathcal{Q}_{6.17a}$ for $\overline{\left[\mathcal{W}_{A_{2k-1}}\right]}^{[0^{k-1},l,0^{k-1}]}_{[0^{k-1},l-2,0^{k-1}]} \times \mathbb{H}^{Nk}$ for $N \geq 1$. This quiver specialises $\mathcal{Q}_{6.16}$ to the case $l' = 0$. The node of rank k filled in black is "ugly", with balance -1, all other nodes are "good", with non-negative balance. Application of the dualisation algorithm to $\mathcal{Q}_{6.17a}$ yields $\mathcal{Q}_{6.17b}$, which is a magnetic quiver for $\overline{\left[\mathcal{W}_{A_{2k-1}}\right]}^{[0^{k-1},l,0^{k-1}]}_{[0^{k-1},l-2,0^{k-1}]}$. 136

6.18 U(k) cyclic polymerisation of $\mathcal{Q}_{6.16}$ to produce quiver $\mathcal{Q}_{6.18}$. 136

6.19 (a) Magnetic quiver $\mathcal{Q}_{6.19a}$ for $\overline{\left[\mathcal{W}_{A_{l-1}}\right]}^{[k,0^{l-3},k]}_{[0^{l-1}]}$. This quiver is $3d$ mirror to $\mathcal{Q}_{6.17b}$.
(b) Magnetic quiver $\mathcal{Q}_{6.19b}$ for $\overline{\left[\mathcal{W}_{A_{l-1}}\right]}^{[k,0^{l-l'-2},N,0^{l'-2},k]}_{[0^{l-l'-1},N,0^{l'-1}]}$. This quiver is $3d$ mirror to $\mathcal{Q}_{6.16}$. 138

6.20 Unframed linear quiver $\mathcal{Q}_{6.20}$. 138

6.21 Construction of a generic Kronheimer-Nakajima quiver from U(k_1) cyclic polymerisation. 138

6.22 U(1) cyclic polymerisation of the finite A_{N+2} quiver to produce $\mathcal{Q}_{6.22}$. 140

6.23 U(1) cyclic polymerisation of the affine $E_6^{(1)}$ quiver to produce $\mathcal{Q}_{6.23}$. 141

6.24 U(2) cyclic polymerisation of the affine $E_6^{(1)}$ quiver to produce $\mathcal{Q}_{6.24}$. 142

6.25 U(1) cyclic polymerisation of the $E_7^{(1)}$ quiver to produce $\mathcal{Q}_{6.25}$. 144

6.26 U(3) cyclic polymerisation of the $E_7^{(1)}$ quiver to produce $\mathcal{Q}_{6.26}$. 145

7.1 Subtraction of the SU(2) orthosymplectic quotient quiver from the orthosymplectic magnetic quiver for $\overline{min.E_7}$ to produce $\mathcal{Q}_{7.1}$. 164

7.2 Subtraction of the SU(2) orthosymplectic quotient quiver from the orthosymplectic magnetic quiver for $\overline{min.E_6}$ to produce $\mathcal{Q}_{7.2}$. 165

7.3 Both alignments of the SU(2) quotient quiver against $\mathcal{Q}_{7.2}$ to produce $\mathcal{Q}_{7.3a}$ and $\mathcal{Q}_{7.3b}$. Their intersection is $\mathcal{Q}_{7.3c}$. 168

7.4 Subtraction of the SU(2) orthosymplectic quotient quiver from the orthosymplectic magnetic quiver for $\overline{min.E_8}$ to produce $\mathcal{Q}_{7.4}$. 171

7.5 Subtraction of two SU(2) orthosymplectic quotient quivers from each long leg of the orthosymplectic magnetic quiver for $\overline{min.E_8}$. The result is quiver $\mathcal{Q}_{7.5}$. . . . 173

7.6 Two alignments of the SU(3) quotient quiver against the magnetic orthosymplectic quiver for $\overline{min.E_7}$ producing $\mathcal{Q}_{7.6a}$ and $\mathcal{Q}_{7.6b}$. Their intersection is $\mathcal{Q}_{7.6c}$. . 176

7.7 Subtraction of the SU(3) orthosymplectic quotient quiver from the orthosymplectic magnetic quiver for $\overline{min.E_8}$. 178

7.8 Subtraction of the SU(3) orthosymplectic quotient quiver from the orthosymplectic magnetic quiver for $\overline{min.E_8}///\mathrm{SU}(3)$. This gives $\overline{min.E_8}///\mathrm{SU}(3) \times \mathrm{SU}(3)$ as a moduli space of dressed monopole operators. 178

7.9 Two alignments of the G_2 quotient quiver against the orthosymplectic quiver for $\overline{min.E_8}$ producing $\mathcal{Q}_{7.9a}$ and $\mathcal{Q}_{7.9b}$. Their intersection is $\mathcal{Q}_{7.9c}$. 182

7.10 Subtraction of the G_2 orthosymplectic quotient quiver from the orthosymplectic magnetic quiver for $\overline{min.E_7} \times \overline{min.E_7}$. 185

7.11 Two alignments of the SO(7) quotient quiver against the orthosymplectic magnetic quiver for $\overline{min.E_7} \times \overline{min.E_7}$ producing $\mathcal{Q}_{7.11a}$ and $\mathcal{Q}_{7.11b}$. Their intersection is $\mathcal{Q}_{7.11c}$. 187

7.12 Four $\frac{1}{4}$M5-branes on an E_6 Klein singularity. The directions $x^{0,1,2,3,4,5}$ are suppressed. The corresponding electric quiver $\mathcal{Q}_{7.12b}$ comes from the F-theory dual description. 189

7.13 Two $\frac{1}{2}$ M5 branes on an E_6 Klein singularity. The directions $x^{0,1,2,3,4,5}$ are suppressed. The corresponding electric quiver $\mathcal{Q}_{7.13b}$ comes from the F-theory dual description. 190

7.14 The subtraction of the SU(3) quotient quiver on the orthosymplectic quiver for $\overline{min.E_8} \times \overline{min.E_8}$ to give $\mathcal{Q}_{7.14}$. This is a magnetic quiver for the $6d$ $\mathcal{N} = (1,0)$ worldvolume theory of two separated $\frac{1}{2}$M5 branes on E_6 Klein singularity. 191

7.15 The Type IIA brane system for the magnetic quiver $\mathcal{Q}_{7.14}$. This is a magnetic quiver for the $6d$ $\mathcal{N} = (1,0)$ worldvolume theory of two $\frac{1}{2}$M5 branes on a Klein E_6 singularity. 192

7.16 One M5 brane on an E_6 Klein singularity. The directions $x^{0,1,2,3,4,5}$ are suppressed. The corresponding electric quiver $\mathcal{Q}_{7.16b}$ comes from the F-theory dual description. 193

7.17 The Type IIA brane system from which the magnetic quiver $\mathcal{Q}_{7.19}$ is read. This is a magnetic quiver for $6d$ $\mathcal{N} = (1,0)$ (E_6, E_6) conformal matter. This configuration can be obtained from that of Figure 7.15 by moving the NS5-brane onto the $O8^-$-plane. 194

7.18 The electric phase of the magnetic Type IIA brane system shown in Figure 7.17 from which $\mathcal{Q}_{7.19}$ is read. 194

7.19 The effect of a small E_8-instanton transition on the magnetic quiver $\mathcal{Q}_{7.14}$ associated to the brane system in Figure 7.15 as the NS5-brane is taken onto the $O8^-$-plane. The resulting quiver $\mathcal{Q}_{7.19}$ is the magnetic quiver for $6d$ $\mathcal{N} = (1,0)$ (E_6, E_6) conformal matter. 194

A.1 Both (incorrect) alignments of the SU(3) quotient quiver against the unitary unframed magnetic quiver for $\overline{min.E_6}$ to give quivers $\mathcal{Q}_{A.1a}$ and $\mathcal{Q}_{A.1b}$. Their intersection is trivial. 232

A.2 Both alignments of the SU(2) quotient quiver against the magnetic quiver for $\overline{min.C_k}$ for $k \geq 4$ giving quivers $\mathcal{Q}_{A.2a}$ and $\mathcal{Q}_{A.2b}$. Their intersection, reached via A_1 KP transitions, is quiver $\mathcal{Q}_{A.2c}$. 234

B.1 In Figure B.1a is a punctured Riemann surface $\mathcal{C}_{N,g}$ of genus g with n punctures, ρ_i, of type A_{n-1}. In Figure B.1b is the corresponding $3d$ mirror which consists of legs which are the $T_{\rho_i}[\mathrm{SU}(n)]$ glued at the common flavour symmetry. There are g adjoint on the central U(n) gauge node corresponding to the genus of the Riemann surface. 237

B.2 In (Figure B.2a) is the gluing of maximal punctures on the Riemann surfaces. In (Figure B.2b) is the perspective on the $3d$ mirror quiver, this is the same as chain polymerisation at the node of U(n). 239

B.3 In Figure B.3a is the gluing of two maximal punctures on the same Riemann surface. In Figure B.3b is the corresponding action on the $3d$ mirror quivers, this differs from cyclic polymerisation. 240

E.1 Most general A-type Kronheimer-Nakajima quiver. The Higgs branch is the moduli space of instantons $\mathcal{M}^{\mathbb{C}^2/\mathbb{Z}_N;\mathrm{SU}(l)}_{(k_1,\cdots,k_N),(l_1,\cdots,l_N)}$, where $l = \sum_{i=1}^{N} l_i$. The Coulomb branch is the moduli space of instantons $\mathcal{M}^{\mathbb{C}^2/\mathbb{Z}_l;\mathrm{SU}(N)}_{(k'_1,\cdots,k'_l),(l'_1,\cdots,l'_l)}$, where the k'_i and l'_i are linear functions of the k_i and l_i respectively. 248

E.2 The Kronheimer-Nakajima quiver with all gauge nodes the same. The Coulomb branch is the moduli space of k SU(N) instantons on $\mathbb{C}^2/\mathbb{Z}_l$ where $l = \sum_{i=1}^{N} l_i$. . 250

E.3 The Kronheimer-Nakajima quiver with all gauge nodes the same. The Coulomb branch is the moduli space of k SU(N) instantons on $\mathbb{C}^2/\mathbb{Z}_l$ where $l = \sum_{i=1}^{N} l_i$. . 251

Chapter 1

Introduction

Symmetries have served as faithful guiding principles in many topics in physics since Noether's elegant formulation of the relationship between continuous symmetries and conservation laws [9]. Quantum field theory (QFT) champions the idea of leveraging symmetries in a problem to gain understanding, which is a welcome oasis in a desert where many mathematical and technical challenges in QFT place themselves adversely to physicists. It is no surprise then, that the best model of the particles and fundamental forces in our Universe to date, the Standard Model, is a QFT which is packed with various gauge, global, and even higher-form symmetries.

The addition of supersymmetry to quantum field theory, transcends the role of symmetries even further [10]. In particular, the connection between algebraic geometry and physics becomes even more apparent. The first to popularise this was Seiberg, when he leveraged holomorphy [11] to show that the $4d$ $\mathcal{N} = 1$ superpotential is (usually) not renormalised. This feat was only possible due to the addition of supersymmetry. As a consequence, problems in supersymmetric gauge theories can be turned into problems in algebraic geometry with its own arsenal of tools.

The study of moduli spaces of vacua in string theory and supersymmetric gauge theories has been of historic importance and exemplifies the intimate connection to geometry. Physically, the moduli space of vacua gives insight into the possible light spectra of particles and residual gauge theories one can reach through the Brout-Englert-Guralnik-Higgs-Hagen-Kibble mechanism [12–15] (or "Higgs mechanism" for short). With enough supersymmetry theories do not admit

a superpotential and so computing the classical moduli space essentially becomes a counting problem. In theories with maximal supersymmetry in d dimensions, one has to account for non-compact scalars, which come from dimensional reduction of the graviton in eleven dimensions, and compact scalars, which come from dimensional reduction of the 3-form in eleven dimensions. The classical moduli space of theories in d dimensions with maximal supersymmetry is given by the coset construction [16–18]

$$\mathcal{M}_d^{32} = E_{n(n)}/H_n \tag{1.1}$$

where $n = 11 - d$, $E_{n(n)}$ is the maximally split real form of the E-sequence member of rank n, and where H_n is the maximally compact subgroup of $E_{n(n)}$ or the R-symmetry of the theory. For $d \geq 6$ the corresponding $E_{n(n)}$ groups correspond to classical groups. Some properties of the moduli space can be summarised through the following formulae relating the number of non-compact scalars, N, and the number of compact scalars C.

$$n = 11 - d = N \tag{1.2}$$

$$\dim H_n = C \tag{1.3}$$

$$\dim \mathcal{M}_d^{32} = N + C \tag{1.4}$$

The moduli space of theories with 16 supercharges still takes the form of a coset. Due to gravitational anomalies, these theories have either $E_8 \times E_8$ or SO(32) gauge symmetry [19], so they must contain one supergravity multiplet and sixteen vector multiplets. The supergravity multiplet contains a non-compact scalar and the vector multiplets contain compact scalars. Through dimensional reduction additional compact scalars arise. The classical moduli space of a theory in d dimensions, where now $d \leq 10$ is [20, 21]

$$\mathcal{M}_d^{16} = \begin{cases} \frac{\mathrm{SO}(26-d,10-d)}{\mathrm{SO}(26-d)\times\mathrm{SO}(10-d)} \times \mathbb{R}^+, & 5 \leq d \leq 10 \\ \frac{\mathrm{SO}(22,6)}{\mathrm{SO}(22)\times\mathrm{SO}(6)} \times \frac{\mathrm{SL}(2,\mathbb{R})}{\mathrm{SO}(2)}, & d = 4 \\ \frac{\mathrm{SO}(24,8)}{\mathrm{SO}(24)\times\mathrm{SO}(8)}, & d = 3 \end{cases} \tag{1.5}$$

since the supergravity multiplet contains two non-compact scalars in four dimensions, and all

scalars are compact in three dimensions. Quantum effects were accounted for by use of the U-duality of string theory [22] in both cases of supergravity theories with 32 and 16 supercharges.

Breaking half of supersymmetry again, to theories with eight supercharges, changes the analysis greatly. The focus of this thesis lies on gauge theories, supersymmetry is now relaxed enough to allow for superpotentials but is also strict enough to constrain their form. The moduli space of vacua is now the space of vevs which minimise the superpotential, these vevs are solutions to the F-term and D-term equations. This uniquely places theories with eight supercharges in a "Goldilocks" zone where one has enough control to extract exact results but also be able to study a range of interesting spaces. In particular, the moduli spaces of vacua are not always symmetric spaces like they are in cases with more supersymmetry. The moduli spaces of theories with eight supercharges also separate into different branches. With the restriction to gauge theories, the only source of scalar fields are in the hypermultiplet, vectormultiplets, and tensor multiplets (for six dimensions only). The branches of the moduli space refer to subspaces where all but one source of scalars can acquire non-trivial vev. The Higgs branch, the moduli space of scalars in the hypermultiplet, is of particular geometric interest as it is a "symplectic singularity" [23]. These moduli spaces and their resolutions have also garnered interest from mathematicians, they are hyper-Kähler varieties and have applications to representation theory, vertex algebras, geometric Langlands, and more [24–29]. This thesis will focus on moduli spaces of theories with eight supercharges and symplectic singularities.

The specific theories studied in this thesis are quiver gauge theories. Quivers encompass the typical Lagrangian description of a gauge theory into a diagram consisting of circles, squares, and lines [30]. As mentioned, there is enough supersymmetry so superpotentials are constrained enough that quivers are mostly equivalent to Lagrangians. The diagrammatic nature of quivers provides a compact notation for gauge theories but can also make explicit certain global symmetries of the theory by the combinatorial data in the quiver.

Quiver gauge theories have close ties to string theory constructions of supersymmetric gauge theories and the two can often be "read off" from each other. The core brane systems that are most amenable to the study of theories with eight supercharges are the Hanany-Witten brane

setups [31]. Originally formulated in Type IIB, these simple diagrams encompass many non-trivial features of $3d$ $\mathcal{N} = 4$ supersymmetric gauge theories while taking advantage of the entire web of string dualities. This formalism has been extended to provide descriptions of theories with eight supercharges in four, five, and six dimensions too [32–34] from the application of T-duality. The analysis from brane systems is not too reliant on things like the DBI action or scattering amplitudes which give details about the gauge theory at hand. Much like with quivers, one will extract information and the physics of the gauge theories from the combinatorial data encoded in the brane systems.

Supersymmetric gauge theories also enjoy global symmetries which act on operators in the theory. These global symmetries are also global symmetries for the moduli space of vacua. The flavour symmetry of a theory is the global symmetry of the Higgs branch for example. The first two questions that spring to a physicist's mind when a quantum field theory enjoys a global symmetry are:

1. What (mixed) anomalies does this global symmetry have?

2. If allowed, how can one gauge this symmetry?

It is the second question that will be most relevant here. In general, the answer is theory dependent. Usually to gauge global symmetries, one would write down a Lagrangian, couple background gauge fields to the Noether current for the global symmetry and add a kinetic term for the gauge fields. However a theory may not admit a known Lagrangian, or additional massless states can appear at certain points in the moduli space or along RG-flow. The prototypical example would be the instanton corrections to the superpotential in $4d$ $\mathcal{N} = 1$ theories [35], but violations of the non-renormalisation theorem for theories with eight supercharges [36] also occur. For example, in four dimensions some theories may have Argyres-Douglas points [37, 38], in five dimensions massless instantons can appear at infinite coupling [39–41], and in six dimensions tensionless strings can appear at infinite coupling [42–45]. The examples given for four, five, and six dimensional theories are all examples of instanton effects in that they deal with co-dimension four objects in the theory. For $3d$ $\mathcal{N} = 4$ theories, monopole operators

appear in the IR which drastically quantum correct the classical Coulomb branch.

Many of these effects have natural interpretation from string theory including being realisable in Hanany-Witten brane systems. From the brane system one can read off a "magnetic quiver" [46] which describes the Higgs branches of a theory with eight supercharges as a moduli space of dressed monopole operators. The magnetic quiver characterises Higgs branches incorporating these non-trivial effects using only the combinatorial data of brane systems. The magnetic quiver and related techniques have been remarkably successful in the study of theories with eight supercharges [47–82, 1, 5, 83–90, 2, 3, 6, 91–98, 7, 99–102, 8, 103, 4, 104–107] in this regard and the work in this thesis follows this theme.

A computation one can do with magnetic quivers is finding the Hilbert series of the moduli space of dressed monopole operators. The Hilbert series enumerates the gauge invariant operators in a theory grading them by the SU(2) R-charge and any weights of the global symmetry algebra. This includes the additional operators which preclude a description from a Lagrangian. The Hilbert series from a magnetic quiver can be computed using the monopole formula [108]. The Hilbert series has an advantage compared to other objects which do similar things, such as superconformal indices, in terms of being simpler to compute and hence more likely to have closed form expressions. Furthermore, although in certain limits the superconformal index becomes a Hilbert series [109], this behaviour is generally not the case. The Hilbert series often provides information about theories that indices cannot, this makes them an extremely suitable object to compute in order to study moduli spaces of theories with eight supercharges.

There are also a host of combinatorial techniques on magnetic quivers which probe the underlying geometric structure of a moduli space. A significant effort is in understanding the various phases a theory can undergo through the Higgs mechanism, and their relationships to each other, which are summarised in a Hasse diagram [110, 47, 49, 75, 83, 6]. Other techniques are theory dependent such as understanding FI deformations of $3d$ $\mathcal{N} = 4$ theories [79, 93].

The central topic of this thesis, gauging global symmetries, can also be realised diagrammatically using magnetic quivers. The techniques described here are developed for $3d$ $\mathcal{N} = 4$ theories but can be applied to magnetic quivers for theories in higher dimensions also. Two

global symmetries $3d$ $\mathcal{N} = 4$ theories enjoy are flavour symmetries and the global symmetry of the Coulomb branch (this may also go by the name of topological symmetry or monopole global symmetry). Gauging the flavour symmetry of $3d$ $\mathcal{N} = 4$ theories is largely unproblematic since there are no gauge anomalies in three dimensions, no parity anomalies for the theories studied here, and the flavour symmetry is treated classically. On the other hand, the gauging of Coulomb branch global symmetries is generically rather challenging. Firstly, one distinction should be made, the Coulomb branch in the UV is an orbifold with its global symmetry being the maximal torus of the gauge group. In the IR, monopole operators, the source of the challenge, appear in the spectrum which correct the Coulomb branch and may enhance the Abelian global symmetry to a non-Abelian symmetry. It is the IR Coulomb branch symmetry that shall concern this thesis.

In the face of these complications there is still hope, as $3d$ $\mathcal{N} = 4$ theories enjoy a particularly interesting and useful duality in the IR which goes by the name of $3d$ mirror symmetry [111]. This is a duality which relates two $3d$ $\mathcal{N} = 4$ theories which flow to the same IR fixed point, up to a swap in certain features such as their Higgs and Coulomb branches, and FI and mass parameters. Historically, this duality was useful to understand the quantum Coulomb branches of a theory through the classical Higgs branch of its mirror. This idea will be leveraged once more in this thesis to extract combinatorial algorithms for gauging Coulomb branch global symmetries. The commutation of gauging these global symmetries and $3d$ mirror symmetry is summarised in Figure 1.1, as well as the corresponding actions on the moduli spaces. The Higgs branch of theories with eight supercharges are hyper-Kähler and so the action of gauging flavour symmetry subgroups corresponds to a hyper-Kähler quotient (HKQ) [25]. By $3d$ mirror symmetry gauging Coulomb branch global symmetry subgroups should also correspond to a hyper-Kähler quotient.

The idea of using $3d$ mirror symmetry captured in Figure 1.1 can also be extended to magnetic quivers and theories in higher dimensions. This is summarised in Figure 1.2. Inspiration from the physics of theories in higher dimensions is particularly useful since the methods to gauge certain flavour symmetries may be extremely constrained either by anomalies or by the specific construction of the higher dimensional theory in question. In turn, a constraint on how to

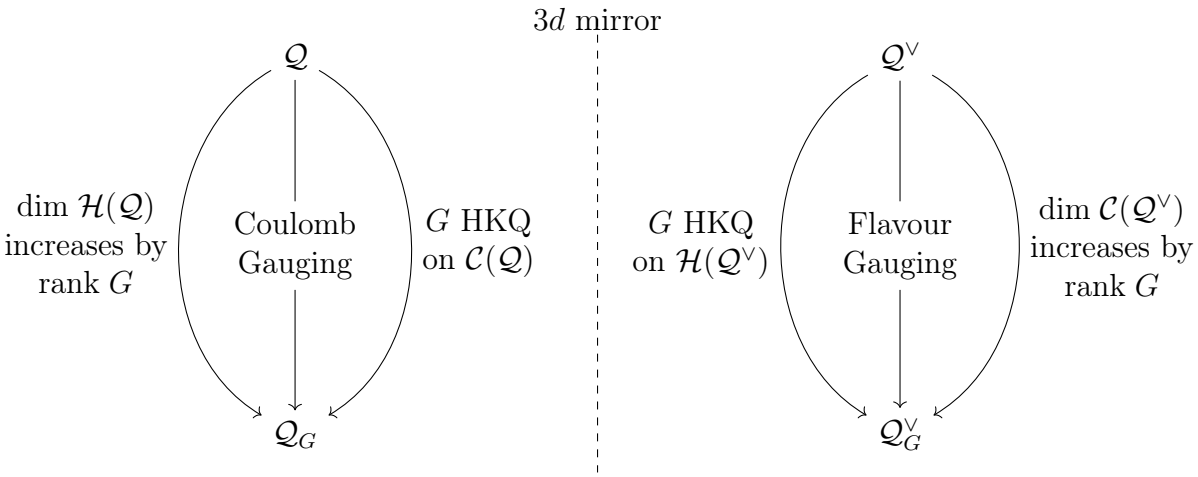


Figure 1.1: Left: Gauging a G subgroup of the Coulomb branch global symmetry of a $3d$ $\mathcal{N}=4$ theory $\mathcal{Q}$ producing $\mathcal{Q}_G$ and the effect on the Higgs and Coulomb branches. Right: Image in the "3d mirror" showing that the $3d$ mirrors of $\mathcal{Q}$ and $\mathcal{Q}_G$, $\mathcal{Q}^\vee$ and $\mathcal{Q}^\vee_G$ respectively are also related by gauging a G subgroup of the flavour symmetry. The corresponding actions on the moduli space are also shown.

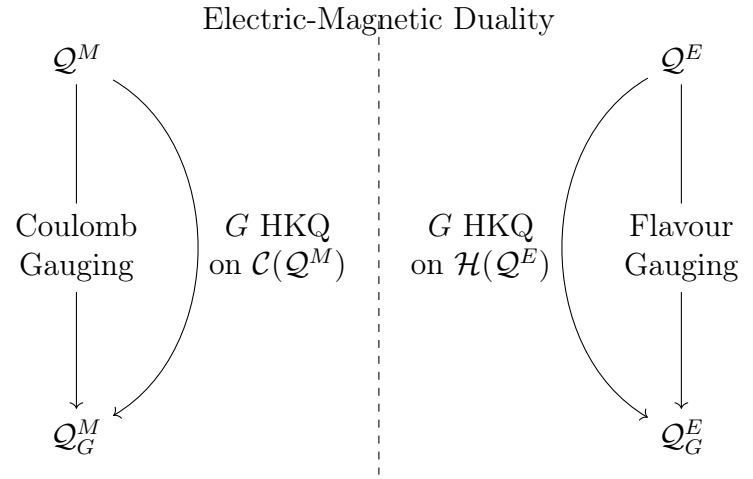


Figure 1.2: Left: Gauging a G subgroup of the Coulomb branch global symmetry of a magnetic quiver $\mathcal{Q}^M$ producing $\mathcal{Q}^M_G$ and the effect on the Coulomb branch. Right: Gauging a G subgroup of the flavour symmetry of an electric $d=4,5,6$ theory $\mathcal{Q}^E$ producing $\mathcal{Q}^E_G$.

realise this gauging through magnetic quivers fixes combinatorial operations precisely.

These techniques can be applied to magnetic quivers for theories in higher dimensions, relating two different theories by gauging. One can also find relationships between two different moduli spaces by hyper-Kähler quotients providing new results in mathematics.

Organisation of the Thesis Chapter 2 lays out the necessary physics background regarding supersymmetric quiver gauge theories in three and six dimensions and their constructions from

Type IIB and Type IIA string theory.

The mathematics background regarding the common types of symplectic singularity encountered in this thesis is covered in Chapter 3.

Chapter 4 introduces the first technique to gauge Coulomb branch global symmetries of $3d$ $\mathcal{N} = 4$ theories. This technique is "quotient quiver subtraction" and gauges $\mathrm{SU}(n)$ subgroups of Coulomb branch global symmetries of quivers with unitary gauge groups. These techniques are applied to moduli spaces of free fields and nilpotent orbits of exceptional algebras among others.

In Chapter 5, a similar "quotient quiver subtraction" technique is introduced which gauges $\mathrm{Sp}(n)$ (possibly coupled to a half-hypermultiplet), and $\mathrm{SO}(n)$ subgroups of the Coulomb branch global symmetry of quivers with unitary gauge groups. These are applied to provide new realisations of some dualities between some $4d$ $\mathcal{N} = 2$ theories using magnetic quivers.

Chapter 6 introduces "quiver polymerisation" which comes in two types - "chain" and "cyclic". The former gauges diagonal $\mathrm{SU}(n)$ symmetries in two different quivers and "chains" them together, the latter gauges a diagonal $\mathrm{U}(n)$ in a single quiver by forming a loop. This technique applies once again to quivers with unitary gauge groups. Notable applications include; hyper-Kähler quotient constructions of the moduli space of instantons, new relationships between nilpotent orbits, and a finite coupling phase of the $6d$ $\mathcal{N} = (1, 0)$ (E_6, E_6) minimal conformal matter theory.

The last technique included in this thesis is given in Chapter 7 which applies to quivers with orthogonal and symplectic gauge groups. This is another type of "quotient quiver subtraction" and gauges $\mathrm{SU}(2)$, $\mathrm{SU}(3)$, G_2, and $\mathrm{SO}(7)$ subgroups of the Coulomb branch global symmetry. There are applications to nilpotent orbits, providing quivers which are "doppelgängers" to quivers with unitary gauge groups, and also new relationships between nilpotent orbits. A significant application is in finding a magnetic quiver for the infinite coupling phase of the $6d$ $\mathcal{N} = (1, 0)$ (E_6, E_6) minimal conformal matter theory and the corresponding Type IIA brane construction.

In Chapter 8 are a summary and conclusions of the work presented in this thesis, as well as some future directions to explore.

Chapter 2

Physics Background

2.1 Introduction

In this Chapter the necessary physics background regarding supersymmetric quiver gauge theories with eight supercharges is reviewed. The review starts with some basic statements about supersymmetry, supermultiplets, and introduces notation for quivers. The remainder of this Chapter will take a closer look into some features of $3d$ $\mathcal{N} = 4$ and $6d$ $\mathcal{N} = (1, 0)$ theories, as well as their constructions in string theory.

2.2 Supermultiplets

In this thesis the focus will lie on supersymmetric quantum field theories in $d = 3$ and 6 dimensions with eight supercharges in Minkowski space. Before approaching each of these in detail, it is worth discussing them in generality first.

These theories enjoy the usual Poincaré spacetime symmetry, generated by translations and Lorentz transformations, as well as supertranslations generated by supercharges which are Lorentz spinors. Altogether, the spacetime symmetry of the theory forms a super-Poincaré algebra. Although these SQFTs have the same amount of supersymmetry, the physics of these

theories varies drastically by dimension.

One obvious way that the physics is different is in the massless field content. Usually in quantum field theory one starts with massless fields which are thought of as representations of the little group $\mathrm{SO}(1, d-3)$. However, with the additional constraint of supersymmetry one works with supermultiplets which are collections of fields with equal numbers of bosonic and fermionic degrees of freedom. Bosonic fields have integer helicity and fermionic fields have half-integer helicity. There are various methods to extract supersymmetry multiplets, such as with ladder operators or through dimensional reduction, but for the purpose of this thesis it is sufficient to quote the results.

As gravity will be decoupled in the theories we study there are only two main supermultiplets to consider; the hypermultiplet and the vector multiplet. Particular emphasis will lie on the bosonic degrees of freedom since these play the most important role in understanding the moduli spaces of vacua.

In d dimensions the hypermultiplet contains two complex scalars $Q, \widetilde{Q}$ and fermions. The bosonic content of the hypermultiplet is the same for $d = 3, 4, 5, 6$ with 8 supercharges.

The vector multiplet in d dimensions contains a gauge field $A^{(1)}$, a collection of $6 - d$ scalars denoted $\phi_{1,\cdots,6-d}$ and some fermions. All of these fields transform in the adjoint of the gauge group.

It is important to note that in six dimensions the vector multiplet does not contain a scalar field. There is an additional supermultiplet in six dimensions which contains a scalar field called the tensor multiplet. The tensor multiplet contains a 2-form $B^{(2)}$, a scalar field, and some fermions.

2.3 Quivers

A quiver is one way to represent a gauge theory in d dimensions, it encodes the gauge symmetry, flavour symmetry, and matter representations in a single diagram consisting of circles, squares,

and lines [30].

Due to the gauge symmetry and in particular supersymmetry, the interactions between the fields are heavily restricted. The more traditional way to represent a theory through a Lagrangian is then almost unambiguous due to these constraints, making quivers almost equivalent to a Lagrangian description (when it exists). Additional data, such as masses or FI parameters, also need to be provided but these will not be considered in this thesis. In the case of six dimensions the number of tensor multiplets will also need to be provided.

The quiver notation is that circular nodes indicate a gauge symmetry, square nodes indicate a flavour symmetry and lines connecting nodes represent a hypermultiplet. Usually the hypermultiplet transforms in the bifundamental representation of the groups it connects, but it may transform in other representations also. In these cases, the specific representation will be labelled with additional notation.

An example is the quiver U(n) SQCD with k flavours and one adjoint hypermultiplet, which is drawn in Figure 2.1. The label n for the gauge node is short-hand for U(n). The adjoint hypermultiplet is denoted by the loop on the U(n) gauge node.

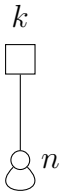


Figure 2.1: Quiver for U(n) gauge theory with k flavours and one adjoint hypermultiplet.

2.4 Moduli Spaces of Vacua

The gauge theories being considered here are constructed from massless multiplets. The fields may gain mass through the Brout-Englert-Guralnik-Higgs-Hagen-Kibble mechanism [12–15] (or Higgs mechanism for short). The scalar fields in the theory are subject to a potential (which is heavily constrained by supersymmetry). About the minima of the potential, located at vacuum expectation values (vev) in field space, the full gauge symmetry is typically broken

to some subgroup resulting in a new massless effective theory and certain other fields, such as W-bosons, gaining mass. Due to the Lorentz invariance of the vacuum only scalar fields can acquire a non-trivial vev and hence one only needs to keep track of scalar fields when studying moduli spaces of vacua.

There may be more than one vev for the theory as is typical in supersymmetric quantum field theories. These could be a discrete number of isolated vevs, but another mathematically rich option is that there may be a continuum of vevs known as the moduli space of vacua.

In this thesis the models that will be studied have moduli spaces of vacua. Even though the vevs may be continuous it is quite possible for special points on the moduli space to result in different effective theories.

One central theme in this thesis is in identifying the moduli spaces of vacua for these supersymmetric theories through a collection of techniques.

2.5 $3d\,\mathcal{N}=4$ Quiver Gauge Theories

In three dimensions the minimal spinor is a Majorana spinor of dimension $2^{\frac{d-1}{2}}=2$. If there are $\mathcal{N}$ spinors that generate the supersymmetry algebra, there are $2\mathcal{N}$ such real supercharges with an R-symmetry which is Spin($\mathcal{N}$). A theory with 8 supercharges in three dimensions has $3d\,\mathcal{N}=4$ supersymmetry with R-symmetry Spin(4). The Lie algebra isomorphism allows the $\mathcal{R}$ symmetry in $3d\,\mathcal{N}=4$ to be thought of as $\mathrm{Spin}(4)\supset \mathrm{SU}(2)_{\mathcal{H}}\times \mathrm{SU}(2)_{\mathcal{C}}$ where the $\mathcal{H}$ and $\mathcal{C}$ refer to "Higgs" and "Coulomb" respectively.

The relevant supermultiplets to consider are the hypermultiplets and vector multiplets. The field content of these supermultiplets are:

- Hypermultiplet: $Q, \widetilde{Q}$ (in $[1]_{\mathcal{H}}$) + fermions
- Vector multiplet: $A^{(1)}$ + $\phi_{1,2,3}$ (in $[2]_{\mathcal{C}}$) + fermions

The two complex scalars $Q, \widetilde{Q}$ in the hypermultiplet is thought of as transforming in the doublet of $\mathrm{SU}(2)_{\mathcal{H}}$. Furthermore the hypermultiplet may be thought of as a direct sum of a chiral and anti-chiral $3d\,\mathcal{N}=2$ multiplet, also denoted Q and $\widetilde{Q}$.

The vector multiplet contains three non-compact scalars $\phi_{1,2,3}$ which transform in the $[2]_{\mathcal{C}}$ and also a gauge field $A^{(1)}$. The gauge field in three dimensions is dual to a compact scalar known as the dual photon, γ. Specifically, $d\gamma^{(0)} = *F^{(2)}$ where $F^{(2)}$ is the field strength for $A^{(1)}$. In terms of $3d\,\mathcal{N}=2$ supermultiplets, the $3d\,\mathcal{N}=4$ supermultiplet is a direct sum of a $3d\,\mathcal{N}=2$ vector multiplet and a chiral multiplet denoted Φ.

The fermionic content will not be too relevant in the remaining discussion.

2.5.1 Moduli Space of Vacua

Since the hypermultiplet and vector multiplet contain scalars the full moduli space of vacua for $3d\,\mathcal{N}=4$ theories can be quite rich since these scalars can independently acquire vevs.

By supersymmetry there is always a trivial vev since the ground state must have zero energy. For simplicity consider first switching off the vevs for scalars in the vector multiplet meaning that only hypermultiplet scalars can acquire non-trivial vevs. This gives a notion of a Higgs branch, $\mathcal{H}$, where only $\mathrm{SU}(2)_{\mathcal{H}}$ acts on it.

Likewise one can switch off the hypermultiplet vevs and allow for non-trivial vector multiplet vevs. This defines the Coulomb branch, $\mathcal{C}$, where only $\mathrm{SU}(2)_{\mathcal{C}}$ acts on it.

Finally, both hypermultiplet and vector multiplet vevs may be non-trivial at the same time. This defines the mixed branch of the theory.

The full moduli space of the theory consists of a union of all of these branches.

$$\mathcal{M} = \mathcal{H} \cup \mathcal{C} \cup_i \mathcal{M}_i \tag{2.1}$$

The physics of each of these branches is quite different due to the different physics of the

operators in the theory which parametrise each of these spaces.

The Higgs and Coulomb branches will be the main focus of this thesis whereas the mixed branch will not be discussed in detail here. Treatments of the mixed branch have appeared in the literature [47, 49].

2.5.2 Higgs Branch

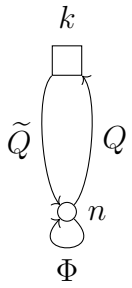
The Higgs branch is parametrised by vevs in the hypermultiplets with vector multiplet vevs switched off. As a first step it is useful to consider the classical physics of the Higgs branch.

The classical Higgs branch is computed by finding gauge invariant solutions to F-term and D-term equations which arise from a cubic superpotential. Geometrically, this is the hyper-Kähler quotient construction for the Higgs branch [25]. In particular, the F-term and D-term equations play the role of complex and real moment maps respectively. Each hypermultiplet contains four real scalars which may be thought of geometrically as $\mathbb{H} \simeq \mathbb{R}^4$. In a theory with gauge symmetry G and n_H hypermultiplets the classical Higgs branch is schematically

$$\mathcal{H}^{\text{classical}} = \mathbb{H}^{n_H} /\!/\!/ G \tag{2.2}$$

where the specific action of the hyper-Kähler quotient, denoted by the three forward slashes, is dependent on the theory in question.

The F-term equation is found from taking derivatives from the superpotential. Supersymmetry constrains the superpotential to be cubic and it is straightforward to read off the superpotential from the quiver. Consider the U(n) gauge theory with k flavours, but rewrite the $3d\,\mathcal{N}=4$ vector and hypermultiplets in terms of $3d\,\mathcal{N}=2$ supermultiplets.



(2.3)

The supermultiplet representations are summarised in Table 2.1. It may be useful to think of Q as an $n \times k$ matrix, $\widetilde{Q}$ as a $k \times n$ matrix and Φ as an $n \times n$ matrix.

Multiplet	U(n)	SU(k)
Q	$[1, 0 \cdots, 0](1)$	$[0, \cdots, 1]$
$\widetilde{Q}$	$[0 \cdots, 1](-1)$	$[1, 0, \cdots, 0]$
Φ	Adj	$[0, \cdots, 0]$

Table 2.1: Representations that the chiral multiplets of $\mathcal{Q}_{2.3}$ transform in.

The superpotential is read from the closed loops formed by the arrows in the quiver and the corresponding F-term is

$$\mathcal{W} = \mathrm{Tr}\left[\widetilde{Q} \cdot \Phi \cdot Q\right], \quad \frac{\partial \mathcal{W}}{\partial \Phi} = Q\widetilde{Q} = 0 \tag{2.4}$$

where the trace is taken over the SU(k) flavour indices.

One expression of the Higgs branch is as the set of matrices Q and $\widetilde{Q}$ subject to the n^2 F-term relations given by $Q\widetilde{Q} = 0$. This is not a physically elegant way to describe the Higgs branch since Q and $\widetilde{Q}$ are not gauge invariant. A more appropriate object is the gauge invariant "meson" defined as

$$M = \widetilde{Q}Q \tag{2.5}$$

which may be thought of as a $k \times k$ matrix.

The F-term relations affect the nilpotency of M since

$$M^2 = (\widetilde{Q}Q)(\widetilde{Q}Q) = \widetilde{Q}(Q\widetilde{Q})Q = 0 \tag{2.6}$$

The classical Higgs branch of U(n) SQCD with k flavours is then

$$\mathcal{H}\left(\mathcal{Q}_{2.3}\right) = \left\{M \in \mathrm{M}(k,\mathbb{C}) | M^2 = 0, \mathrm{Tr}M = 0, \mathrm{Rk}M \leq n\right\} \tag{2.7}$$

The treatment of classical Higgs branches for all such quiver theories follows similar steps to the ones taken above. This may become tedious to solve for more complicated quivers and so alternative methods such as Hilbert series for the Higgs branch become more tractable, which will be introduced shortly. The use of Hilbert series also helps with the complication that Higgs branches can be a union of moduli spaces and it may be possible to identify these constituent parts through inspection of a Hilbert series [112, 80].

The discussion so far has been about the classical Higgs branch for $3d\,\mathcal{N}=4$ quiver gauge theories. The quantum Higgs branch is believed to be exactly the same due to a non-renormalisation theorem [36]. This theorem does not hold if there is some mechanism by which additional massless states can arise in the theory, possibly at special points on the Coulomb/tensor branch. No such mechanism has been discovered for $3d\,\mathcal{N}=4$ theories so far, but examples for theories in dimensions $4, 5, 6$ with eight supercharges exist.

All of the Higgs branches that appear in this thesis are examples of *symplectic singularities*. A few more details about these spaces will be given in Chapter 3.

2.5.3 Higgs Branch Hilbert Series – Weyl Integration

The Hilbert series of a moduli space is a rational function which enumerates gauge invariant operators parametrising the moduli space and grades them according to their R-charge and the weights they transform in with respect to the global symmetry of the moduli space. The strategy

is to take all the basic quarks in the theory, symmetrise them in all allowed combinations (many of which will not be gauge invariant) and then to project out the gauge invariant combinations.

The plethystics program and Master space program [113–117] gives a systematic way to do this for the Higgs branch. The first ingredient is the Plethystic Exponential (PE) which is key in producing the symmetrisations of quarks. The PE of a function $f(t, x_i)$ is

$$\mathrm{PE}[f(t,x_i)] = \exp\left(\sum_{k=1}^{\infty} \frac{f(t^k, x_i^k) - f(0,0)}{k}\right). \tag{2.8}$$

The inverse of the plethystic exponential is the plethystic logarithm (PL). Although the PL will not be used in the construction of the Higgs branch Hilbert series, it is worth introducing it now given the opportunity. The PL is given by

$$\mathrm{PL}[f(t,x_i)] = \sum_{k=1}^{\infty} \frac{\mu(k)\log f(t^k, x_i^k)}{k}, \tag{2.9}$$

where $\mu(k)$ is the Möbius function [118] and is defined for positive integer k as

$$\mu(k) = \begin{cases} +1, & \text{If } k \text{ is square-free with an even number of prime factors} \\ -1, & \text{If } k \text{ is square-free with an odd number of prime factors} \\ 0, & \text{If } k \text{ has a squared prime factor.} \end{cases} \tag{2.10}$$

The computation of the Hilbert series proceeds with the Weyl integration formula

$$\mathrm{HS}_{\mathcal{H}}(t; x_1, \cdots, x_r) = \oint d\mu_G \mathrm{PE}\left[\chi_{\mathrm{matter}} t - \chi^G_{\mathrm{Adj}} t^2\right] \tag{2.11}$$

where G is the gauge group, $x_{1,\cdots,r}$ are fugacities for the flavour symmetry, t is a fugacity for $\mathrm{SU}(2)_{\mathcal{H}}$, χ_{matter} is the character of the pseudoreal matter representations (written in terms of the flavour symmetry and gauge symmetry fugacities) and χ^G_{Adj} is the character of the adjoint representation of the gauge group, written in terms of gauge group fugacities. The $d\mu_G$ denotes

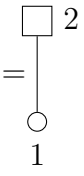
the Haar measure for the gauge group which is given by the following formula

$$d\mu_G = \prod_{i=1}^{\text{rank G}} \left(\frac{dy_i}{y_i}\right) \left(\prod_{\alpha\in\Delta^+} (1-y^\alpha)\right) \tag{2.12}$$

where y^α refers to a monomial, in terms of G character fugacities, associated to the positive root α of G[1].

The interpretation of the Weyl integration formula follows the hyper-Kähler quotient construction of [25]. The $\chi_{\text{matter}}t$ denotes the quarks, which transform with highest weight 1 under $\text{SU}(2)_{\mathcal{H}}$, and the $-\chi^G_{\text{Adj}}t^2$ denotes the particular F-term relation, which transforms under weight 2 under $\text{SU}(2)_{\mathcal{H}}$. The condition on having χ_{matter} being pseudoreal is a realisation of the hyper-Kähler quotient construction starting with $\mathbb{H}^{n_H}$ which has $\text{Sp}(n_H)$ symmetry and the specific action of the hyper-Kähler quotient by the gauge group being associated to its embedding inside $\text{Sp}(n_H)$. The commutant of the gauge group inside $\text{Sp}(n_H)$ is the flavour symmetry of the theory. Taking the PE of all of these quarks, symmetrises all of the possible hypermultiplet contributions which may or may not be gauge invariant. Taking the integral over the gauge group fugacities projects out only the gauge invariant part.

As an example consider the computation of the Higgs branch Hilbert series of the following quiver Q

$Q =$ 

. (2.13)

This quiver has a U(1) gauge node and flavour symmetry SU(2). There is matter which transforms in the bifundamental representation of the U(1) gauge symmetry and SU(2) flavour symmetry. This has character $\chi_{\text{matter}} = q(x+1/x)$ where q and x are fugacities for U(1) and SU(2). There is also a U(1) vector multiplet. The character of the "adjoint" of U(1) is trivial.

[1] In LieArt the positive roots are computed in the so-called `AlphaBasis`.

The Haar measure for the U(1) gauge group is $d\mu_{\mathrm{U}(1)} = dq/q$. Thus

$$\mathrm{HS}\left[\mathcal{H}(\mathcal{Q})\right] = \oint_{|q|=1} \frac{dq}{q} \mathrm{PE}\left[(qx + q/x + x/q + 1/qx)\, t - t^2\right] \tag{2.14}$$

$$= \frac{1 - t^4}{(1 - x^2t^2)(1 - t^2)(1 - t^2/x^2)}. \tag{2.15}$$

This describes the variety $\mathbb{C}^2/\mathbb{Z}_2$, which is consistent with the analysis using the superpotential

$$\mathcal{H}\left(\mathcal{Q}\right) = \left\{ \begin{pmatrix} a & b \\ c & -a \end{pmatrix}, a, b, c \in \mathbb{C} \middle| a^2 + bc = 0 \right\} \tag{2.16}$$

Note that the relation $a^2 + bc = 0$ is the defining relation of $\mathbb{C}^2/\mathbb{Z}_2$.

The Hilbert series methods for Higgs branches described above are simplest in gauge theories which enjoy "complete Higgsing". Theories with complete Higgsing are gauge theories where the gauge symmetry is completely broken at generic points on the Higgs branch, the Higgs branch dimension is computed as dim $\mathcal{H}$ = #hypers − #vectors. In contrast, a theory with incomplete Higgsing has the gauge group broken to only a non-trivial subgroup of the gauge symmetry. In this case the dimension of the Higgs branch is dim $\mathcal{H}$ > #hypers − #vectors.

If the theory enjoys incomplete Higgsing then the form of the Weyl integration is not applicable due to the incorrect incorporation of the F-term. One may be concerned that the Weyl integration formula could be incorrectly applied to theories with incomplete Higgsing. Fortunately, the Weyl integration formula also serves as a diagnostic for theories with incomplete Higgsing. If a theory has incomplete Higgsing then the dimension of the Higgs branch dim $\mathcal{H}$ > #hypers − #vectors. The result of the Weyl integration gives the dimension of the Higgs branch and if one finds that the inequality is satisfied then the theory has incomplete Higgsing and discard the Hilbert series computation.

General corrections to the Weyl integration for theories with incomplete Higgsing remains and open problem. The most reliable course of action is to solve the F-term equations directly.

All of the considerations above apply more generally when gauging a global symmetry subgroup

G of a moduli space $\mathcal{M}$ with global symmetry $G_{\mathcal{M}}$. Suppose that $G_{\mathcal{M}} \supset G \times G_F$ where G_F is the commutant of G inside $G_{\mathcal{M}}$. Then the Hilbert series of the hyper-Kähler quotient $\mathcal{M}///G$ is also given by the Weyl integration formula

$$\mathrm{HS}_{\mathcal{M}///G}(t; x_1, \cdots, x_r) = \oint d\mu_G \mathrm{HS}_{\mathcal{M}}(t; x_1, \cdots, x_r; \{y_i\}) \mathrm{PE}\left[-\chi^G_{\mathrm{Adj}} t^2\right] \tag{2.17}$$

where the $\{y_i\}$ are the fugacities for G. This Weyl integration formula is the primary check of the results in the latter Chapters of this thesis.

2.5.4 Coulomb Branch

The Coulomb branch is parametrised by the non-compact scalars in the vector multiplet $\phi_{i=1,2,3}$ which transform in the adjoint representation of the gauge group G with vevs in the hypermultiplets switched off.

A classical analysis of the Coulomb branch begins with the potential for the scalars in the vector multiplet takes the form of

$$V \sim \sum_{i<j} \mathrm{Tr}[\phi_i, \phi_j]^2 \tag{2.18}$$

where the trace is over the gauge group G.

Such a potential is zero only if the $\phi_{1,2,3}$ commute with each other. This means that the vevs take values in the Cartan subalgebra of G. By the adjoint Higgs mechanism, the gauge group G is broken maximally to the maximal torus $\mathrm{U}(1)^r$ where r is the rank of the gauge group. Since gauge fields in three dimensions are dual to compact scalars, the r vector multiplets that remain after the adjoint Higgs mechanism may also take a vev. Finally, the Coulomb branch is determined up to equivalent vevs. As the gauge group is broken to the maximal torus, the Weyl group $\mathcal{W}_G$ of the gauge group acts on it, leading to equivalences between vevs. The classical Coulomb branch is therefore

$$\mathcal{C}^{\mathrm{classical}} = \left(\mathbb{R}^3 \times S^1\right)^r / \mathcal{W}_G \tag{2.19}$$

Unlike the Higgs branch, the Coulomb branch receives quantum corrections [119, 120]. In the UV, where the QFT is weakly coupled, the Coulomb branch is the classical Coulomb branch. In the IR however, the QFT is strongly coupled and additional monopole operators appear in the low energy spectrum [121]. These are local disorder 't Hooft monopole operators [122] defined by the Dirac monopole singularity of gauge fields at the insertion point of the operator in the Euclidean path integral. An analysis of the IR Coulomb branch based on a Lagrangian becomes much more challenging.

The modern perspective of the Coulomb branch as a moduli space of dressed monopole operators [31, 123, 108] provides an alternative avenue for the study of the Coulomb branch. The study of the (IR) Coulomb branch becomes the counting of all dressed monopole operators.

For $3d$ $\mathcal{N}=4$ theories, the Coulomb branch is also a symplectic singularity. Developments in the mathematics literature prove that Coulomb branches cannot be a union of moduli spaces [27, 124, 125] unlike Higgs branches.

There is also a notion of complete and incomplete Higgsing for the Coulomb branch, although this is more subtle to define precisely since the gauge group can only be broken at most to the maximal torus. A characterisation of complete Higgsing is that the Coulomb branch is a moduli space with dimension equal to the rank of the gauge group and the converse for incomplete Higgsing.

2.5.5 Coulomb Branch Hilbert Series – The Monopole Formula

The monopole formula allows for the computation of the Hilbert series of a moduli space of 1/4-BPS monopoles such as the Coulomb branch of $3d$ $\mathcal{N}=4$ theories and is presented below, [108],

$$\mathrm{HS}_G(t,z)=\sum_{m\in\Gamma^*_{\hat{G}}/\mathcal{W}_{\hat{G}}} z^{J(m)}t^{2\Delta(m)}P_G(t^2,m). \tag{2.20}$$

The interpretation of the formula is to treat the Coulomb branch as a moduli space of monopole operators dressed by Casimir invariants of the unbroken gauge group in the presence of some

magnetic flux m. The monopole formula grades the monopole operators by the SU(2) R-charge $\Delta(m)$ and the $\mathrm{U}(1)^{\mathrm{rank}\,G}$ topological symmetry $\mathrm{U}(1)^r_J$. The dressing function $P_G(t^2,m)$ counts the gauge invariants of the unbroken symmetry. This sum is performed over all of the possible magnetic fluxes for the gauge groups. The Dirac quantisation condition means that the sum is performed over the weights in the Weyl chamber of the weight lattice of the Langlands dual gauge group $\Gamma^*_{\hat{G}}/\mathcal{W}_{\hat{G}}$.

The R-charge is given by the formula below [123, 126, 127],

$$\Delta(m) = -\sum_{\alpha\in\Delta^+}|\alpha(m)| + \frac{1}{2}\sum_{i=1}^{n}\sum_{\rho_i\in\mathcal{R}_i}|\rho_i(m)|. \tag{2.21}$$

where Δ^+ is the set of positive roots of the gauge symmetry and ρ_i are the weights of the matter-field representations $\mathcal{R}_i$.

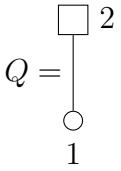
The topological symmetry in the UV, $\mathrm{U}(1)^r_J$, may get enhanced to a non-Abelian group of rank r due to the appearance of monopole operators in the IR. The topological fugacities, when this enhancement occurs, have the interpretation of the simple roots of the non-Abelian global symmetry algebra. One can use the Cartan matrix to map the simple roots into characters and hence find the Hilbert series in terms of characters.

The dressing factor is given as

$$P_G(t^2,m) = \prod_i \frac{1}{1-t^{2d_i(m)}} = \oint d\mu_H \mathrm{PE}\left[\chi^H_{\mathrm{adj}}t\right] \tag{2.22}$$

where the $d_i(m)$ are the degrees of the Casimir invariants of the gauge group $H\subset G$ which is left unbroken by the magnetic flux m.

As an example consider the computation of the Coulomb branch Hilbert series of the following quiver Q

$Q =$ 

. (2.23)

The Dirac quantisation condition for the magnetic charge for the U(1) gauge group constrains $-\infty \leq m \leq \infty$ for integer charge m. As U(1) is Abelian, it does not have any roots and therefore the only contribution to the R-charge is from the matter. This gives $\Delta(m) = |m|$. The dressing function is $P_{\mathrm{U}(1)}(t^2, m) = 1/(1-t^2)$.

$$\mathrm{HS}\left[\mathcal{C}(Q)\right] = \sum_{-\infty \leq m \leq \infty} z^m t^{2|m|} \frac{1}{1-t^2} \tag{2.24}$$

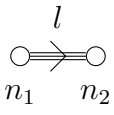
$$= \frac{1-t^4}{(1-t^2 z)(1-t^2)(1-t^2/z)}. \tag{2.25}$$

Upon the variable redefinition $z \to x^2$, this results in the same Hilbert series for $\mathbb{C}^2/\mathbb{Z}_2$.

The monopole formula will also be used to compute the moduli space of dressed monopole operators of magnetic quivers, introduced later, which describe Higgs branches of theories with eight supercharges.

2.5.6 Non-simply laced edges

The monopole formula can be applied to quivers which contain edges which do not have a natural field theory interpretation. A common example of this are non-simply laced edges, an example of such an edge connecting a $\mathrm{U}(n_1)$ and $\mathrm{U}(n_2)$ gauge node with multiplicity l is drawn below



(2.26)

The interpretation of such an edge is similar to those encountered in Dynkin diagrams where the simple roots of $\mathrm{U}(n_1)$ are longer by a factor of l compared to those of $\mathrm{U}(n_2)$. In the conformal dimension formula this factor of l is incorporated by taking the usual contribution of a hypermultiplet connecting the two gauge nodes and then multiplying every magnetic charge associated to $\mathrm{U}(n_1)$ by l.

As non-simply laced edges do not have field theory interpretations (yet) it is unclear how to analyse the Higgs branches of quivers containing these edges. Non-simply laced edges are still physical in that for some values of l there is a realisation from string theory constructions using orientifold planes or S-folds [128–131].

2.5.7 "Good", "Bad", and "Ugly" Theories

The monopole formula does not always converge if there are monopole operators with negative conformal dimension. There are three types of theory as identified in [123] which reflect the values of the conformal dimension of monopole operators and the corresponding effect on the moduli space.

These theories go by the names – "good", "bad" and "ugly".

- A "good" theory is one where all monopole operators have charges $\Delta \geq 1$. The Coulomb branch is a symplectic singularity.
- An "ugly" theory is one where some monopole operators have a charge $\Delta = 1/2$. There are free twisted hypermultiplets in the spectrum which contribute free spaces to the Coulomb branch. If there are also monopole operators with $\Delta \geq 1$ then the Coulomb branch is a product of a free space with a symplectic singularity.
- A "bad" theory is one where at least one monopole operator has a charge $\Delta \leq 0$. The Coulomb branch is smooth.

Throughout this thesis, we will try to forgo the names of "good", "ugly", and "bad" and refer to the first two types as "computable" (in the sense of the monopole formula) and the last as "incomputable".

It is also useful to identify when a theory has a computable or incomputable Coulomb branch or even what possible global symmetry enhancements will be, even before attempting an explicit computation. For unitary quiver gauge theories there is a simple rule of thumb to determine

this. Following the notation for Cartan matrices, an adjacency matrix A_{ij} is computed for the gauge nodes, with any labelling of the gauge nodes. With this labelling of the gauge nodes, the ranks of the gauge nodes are collected into a vector with components r_i as well as any flavours f_i. The excess of each node is determined as

$$e_i = \sum_j -A_{ij} r_j + f_i. \tag{2.27}$$

If the $e_i \geq 0 \ \forall i$ then the theory is likely to be computable and is called "balanced" when saturating the inequality. In this case there is likely to be an enhancement of the global symmetry by the group corresponding to the Dynkin diagram formed by the balanced nodes. A few more non-trivial Coulomb branch global symmetry enhancements were identified in [64]. If there is at least one $e_i = -1$ then the theory likely to be computable and there may be a free part to the Coulomb branch. If there is at least one $e_i < -1$ then the theory is incomputable.

This rule of thumb does not always correctly identify the computability of a theory. A more explicit test, such as by computing the R-charge and checking if negative charge monopole operators arise, will precisely determine this.

2.5.8 Alternative methods to computing Hilbert series

In certain cases, if the quiver is "star-shaped" there are methods which include gluing Hall-Littlewood functions and Slodowy slices which tend to be more efficient than using the monopole formula [132–134]. This is rather laborious machinery to introduce here considering that the results of the computation are of more interest in this thesis rather than the method of computation. A brief overview on these methods can be found in Appendix C.

2.5.9 Highest Weight Generating Function

The Hilbert series gives a description of the generators and relations that parametrise a moduli space. However, these can often be complicated expressions and involve symmetrisation of some

basic gauge invariant operators and their relations.

Instead of using characters of irreps of global symmetries in the Hilbert series, one may trade these for Dynkin labels. This is the notion of a Highest Weight Generating function (HWG). The *highest weight fugacities* μ_i are introduced with the correspondence to Dynkin labels as,

$$[n_1, \cdots, n_r] \leftrightarrow \mu_1^{n_1} \cdots \mu_r^{n_r} \tag{2.28}$$

which is also notation that will be adopted for labelling representations.

Thus for a given Hilbert series, the HWG for some compact group with rank r as [135],

$$\mathrm{HWG}(t; \mu_1 \cdots, \mu_r) = \sum_{k_1=0}^{\infty} \cdots \sum_{k_r=0}^{\infty} \int_G d\mu_G \chi([\mu_1^{k_1}, \cdots \mu_r^{k_r}]) \mathrm{HS}(t; x_1, \cdots x_r) \mu_1^{k_1} \cdots \mu_r^{k_r}. \tag{2.29}$$

The interpretation of this formula is quite simple. Characters of compact Lie groups are orthogonal due to the Peter-Weyl theorem. In the Hilbert series, the coefficients of t are precisely these characters of the global symmetry. The above formula projects the characters that appear in the Hilbert series and replaces it with the highest weight fugacities associated to the Dynkin labels of that representation.

An important distinction is that the HWG is not a Hilbert series. The generators and relations of the variety cannot be directly read from the HWG. The HWG must be converted into a Hilbert series in order to do that. The advantage of using the HWG for some analyses is that it is often simpler than the Hilbert series and many theories which fall into natural families (perhaps labelled by some parameters) can have a HWG which is also dependent on these parameters. It is much harder to find a universal expression for the Hilbert series for a family of theories in general.

2.5.10 $3d$ Mirror Symmetry

Some pairs of theories may exhibit $3d$ mirror symmetry [111]. This is an IR duality between two $3d$ $\mathcal{N}=4$ gauge theories which flow to the same IR fixed point but exchanges some properties of these theories. Their Higgs and Coulomb branches are exchanged which is non-trivial as the physics of Higgs branches is classical and to do with mesons and baryons whereas Coulomb branch is not classical and the physics is related to dressed monopole operators. This duality also exchanges the masses and FI parameters of these theories. One way of understanding this duality is through the exchange of the $\mathrm{SU}(2)_{\mathcal{H}} \leftrightarrow \mathrm{SU}(2)_{\mathcal{C}}$ factors.

In string theory, $3d$ mirror symmetry is realised as the action of S-duality on D3, D5, and NS5 Type IIB brane systems [31].

Historically, this duality was particularly useful in studying the Coulomb branches of $3d$ $\mathcal{N}=4$ theories since they receive quantum corrections and their dual Higgs branches do not. With the discovery of the monopole formula, Coulomb branches are just as simple to study as Higgs branches.

2.5.11 Framed and Unframed Quivers

In any "unframed" quiver gauge theory with unitary gauge groups, i.e. without any flavour node, there exists an overall centre-of-mass $\mathrm{U}(1)_{\mathrm{COM}}$ symmetry that is ungauged by the choice of framing i.e. specification of flavours. This centre-of-mass $\mathrm{U}(1)_{\mathrm{COM}}$ is the centre of the gauge group and hence one can consider which parts of the spectrum are invariant under its action. The electric spectrum is invariant under its action and so one does not need to fix $\mathrm{U}(1)_{\mathrm{COM}}$ to use the Weyl integration formula to find the Hilbert series of the Higgs branch (except one also has to remove a trivial factor of $\mathbb{H}$ for the singular part). The magnetic spectrum does depend on the action of $\mathrm{U}(1)_{\mathrm{COM}}$. In the monopole formula this is reflected in the choice of origin for the system of monopole charges, and such a choice is indeed necessary for the monopole formula to evaluate without divergence. In modern terminology, the $\mathrm{U}(1)_{\mathrm{COM}}$ symmetry is a magnetic zero-form symmetry and its gauging/ungauging is dual to the ungauging/gauging of

a dual U(1) electric one-form symmetry, this does not affect the electric spectrum but does affect the magnetic spectrum.

Returning to the monopole formula, as observed in [136], this choice of origin, providing it is made amongst monopole charges associated with long roots, does not affect the Coulomb branch calculation in a fundamental manner, since the impact on the refined Hilbert series can be compensated by a suitable choice of map between topological symmetry fugacities and global symmetry fugacities. This in turn makes it possible to treat framed unitary magnetic quivers within equivalence classes represented by an *unframed* quiver that only contains gauge nodes, as discussed in [137].

A framed unitary quiver can be converted to its *unframed* representative as follows.

1. Replace every flavour node of n by a flavour node of 1, increasing the multiplicity of direct links between it and other nodes by a factor of n to compensate.
2. Redraw the diagram to superimpose all the flavour nodes of 1.
3. Convert the flavour node of 1 to a U(1) gauge node.

The techniques discussed in the latter Chapters of this thesis are diagrammatic in terms of the quivers and so it is simpler to work with unframed quivers, rather than to pick a framing which can complicate the application of these techniques.

For quivers with orthogonal and symplectic gauge groups, so called "orthosymplectic" quivers, the centre symmetry is discrete, typically $\mathbb{Z}_2$. Therefore unframed orthosymplectic quivers are not equivalence classes of framed quivers. The action of the centre discrete symmetry, similarly does not affect the electric spectrum but does affect the magnetic spectrum. In the monopole formula this manifests itself as receiving contributions from multiple lattices [138]. In the examples considered here the centre symmetry is $\mathbb{Z}_2$ and all Coulomb branch Hilbert series computed for unframed orthosymplectic quivers receive contributions from an integer lattice and a half-integer lattice. Framed orthosymplectic quivers have this discrete symmetry fixed and only receive contributions from the integer lattice in the monopole formula.

2.6 $6d\ \mathcal{N} = (1,0)$ Theories

Let us review some field theory constructions of $6d\ \mathcal{N} = (1,0)$ theories. In six dimensions the minimal spinor is a symplectic Majorana-Weyl spinor which can be left-handed or right-handed. Each symplectic Majorana-Weyl spinor carries $2^{\frac{d}{2}-1} = 4$ real supercharges. Since the spinor representation in six dimensions is complex, the supercharges transform in the fundamental representation of $\mathrm{Sp}(\mathcal{N}_L) \times \mathrm{Sp}(\mathcal{N}_R)$ where the first factor rotates left-handed spinors and the second rotates the right-handed spinors. A theory with 8 supercharges in six dimensions has $6d\ \mathcal{N} = (1,0)$ supersymmetry where the left-handed spinor is chosen, the R-symmetry is $\mathrm{Sp}(1)$.

As mentioned there are three massless supermultiplets that will be used; the hypermultiplet, vector multiplet, and tensor multiplet. In terms of the massless little group, $\mathrm{Spin}(4)$ which will be treated as $\mathrm{SO}(4)$, and the $\mathrm{Sp}(1)_R$ R-symmetry the fields transform in the following representations written in terms of Dynkin labels

- Hypermultiplet: $\underbrace{[0,0]_{\mathrm{SO}(4)}[1]_{\mathrm{Sp}(1)}}_{\text{Scalars}} + \underbrace{[1,0]_{\mathrm{SO}(4)}[1]_{\mathrm{Sp}(1)}}_{\text{Fermions}}$
- Vector multiplet: $\underbrace{[1,1]_{\mathrm{SO}(4)}[0]_{\mathrm{Sp}(1)}}_{\text{Gauge field}} + \underbrace{[0,1]_{\mathrm{SO}(4)}[1]_{\mathrm{Sp}(1)}}_{\text{Fermions}}$
- Tensor multiplet: $\underbrace{[2,0]_{\mathrm{SO}(4)}[0]_{\mathrm{Sp}(1)}}_{\text{a.s.d. 2-form}} + \underbrace{[1,0]_{\mathrm{SO}(4)}[1]_{\mathrm{Sp}(1)}}_{\text{Fermions}} + \underbrace{[0,0]_{\mathrm{SO}(4)}[0]_{\mathrm{Sp}(1)}}_{\text{Scalar}}$

There are scalar fields in the hypermultiplet and tensor multiplet but not in the vector multiplet. This means there is a notion of a Higgs branch and tensor branch but not a Coulomb branch.

Note also that the anti-self-dual 2-form, $B^{(2)}$ that appears in the tensor multiplet causes some complication with writing down Lagrangians due to the vanishing kinetic term. Although there are treatments for writing Lagrangians for anti-self-dual forms in QFT [139–143], by working with quivers one avoids this subtlety.

Furthermore one naïvely would expect six dimensional theories to be non-renormalisable. However in many cases there is an SCFT UV completion and possibly a string theory construction which makes these theories sensible in the IR. If there is a string theory construction of a six

dimensional theory then one may also describe theories which are not conformal such as little string theories [144–146].

Gauge and gravitational anomalies heavily restrict the gauge theories one can have. A partial list of the allowed gauge theories is in [147–152].

2.6.1 Tensor Branch

The tensor branch is the moduli space of vacua associated to scalars in the tensor multiplet. Due to supersymmetry the scalars in the tensor multiplet are not subject to any potential and can take the value of any real number.

The anti-self-dual 2-form $B^{(2)}$ in the tensor multiplet implies the existence of additional codimension four objects in the spectrum. This is seen through the equations of motion and Bianchi identity in the presence of sources

$$d *_6 H^{(3)} = \delta^{(4)} \tag{2.30}$$

$$dH^{(3)} = \delta^{(4)} \tag{2.31}$$

In six dimensions these codimension four objects are dyonic strings. The dyonic strings in six dimensions function similarly to dyonic particles in four dimensions. In particular, there is an analogue to the BPS bound for dyonic strings where the tension of the string T is proportional to the vev of the tensor multiplet. An additional consequence of supersymmetry is that the interaction term between the vector multiplet and tensor multiplet fixes the gauge coupling $1/g^2$ to be proportional to the vev of the tensor multiplet scalar.

$$T \sim \langle \phi \rangle \sim \frac{1}{g^2} \tag{2.32}$$

These equivalences make six dimensional physics unique in that there are no free (continuous) parameters. All of the different phases of the theory can be reached by suitable choice of vev.

2.6.2 Higgs Branch

The Higgs branch of six dimensional theories is a symplectic singularity but is not classically exact. The dyonic strings present in six dimensions complicate the analysis when they become tensionless when a tensor multiplet scalar has trivial vev. This includes a new set of massless states in the spectrum which changes the Higgs branch. Setting a vev to zero is also equivalent to setting a gauge coupling to infinity, this means that the usual perturbative QFT techniques fail.

As mentioned, different phases of six dimensional theories may be accessed by suitable choices of vev. In terms of the Higgs branch geometry, the most important delineation is in whether a tensor multiplet scalar has zero or non-zero vev. If all of these vevs are non-zero then the Higgs branch is a classical moduli space of baryons and mesons. If tensor multiplet vevs are then set to zero in turn then the Higgs branch changes in some way as each vev is set to zero.

The way the Higgs branch changes depends on the particular theory in question, however there are "rules of thumb" which indicate what effect takes place based on an F-theory [153] construction of the gauge theory. The four possible effects discovered so far are [45, 154, 46, 155, 156, 72, 1, 92]

(-1). Small E_8 instanton transition

(-2). Discrete group gauging

(-3). Continuous group gauging

(-4). Klein D_4 transition

where the labelling refers to the F-theory notation for the self-intersecting curve supporting the gauge group which goes to infinite coupling.

The main tool to fully understand the quantum Higgs branch of a six dimensional theory is the *magnetic quiver*. These are mainly derived through brane constructions and so will be elaborated upon in Section 2.8.

2.7 Type IIB Brane Constructions for $3d\,\mathcal{N}=4$ Theories

String theory constructions allow for an additional perspective into the physics of gauge theories. Throughout this thesis, a low energy limit will be taken so that the effects of gravity can be neglected which is suitable for the study of gauge theories. Furthermore, the rich web of dualities in string theory may be utilised to explain various phenomena in gauge theory from a "top-down" perspective.

The most relevant construction for this work is the Hanany-Witten [31] brane system. This was originally formulated in Type IIB string theory and gave a construction of $3d\,\mathcal{N}=4$ gauge theories using NS5, D5, and D3 branes. Simple generalisations of this framework yielded similar brane systems for gauge theories in four, five, and six dimensions. It is worth seeing in detail how this construction works with a short review.

The occupation of the NS5, D5, and D3 branes in $\mathbb{R}^{10}$ is summarised in Table 2.2. All three branes share the $x^{0,1,2}$ directions, which is where the $3d\ \mathcal{N}=4$ SQFT lives. There are also directions which are occupied only by some of the branes, the $x^{3,4,5}$ directions occupied by the NS5 brane specifies an $\mathbb{R}^3$ with SO(3) symmetry which represents the $\mathrm{SU}(2)_{\mathcal{C}}$ R-symmetry, similarly the $x^{7,8,9}$ directions specifies another $\mathbb{R}^3$ with SO(3) symmetry which represents the $\mathrm{SU}(2)_{\mathcal{H}}$ R-symmetry.

	x^0	x^1	x^2	x^3	x^4	x^5	x^6	x^7	x^8	x^9
NS5	✓	✓	✓	✓	✓	✓				
D5	✓	✓	✓					✓	✓	✓
D3	✓	✓	✓				✓			

Table 2.2: Occupation of NS5, D5, and D3 branes in spacetime for Hanany-Witten setup.

The gauge theory that lives on an infinite D3 worldvolume is the $4d\,\mathcal{N}=4$, U(1) super-Yang-Mills theory. The $4d\ \mathcal{N}=4$ vectormultiplet can be dimensionally reduced to a $3d\ \mathcal{N}=8$ vectormultiplet which decomposes into a $3d\,\mathcal{N}=4$ vectormultiplet and a hypermultiplet.

In the Hanany-Witten brane setup the D3 branes end on NS5 branes or D5 branes and so this amounts to putting either Dirichlet or Neumann boundary conditions on the $3d\,\mathcal{N}=4$ vector

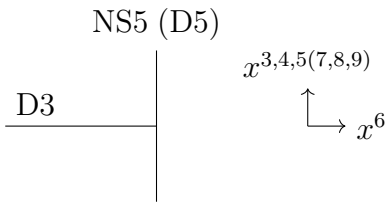


Figure 2.2: D3 brane ending on either an NS5 or D5.

multiplet or hypermultiplet.

As a D3 brane ends on an NS5 (D5) brane, shown in Figure 2.2, there are three moduli corresponding to the $x^{3,4,5}(x^{7,8,9})$ directions the D3 brane can occupy in the five brane world volume. These are the scalar fields in the $3d$ $\mathcal{N}=4$ vector multiplet (hypermultiplet). The moduli coming from the gauge field depends on whether the field strength has Dirichlet or Neumann boundary conditions. In terms of the brane set up in Figure 2.2, Dirichlet boundary conditions require that $F_{\mu\nu}=0$ on the boundary of the D3 brane and Neumann boundary conditions require that $F_{\mu 6}=0$. The gauge field in $4d$ dimensionally reduces to a gauge field a_μ in $3d$, which is taken to be independent of x^6, with field strength $F_{\mu\nu}$, and to a compact scalar b which is defined such that $\partial_\mu b = F_{\mu 6}$.

When the D3 ends on an NS5, Neumann boundary conditions are placed on the field strength, killing b and leaving a_μ. Combined with the three moduli corresponding to the position of the D3 brane in the $x^{3,4,5}$ direction one finds a $3d$ $\mathcal{N}=4$ vector multiplet living on the D3 brane.

If instead, the D3 ends on a D5 brane, Dirichlet boundary conditions are placed on the field strength, projecting out a_μ and leaving b. Combined with the three moduli corresponding to the position of the D3 brane in the $x^{7,8,9}$ direction one finds a $3d$ $\mathcal{N}=4$ linear multiplet living on the D3 brane.

Now consider ending the D3 brane from two sides with five branes. In this case there are three possible options: NS5 branes at either end, D5 branes at either end, or one of each type. For the purposes of this work, only the zero modes of the low energy spectrum of the theory living on the D3 worldvolume are taken. In this sense, the brane system does not provide a precise description of the details of the gauge theory living on the D3 brane worldvolume. Instead the combinatorial data in the brane system is used to provide a description of the low energy

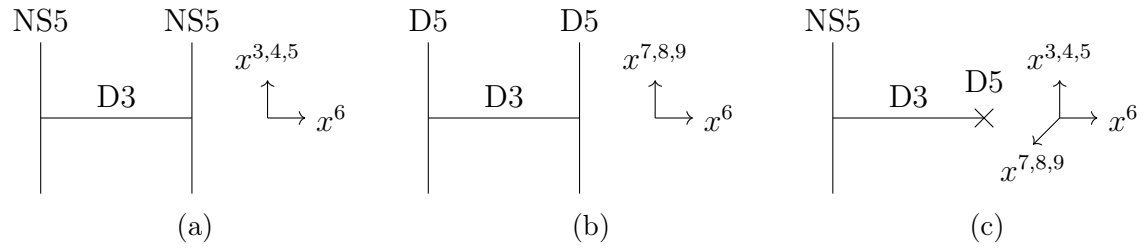


Figure 2.3: D3 brane ending between five branes.

physics of the gauge theory on the D3 brane.

When the D3 brane ends between two NS5 branes, as in Figure 2.3a, the supermultiplet living on the D3 brane is an electric U(1) $3d$ $\mathcal{N} = 4$ vector multiplet. However, when the D3 brane ends between two D5 branes, as in Figure 2.3b, with the understanding that one takes only the zero modes, the supermultiplet living on the D3 worldvolume is an electric $3d$ $\mathcal{N} = 4$ hypermultiplet. Finally, when the D3 brane ends between an NS5 and a D5 on either side, as in Figure 2.3c, there is no supermultiplet living on the D3 as there are no position moduli and all components of the field strength are projected out.

If there are stacks of n D3 branes between five branes then the supermultiplet living on the D3 worldvolume is an electric U(n) $3d$ $\mathcal{N} = 4$ vector multiplet if between two NS5, n electric hypermultiplets if between two D5, and no supermultiplet if between one of each five brane.

To generalise the discussion so far, a pair of simple Hanany-Witten brane systems are shown in Figure 2.4 with the corresponding electric $3d$ $\mathcal{N} = 4$ gauge theory that lives on the D3 worldvolume. The massless spectra should be thought of as arising from fundamental strings which stretch between the D3 branes giving rise to bifundamental matter.

The discussion so far considers the so called "electric spectrum" as it deals with fundamental strings ending between the D3 branes. The end of the fundamental string is an electric source for the 1-form gauge field living on the D3 worldvolume. However, one may also consider the "magnetic spectrum" which comes from D1 ending between the D3 branes. In this case the end of the D1 is a magnetic source for the 1-form gauge field on the D3 brane worldvolume. In fact the end of the D1 in the D3 world volume is interpreted as a 't Hooft Polyakov monopole. Generally, a Dp brane ending on a D(p+2) brane is interpreted as a 't Hooft Polyakov monopole.

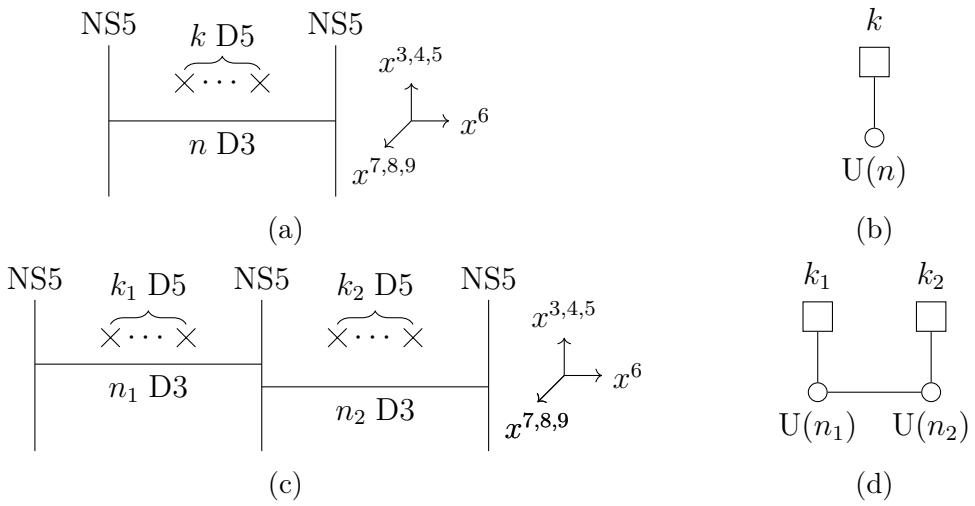


Figure 2.4: Simple Type IIB Hanany-Witten brane setup and the corresponding electric quiver theory that lives on the D3 worldvolume

There is then an associated magnetic supermultiplet that lives on the D3 brane worldvolume. When the D3 brane ends between two NS5 branes one may also view the supermultiplet living on the D3 brane as a magnetic (twisted) hypermultiplet. Similarly when the D3 brane ends between two D5 branes one may view the supermultiplet as a magnetic U(n) (twisted) vectormultiplet.

All of the discussion so far then follows exactly the same logic except with the exchange of the labels NS5 $\leftrightarrow$ D5 and electric $\leftrightarrow$ magnetic.

2.7.1 Brane Creation and Annihilation

Although this Section discusses Type IIB brane systems, it will be constructive to consider a generic D($p+2$) brane in either Type IIA or Type IIB in the remainder for $p \geq 3$.

A non-trivial effect occurs when an NS5 crosses a D($p+2$) in the Hanany-Witten brane set up since the worldvolumes of the branes link each other. As the branes cross there is creation/annihilation of Dp branes as shown in Figure 2.5. A thorough technical argument for the effect is given in [31].

A consequence of the analysis of [31] is a simple formula for the linking number of the NS5

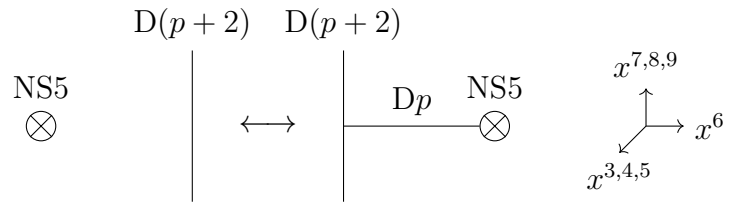


Figure 2.5: Depiction of the brane creation/annihilation effect.

brane and D$(p+2)$. Usually, the linking number is defined as a flux integral

$$L_{\text{NS}} = \int_{\mathbb{R}^3} \frac{H^{(3)}}{2\pi} \tag{2.33}$$

$$L_{\text{D}(p+2)} = -\int_{\mathbb{R}^{6-p}} \frac{G^{(6-p)}}{2\pi} \tag{2.34}$$

where $H^{(3)}$ is the field strength for the NSNS 2-form and $G^{(6-p)}$ is the field strength for the RR $C^{(5-p)}$ which is magnetically sourced by the D$(p+2)$. The integrals reduce to the following simple formulae

$$L_{\text{NS}} = \frac{1}{2}\left(r_{\text{D}(p+2)} - l_{\text{D}(p+2)}\right) + \left(l_{\text{D}p} - r_{\text{D}p}\right) \tag{2.35}$$

$$L_{\text{D}(p+2)} = \frac{1}{2}\left(r_{\text{NS5}} - l_{\text{NS5}}\right) + \left(l_{\text{D}p} - r_{\text{D}p}\right) \tag{2.36}$$

where r, l refer to the number of branes, of the type in the subscript, that end on the right or left (in the x^6) direction. The choice of sign for branes ending on the left or right is somewhat arbitrary so long as there is a relative sign between them. Importantly, the brane transitions do not change the total linking number of a brane system.

To a given brane system there is an electric phase, where all Dp branes are suspended between NS5 branes, and a magnetic phase where all Dp branes are suspended between D$(p+2)$ branes. From each phase, one can read an electric quiver or magnetic quiver respectively. It is through the brane creation/annihilation effect that one can take a brane system from the electric phase to the magnetic or vice versa.

The relationship between electric and magnetic quivers, in generic dimensions, is that the Higgs branch of the electric quiver happens to be equal to the moduli space of monopole operators of the magnetic quiver. For 3d $\mathcal{N} = 4$ theories the statement is stronger and the electric and

magnetic quivers are $3d$ mirror [111]. Two theories, A and B, which are $3d$ mirror enjoy the property that

$$\mathcal{H}(A) = \mathcal{C}(B) \tag{2.37}$$

$$\mathcal{C}(A) = \mathcal{H}(B) \tag{2.38}$$

The string theory explanation is due to S-duality in Type IIB swapping D5 and NS5 [31].

2.7.2 Orientifold Planes

Orientifold planes are objects in string theory which incorporate the action of a discrete space-time symmetry and parity on the worldsheet of fundamental strings. There are four such orientifold planes; Op^-, Op^+, $\widetilde{\text{O}p^-}$, and $\widetilde{\text{O}p^+}$. These four types arise, for $p \leq 5$, due to the possible $\mathbb{Z}_2 \times \mathbb{Z}_2$ charges, defined by a (twisted) cohomology, arising from the NS 2-form and the RR $(5-p)$-form, where in Type IIB $p = 3, 5$. The trivial and non-trivial $\mathbb{Z}_2$ arising from the NS 2-form is denoted by $\pm$ respectively and the trivial and non-trivial $\mathbb{Z}_2$ arising from the RR sector is denoted by the lack of a tilde or with tilde. Orientifold planes can still be defined for $p \geq 6$ through the action on Chan-Paton factors and come in the same four types.

When Dp branes are placed in parallel to an Op plane, the electric and magnetic gauge groups on the Dp worldvolume change due to the way that fundamental strings or D$(p-2)$ branes end between the Dp branes and their mirror images. The electric and magnetic gauge groups as well as the charge of the orientifold planes (in units of D-brane charge), and notation used throughout this thesis is summarised in Table 2.3 [129]. A further bit of notation is that any Dp brane numbers will denote the number of full branes on the orientifold.

Orientifold	Charge	Electric	Magnetic	Notation
Op^-	-2^{p-5}	D	D	
Op^+	$+2^{p-5}$	C	B	.....
$\widetilde{\text{O}p^-}$	$\frac{1}{2} - 2^{p-5}$	B	C	_____
$\widetilde{\text{O}p^+}$	$+2^{p-5}$	C	C	- - - - -

Table 2.3: Gauge algebra for electric and magnetic BPS states with orientifold planes.

It shall be important to understand what the electric vector multiplets are in the presence of each type of O(p+2) plane [130]. The electric vector multiplet when $2n$ Dp branes pass through an O$(p+2)^-$ plane has gauge group Sp(n). Similarly, the electric vector multiplet when $2n$ Dp branes end on an O$(p+2)^+$ plane, has gauge group SO($2n$). In the presence of an $\widetilde{\text{O}(p+2)^+}$, the electric vector multiplet for a stack of $2n+1$ Dp has SO($2n+1$) gauge symmetry. The last case is when $2n$ Dp branes pass through an $\widetilde{\text{O}(p+2)^-}$, in which case the resulting gauge group is Sp(n) with a half-hypermultiplet.

Another kind of orientifold that will be used in this thesis is the ON which incorporates an orbifold by $(-1)^{F_L}$ [157, 128, 158–160]. The ON plane also comes with four possible $\mathbb{Z}_2 \times \mathbb{Z}_2$ charges and is S-dual to the O5 plane with the same charge. The ON plane is still a valid object in Type IIA and is thought of as the T-dual to the ON in Type IIB. There is an electric gauge algebra on the NS5 brane worldvolume when D1 can end following the same assignment as in Table 2.3. The electric quiver has gauge nodes arranged in the Dynkin diagram of the electric gauge algebra on the NS5 brane.

The effect of the O($p+2$) and ON swaps when considering the magnetic quiver. Magnetic vector multiplets get the Dynkin type ending in the presence of O($p+2$) and have classical group algebra in the presence of ON.

Finally, due to the combination of actions of the orientifolds as a Klein four-group, if any two of the Op, O($p+2$), or ON are present in a brane system, then the action of the third is automatically generated [131].

The brane creation/annihilation effect is also modified in the presence of orientifold planes. Firstly recall that orientifold Op planes change their type as they pass through a (half) D(p+2) brane or (half) NS5 brane, flipping the charge of the RR $\mathbb{Z}_2$ charge and NS $\mathbb{Z}_2$ charge respectively [161, 131, 160]. This effect is responsible for the alternating sequence of orthogonal and symplectic gauge groups in orthosymplectic quivers. Secondly, any brane creation or annihilation effects must preserve the linking number, which now get additional contributions from the charge of the orientifold planes.

$$L_{\mathrm{NS}} = \frac{1}{2}\left(r_{\mathrm{D}(p+2)} - l_{\mathrm{D}(p+2)}\right) + \left(l_{\mathrm{D}p} - r_{\mathrm{D}p}\right) + \left(q^L_{\mathrm{O}p} - q^R_{\mathrm{O}p}\right) \tag{2.39}$$

$$L_{\mathrm{D}(p+2)} = \frac{1}{2}\left(r_{\mathrm{NS5}} - l_{\mathrm{NS5}}\right) + \left(l_{\mathrm{D}p} - r_{\mathrm{D}p}\right) + \left(q^L_{\mathrm{O}p} - q^R_{\mathrm{O}p}\right) \tag{2.40}$$

Thus for each of the four orientifold planes the transitions are summarised in Figure 2.6.

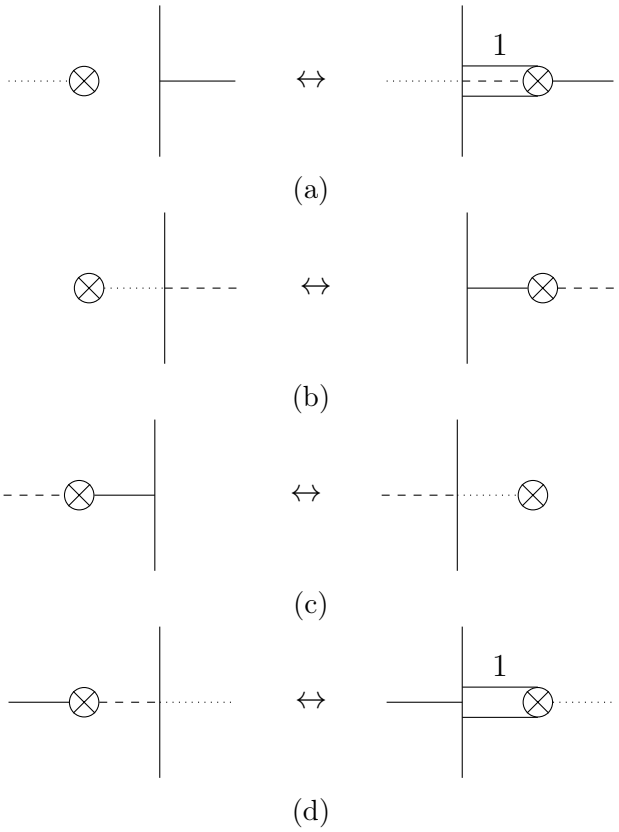


Figure 2.6: Summary of brane creation effect in the presence of Op planes. The circle with a cross indicates an NS5 brane and vertical lines indicate a D$(p+2)$ brane.

2.8 Type IIA Brane Construction for $6d\ \mathcal{N} = (1,0)$ Theories

Type IIA brane systems with NS5, D8, and D6 branes, possibly with orientifold planes, give rise to $6d\ \mathcal{N} = (1,0)$ gauge theories on the D6 worldvolume.

The spacetime occupation is summarised in Table 2.4. These brane systems may be thought of as arising from the Type IIB brane systems for $3d\ \mathcal{N} = 4$ gauge theories and applying T-duality

in each of the $x^{3,4,5}$ directions.

	x^0	x^1	x^2	x^3	x^4	x^5	x^6	x^7	x^8	x^9
NS5/ON	✓	✓	✓	✓	✓	✓				
D8/O8	✓	✓	✓	✓	✓	✓		✓	✓	✓
D6/O6	✓	✓	✓	✓	✓	✓	✓			

Table 2.4: Occupation of NS5, D8, and D6 branes in spacetime for Hanany-Witten setup.

All three branes share the $x^{0,1,2,3,4,5}$ directions which is where the $6d$ $\mathcal{N} = (1,0)$ SQFT lives. There is no longer any direction which is occupied solely by the NS5 brane, this is indicative of the inexistence of a Coulomb branch in six dimensions. However, the $x^{7,8,9}$ directions are occupied solely by D8 branes which defines, as before, an $\mathbb{R}^3$ with SO(3) symmetry which represents the $\mathrm{SU}(2)_{\mathcal{H}} \simeq \mathrm{Sp}(1)_{\mathcal{H}}$ R-symmetry.

There are some additional considerations to take when studying these brane systems. Firstly, in the presence of D8 branes the usual Type IIA string theory gets modified to the massive Type IIA string theory. The name comes from the fact that there is now a Romans' mass term for the NSNS 2-form [162]. In the corresponding supergravity this mass is related to a cosmological constant which is in turn related to the D8 brane charge. For the purposes of this thesis, it is important to note that since the D8 brane is codimension one in spacetime it acts as a domain-wall and the cosmological constant m jumps by one as it crosses a (full) D8 brane [34, 32].

Secondly, the electric phase of these Type IIA brane systems would require D6 branes to end between NS5 branes. Naïvely this is problematic as the NS5 brane will not be able to absorb the RR flux since the end of the D6 brane occupies the same dimensions as the NS5 brane worldvolume. The solution lies in the fact that the Romans' mass term can compensate the RR charge violation. The only constraint is that the net number of D6 branes ending to the left and right of the NS5 brane is equal to m for the particular D8 interval that the NS5 is located in. As a corollary, usually in the presence of O6 planes NS5 branes are stuck on the orientifold. However, in a D8 interval with $m = 0$ it will be possible to recombine half NS5 on the orientifold and lift them off so that nothing ends on them. This result is crucial when

transitioning from the electric phase to the magnetic phase of the brane system.

Thirdly, a point about the interpretation of brane systems. The Higgs branch of six dimensional theories receive non-trivial corrections whenever tensionless strings appear in the spectrum. The tension of these dyonic strings is proportional to the vev of the scalar in the tensor multiplet. In the Type IIA brane system this vev is represented by the separation of NS5 branes (and potentially also their images in an O8). This is sensible since a $6d$ $\mathcal{N} = (2, 0)$ tensor multiplet lives on the NS5 worldvolume. Hence, the appearance of tensionless strings can be represented combinatorially by making NS5 branes coincident. The physics of strongly interacting NS5 branes is challenging to describe but the brane system is not supposed to capture this physics. The brane system only describes the zero modes in the worldvolume theory of the D6 branes. It is crucial to reiterate that the brane system only provides combinatorial data and that it should not be taken too literally.

Another peculiar feature of some of these Type IIA brane systems is in the use of negatively charged D6 branes. Despite their presence in a string background being associated to supersymmetry breaking [163–165] many consistent results in $6d$ $\mathcal{N} = (1, 0)$ gauge theories can be computed with their presence [166, 167, 72]. In particular their magnetic quivers, with a set of brane constructions in [72, 91]. The usual rules of Hanany-Witten brane systems apply as before regardless of the charge of the D6 branes. This is another case where one uses combinatorial data of a brane system without trying to make sense of it too literally.

2.8.1 Magnetic Quivers

Now it is time to introduce one of the central physical constructions used in this thesis, the magnetic quiver.

In these Type IIA brane systems for $6d$ $\mathcal{N} = (1, 0)$ theories there is the electric phase, where one thinks of fundamental strings ending between D6 and NS5, and the magnetic phase, where one thinks of D4 ending between D6 and NS5 branes. Again, the D4 branes should be thought of as 't Hooft Polyakov monopoles in the D6 worldvolume theory. From each phase of the

brane system, which are reached by brane creation and annihilation moves, one may read off the electric quiver and a magnetic quiver. In Type IIB Hanany-Witten brane systems, the electric and magnetic quivers are $3d$ mirror, the analogue of this in higher dimensions is that the Higgs branch of the electric quiver is equal to the moduli space of monopoles defined by the magnetic quiver. This can be verified explicitly with Hilbert series computations by comparing the classical Higgs branch of the $6d$ $\mathcal{N}=(1,0)$ theory with the moduli space of monopoles of the magnetic quiver computed through the monopole formula. In this sense, the magnetic quiver is an "auxiliary $3d$" theory characterising Higgs branches of higher dimensional theories with eight supercharges as equivalent to the "Coulomb branch" of the magnetic quiver.

$$\mathcal{H}\left(\mathcal{Q}^{d=4,5,6}\right)=\mathcal{C}\left(\mathcal{Q}_M^{3d}\right) \tag{2.41}$$

Crucially however, magnetic quivers are intimately tied to the physics of the higher dimensional theory usually through brane systems and also give descriptions of non-perturbative effects for which Lagrangian-based Higgs branch constructions are not known.

The magnetic phase of the Type IIA brane systems for $6d$ $\mathcal{N}=(1,0)$ theories are reached when D6 end between D8 and not NS5. Therefore to reach the magnetic phase, brane moves are performed to get the NS5 into a D8 brane interval with zero cosmological constant. From there, one can move NS5 in the $x^{7,8,9}$ directions away from the D6 or O6 planes. The rules for reading magnetic quivers from Type IIA brane systems for $6d$ $\mathcal{N}=(1,0)$ theories, first established in [46, 155], are almost identical to those established in the previous sections for Type IIB brane systems. The only difference is that the fundamental magnetic object, the D4, ending between a D6 and NS5 gives rise to a magnetic vector multiplet and an adjoint hypermultiplet instead of a flavour. This is because the D6 (on an interval) and NS5 occupy the same number of (non-compact) spacetime dimensions. Another rule involves when multiple NS5 branes coincide in the brane system, this corresponds to tuning a gauge coupling in the $6d$ theory to infinity where the Higgs branch may receive a correction. In general a stack of NS5

branes corresponds to the following in the magnetic quiver,



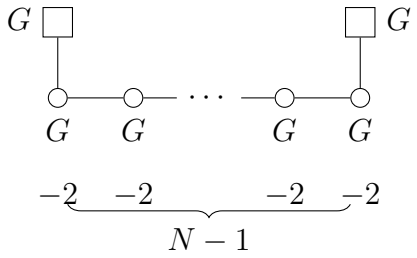
(2.42)

and this is similar in the presence of O6 planes when the gauge group in the magnetic quiver is no longer unitary. For example n (half) NS5 branes above an O6$^-$ gives an Sp(n) gauge group with $[0, 1, 0, \cdots, 0]_{\mathrm{Sp}(n)}$ in the magnetic quiver. When $n = 1$, the loop on the U(1) contributes a trivial free hypermultiplet, or in the presence of orientifold planes, the antisymmetric representation Sp(1) is trivial so in either case the loop can be suppressed in the magnetic quiver.

$6d\ \mathcal{N} = (1, 0)$ Conformal Matter

These rules are illustrated with a simple set of examples considered in [46, 155]. However, this is also an opportunity to consider a general setup which plays an important role in Chapter 6 and Chapter 7. The general setup is an M-theory background on $\mathbb{R}^7 \times \mathbb{C}^2/\Gamma_{ADE}$ where Γ_{ADE} is a discrete subgroup of SU(2). The corresponding gauge theory is the $7d$ $\mathcal{N} = 1$ super-Yang-Mills with gauge group $G = ADE$. If one adds N M5 branes to the setup breaking half of supersymmetry, the background is now $\mathbb{R}^6 \times \mathbb{R} \times \mathbb{C}^2/\Gamma_{ADE}$, with the $\mathbb{R}^6$ corresponding to the M5 worldvolume and $\mathbb{R}$ being a direction that M5 are separated along. The M5 act as domain-walls in the $7d$ theory giving multiple gauge groups connected by some generalised notion of bifundamental matter. Taking zero modes along the M5 separation direction results in the following $6d$ $\mathcal{N} = (1, 0)$ gauge theory referred to as rank N (G, G) conformal matter [168], which enjoys $N - 1$ gauge groups each with their own gauge coupling which can be set to infinity giving many different phases of the Higgs branch. The labels of -2 refer to the

self-intersection number of the $\mathbb{CP}^1$ in the base of the dual F-theory construction.

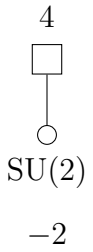


(2.43)

The case of $N = 1$, termed minimal conformal matter, is particularly special since the corresponding $6d$ theory plays the role of "bifundamental matter". One would expect that the Higgs branch of such a theory is a moduli space of free hypermultiplets, however this is generically not the case and the Higgs branch is a non-trivial symplectic singularity.

(A, A) Conformal Matter

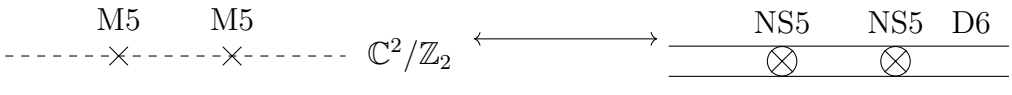
The first simple example of reading magnetic quivers starts by taking $G = \mathrm{SU}(2)$ and $N = 2$. The above $6d$ $\mathcal{N} = (1,0)$ theory becomes SU(2) gauge theory with four flavours, which is written as



(2.44)

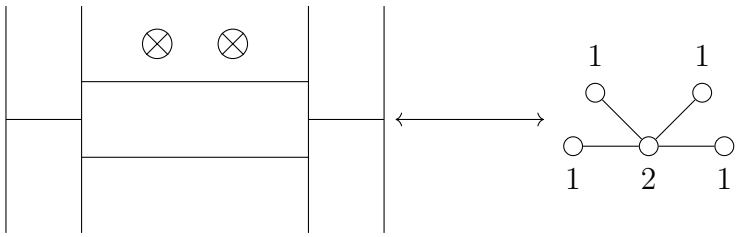
where the -2 refers to the self-intersection number of the $\mathbb{CP}^1$ in the base of an F-theory construction.

In this case, one can take the M-theory background and reduce on a circle which the M5 wraps to Type IIA. The M5 branes become NS5 branes and the $\mathbb{C}^2/\mathbb{Z}_2$ become two D6 branes. This is because the Klein A_k singularity in M-theory backgrounds can be thought of as the transverse space to a stack of $k+1$ KK monopoles which become D6 branes in Type IIA.



(2.45)

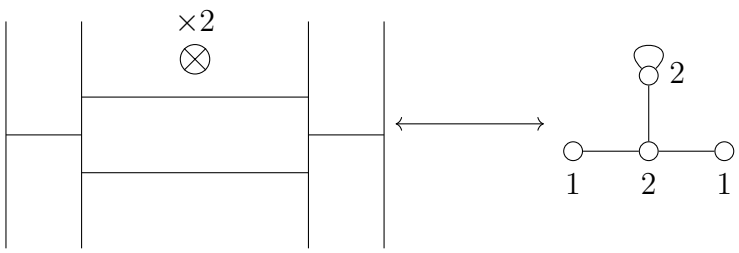
The Type IIA brane system on the right hand side has two semi-infinite D6 branes on the left and right which can end on D8 branes without further breaking supersymmetry. The way the D6 branes can end on the D8 branes depends on a particular partition of 2 since either both D6 can end on the same D8 or each D6 can end on one D8 each. Let us take the latter choice, and also suppose that there are additional D8 branes at infinity which result in the interval in which the NS5 branes sit to have zero cosmological constant. Upon lifting the NS5 branes away from the D6 the Type IIA brane system and corresponding magnetic quiver are given below.



(2.46)

The classical Higgs branch of SU(2) with four flavours is the moduli space of one SO(8) instanton on $\mathbb{C}^2$ or alternatively the minimal nilpotent orbit of SO(8) denoted $\overline{min.D_4}$, which is also given by the moduli space of monopoles of the magnetic quiver above which is the affine $D_4^{(1)}$ quiver.

The infinite coupling limit of SU(2) with four flavours corresponds to placing the NS5 branes on top of each other. This is drawn below with the corresponding magnetic quiver.

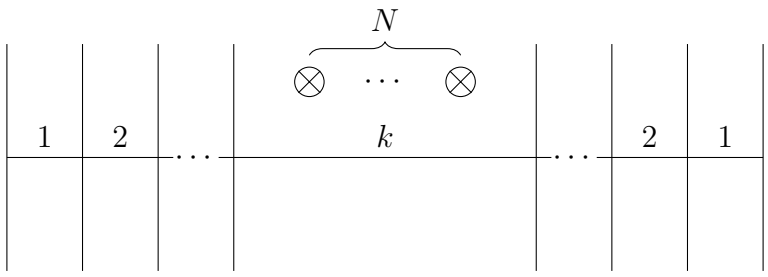


(2.47)

The Higgs branch of SU(2) with four flavours at infinite coupling cannot be computed classically

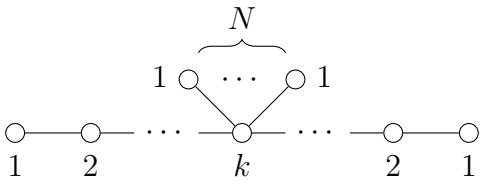
due to the tensionless strings in the spectrum. However, the moduli space of monopoles given by the magnetic quiver identifies the Higgs branch to as a moduli space called the $\overline{n.min.B_3}$ which is a nilpotent orbit and will be introduced more formally in Chapter 3. In fact, there is a $\mathbb{Z}_2$ quotient acting on the finite coupling Higgs branch which results in the infinite coupling Higgs branch, which is seen in the brane system by making the two NS5 coincident. The mathematical relationship between the moduli spaces is also known in the mathematics literature [169].

This construction can be generalised for $G = \mathrm{SU}(k)$, with $\Gamma_G = \mathbb{C}^2/\mathbb{Z}_k$ and for general N. Upon reducing the M-theory setup to Type IIA, each M5 brane becomes an NS5 and the $\mathbb{C}^2/\mathbb{Z}_k$ singularity becomes a stack of k D6 branes. Then choosing to end the k semi-infinite D6 branes on one D8 brane each with additional D8 branes at infinity to make the intervals containing the NS5 have zero cosmological constant results in the following Type IIA brane system with all NS5 branes separated.



(2.48)

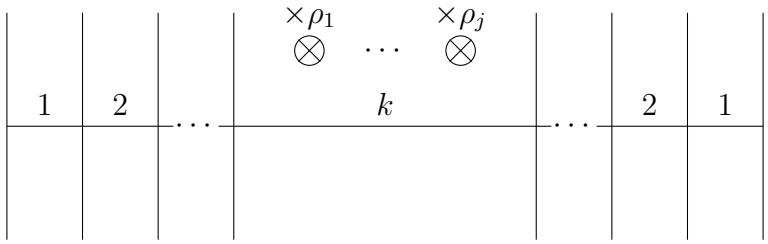
From the brane system one reads the following magnetic quiver



(2.49)

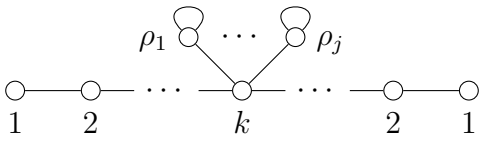
There are many possible combinations in which the some of the $N-1$ gauge couplings in $6d$ can be set to infinity. In the brane system this corresponds to all of the possible ways the NS5 branes can be coincident or not, which is in one-to-one correspondence with all partitions $\rho = (\rho_1, \rho_2, \cdots, \rho_j)$ of N where each element of the partition denotes how many NS5 are

coincident. The most generic brane system and magnetic quiver is then



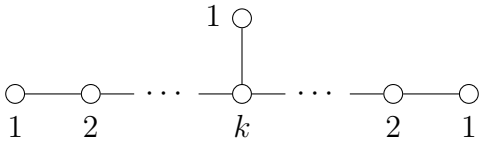
(2.50)

From the brane system one reads the following magnetic quiver



(2.51)

The minimal conformal matter case with $N = 1$, gives a magnetic quiver which takes the following form



(2.52)

which upon evaluating the Hilbert series with the monopole formula indicates the moduli space is $\mathbb{H}^{k^2}$.

(D, D) Conformal Matter

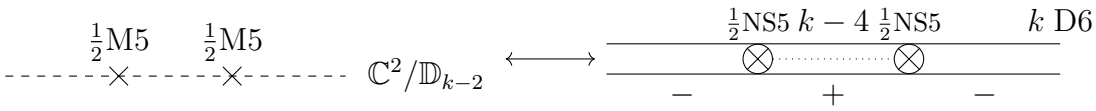
The next natural case to consider is to take N M5 branes on a Klein D_k singularity $\mathbb{C}^2/\mathbb{D}_{k-2}$ where $\mathbb{D}_{k-2}$ is the dihedral group of order $4k - 8$. Much of the analysis from the previous Subsection carries over, except for some additional subtleties. Take first, the case of one M5

brane on $\mathbb{C}^2/\mathbb{D}_{k-2}$, the naïve reduction to Type IIA would be the following



(2.53)

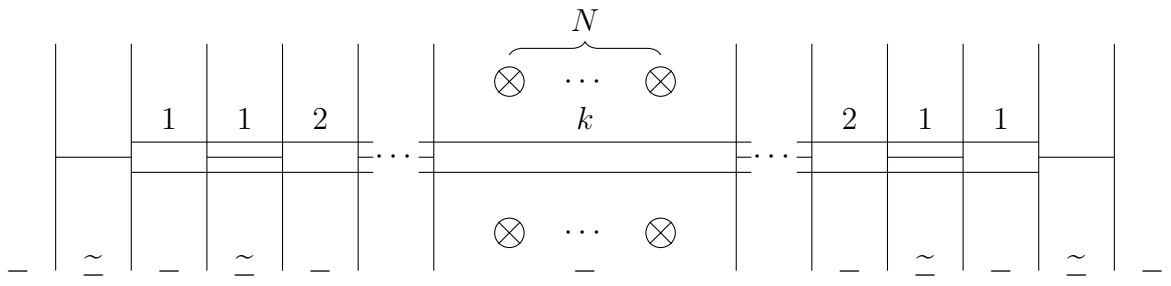
where one full NS5 has k D6 branes ending to the left and right on top of an O6$^-$ plane. However an NS5 brane on top an orientifold plane splits into two half NS5 branes. This is suggestive of the fractionation of the M5 branes and the following picture



(2.54)

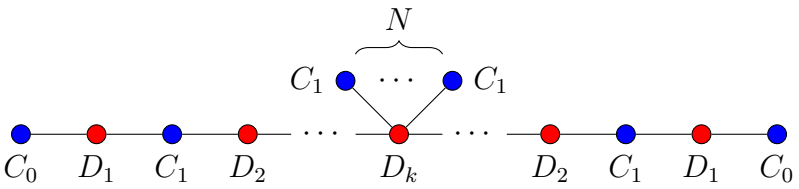
where there are $k-4$ D6 branes between the (half) NS5 branes to preserve the cosmological constant in the interval.

With this additional input, take N M5 branes on $\mathbb{C}^2/\mathbb{D}_{k-2}$ and reduce to Type IIA. Upon ending all D6 branes between the (half) D8 and ensuring that the interval containing the (half) NS5 has zero cosmological constant, the magnetic phase of the Type IIA brane system is



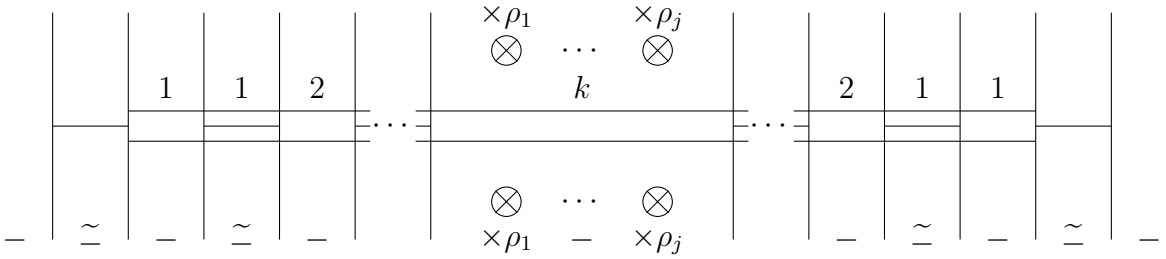
(2.55)

and results in the following magnetic quiver

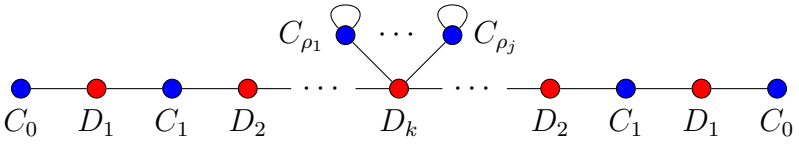


(2.56)

The C_0 refers to a trivial group and it does not contribute to computation of moduli spaces so it can be suppressed, however it is included here to reflect the total number of D8 branes in the brane system. There are again multiple ways to take the $N-1$ gauge couplings to infinity, corresponding to partitions $\rho = (\rho_1, \rho_2, \cdots, \rho_j)$ of N. The most generic Type IIA brane system and corresponding magnetic quiver are



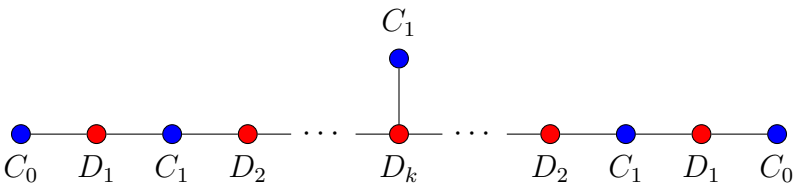
(2.57)



(2.58)

where the loops refer to antisymmetric matter.

In this case the minimal conformal matter, $N = 1$, has the following magnetic quiver



(2.59)

evaluation of the Hilbert series for this moduli space indicates that it is not a moduli space of

free hypermultiplets and is instead a more complicated symplectic singularity. The HWG is

$$\text{HWG}\left[\mathcal{C}\left(\mathcal{Q}_{2.59}\right)\right] = \text{PE}\left[\sum_{i=1}^{k-1}\mu_{2i}t^{2i} + t^4 + \mu_{2k}\left(t^{k-2}+t^k\right)\right] \tag{2.60}$$

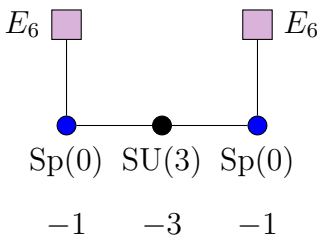
where the μ_i are highest weight fugacities for SO$(4k)$.

(E,E) Conformal Matter

In this case, there is no known Type IIA brane system to reduce the M-theory setup to. Instead one relies on F-theory constructions. Take the simplest case of the M-theory setup of one M5 brane on an E-type Klein singularity which is dual to the F-theory construction of two intersecting D7 branes which wrap one of two intersecting $\mathbb{CP}^1$ in the base of an elliptic fibration with the singular fibres of type Kodaira type IV^*, III^*, or II^* for $E_{6,7,8}$ respectively.

This elliptic fibration is too singular at the intersection point and so blowups are performed to reduce the degree of singularity of the fibration. The blowups add additional $\mathbb{CP}^1$ in the base with a finite size which also support gauge groups. The size of these $\mathbb{CP}^1$ corresponds to the gauge coupling in $6d$. Therefore, the notion of (E,E) minimal conformal matter is dual to a particular gauge theory in $6d$. The number of gauge groups corresponds to the number of intervals between the M5 which determines the number of M5 fractions.

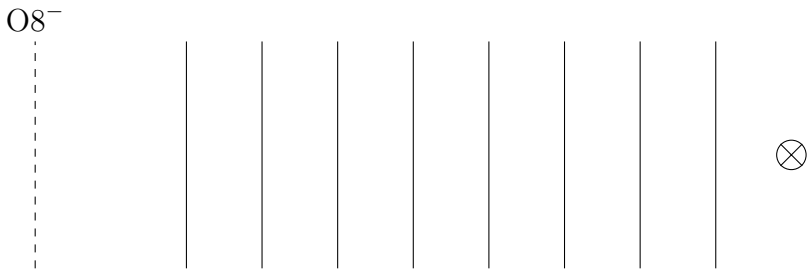
For the case of E_6, which is considered in Chapter 6 and Chapter 7, the M5 branes fractionate into four and the dual gauge theory is



(2.61)

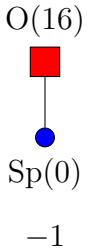
Small E_8 Instanton Transition

A second non-trivial dictionary between brane systems and magnetic quivers concerns when (half)NS5 branes are placed on top of O8 planes, the "half" is dropped in the following. Consider an NS5 brane next to an O8$^-$ and eight D8 branes.



(2.62)

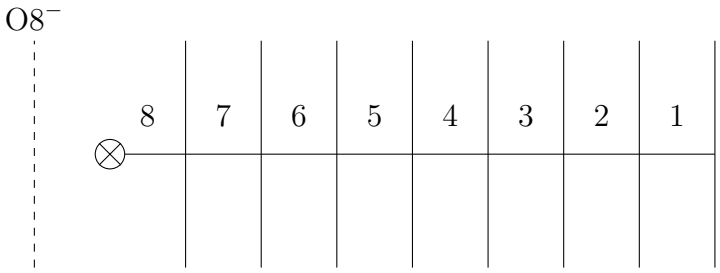
The electric gauge theory is the following



(2.63)

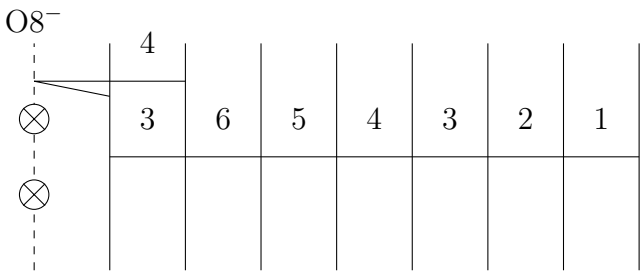
where the Sp(0) refers to a trivial gauge group but with a dynamical tensor multiplet. This is because there is a non-trivial distance between the NS5 brane and its image in the O8$^-$. The O(16) flavour symmetry is due to the eight D8 branes on top of the O8$^-$ plane. The label -1 refers to the self-intersection number of the $\mathbb{CP}^1$ in the base of the F-theory construction.

The NS5 brane is now brought near the O8$^-$ plane accounting for D6 brane creation.



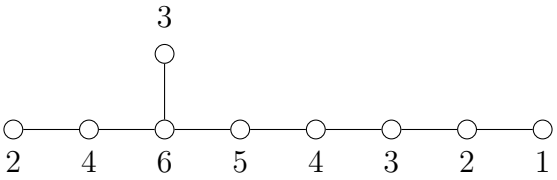
(2.64)

When the NS5 brane reaches the O8$^-$ plane, it can recombine with its image and the D6 brane pass through the O8 resulting in the following brane system



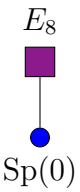
(2.65)

The magnetic quiver is the affine $E_8^{(1)}$ quiver



(2.66)

where the two NS5 on the O8$^-$ are read as a gauge node in the magnetic quiver. The corresponding electric quiver is



(2.67)

The Coulomb branch of the magnetic quiver is the moduli space of one E_8 instanton on $\mathbb{C}^2$ which has dimension 29. The jump in Higgs branch dimension from 0, at finite coupling, to 29, at infinite coupling, is indicative of the gravitational anomaly cancellation condition which trades a tensor multiplet for 29 hypermultiplets. The affine $E_8^{(1)}$ quiver is a sensible magnetic quiver as the above Type IIA construction is dual to the M-theory background of an M5 brane next to an M9 wall [170, 171] with an M2 brane ending between them. When the M5 is away from the M9 there are no massless states. When the M5 is on the wall it is an instanton inside the M9 with gauge symmetry E_8. The theory on the M5 brane is called an E-string theory since the ends of the M2 are string-like objects.

Chapter 3

Background on Symplectic Singularities

3.1 Introduction

Having introduced the main physics concepts that will appear in this thesis, it is time to rip off the plaster and delve into the mathematical background that will be needed. This will mostly encompass a type of moduli space omnipresent when dealing with moduli spaces of theories with eight supercharges called *symplectic singularities*. Within symplectic singularities there are many different constructions of varieties, the most common in this thesis will be orbifolds, nilpotent orbits, and affine Grassmannian slices. In addition, some Hilbert series divination will be covered to extract as much information about a moduli space as possible.

This review will be aimed towards physicists and will provide only loose definitions and focus more on the results of mathematical theorems. The reader is encouraged to look at the references and those contained within for a formal treatment of these topics.

3.2 Symplectic Singularities

The moduli spaces of vacua that will be encountered in this thesis fall within a family of geometric spaces called "symplectic singularities".

Firstly a Poisson variety is one whose coordinate ring has a Poisson bracket on it which satisfies, skew-symmetry, the Jacobi identity, and Leibniz rule. For some functions f, g, h on the variety these properties are respectively

$$\{f, g\} + \{g, f\} = 0 \tag{3.1}$$

$$\{f, \{g, h\}\} + \{g, \{h, f\}\} + \{h, \{f, g\}\} = 0 \tag{3.2}$$

$$\{f, gh\} - \{f, g\}h - g\{f, h\} = 0 \tag{3.3}$$

Much like in classical mechanics, the study of Poisson brackets is associated to symplectic geometry through the duality of the Poisson bracket and antisymmetric (or symplectic) form.

The formal definition of a symplectic singularity was given by Beauville [23] which roughly states that a symplectic singularity is a hyper-Kähler variety (a variety of even complex dimension) with a holomorphic symplectic form which can be degenerate at finitely many points, but extends to a symplectic form on any resolution of this variety.

Poisson varieties admit a foliation into "symplectic leaves" which are sub-varieties of the Poisson variety and need not be of the same dimension [172]. Symplectic singularities, which are also Poisson varieties have a similar property [173, 174], they admit a finite stratification which have partial order. This partial order is captured in an object called a Hasse diagram. In the physics literature many techniques have been developed to determine the Hasse diagrams of moduli spaces of theories with eight supercharges [110, 47, 75, 83, 6, 95, 8].

3.3 Poisson Brackets

Before tackling a variety with singularities it will be instructive to consider a space without singularities. The space $\mathbb{C}^2$ can be parametrised by two complex coordinates (z_1, z_2) with an overall SO(4) symmetry rotating the four real coordinates.

The SO(4) symmetry can be split into two factors of SU(2) as

$$\mathrm{SO}(4) \simeq \mathrm{SU}(2)_R \times \mathrm{SU}(2) \tag{3.4}$$

where the first $\mathrm{SU}(2)_R$ will be interpreted as an R-symmetry in a physical context and the second SU(2) is the global symmetry of $\mathbb{C}^2$.

The holomorphic coordinates (z_1, z_2) and the corresponding anti-holomorphic coordinates $(\bar{z}_1, -\bar{z}_2)$ are acted upon by these two symmetries as shown in Table 3.1.

Weights		SU(2)	
		1	−1
$\mathrm{SU}(2)_R$	1	z_1	z_2
	−1	$-\bar{z}_2$	$\bar{z}_1$

Table 3.1: Action of SU(2) and $\mathrm{SU}(2)_R$ on the holomorphic and anti-holomorphic coordinates of $\mathbb{C}^2$.

The SU(2) global symmetry acts across the columns of the matrix whereas the $\mathrm{SU}(2)_R$ acts non-holomorphically down the column of the matrix. The numbers 1 and −1 denote the weight under which each of the coordinates transforms. Importantly, holomorphic functions on $\mathbb{C}^2$ are associated to the highest weights of $\mathrm{SU}(2)_R$.

A way to analyse $\mathbb{C}^2$ is to consider the Poisson bracket of holomorphic functions on $\mathbb{C}^2$. Given two holomorphic functions $f(z_1, z_2)$ and $g(z_1, z_2)$ the Poisson bracket is defined (in canonical coordinates) as

$$\{f(z_1, z_2), g(z_1, z_2)\} = \frac{\partial f}{\partial z_1}\frac{\partial g}{\partial z_2} - \frac{\partial f}{\partial z_2}\frac{\partial g}{\partial z_1} = \frac{\partial f}{\partial z_i}\Omega^{ij}\frac{\partial g}{\partial z_j} \tag{3.5}$$

From this definition it is clear to see that the Poisson bracket is: anti-commuting, bilinear, obeys the Leibniz property, and the Jacobi identity. The explicit connection to the symplectic form Ω is also given in these coordinates.

Given the linearity of functions it is sufficient to consider simple monomials of the form $z_1^a z_2^b$ where $a, b \in \mathbb{Z}_{\geq 0}$, the degree of the monomial is $a+b$. The degree two monomials are particularly interesting as the Poisson bracket between them also results in a degree two monomial. In other

words, the degree two monomials are elements of the Lie algebra which acts on the functions on the space. This Lie algebra is the global symmetry of the moduli space.

To explicate this, there are three monomials of degree two on $\mathbb{C}^2$; z_1^2, z_1z_2, z_2^2. Of the six Poisson brackets three are of particular relevance

$$\{z_1^2, z_1z_2\} = 2z_1^2, \quad \{z_1z_2, z_1z_2\} = 0, \quad \{z_2^2, z_1z_2\} = -2z_2^2 \tag{3.6}$$

as they clearly form the Lie algebra of SU(2), the global symmetry of the space.

Physically, the coordinates on the space will correspond to chiral operators in the SQFT and the Poisson bracket is the algebra of these operators.

3.3.1 Example: $\mathbb{C}^2/\mathbb{Z}_n$

The next simplest example is the Klein A_{n-1} singularity. There are again two holomorphic complex coordinates (z_1, z_2) which transform under the action of $\mathbb{Z}_n$ as

$$(z_1, z_2) \to (e^{2\pi i/n} z_1, e^{-2\pi i/n} z_2) \tag{3.7}$$

Any function on $\mathbb{C}^2/\mathbb{Z}_n$ must respect the $\mathbb{Z}_n$ action so the most lowest degree monomials are z_1^n, z_1z_2, z_2^n.

If $n \neq 2$ then z_1z_2 is the only degree two monomial and the Poisson bracket is trivial

$$\{z_1z_2, z_1z_2\} = 0 \tag{3.8}$$

indicating that there is a U(1) global symmetry.

If $n = 2$ then z_1^2, z_1z_2, z_2^2 are all degree two functions with the Poisson brackets indicating an SU(2) global symmetry as before.

3.4 Hilbert Series

The computation of Poisson brackets is extremely useful in physics to derive precise operator algebras, the cost is that it becomes extremely complicated to do so for exotic moduli spaces. Examples of Poisson brackets for moduli spaces of theories with eight supercharges have appeared in [76, 107].

The general strategy of computing Hilbert series employed in the previous Chapter was to grade operators under the $\mathrm{SU}(2)_R$ symmetry and global symmetry and then to count them modulo gauge invariance. When studying symplectic singularities a similar approach is taken.

3.4.1 Example: $\mathbb{C}^2$

The monomials on $\mathbb{C}^2$ take the form $z_1^a z_2^b$ for $a, b \in \mathbb{Z}_{\geq 0}$. Assign two variables $t_{1,2}$ which counts the degree of $z_{1,2}$ in a particular monomial. The Hilbert series is a generating function which enumerates all of the functions on a variety at all degrees. For this example the Hilbert series $HS_{\mathbb{C}^2}(t_1, t_2)$ is computed as

$$\mathrm{HS}_{\mathbb{C}^2}(t_1, t_2) = \sum_{a,b=0}^{\infty} t_1^a t_2^b \tag{3.9}$$

$$= \frac{1}{(1-t_1)(1-t_2)} \tag{3.10}$$

The choice of variable $t_{1,2}$ is natural but does not make any of the symmetries of $\mathbb{C}^2$ apparent. Recall that $z_{1,2}$ transform with weight one under $\mathrm{SU}(2)_R$ and as ± 1 under the $\mathrm{SU}(2)$ global symmetry. The following variable redefinition makes this apparent

$$t_1 \to tx, \quad t_2 \to t/x \tag{3.11}$$

where t is a variable which counts the degree of functions under $\mathrm{SU}(2)_R$ and x is a variable which denotes the weight a function transforms with under the $\mathrm{SU}(2)$ global symmetry. The

Hilbert series then becomes

$$\mathrm{HS}_{\mathbb{C}^2}(t,x) = \frac{1}{(1-tx)(1-t/x)} \tag{3.12}$$

$$= 1 + (x + x^{-1})t + (x^2 + 1 + x^{-2})t^2 + O(t^3) \tag{3.13}$$

where the expression has been expanded up to order t^2.

The advantage of such a choice of variables is that the coefficients of t are characters of the representation of the global symmetry that the holomorphic functions transform in.

3.4.2 Example: $\mathbb{C}^2/\mathbb{Z}_n$

The basic monomials for this variety are $z_1^n, z_1 z_2, z_2^n$ which are subject to the relation $(z_1^n)(z_2^n) = (z_1 z_2)^n$. The relation prevents overcounting of holomorphic functions.

The Hilbert series written in terms of the variables $t_{1,2}$ is

$$\mathrm{HS}_{\mathbb{C}^2/\mathbb{Z}_n}(t_1,t_2) = \frac{1 - t_1^n t_2^n}{(1-t_1^n)(1-t_1 t_2)(1-t_2^n)} \tag{3.14}$$

but redefining the coordinates to make the symmetries explicit

$$t_1 \to t q^{1/n}, \quad t_2 \to t q^{-1/n} \tag{3.15}$$

gives a new Hilbert series

$$\mathrm{HS}_{\mathbb{C}^2/\mathbb{Z}_n}(t,q) = \frac{1 - t^{2n}}{(1-t^n q)(1-t^2)(1-t^n/q)} \tag{3.16}$$

3.4.3 Hilbert Series Divination

The Hilbert series contains surprisingly more information about a variety than one may expect. It will be useful to summarise some properties of Hilbert series for particular varieties.

The first observation is that the coefficient of the t^2 term of a refined Hilbert series is the character of the adjoint representation of the global symmetry, up to some fugacity maps. This is because the degree two functions on a variety form the Lie algebra of the global symmetry. In the monopole formula, the z_i are fugacities associated to the U(1) topological symmetry of unitary gauge groups. They have the interpretation of simple roots of the global symmetry algebra and hence one would have to map these to fugacities of highest weight, typically using the Cartan matrix of the global symmetry algebra, to fully realise the character of the global symmetry. If one uses the Cartan matrix, the map between simple root fugacities and weight fugacities is

$$z_i = \prod_j x_j^{A_{ji}} \tag{3.17}$$

although one may need different maps and there is no general principle to find them. If the Hilbert series is unrefined then the t^2 term is the dimension of the adjoint representation of the Hilbert series.

A second observation is that the pole of an unrefined Hilbert series at $t = 1$ is the complex dimension of the variety. This dimension should be even if the moduli space is to be a symplectic singularity.

3.5 Nilpotent Orbits

The closures of nilpotent orbits of classical and exceptional Lie algebras are one type of symplectic singularity which will be particularly important in this thesis. A review of this topic will follow ideas and proofs (not stated here) in [175] and references within. Only statements of the results will be required here.

Nilpotent orbits of a Lie algebra $\mathfrak{g}$ are moduli spaces of the orbit of inequivalent elements under the co-adjoint action of $\mathfrak{g}$. The closure of a nilpotent orbit is the union of nilpotent orbits generated by Lie algebra elements of "lower nilpotency". The nilpotent orbits of a Lie algebra $\mathfrak{g}$ are in one-to-one correspondence with the different possible embeddings $G \hookleftarrow \mathrm{SU}(2)$, due

to theorems of Jacobson-Morozov [176, 177] and Kostant [175]. This embedding is specified by a homomorphism $\rho : G \to \mathrm{SU}(2)$. These embeddings of SU(2) into a Lie group G, are classified by Dynkin [178] in terms of weighted Dynkin diagrams. This gives an equivalence between weighted Dynkin diagrams and nilpotent orbit closures. The nilpotent orbit closures of classical groups were classified in the work of Kraft-Procesi [179, 180] and exceptional nilpotent orbits were classified in the work of Bala-Carter [181, 182].

A simple way to define these embeddings of SU(2) inside G is through characters. The characters of G are expressed in terms of a set of $r = \text{rank } G$ fugacities called Cartan subalgebra (CSA) fugacities, $\{x_1, \cdots, x_r\}$, associated to the weights of G, ρ maps these fugacities to powers of the CSA fugacity associated to SU(2) denoted x. The specific labelling of $x_1, \cdots, x_r$ is through the corresponding node in the Dynkin diagram corresponding to that particular (co)weight. Alternatively, the action of ρ can be seen in terms of simple roots fugacities $\{z_1, \cdots, z_r\}$ associated to the roots of G or equivalently the co-weights of G, ρ then maps these to the simple root fugacity z for SU(2).

$$\rho : \{x_1, \cdots, x_r\} \to \{x^{w_1}, \cdots, x^{w_r}\}, \tag{3.18}$$

$$\rho : \{z_1, \cdots, z_r\} \to \{z^{q_1/2}, \cdots, z^{q_r/2}\}, \tag{3.19}$$

where the exponents q_i and w_j are necessarily related by the Cartan matrix of G:

$$q_i = \sum_j A_{ij} w_j \tag{3.20}$$

These maps can be used to decompose irreps of G into irreps of SU(2) and this permits the labelling of nilpotent orbits in any one of a number of equivalent ways [175]:

1. By the *Characteristic*, or *root map*, the set of ordered exponents $[q_1, \cdots, q_r]$,

2. By the *weight map* set of ordered exponents $[w_1, \cdots, w_r]$,

3. By the *partition*[1] which enumerates the dimensions and multiplicity of SU(2) irreps in

[1] $(\ldots, n_i^{m_i}, \ldots)$ denotes a partition where the superscript m_i gives the multiplicity of the dimension n_i in the partition.

the vector/fundamental of G under the map ρ.

For exceptional nilpotent orbits one can use another labelling of the nilpotent orbits called the Bala-Carter labelling. The maps between Bala-Carter labels and the characteristic may be found in [175].

Explicit constructions of some nilpotent orbits as a Higgs branch or Coulomb branch of a $3d$ $\mathcal{N}=4$ theory was done in [183–185] using this data. Most notably there are (hyper-Kähler quotient) Higgs branch constructions of all classical group nilpotent orbit closures also following work in [179, 180], but only a limited number of Coulomb branch constructions. For exceptional nilpotent orbits there are no known hyper-Kähler quotient Higgs branch constructions and again only a limited number of Coulomb branch constructions. However the Hilbert series for all nilpotent orbits can be computed from the characteristic with the nilpotent orbit localisation formula regardless if an explicit quiver is known [186, 184].

The systematic Coulomb branch constructions for some nilpotent orbits are limited to orbits which have the so-called property of *height* less than 3 [187]. This height is computed as

$$h = \sum_{i=1}^{r} q_i h_i^\vee \tag{3.21}$$

If $h \leq 2$ the Coulomb branch construction is defined by a quiver which forms the Dynkin diagram of G with $\mathrm{U}(w_i)$ gauge nodes and q_i flavours. In particular, the unframed quiver for the minimal nilpotent orbits for all semi-simple Lie algebras is the affine Dynkin quiver. Systematic Coulomb branch constructions for nilpotent orbits of height $h \geq 3$ are not known and cases are found sporadically in the literature.

A typical way of labelling the closures of nilpotent orbits is by group and partition data as $\overline{\mathcal{O}}_\rho^G$, where the overline clarifies that we are referring to the closure of the orbit. The partition data allows the nilpotent orbits of G to be organised as a Hasse diagram, and certain orbits in this poset carry canonical names. These include the minimal orbit $\overline{min.G}$, "next to" minimal orbits $\overline{n.min.G}$ (where we can use $n.$ multiple times to indicate how far an orbit is from the minimal), the sub-regular orbit $\overline{sub.reg.G}$ and the maximal or regular orbit $\overline{max.G}$ (also termed

the nilcone $\mathcal{N}$).

Normal and Non-normal Orbits

Most of the nilpotent orbits that will be encountered in this thesis are "normal" nilpotent orbits. These orbits are Calabi-Yau and contain only rational Gorenstein singularities [188], their Hilbert series have palindromic numerators [189, 183]. A non-normal orbit is one which (anti-climactically) is not normal, and so their Hilbert series will not have a palindromic numerator.

Higgs branches of theories with eight supercharges can be either normal or non-normal. However Coulomb branches are always normal [27], and so any quiver construction associated with a non-normal orbit actually produces its normalisation. The normalisation of a variety is unique and essentially includes additional functions on the chiral ring required to make the variety normal. Non-normal nilpotent orbits for classical and exceptional Lie algebras were identified in [179, 180, 190].

3.6 Slodowy Slices and Intersections

A closely related concept to nilpotent orbits is the notion of a Slodowy slice [191]. To a given nilpotent orbit, specified by ρ, are transverse spaces formed by the generators of the Lie algebra $\mathfrak{g}$ which are not included in the embedding ρ. These spaces are termed Slodowy slices, or Slodowy intersections if restricted by a superior orbit in the poset. Each such transverse space within $\mathfrak{g}$ is defined by a pair of orbits and is notated $\mathcal{S}^G_{\rho,\sigma}$, where the slice is taken from σ to ρ. For further background on Slodowy slices and intersections see [133, 134].

The Slodowy slice of an orbit, labelled by data ρ, to the maximal orbit (or nilcone) $\mathcal{N}$ is defined as

$$\mathcal{S}^G_{\mathcal{N},\rho} := \mathcal{N} \cap \overline{\mathcal{O}}_\rho. \tag{3.22}$$

The Slodowy slice to the maximal orbit is by definition trivial and the Slodowy slice to the trivial orbit is by definition the nilcone. However, for other orbits the Slodowy slice is not

trivial and in fact they form a partial order by their dimension. This is because the dimension of the Slodowy slice $\mathcal{S}^G_{\mathcal{N},\rho}$ and the dimension of the orbit $\overline{\mathcal{O}}_\rho$ must sum to the dimension of the nilcone $\mathcal{N}$. This is by definition of the Slodowy slice as a space transverse to $\overline{\mathcal{O}}_\rho$ and $\mathcal{N}$. As the orbits have a partial order then so must the Slodowy slices $\mathcal{S}^G_{\mathcal{N},\rho}$.

In certain cases, if there is a quiver whose Higgs/Coulomb branch corresponds to $\mathcal{S}^G_{\rho,\sigma}$ then its Coulomb/Higgs branch may correspond to $\mathcal{S}^{G^\vee}_{\sigma^\vee,\rho^\vee}$ where the superscript $\vee$, denotes a dual group or partition. This goes by the name of Lusztig-Spaltenstein or also Barbasch-Vogan duality in the mathematics literature [192, 193], but physically it represents the duality of the electric and magnetic spectrum of a theory. Typically, this maps spectra associated to a group G to the Langlands dual group $G^\vee$ however for certain theories where the Higgs/Coulomb branch is an orbit, slice, or intersection inside the $G = C_n$ nilcone then the Coulomb/Higgs branch may also be in the same C_n nilcone. This goes by the name of metaplectic duality [194], this is also a type of duality between electric and magnetic spectra if one considers $\widetilde{\mathrm{O}}^+$ planes for example.

3.7 Affine Grassmannian

The affine Grassmannian is another type of algebraic object that shares intimate connections to brane systems and quiver gauge theories, a limited set of references include [195–201, 28, 202, 203].

To define the affine Grassmannian, one makes some analogies with matrix groups defined over some field. One can consider such a group and take the right quotient by the same matrix group defined over its ring of integers. This defines a lattice.

The affine Grassmannian is constructed similarly where we first construct the objects

$$G((t)) = \{M \in \mathrm{GL}\left(n, \mathbb{C}((t))\right), P_j(M) = 0\} \tag{3.23}$$

$$G[[t]] = \{M \in \mathrm{GL}\left(n, \mathbb{C}[[t]]\right), P_j(M) = 0\}. \tag{3.24}$$

The first object, $G((t))$, is a subgroup of the general linear group, $\mathrm{GL}\left(n, \mathbb{C}((t))\right)$, over the field

of Laurent series in variable t, $\mathbb{C}((t))$. The elements of $G((t))$ are subject to some polynomial constraints $P_j(M)$ for $j = 1, \cdots, J$ which are the analogous defining constraints on the matrices for the groups $\mathrm{SL}(n, \mathbb{C})$, $\mathrm{SO}(n, \mathbb{C})$, and $\mathrm{Sp}(n, \mathbb{C})$ (of rank n). The second object, $G[[t]]$, is a subgroup of the general linear group, $\mathrm{GL}(n, \mathbb{C}[[t]])$, over the field of formal power series (not necessarily convergent) in variable t, $C[[t]]$. The elements of $G[[t]]$ are subject to the same constraints $P_j(M)$.

The field $\mathbb{C}[[t]]$ plays the role of the "ring of integers" of $\mathbb{C}((t))$ and so one can define the set of inequivalent lattices as the affine Grassmannian

$$Gr_G = G((t))/G[[t]], \tag{3.25}$$

where the action of $G[[t]]$ is on the right and corresponds to changes of basis of the lattice.

The left action of $G[[t]]$ gives an orbit of the affine Grassmannian which is parametrised by some coweight λ of G. The closure of this orbit is given by the union of orbits with coweights $\mu \leq \lambda$.

For any algebraic group G there is a partial order on the coweights where $\mu \geq \lambda$ if $\mu - \lambda \in \Lambda_0^+$ where Λ_0^+ is the positive coroot lattice. Then the transverse slice in the affine Grassmannian of G from λ to μ is given by the following Coulomb branch

$$\overline{[\mathcal{W}_G]}_\lambda^\mu = \mathcal{C}\begin{pmatrix}\text{Gauge nodes form finite Dynkin diagram of } G \\ \text{with flavours given by } \mu \text{ and balance given by } \lambda\end{pmatrix}. \tag{3.26}$$

The information about the flavours and the balance of the gauge nodes is sufficient to determine the rank of the gauge nodes.

A similar construction for slices in the "double affine Grassmannian" is given as Coulomb branches of framed affine G-quivers [204, 205]. Physically, the Coulomb branches of these framed affine quiver typically correspond to the moduli space of G instantons on an A-type Klein singularity.

Chapter 4

Quotient Quiver Subtraction

4.1 Introduction

A motivation for studying quiver gauge theories is that their graphical nature allows for simple diagrammatic and combinatorial operations that represent actions on the moduli spaces of vacua. As a consequence, information about the structure of these moduli spaces can often be found in an efficient way. The central topic of this thesis is to demonstrate that the gauging of $3d$ $\mathcal{N}=4$ Coulomb branch isometry subgroups, which is typically very challenging to do, is no exception.

Gauging global symmetry subgroups of $3d$ $\mathcal{N}=4$ theories can also be viewed geometrically as actions on the moduli space. The Coulomb branch of a $3d$ $\mathcal{N}=4$ theory, is always a symplectic singularity provided there are no operators with negative conformal dimension. One can consider taking the hyper-Kähler quotient by some subgroup of its global symmetry. Physically, such a hyper-Kähler quotient is a gauging of the theory that incorporates the action of a moment map. The study of hyper-Kähler quotients in physics typically appears when discussing Higgs branches of theories with eight supercharges [24–26] and so this work complements that by studying hyper-Kähler quotients on Coulomb branches of $3d$ $\mathcal{N}=4$ theories. Coulomb branches have a benefit compared to Higgs branches, in that it is possible to construct moduli spaces with exceptional group global symmetries directly. Exceptional group symmetries only

arise from Higgs branches when additional quantum effects are accounted for, an example would be the rank 1 theories with $E_{6,7,8}$ global symmetry [206–209].

In addition to the progress from the physics side, there are new mathematical results that can be extracted by studying such gaugings. For example, Kobak and Swann [210] showed that the hyper-Kähler quotients of classical orbits by continuous symmetry groups are hyper-Kähler, and provide several such examples, based mainly on hyper-Kähler quotients by low rank unitary groups, where the resulting space is also a nilpotent orbit. In Section 4.4 examples of hyper-Kähler quotients of exceptional nilpotent orbits by non-Abelian groups will be studied.

In this Chapter a precise procedure for gauging SU(n) Coulomb branch isometry subgroups called *quotient quiver subtraction* is presented. A full list of the rules for SU(n) hyper-Kähler quotients via *quotient quiver subtraction* will be provided in Section 4.2, but we can preview some key features.

In particular, we only work with those magnetic quivers where there is a *Dynkin type* embedding of SU(n) into the global symmetry $\mathcal{G}_\mathcal{C}$, and the diagrammatic selection rules avoid those magnetic quivers where *incomplete Higgsing* occurs, so that the simple Weyl integration methods can be applied.

The rules involve the subtraction of a *quotient quiver* with gauge nodes of the form $(1) - (2) - \cdots - (n) - \cdots - (2) - (1)$. Such a quiver has an incomputable Coulomb branch Hilbert series [123]. Nevertheless, such a quotient quiver can often be subtracted from computable magnetic quivers that have a corresponding "external leg" to produce valid magnetic quiver(s), whose Coulomb branches have the correct dimensions for a hyper-Kähler quotient.

A significant feature of the rules is that, in certain cases, they identify that the hyper-Kähler quotient of a Coulomb branch is a union of Coulomb branches. Methods similar to [80] are used to evaluate the HS of such unions and to illuminate their underlying structures. This is particularly interesting as Coulomb branches cannot be unions of moduli spaces [27, 124, 125] but a hyper-Kähler quotient of a Coulomb branch can.

The SU(n) quotient quiver subtraction algorithm is applied to examples including moduli spaces

of free fields (reproducing known results), exceptional nilpotent orbits, and to adjacent examples related to dualities of $4d$ $\mathcal{N}=2$ theories.

Organisation of the Chapter In Section 4.2 the rules for SU(n) quotient quiver subtraction are presented. In Section 4.3 a few warm-up applications of SU(n) quotient quiver subtraction on magnetic quivers for moduli spaces of free fields are given. These recover known results about hyper-Kähler quotients on free spaces. In Section 4.4 the rules of SU(n) quotient quiver subtraction are applied to find hyper-Kähler quotients of exceptional nilpotent orbits. Many new conjectures for relationships between orbits and/or slices in the affine Grassmannian are obtained. For low rank cases we check these relationships by computing HS and/or HWGs.

4.2 Method of quotient quiver subtraction for SU(n) hyper-Kähler quotients

4.2.1 Rules for SU(n) hyper-Kähler quotient by quotient quiver subtraction

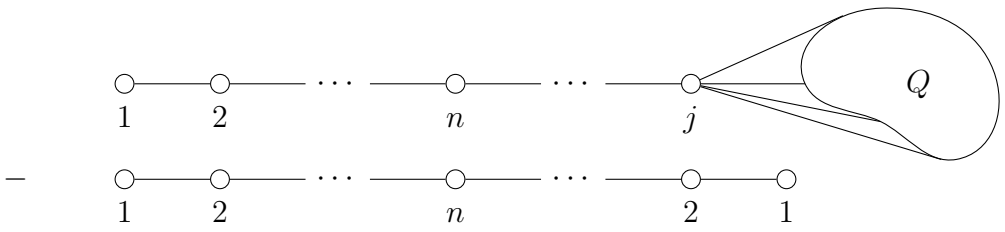


Figure 4.1: Schematic drawing of a valid target quiver (top) having a junction and an external leg. The target quiver for the quotient quiver subtraction must have a leg that starts as $(1)-\cdots-(n)$. If the quotient quiver (bottom) overlaps a junction node of rank j on the target quiver, this must align with a node of rank $2 \leq j$ on the quotient quiver. The remainder of the target quiver, denoted Q, can take any "good" or "ugly" form.

When carrying out SU(n) hyper-Kähler quotient by quotient quiver subtraction, it is convenient to work with unframed quivers throughout. The overall centre of mass U(1) may be fixed at the end of the algorithm.

The SU(n) *quotient quiver* is defined as the unframed quiver $(1)-(2)-\cdots-(n)-\cdots-(2)-(1)$ and the *target quiver* as the unitary magnetic quiver for which the SU(n) hyper-Kähler quotient of its Coulomb branch is desired. The procedure for performing an SU(n) hyper-Kähler quotient by quotient quiver subtraction is then as follows. At each stage of the procedure there are selection rules (in bold) that should be applied before continuing.

1. Select a computable unitary magnetic quiver as the target.

   Long Framing Rule The target quiver must be framed only on long nodes, otherwise unframing will give an ambiguous result.

2. Transform the target quiver into its unframed form.

   External Leg Rule The unframed target quiver must have at least one external leg with gauge nodes of $(1)-(2)-\cdots-(n)$. For a non-simply laced target quiver, this leg must correspond to long roots. Multiple legs may give a choice of hyper-Kähler quotients.

3. Align the quotient quiver against this external leg and subtract its gauge nodes from the target.

   Single Edge Rule The edges of the quotient quiver are simply laced and can only be subtracted from a section of the target quiver with single edges.

   Junction Rule If the quotient quiver extends beyond a junction in the target quiver, the junction must align with a trailing node of 2 in the quotient quiver, as drawn in Figure 4.1.

   Union Rule If the quotient quiver extends past the junction, then all possible alignments must lead to valid diagrams.

   Adjoint Hypers Rule Any nodes with an adjoint hypermultiplet must survive the quotient quiver subtraction.

4. Restore the original balance of all surviving gauge nodes with a single U(1) gauge node with appropriate numbers of hypers from the surviving gauge nodes connecting to it.

Rebalancing Rule The resulting framed quiver(s) must contain no node (gauge or flavour) with negative rank.

5. If a particular alignment of the quotient quiver breaks the target into disconnected pieces, then its contribution to the moduli space is the Cartesian product of the Coulomb branches of these disjoint magnetic quivers.

6. If the target quiver contains a junction, and there are multiple possible alignments of the quotient quiver, each alignment is taken as yielding a different quiver, and the desired moduli space is the union of the Coulomb branches of these magnetic quivers.

By way of explanatory comments:

- Recall that the Hilbert series from applying the monopole formula to a simply laced magnetic quiver is insensitive to the choice of framing, and that for a non-simply laced quiver, the HS is insensitive to choice of framing amongst long nodes [136]. Quiver subtraction requires compatible framing, so that the framing on the target quiver and the quotient quiver need to be aligned before subtraction, if this is possible, by judicious shifts in framing. Alternatively, one can work with unframed quivers in both cases, and this is the diagrammatic approach that is simpler for SU(n) quotient quiver subtraction.

- The External Leg Rule requires that an external leg of $(1) - (2) - \cdots - (n)$ must be available for subtraction of the quotient quiver. By construction, this leg has a chain of $n-1$ balanced nodes and so contains the Dynkin diagram of A_{n-1}, thereby ensuring that there is a Dynkin type embedding of SU(n), and permitting comparison with the result from Weyl integration. The sum of the ranks of the (unframed) quotient quiver is n^2 and so, when it is subtracted, the (quaternionic) dimension of the framed target quiver's Coulomb branch is reduced by n^2-1 (allowing for the dimension 1 increase from the initial unframing). This matches with the expectation from Weyl integration for an SU(n) hyper-Kähler quotient whenever there is complete Higgsing.

- The unframing of the target quiver re-introduces the centre-of-mass U(1) to the global

symmetry. Thus the subtraction of the SU(n) quotient quiver (of dimension n^2) from the unframed target quiver is consistent with an SU(n) hyper-Kähler quotient.

- The External Leg Rule also requires the external leg to lie within the long roots of the target quiver. This is because the quotient quiver corresponds to long roots and so cannot be subtracted from short roots.

- Empirically, we find that quotient quiver subtraction does not match Weyl integration under violation of the Adjoint Hypers Rule.

- The Single Edge Rule forbids the quotient quiver being aligned against a part of the target quiver with non-simply laced edges or multiple hypers. This is because quiver subtraction is undefined in these cases.

- The Rebalancing Rule ensures that the resulting quiver will not have any nodes (gauge or flavour) with negative rank. This is because magnetic quivers with negative rank nodes do not have natural interpretations.

- The Junction Rule is an empirical rule for target quivers where the quotient quiver extends past a junction. If this rule is violated, then we have found that incomplete Higgsing occurs under Weyl integration and we are unable to validate the result from quiver subtraction. Conversely, the requirement that a junction should align with a node of at most rank 2 on the quotient quiver leads to any alternative resulting quivers having an intersection related by A-type Kleinian singularities; and this appears to be sufficient to ensure complete Higgsing.

- The Union Rule ensures that the union of the Coulomb branches of the alternative magnetic quivers can be constructed.

- The interpretation of the Coulomb branch of disconnected quivers is the natural one of a Cartesian product of Coulomb branches. In terms of HS, it is the usual multiplicative product.

- In a magnetic quiver each gauge node is associated to a different root fugacity, and the requirement of a Dynkin type embedding fixes a specific labelling of the nodes by

fugacities. So even if alternative alignments of the quotient quiver are related by outer automorphism, they represent different moduli spaces, and have to be treated as distinct components of the union.

- A trivial comment is that if multiple SU(n) hyper-Kähler quotient are to be computed then one simply does quotient quiver subtraction for each SU(n) in turn. The order in which this is done may affect the final result.

Some examples that illustrate pathological outcomes from violating the selection rules are contained in Appendix A.

Whenever alternative magnetic quivers result from quotient quiver subtraction, it remains to find their union. We compute the Hilbert series for the union of the Coulomb branches of a set of quivers $\{Q_i\}$, where $i = 1, \cdots, n$, using the *Unions of Cones* formula [80]:

$$\begin{aligned}\mathrm{HS}\left(\mathcal{C}\left(Q_1 \cup Q_2 \cup \cdots \cup Q_n\right)\right) = \sum_i \mathrm{HS}\left(\mathcal{C}\left(Q_i\right)\right) - \sum_{1\leq i<j\leq n} \mathrm{HS}\left(\mathcal{C}\left(Q_i \cap Q_j\right)\right) \\ + \cdots + \sum_{1\leq i_1<i_2<\cdots<i_p\leq n} (-1)^{p-1}\mathrm{HS}\left(\mathcal{C}\left(Q_{i_1} \cap \cdots \cap Q_{i_p}\right)\right) + \cdots .\end{aligned} \tag{4.1}$$

The magnetic quivers for the intersections can be found by carrying out Kraft-Procesi quiver subtractions from each component of the union down to a common quiver.

This decomposition of the union as a signed sum of Coulomb branches is the reason quotient quiver subtraction provides additional insight into the structure of a hyper-Kähler quotient compared with Weyl integration. While it is a challenge to decompose a moduli space into its constituent parts from an HS alone, with quotient quiver subtraction, each alignment directly identifies the magnetic quiver for each constituent part of the moduli space.

We test our conjecture that the SU(n) hyper-Kähler quotient of the Coulomb branch of the target quiver corresponds to the union of Coulomb branches from different possible alignments with many examples in the course of this work. To validate a quotient quiver subtraction, we compare the results to those from an SU(n) hyper-Kähler quotient by Weyl integration. We do

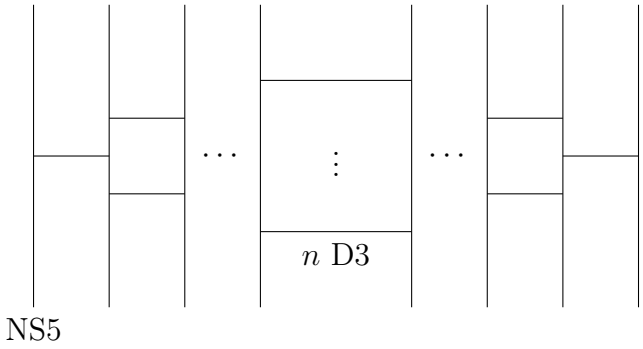


Figure 4.2: Type IIB brane system for the SU(n) quotient quiver. There are $2n$ NS5 branes with $2n-1$ intervals on which D3 branes are suspended.

this using the Dynkin type embedding of SU(n) into $G_{\mathcal{C}}$ associated with the external leg, all as described further in each example.

4.2.2 A physical interpretation of the SU(n) quotient quiver

As mentioned, one cannot compute the Coulomb branch Hilbert series of the SU(n) quotient quiver. However, we can go to the Type IIB Hanany-Witten brane system [31] for the SU(n) quotient quiver which is drawn in Figure 4.2. It is clear that from the point of view of the NS5 brane that this is the moduli space of an SU($2n$) monopole with magnetic charges $(1, 2, \cdots, n, \cdots, 2, 1)$. The moduli space of such a monopole has been found in the mathematics literature as T^*SL(n) [211, 212]. The moduli space T^*SL(n) is smooth and compact and it is at present unclear how this is connected to the SU(n) hyper-Kähler quotient, a singular operation, of Coulomb branches which are also singular and non-compact.

An alternative viewpoint is that the SU(n) quotient quiver can be viewed as a cylinder in a class $\mathcal{S}$ theory with algebra A_{n-1}[1]. The cylinder plays an important role in gauging flavour symmetries in class $\mathcal{S}$ and so it is curious that it appears in the context of $3d$ $\mathcal{N}=4$ theories also.

[1]We thank Tudor Dimofte for discussions about this point.

4.3 Moduli Space of Free Fields

We begin with magnetic quivers for some of the moduli spaces of free fields and apply the rules presented in Section 4.2 to compute the SU(n) hyper-Kähler quotient of the Coulomb branch using SU(n) quotient quiver subtraction. Additionally, we compare SU(n) quotient quiver subtraction where the explicit embedding used will be given when studying each example.

4.3.1 Moduli Space of Free Fields SU(2) hyper-Kähler quotient

$\mathbb{H}^{2k}///\mathrm{SU}(2), k \geq 2$

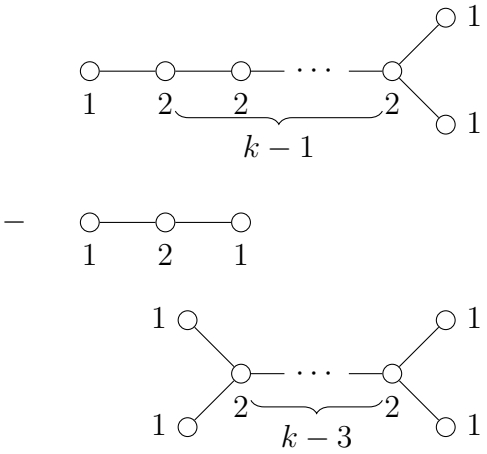


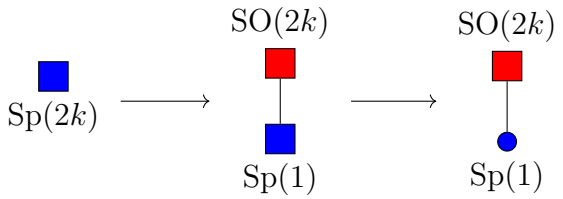
Figure 4.3: One subtraction of the SU(2) quotient quiver from the magnetic quiver $\mathcal{Q}_{4.3}$ for $\mathbb{H}^{2k}$ to produce the magnetic affine $D_k^{(1)}$ quiver for $\overline{min.D_k}$.

The unframed magnetic quiver $\mathcal{Q}_{4.3}$ for $\mathbb{H}^{2k}$ is drawn in the top of Figure 4.3. This quiver takes the form of the finite D_{k+2} Dynkin diagram. The Coulomb branch has an Sp($2k$) global symmetry which can branch as Sp($2k$) $\to$ SO($2k$) $\times$ SU(2) global symmetry. Although there are two ends from which a SU(2) quotient quiver may be subtracted in accordance with the rules in Section 4.2, consider the possibility drawn in Figure 4.3, which results in the affine $D_k^{(1)}$ quiver which is a magnetic quiver for $\overline{min.D_k}$. This is written as an operation on moduli spaces as

$$\mathbb{H}^{2k}///\mathrm{SU}(2) = \overline{min.D_k}, \quad k \geq 2. \tag{4.2}$$

This result has been tested explicitly for $k = 2, \cdots, 6$, finding agreement with Weyl integration.

The result (4.2) is naturally viewed from the Higgs branch perspective by taking a collection of $2k$ free hypermultiplets with $\mathrm{Sp}(2k)$ global symmetry, decomposing them into $\mathrm{Sp}(1) \times \mathrm{SO}(2k)$ representations where $\mathrm{Sp}(1) \simeq \mathrm{SU}(2)$ and then gauging the $\mathrm{Sp}(1)$.



(4.3)

The resulting quiver is the $3d$ mirror of the affine $D_k^{(1)}$ quiver and hence demonstrates quotient quiver subtraction as a dual operation to gauging flavour symmetry subgroups.

$\mathbb{H}^{2k+1}///\mathrm{SU}(2), k \geq 2$

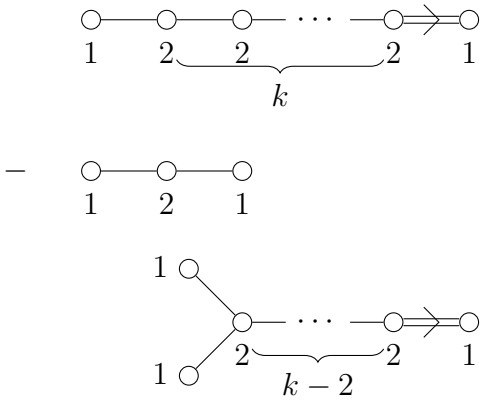


Figure 4.4: Subtraction of the SU(2) quotient quiver from the magnetic quiver $\mathcal{Q}_{4.4}$ for $\mathbb{H}^{2k+1}$ to produce the magnetic affine $B_k^{(1)}$ quiver for $\overline{min.B_k}$.

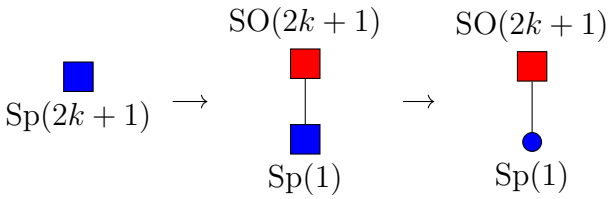
The unframed magnetic quiver $\mathcal{Q}_{4.4}$ for $\mathbb{H}^{2k+1}$ is drawn in the top of Figure 4.4. This quiver takes the form of the finite B_{k+2} Dynkin diagram. The Coulomb branch has $\mathrm{Sp}(2k+1)$ global symmetry which branches as $\mathrm{Sp}(2k+1) \to \mathrm{SO}(2k+1) \times \mathrm{SU}(2)$ global symmetry. There is only one place from which a SU(2) quotient quiver may be subtracted in accordance with the rules in Section 4.2. This is shown in Figure 4.4 and results in the magnetic affine $B_k^{(1)}$ quiver for

$\overline{min.B_k}$. As actions on moduli spaces this is expressed as

$$\mathbb{H}^{2k+1}///\mathrm{SU}(2) = \overline{min.B_k}, \quad k \geq 2. \tag{4.4}$$

This result has been tested explicitly for $k = 1, \cdots, 5$, finding agreement with Weyl integration.

The result (4.4) is also naturally viewed from the Higgs branch perspective by taking a collection of $2k$ free hypermultiplets with $\mathrm{Sp}(2k+1)$ global symmetry, decomposing them into $\mathrm{Sp}(1) \times \mathrm{SO}(2k+1)$ representations and then gauging the $\mathrm{Sp}(1)$. Despite the resulting gauge theory having a Witten anomaly [213] one can still view this gauge theory as a construction for the nilpotent orbit closure.



(4.5)

4.4 Exceptional Orbits

We now consider the possible $\mathrm{SU}(n)$ hyper-Kähler quotients that one can take from exceptional orbits using quotient quiver subtraction. Unlike, the classical case, there are no families of exceptional orbits, so these orbits are considered on a case-by-case basis. Furthermore, these hyper-Kähler quotients have no known analogue as a Higgs branch hyper-Kähler quotient. The following results are hence unique and non-trivial tests of the quotient quiver subtraction algorithm.

The SU(2) hyper-Kähler quotients of $\overline{min.F_4}$, $\overline{min.E_6}$, $\overline{min.E_7}$,and $\overline{min.E_8}$ are examined. As well as the SU(3) hyper-Kähler quotient of $\overline{min.E_7}$ and $\overline{min.E_8}$ (the latter was first computed in [72]). Finally the SU(4) hyper-Kähler quotient of $\overline{min.E_8}$ is studied.

The relevant embedding of $\mathrm{SU}(n)$ into the adjoint will be given when studying each example.

The notation for the embedding uses highest weight fugacities with ν reserved for SU(n) and μ for global symmetries which are commutants.

4.4.1 Exceptional Orbit SU(2) hyper-Kähler quotient

$\overline{min.F_4}///\mathrm{SU}(2)$

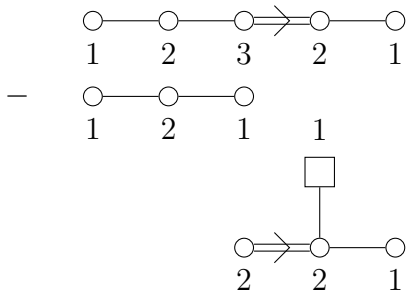


Figure 4.5: Quiver subtraction of the SU(2) quotient quiver from an unframed magnetic quiver for $\overline{min.F_4}$ to produce quiver $\mathcal{Q}_{4.5}$.

The affine $F_4^{(1)}$ magnetic quiver for $\overline{min.F_4}$ is shown at the top of Figure 4.5, together with the subtraction of the SU(2) quotient quiver to result in quiver $\mathcal{Q}_{4.5}$. Note that the subtraction occurs on the long side, in accordance with the External Leg Rule. The rebalancing is done with a flavour node as the node that requires rebalancing is on the short side of the quiver. The Coulomb branch of $\mathcal{Q}_{4.5}$ is $\overline{n.min.C_3}$. We conclude that:

$$\overline{min.F_4}///\mathrm{SU}(2) = \overline{n.min.C_3}. \tag{4.6}$$

We have checked this explicitly using the embedding of $F_4 \hookleftarrow \mathrm{Sp}(3) \times \mathrm{SU}(2)$, where the fundamental of F_4 decomposes in the following way:

$$(\mu_1)_{F_4} \to \mu_1^2 + \nu^2 + \mu_3\nu \tag{4.7}$$

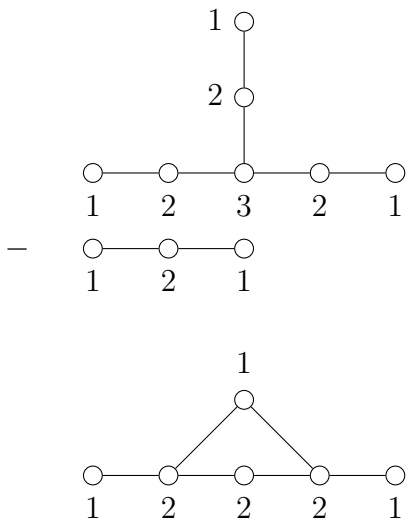


Figure 4.6: Quiver subtraction of the SU(2) quotient quiver from an unframed magnetic quiver for $\overline{min.E_6}$ to produce quiver $\mathcal{Q}_{4.6}$.

$\overline{min.E_6}///\mathrm{SU}(2)$

A magnetic quiver for $\overline{min.E_6}$ is shown at the top of Figure 4.6, together with the subtraction of the SU(2) quotient quiver to result in the quiver $\mathcal{Q}_{4.6}$. The Coulomb branch of $\mathcal{Q}_{4.6}$ is $\overline{n.min.A_5}$. We conclude that:

$$\overline{min.E_6}///\mathrm{SU}(2) = \overline{n.min.A_5}. \tag{4.8}$$

There is an embedding of $E_6 \hookleftarrow \mathrm{SU}(6) \times \mathrm{SU}(2)$ where the adjoint of E_6 decomposes in the following way:

$$(\mu_6)_{E_6} \to \mu_1\mu_5 + \nu^2 + \mu_3\nu \tag{4.9}$$

We have used this to compute the hyper-Kähler quotient explicitly by Weyl integration and find agreement with quiver subtraction.

Extended E_6 quiver $\overline{min.E_6} \times \mathbb{H}^2///\mathrm{SU}(2)$

One can take the affine E_6 shown in the top of Figure 4.6 and extend one leg by a further node of U(2). This is shown in Figure 4.7 with the U(2) node, in between the U(1) and another U(2) node, having a balance of -1. The Hilbert series of the Coulomb branch of this quiver is

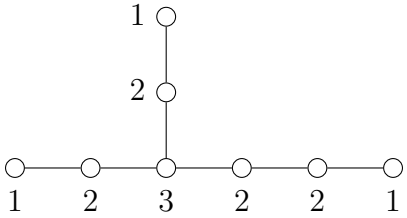


Figure 4.7: Magnetic quiver $\mathcal{Q}_{4.7}$ for $\overline{min.E_6} \times \mathbb{H}^2$.

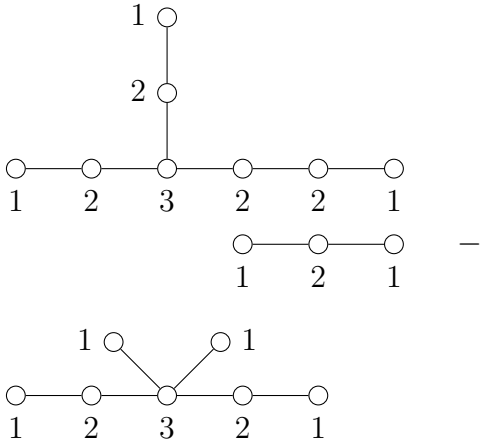


Figure 4.8: Subtraction of the SU(2) quotient quiver from the unframed magnetic quiver $\mathcal{Q}_{4.7}$ for $\overline{min.E_6} \times \mathbb{H}^2$ to produce the magnetic quiver $\mathcal{Q}_{4.8}$.

computed as

$$\mathrm{HS}\left[\mathcal{C}(\mathcal{Q}_{4.7})\right] = \frac{\left(\begin{array}{l} 1 + 56t^2 + 945t^4 + 6776t^6 + 23815t^8 + 43989t^{10} \\ \quad + 43989t^{12} + 23815t^{14} + 6776t^{16} + 945t^{18} + 56t^{20} + t^{22} \end{array}\right)}{(1-t)^4(1-t^2)^{22}}. \tag{4.10}$$

The moduli space is $\overline{min.E_6} \times \mathbb{H}^2$ and the global symmetry is $E_6 \times \mathrm{Sp}(2)$ which is confirmed from the t^2 coefficient of the above HS. One alignment and subtraction of the SU(2) quotient quiver from $\mathcal{Q}_{4.7}$ is shown in Figure 4.8 to produce quiver $\mathcal{Q}_{4.8}$. The Hilbert series of the Coulomb

branch of $\mathcal{Q}_{4.8}$ is

$$\mathrm{HS}\left[\mathcal{C}(\mathcal{Q}_{4.8})\right] = \frac{\left(\begin{array}{l} 1+6t+41t^2+206t^3+900t^4+3326t^5+10846t^6+31100t^7+79677t^8 \\ \quad +183232t^9+381347t^{10}+720592t^{11}+1242416t^{12}+1959850t^{13}+2837034t^{14} \\ \quad +3774494t^{15}+4624009t^{16}+5220406t^{17}+5435982t^{18}+\text{palindrome}+t^{36} \end{array}\right)}{(1-t^2)^{16}(1-t^3)^4(1+t+t^2)^6}, \tag{4.11}$$

the coefficient of the t^2 term indicates that the global symmetry of $\mathcal{C}(\mathcal{Q}_{4.8})$ is U(6).

We conclude that

$$\left(\overline{min.E_6}\times\mathbb{H}^2\right)///\mathrm{SU}(2) = \mathcal{C}(\mathcal{Q}_{4.8}). \tag{4.12}$$

The above result is verified from Weyl integration by integrating over the SU(2) in the global symmetry of $\mathcal{C}(\mathcal{Q}_{4.7})$.

This result realises the Higgs branch side of a set of $4d$ $\mathcal{N}=2$ dualities contained in [214, 215, Table 2 Ex. 15]. In this case the proposed duality is between SU(3) gauge theory with 6 flavours at infinite coupling and the gauging of the SU(2) in a rank 1 E_6 SCFT with a free fundamental hyper of SU(2).

The Coulomb branch of $\mathcal{Q}_{4.7}$ is exactly the Higgs branch of the latter theory. The gauging of SU(2) is implemented through the quiver subtraction to produce $\mathcal{Q}_{4.8}$. The quiver $\mathcal{Q}_{4.8}$ is indeed the $3d$ mirror for SU(3) with 6 flavours.

$\overline{min.E_7}///\mathrm{SU}(2)$

An unframed magnetic quiver for $\overline{min.E_7}$ is shown at the top of Figure 4.9, followed by the subtraction of the SU(2) quotient quiver to give $\mathcal{Q}_{4.9}$. The Coulomb branch of $\mathcal{Q}_{4.9}$ is $\overline{n.n.min.D_6}$. We conclude that:

$$\overline{min.E_7}///\mathrm{SU}(2) = \overline{n.n.min.D_6}. \tag{4.13}$$

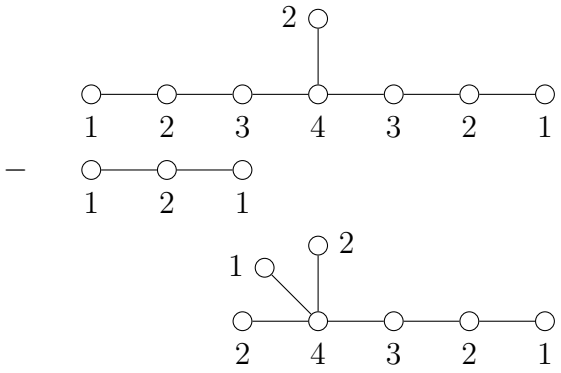


Figure 4.9: Quiver subtraction of the SU(2) quotient quiver from an unframed magnetic quiver for $\overline{min.E_7}$ to produce quiver $\mathcal{Q}_{4.9}$.

We have checked this explicitly using the embedding of $E_7 \hookleftarrow \mathrm{SO}(12)\times\mathrm{SU}(2)$ which decomposes the adjoint as:

$$(\mu_1)_{E_7} \to \mu_2 + \nu^2 + \mu_6\nu \tag{4.14}$$

This example realises the Higgs branch side of the $4d\,\mathcal{N}=2$ duality proposed in [214, 215, Table 2 Ex. 7], which claims that Sp(2) with six flavours is dual to the SU(2) gauging of the rank 1 E_7 theory. The quotient quiver subtraction in Figure 4.9 explicitly takes the magnetic quiver for the rank 1 E_7 theory and gauges SU(2) through quotient quiver subtraction to produce $\mathcal{Q}_{7.1}$ which is a magnetic quiver for Sp(2) with six flavours.

$\overline{min.E_8}///\mathrm{SU}(2)$

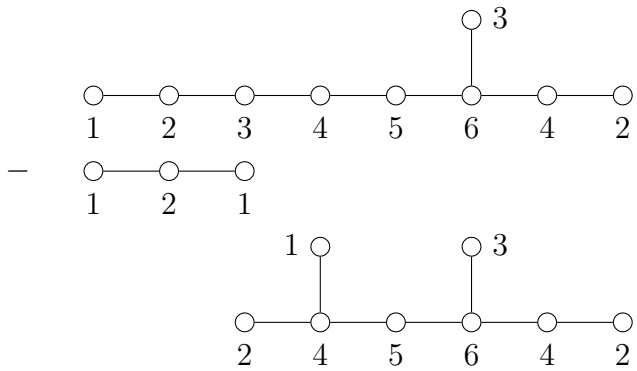


Figure 4.10: Quiver subtraction of the SU(2) quotient quiver from an unframed magnetic quiver for $\overline{min.E_8}$ to produce quiver $\mathcal{Q}_{4.10}$.

An unframed magnetic quiver for $\overline{min.E_8}$ is given at the top of Figure 4.10 followed by the

subtraction of the SU(2) quotient quiver to produce $\mathcal{Q}_{4.10}$. The Coulomb branch of $\mathcal{Q}_{4.10}$ is $\overline{n.min.E_7}$. We conclude that:

$$\overline{min.E_8}///\mathrm{SU}(2) = \overline{n.min.E_7}. \tag{4.15}$$

We have checked this explicitly using the Dynkin-type embedding of $E_8 \hookleftarrow E_7 \times \mathrm{SU}(2)$ under which the adjoint of E_8 decomposes as:

$$(\mu_7)_{E_8} \to \mu_1 + \nu^2 + \mu_6\nu \tag{4.16}$$

4.4.2 Exceptional Orbit SU(3) hyper-Kähler quotient

It is important to note that $\overline{min.E_6}$ is not amenable to subtraction by the SU(3) quotient quiver as the junction occurs on a node of rank 3 on the quotient quiver as opposed to a node of rank 2 as required by the Junction Rule.

$\underline{\overline{min.E_7}///\mathrm{SU}(3)}$

The unframed magnetic quiver for the $\overline{min.E_7}$ permits two possible alignments for subtraction of an SU(3) quotient quiver, as shown in Figure 4.11. The resulting quivers $\mathcal{Q}_{4.11a}$ and $\mathcal{Q}_{4.11b}$ are magnetic quivers for the nilpotent orbits $\overline{\mathcal{O}}^{A_5}_{(2^3)}$ and $\overline{\mathcal{O}}^{A_5}_{(3,1^3)}$, respectively. We conclude that:

$$\overline{min.E_7}///\mathrm{SU}(3) = \overline{\mathcal{O}}^{A_5}_{(2^3)} \cup \overline{\mathcal{O}}^{A_5}_{(3,1^3)} \tag{4.17}$$

The intersection, reached in both cases by an A_1 KP transition, is the quiver $\mathcal{Q}_{4.11c}$, which is a magnetic quiver for $\overline{n.min.A_5}$. There is an embedding of $E_7 \hookleftarrow \mathrm{SU}(6) \times \mathrm{SU}(3)$ which decomposes the adjoint of E_7 as:

$$(\mu_1)_{E_7} \to \mu_1\mu_5 + \nu_1\nu_2 + \mu_2\nu_2 + \mu_4\nu_1 \tag{4.18}$$

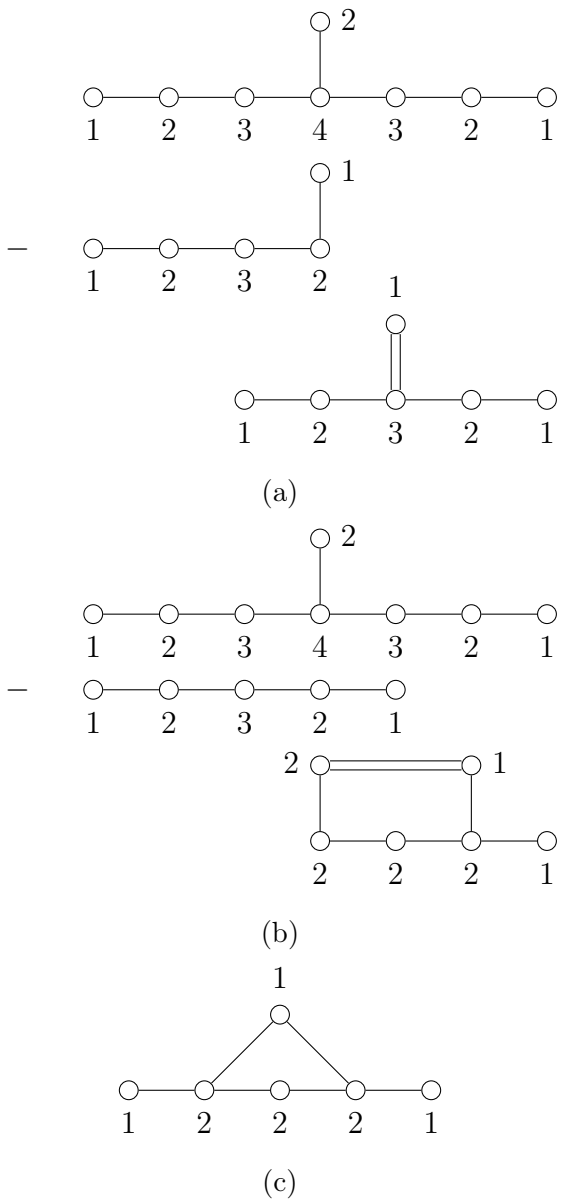


Figure 4.11: Both alignments of the SU(3) quotient quiver against $\overline{min.E_7}$ to produce quivers $\mathcal{Q}_{4.11a}$ and $\mathcal{Q}_{4.11b}$. Their intersection, reached via A_1 Kraft-Procesi transitions, is $\mathcal{Q}_{4.11c}$.

and we have used this to compute the hyper-Kähler quotient using Weyl integration and to verify the above result.

$\overline{min.E_8}///\mathrm{SU}(3)$

The computation of this SU(3) hyper-Kähler quotient was first done in [72] both using a diagrammatic quiver subtraction of the SU(3) quotient quiver from affine $E_8^{(1)}$ quiver, as reproduced in Figure 4.12, and explicitly using Weyl integration. The resulting diagram is not a

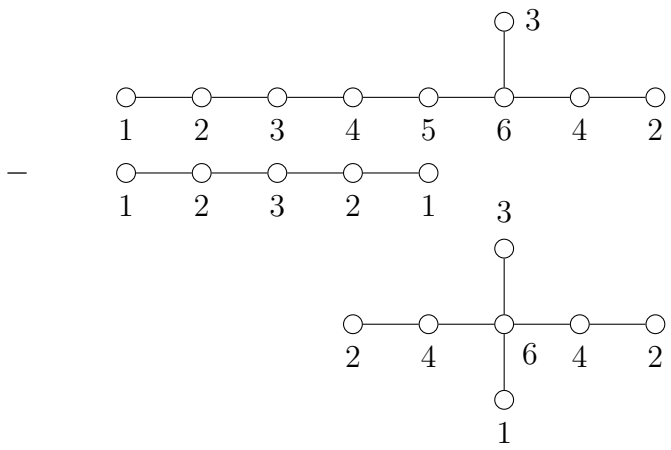


Figure 4.12: Quiver subtraction of the SU(3) quotient quiver from an unframed magnetic quiver for $\overline{min.E_8}$ to produce quiver $\mathcal{Q}_{4.12}$.

magnetic quiver for an E_6 orbit, but turns out to be a magnetic quiver for the double cover of the 21-dimensional orbit of E_6. The quiver $\mathcal{Q}_{4.12}$ is also a slice in the affine Grassmannian of E_6 and so we find:

$$\overline{min.E_8}///\mathrm{SU}(3) = \mathbb{Z}_2 \text{ cover } \overline{\mathcal{O}}_{E_6}^{A_2} = \left[\overline{\mathcal{W}_{E_6}}\right]_{[0,0,0,0,0,0]}^{[0,0,1,0,0,0]} \tag{4.19}$$

This is explicitly checked using Weyl integration with the embedding $E_8 \hookleftarrow E_6 \times \mathrm{SU}(3)$ which decomposes the adjoint as

$$(\mu_7)_{E_8} \to \mu_6 + \nu_1\nu_2 + \mu_1\nu_1 + \mu_5\nu_2 \tag{4.20}$$

4.4.3 Exceptional Orbit SU(4) hyper-Kähler quotient

$\overline{min.E_8}///\mathrm{SU}(4)$

Subtraction of the SU(4) quotient quiver from the unframed magnetic quiver for $\overline{min.E_8}$ has two possible alignments, as shown in Figure 4.13, which produce quivers $\mathcal{Q}_{4.13a}$ and $\mathcal{Q}_{4.13b}$. These are both slices in the affine Grassmannian of D_5, being $\left[\overline{\mathcal{W}_{D_5}}\right]_{[0,0,0,0,0]}^{[0,2,0,0,0]}$ and $\left[\overline{\mathcal{W}_{D_5}}\right]_{[0,0,0,0,0]}^{[1,0,0,2,0]}$, respectively. The latter can also be identified as the normalisation of the orbit $\overline{\mathcal{O}}_{(3^2,2^2)}^{D_5}$, calculated using the

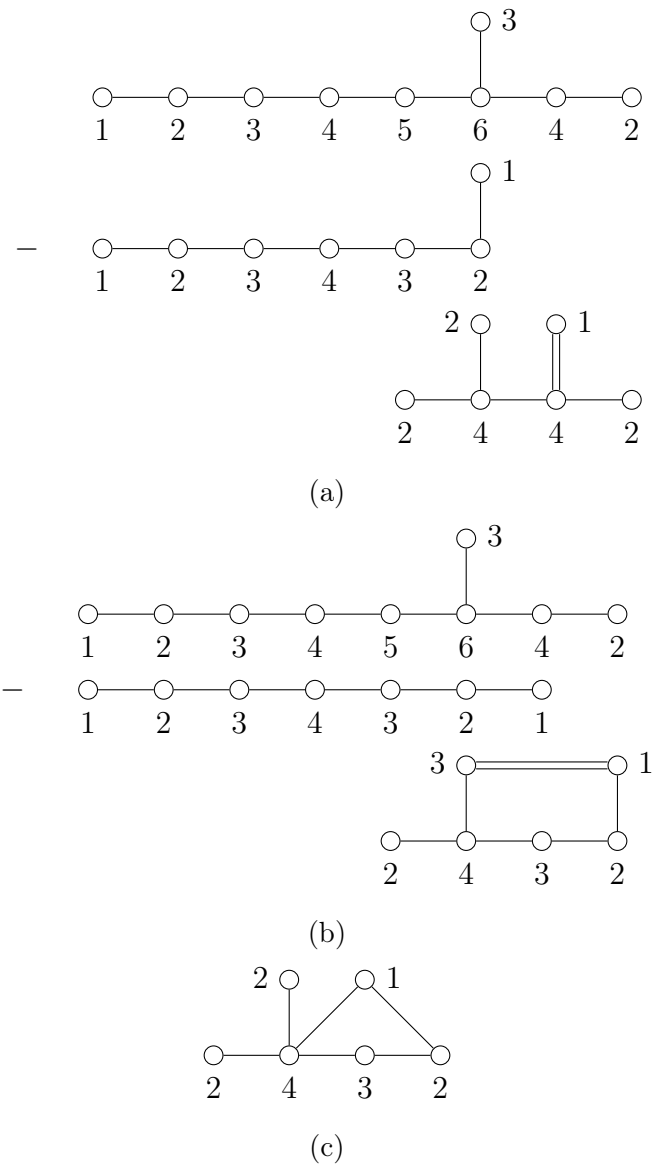


Figure 4.13: Both alignments of the SU(4) quotient quiver against $\overline{min.E_8}$ to produce quivers $\mathcal{Q}_{4.13a}$ and $\mathcal{Q}_{4.13b}$. Their intersection, reached via A_1 KP transitions, is $\mathcal{Q}_{4.13c}$.

Nilpotent Orbit Normalisation formula [184]. We conclude that:

$$\overline{min.E_8}///\mathrm{SU}(4) = \overline{[\mathcal{W}_{D_5}]}^{[0,2,0,0,0]}_{[0,0,0,0,0]} \cup \overline{[\mathcal{W}_{D_5}]}^{[1,0,0,2,0]}_{[0,0,0,0,0]} \tag{4.21}$$

The intersection $\mathcal{Q}_{4.13c}$, related in both cases by an A_1 KP transition, is a magnetic quiver whose Coulomb branch is also a slice in the affine Grassmannian of D_5, $\overline{[\mathcal{W}_{D_5}]}^{[1,0,1,0,0]}_{[0,0,0,0,0]}$. Comparison of the volumes of the Coulomb branches indicates it is also the double cover of the orbit $\overline{\mathcal{O}}^{D_5}_{(3^2,1^4)}$. This is in accordance with the Springer correspondence and geometric Satake equivalence, as discussed in [216].

This identity can be checked explicitly using Weyl integration under the embedding of $E_8 \hookleftarrow \mathrm{SO}(10) \times \mathrm{SU}(4)$ which decomposes the fundamental of E_8 as:

$$(\mu_7)_{E_8} \to \mu_2 + \nu_1\nu_3 + \mu_5\nu_3 + \mu_4\nu_1 + \mu_1\nu_2 \tag{4.22}$$

Chapter 5

Quotient Quiver Subtraction – Classical Groups

5.1 Introduction

The previous Chapter introduced SU(n) quotient quiver subtraction which is a combinatorial procedure for gauging SU(n) subgroups of the (IR) Coulomb branch isometry of quivers with unitary gauge groups.

In this Chapter the combinatorial method for gauging Sp(n), SO(n), and Sp(n) coupled to a half-hypermultiplet of Coulomb branch global symmetry subgroups is presented. The derivation of the rules uses Type IIB brane systems with O5 planes and their S-dual the ON. The use of brane systems makes the duality between flavour symmetry gauging and Coulomb branch global symmetry gauging explicit. The resulting algorithms also involve a subtraction of quivers but also involve changing the graph type to that of Dynkin type B, C, or D.

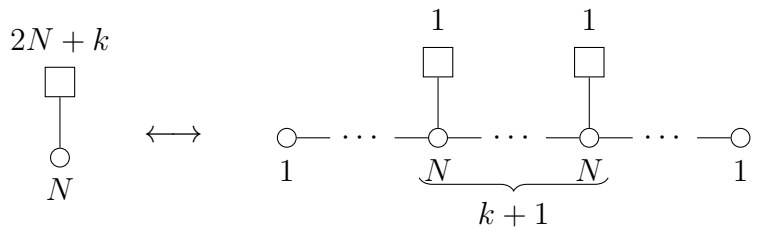
The prescription for these quotient quiver subtraction algorithms, much like in the previous Chapter, applies to quivers with a long enough leg of gauge nodes going from $(1) - (2) - \cdots$ which supports the symmetry being gauged. Furthermore it deals only with cases with *complete Higgsing* of the symmetry being gauged.

The Sp(n) and SO(n) quotient quiver subtraction are used to provide alternative checks of certain $4d$ $\mathcal{N}=2$ dualities in [215], with a more direct approach to deriving magnetic quivers. Further examples provide new relationships between the Higgs branches of certain rank-1 $4d$ $\mathcal{N}=2$ theories under gauging.

Organisation of the Chapter. Section 5.2 introduces the quotient quiver subtraction process for Sp(n) groups, Sections 5.3 and 5.4 repeat the process for SO($2n$) and SO($2n+1$) groups respectively. The case of gauging an Sp(n) with the addition of a half hypermultiplet is done in Section 5.5.

5.2 Sp(n) Quotient Quivers

An extension of the unitary Coulomb branch gauging algorithm given in Chapter 4 involves classical Lie groups of BCD-type. In the following derivation, the logic of appealing to the mirror-theory is made clear, alongside its underpinning in brane systems.



(5.1)

Consider the U(N) SQCD with $2N+k$ flavours in the left hand side of (5.1). Gauging an Sp(n) subgroup of the flavour symmetry returns the theory $\mathcal{Q}_{5.1a}$ in Figure 5.1a with Type IIB brane system realisation in Figure 5.1b. The gauging of an Sp(n) Coulomb branch global symmetry is seen through the corresponding $3d$ mirrors. The $3d$ mirror theory of $\mathcal{Q}_{5.1a}$ is $\mathcal{Q}_{5.1c}$ drawn in Figure 5.1c. The corresponding S-dual brane system is given in Figure 5.1d. Comparing $\mathcal{Q}_{5.1c}$ to the $3d$ mirror of the U(N) SQCD theory, in the right hand side of (5.1) leads to a candidate for the quotient quiver, given in (5.2). Figure 5.1c also shows that a second operation, here termed "splitting", is necessary in order to correctly realise the gauging. Morally, this is the

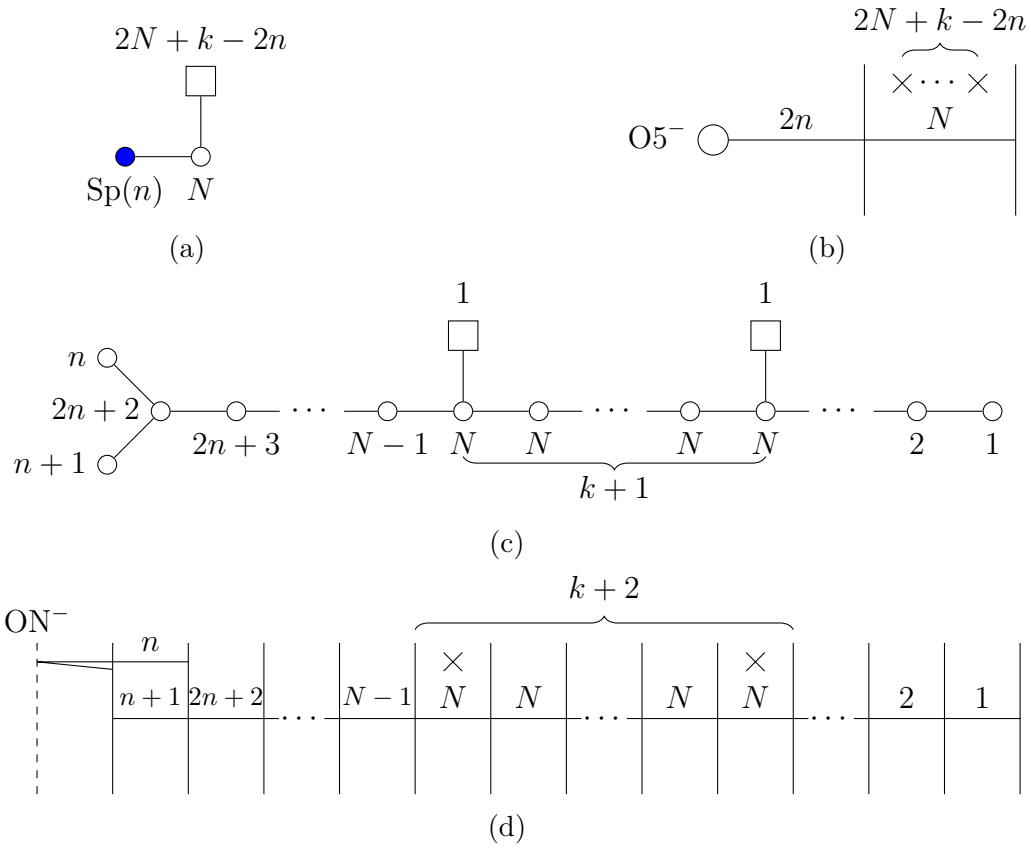
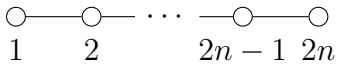


Figure 5.1: Gauging an Sp(n) flavour subgroup of U(N) SQCD with $2N+k$ flavours gives the theory drawn in Figure 5.1a with the corresponding Type IIB brane system drawn in the electric phase in Figure 5.1b. The 3d mirror theory is drawn in $\mathcal{Q}_{5.1c}$ with its corresponding Type IIB brane system in electric phase drawn in Figure 5.1d.

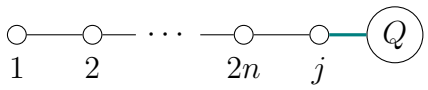
effect of an ON$^-$ plane. Note that the total rank of the quotient quiver (5.2) is $n(2n+1)$, equal to the dimension of Sp(n) – the splitting operation does not change the rank of the theory. Note also that rebalancing with an additional U(1) gauge node is not required for Sp(n) gauging.

Sp(n) Quotient Quiver  (5.2)

Formal Statement of the Rule The Sp(n) quotient quiver subtraction procedure gauges an Sp(n) subgroup of the Coulomb branch symmetry of any generic, framed or unframed unitary target quiver. The precise rules are given below.

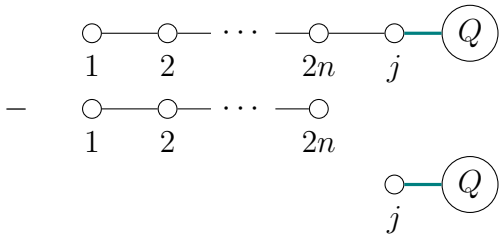
1. Take a target quiver with a long leg of gauge nodes up to at least U($2n$) and at least one

more non-negatively balanced gauge node, denoted U(j). The edge in teal denotes some generic connection to the rest of the quiver Q, the only restriction is that the long leg must correspond to long roots of the Coulomb branch global symmetry algebra.



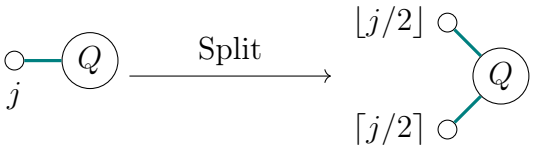
(5.3)

2. Align the Sp(n) quotient quiver against the leg of the target quiver and subtract the ranks of the quotient quiver from those of the target. This deletes the gauge nodes from U(1) up to U($2n$) in the maximal chain, leaving only U(j). Rebalancing is not required.



(5.4)

3. Split the U(j) into two gauge nodes of U($\lceil j/2 \rceil$) and U($\lfloor j/2 \rfloor$), which inherit all links and flavours of the U(j) node in teal.



(5.5)

Comments Note that the case of Sp(1) quotient quiver subtraction precisely matches that of the SU(2) quotient quiver subtraction introduced in Chapter 4. Note also that the Sp(n) quotient quiver is "half" of the SU($2n$) quotient quiver, indicating the $\mathbb{Z}_2$ which relates the two groups.

The change in the Higgs branch dimension after performing Sp(n) quotient quiver subtraction is

$$\Delta \dim \mathcal{H} = \left[-n^2 - (n+1)^2\right] - \left[\sum_{i=1}^{2n} i(i+1) - \sum_{i=1}^{2n+1} i^2\right]$$

$$= n = \text{Rk}\left(\text{Sp}(n)\right) \tag{5.6}$$

which is precisely the expected increase in Higgs branch dimension.

The Sp(n) quotient quiver subtraction requires a long leg of gauge nodes of the form $(1)-(2)-\cdots-(2n)-(j)-$ where the U($2n$) and U(j) nodes do not have to be balanced. Such a tail has at least $2n-1$ balanced gauge nodes contributing at least SU($2n$) Coulomb branch global symmetry. The Sp(n) is embedded inside this SU($2n$) as

$$[1,0,\cdots,0,1]_{\text{SU}(2n)} \to [2,0,\cdots,0]_{\text{Sp}(n)} + [0,1,0\cdots,0]_{\text{Sp}(n)} \tag{5.7}$$

This explains the origin of the Sp(n) symmetry that appears in the long leg. There may be an overall enhancement of the Coulomb branch global symmetry in the starting quiver, in which case the Sp(n) symmetry being gauged may admit an embedding directly into the enhanced global symmetry. Nevertheless, the Sp(n) symmetry should be thought of as sourced by the long leg of gauge nodes.

As mentioned, Sp(1) quotient quiver subtraction is identical to SU(2) quotient quiver subtraction, with many examples contained within [1]. Non-trivial examples of the algorithm begin with Sp(2), which requires a quiver with a maximal chain up to U(4) and at least one more non-negatively balanced gauge node.

5.2.1 $\overline{min.E_8}//\text{Sp}(2)$

Consider Sp(2) quotient quiver subtraction on the affine $E_8^{(1)}$ quiver, shown in two steps in Figure 5.2. The resulting theory is $\mathcal{Q}_{5.2}$, with unrefined Coulomb branch Hilbert series given

as

$$\mathrm{HS}\left[\mathcal{C}\left(\mathcal{Q}_{5.2}\right)\right] = \frac{\left(\begin{array}{l} 1+36t^2+812t^4+12735t^6+150112t^8+1375706t^{10}+10079822t^{12} \\ +60251599t^{14}+298785809t^{16}+1245721768t^{18}+4415307757t^{20} \\ +13424410658t^{22}+35275096941t^{24}+80598415736t^{26}+160929609663t^{28} \\ +281921275764t^{30}+434675562921t^{32}+591245656950t^{34} \\ +710641440658t^{36}+755494093072t^{38}+\cdots+t^{76} \end{array}\right)}{(1-t^2)^{19}(1-t^4)^{19}} \tag{5.8}$$

which does not illuminate the identity of the moduli space as a symplectic singularity but does identify the Coulomb branch global symmetry as SO(11) [64].

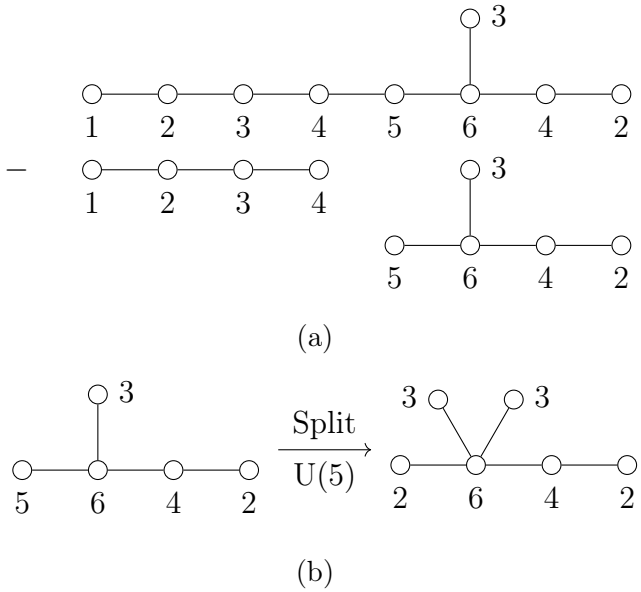


Figure 5.2: Sp(2) quotient quiver subtraction on the affine $E_8^{(1)}$ quiver which occurs in two steps. The first step is shown in 5.2a and involves the subtraction of the Sp(2) quotient quiver from the maximal leg. The second step, shown 5.2b, is the splitting of the U(5) node into a U(2) and U(3), producing the resulting quiver $\mathcal{Q}_{5.2}$. Note the emergence of an S_2 outer automorphism between the two U(3) gauge nodes.

The explicit Hilbert series of the hyper-Kähler quotient may be computed with Weyl integration with the following embedding $E_8 \hookleftarrow \mathrm{SO}(11) \times \mathrm{Sp}(2)$ which decomposes the adjoint as

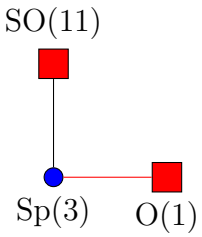
$$(\mu_7)_{E_8} \to \mu_2 + \nu_1^2 + \mu_1\nu_2 + \mu_5\nu_1 \tag{5.9}$$

where the $\mu_{1,2,3,4,5}$ and $\nu_{1,2}$ are highest weight fugacities for SO(11) and Sp(2) respectively.

The result from Weyl integration confirms that

$$\overline{min.E_8}///\mathrm{Sp}(2) = \mathcal{C}\left(\mathcal{Q}_{5.2}\right) \tag{5.10}$$

This construction is a realisation of the proposed duality of certain $4d$ $\mathcal{N}=2$ theories in [215, Table 2 Ex. 1] through magnetic quivers. The pertinent example here is that of the Sp(2) flavour symmetry gauging of the rank 1 E_8 SCFT [206–209] being dual to the following quiver $\mathcal{Q}_{5.11}$



(5.11)

where the red edge denotes a "bi-spinor". In [215, Table 2] this theory is given as Sp(3) with $\mathbf{14} \oplus 11 \cdot \mathbf{6}$. The $11 \cdot \mathbf{6}$ unambiguously refers to the 11 half-hypers. However, there are two 14-dimensional representations of Sp(3), the antisymmetric, $[0,1,0]$, and "spinor", $[0,0,1]$ (with the condition that the highest antisymmetric representation of Sp(n) is called the spinor). Cancellation of the Witten anomaly [213] requires the total Dynkin index of the matter representations to be an integer. The eleven half-hypers each contribute $T([1,0,0]) = 1/2$, the Dynkin index of the spinor is $T([0,0,1]) = 5/2$ which gives the desired cancellation, whereas the Dynkin index for the antisymmetric is $T([0,1,0]) = 2$ which does not give the required cancellation. Furthermore, the continuous commutant of Sp(2) inside E_8 is SO(11). The spinor is a pseudoreal representation meaning that there is an additional discrete O(1) flavour symmetry. The antisymmetric representation is real meaning that there would be an additional Sp(1) flavour symmetry which does not fit with the embedding of Sp(2) inside E_8.

For the purposes of this work, where the focus lies on magnetic quivers, the duality proposed in [215] suggests that the Coulomb branch of $\mathcal{Q}_{5.2}$ and the Higgs branch of $\mathcal{Q}_{5.11}$ are the same.

It is straightforward to compute the Higgs branch Hilbert series of $\mathcal{Q}_{5.11}$ to find agreement

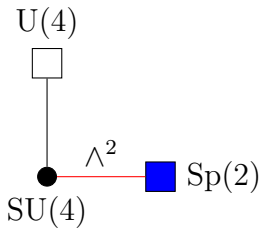
$$\mathcal{H}\left(\mathcal{Q}_{5.11}\right) = \mathcal{C}\left(\mathcal{Q}_{5.2}\right) \tag{5.12}$$

In particular this makes $\mathcal{Q}_{5.2}$ an example of a magnetic quiver for a rank-3 four dimensional theory. Magnetic quivers for rank-1 and rank-2 theories were studied in [51, 217]. The $\mathrm{O}(1) \simeq \mathbb{Z}_2$ flavour symmetry in $\mathcal{Q}_{5.11}$ is expressed in $\mathcal{Q}_{5.2}$ as the $\mathbb{Z}_2$ exchanging the two U(3) gauge nodes.

5.2.2 $(\overline{min.E_6} \times \mathbb{H}^{12})///\mathrm{Sp}(2)$

There is another proposed duality in [215, Table 2 Ex. 16] which states that the Sp(2) flavour symmetry gauging of the rank 1 E_6 SCFT [206–209] coupled to 12 free hypers is dual to SU(4) with four fundamental flavours and two antisymmetric.

The electric quiver is given below



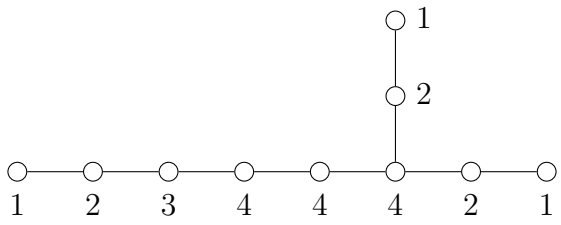
(5.13)

with the (unrefined) Higgs branch Hilbert series computed as

$$\mathrm{HS}\left[\mathcal{H}\left(\mathcal{Q}_{5.13}\right)\right] = \frac{\left(\begin{array}{l} 1+17t^2+36t^3+220t^4+564t^5+2192t^6+5456t^7+15897t^8+35388t^9 \\ +84385t^{10}+165040t^{11}+330357t^{12}+558676t^{13}+948191t^{14}+1360392t^{15} \\ +1931582t^{16}+2222620t^{17}+2460927t^{18}+1755844t^{19}+745362t^{20} \\ -1855388t^{21}-4328851t^{22}-8203044t^{23}-10166289t^{24}-12396256t^{25} \\ -10389664t^{26}-8125224t^{27}-936407t^{28}+4603732t^{29}+13037971t^{30} \\ +16246308t^{31}+19779930t^{32}+\cdots+t^{64} \end{array}\right)}{(1-t^2)^9(1-t^3)^{12}(1-t^4)^9} \tag{5.14}$$

The Hilbert series shows that the moduli space has global symmetry U(4) × Sp(2) as expected. The (quaternionic) dimension of the Higgs branch is 13 from counting $\dim \mathcal{H}\left(\mathcal{Q}_{5.13}\right) = \#\text{hypers} - \#\text{vectors}$. This is not immediately apparent in the Hilbert series above due to negative terms in the numerator, however the order of the pole of the Hilbert series at $t = 1$ is indeed 26 which means that the quaternionic dimension is 13.

The proposed dual to $\mathcal{Q}_{5.13}$ takes the rank 1 E_6 theory coupled to 12 free hypers and gauges Sp(2). In terms of magnetic quivers, the rank 1 E_6 theory has a magnetic quiver given by the affine $E_6^{(1)}$ quiver. The coupling of twelve free hypers can be done by the method of *quiver extension* [2] which is a form of quiver addition. The quiver extension needed in this example adds the finite A_4 quiver three times to the $E_6^{(1)}$ quiver resulting in the following magnetic quiver for the rank 1 E_6 theory coupled to 12 free hypers



(5.15)

The Sp(2) gauging proceeds with quotient quiver subtraction shown in Figure 5.3 to produce

$\mathcal{Q}_{5.3}$. Computation of the Coulomb branch Hilbert series indeed confirms that

$$\mathcal{C}\left(\mathcal{Q}_{5.3}\right) = \mathcal{H}\left(\mathcal{Q}_{5.13}\right) \tag{5.16}$$

so $\mathcal{Q}_{5.3}$ is a magnetic quiver for the Higgs branch of the $4d$ $\mathcal{N} = 2$ theory $\mathcal{Q}_{5.13}$.

This magnetic quiver was proposed in [218] through methods studying the theory $\mathcal{Q}_{5.13}$ as a class $\mathcal{S}$ theory and considering its S-dual frames. It may also be found from the explicit Type IIA brane system for SU(4) gauge theory with four flavours and two antisymmetric [131]. Quotient quiver subtraction provides an alternative construction for the magnetic quiver.

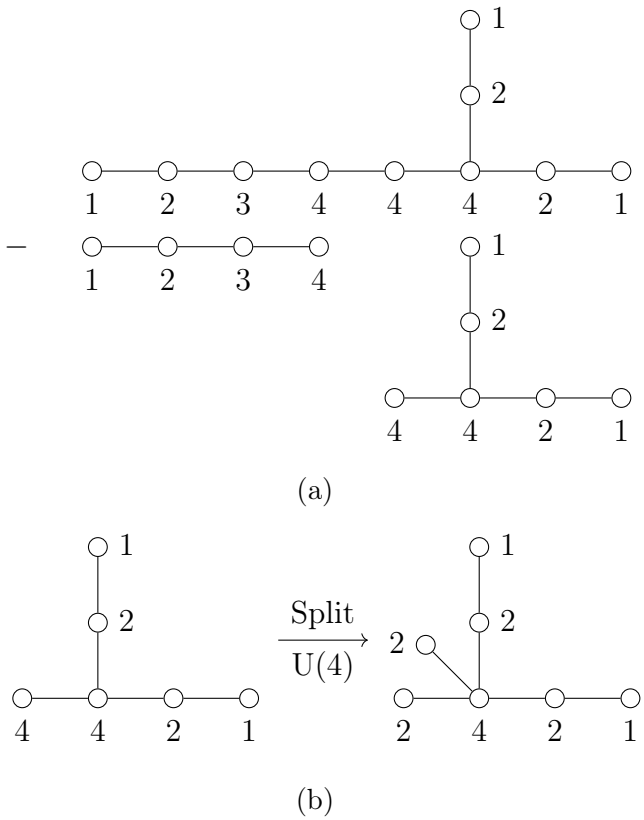
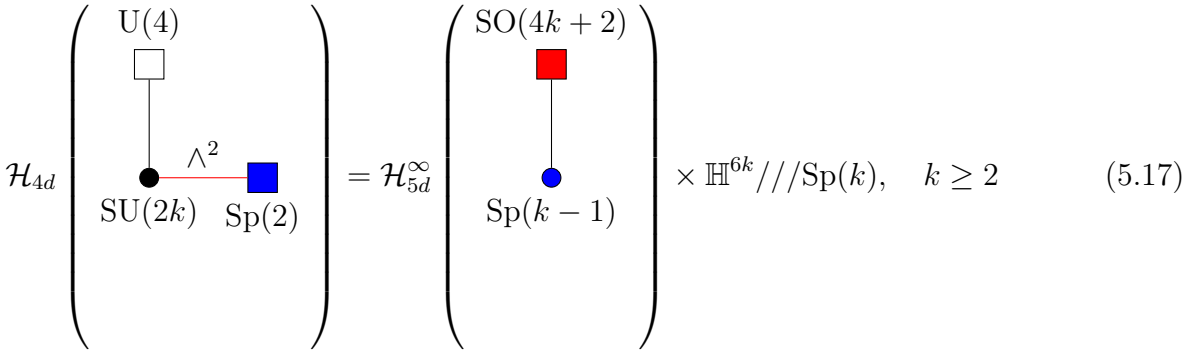


Figure 5.3: Sp(2) quotient quiver subtraction on the extended affine $E_6^{(1)}$ quiver $\mathcal{Q}_{5.15}$ which occurs in two steps. The first step is shown in 5.3a and involves the subtraction of the Sp(2) quotient quiver from the maximal leg. The second step, shown 5.3b, is the splitting of the U(4) node into two U(2) nodes producing the resulting quiver $\mathcal{Q}_{5.3}$.

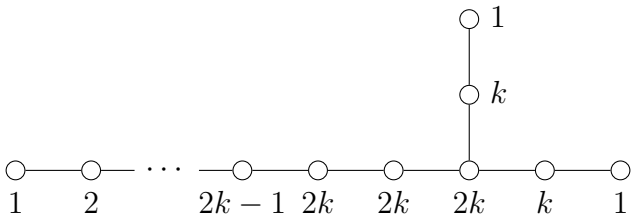
The arguments above can be employed to generalise the duality proposed in [215, Table 2 Ex.

16] to a one-parameter family of dualities. Specifically that



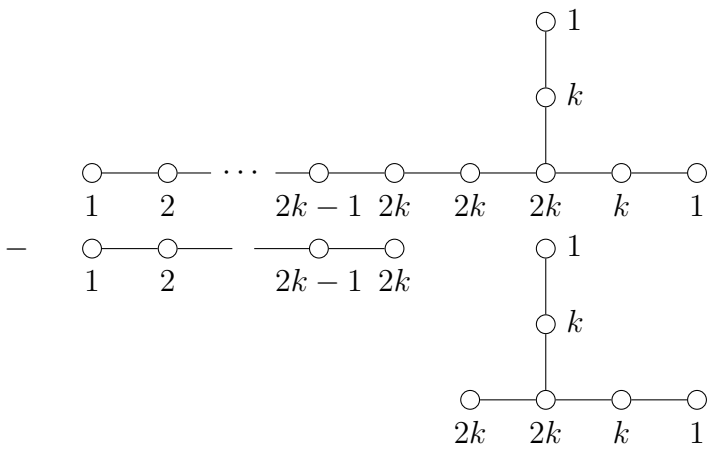
(5.17)

The magnetic quiver for the $5d$ theory can be extended by three nodes of $\mathrm{U}(2k)$ to incorporate the $\mathbb{H}^{6k}$ producing the following quiver

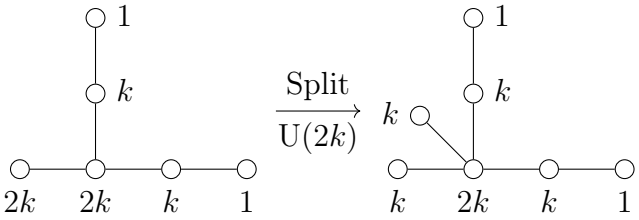


(5.18)

Then performing $\mathrm{Sp}(k)$ quotient quiver subtraction on $\mathcal{Q}_{5.18}$ is shown in Figure 5.4 to produce $\mathcal{Q}_{5.4}$ which is precisely what one reads from the Type IIA brane system for the $4d$ quiver in (5.17).



(a)



(b)

Figure 5.4: Sp(k) quotient quiver subtraction on $\mathcal{Q}_{5.18}$ which occurs in two steps. The first step is shown in 5.4a and involves the subtraction of the Sp(k) quotient quiver from the maximal leg. The second step, shown 5.4b, is the splitting of the U($2k$) node into two U(k) nodes producing the resulting quiver $\mathcal{Q}_{5.4}$.

5.3 SO($2n$) Quotient Quivers

The starting point for the analysis is once again the U(N) SQCD with $2N + k$ flavours given in (5.1). Gauging an SO($2n$) flavour symmetry subgroup (where $N \geq 2n + 1$ ensures positive balance) results in the theory $\mathcal{Q}_{5.5a}$ given in Figure 5.5a with Type IIB brane system in Figure 5.5b. This theory has an SU($2N + k - 2n$) flavour symmetry – the commutant of SO($2n$) inside SU($2N + k$) – and a Higgs branch of dimension $N(N + k) - n(2n + 1)$. The magnetic theory is $\mathcal{Q}_{5.5c}$ given in Figure 5.5c, alongside its brane system in Figure 5.5d. Comparing the magnetic theory of the SQCD before (5.1) and after (Figure 5.5c) gauging identifies the quotient quiver (5.19) and the subtraction prescription, given below.

Note that the total rank of the gauge nodes of the quotient quiver (5.19) is $n(2n-1)$, the same

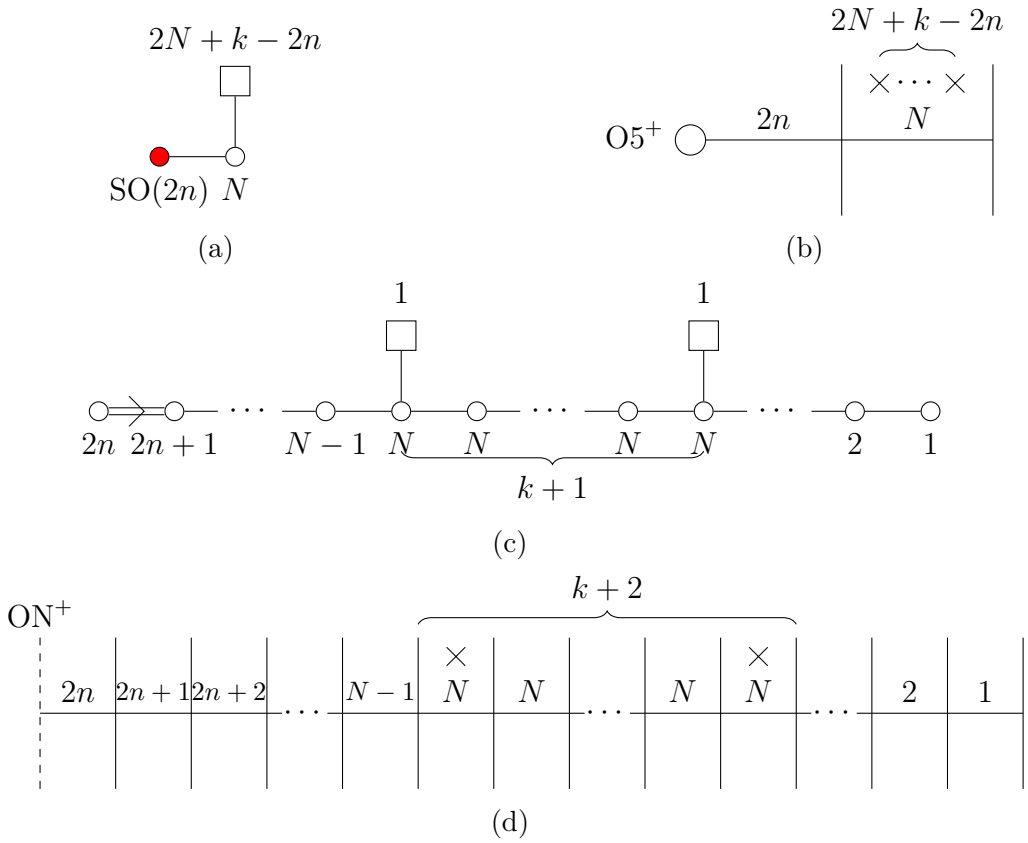
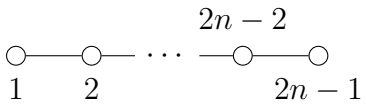


Figure 5.5: Gauging an SO($2n$) flavour subgroup of U(N) SQCD with $2N+k$ flavours returns the theory in Figure 5.5a, realised from the brane system in Figure 5.5b. The magnetic theory is conjectured to be Figure 5.5c, associated to the brane system in Figure 5.5d, related to that of Figure 5.5b by brane-creation and S-duality. Comparison to the mirror of the SQCD in (5.1) leads to the conjectural quotient quiver (5.19).

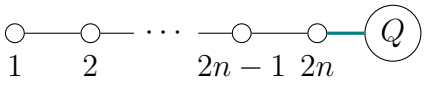
as the dimension of SO($2n$).

SO($2n$) Quotient Quiver  (5.19)

Formal statement of the rule The conjectured operation to gauge an SO($2n$) subgroup of the Coulomb branch global symmetry requires a long leg up to at least U($2n$) and involves the following steps.

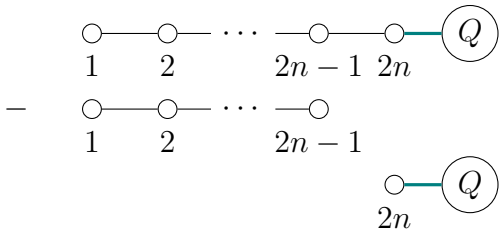
1. Take a target quiver with a long leg of gauge nodes up to at least U($2n$). As in Section

5.2, the edge in teal denotes some generic connection to the rest of the quiver Q.



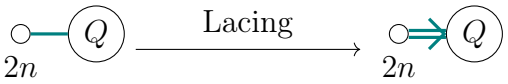
(5.20)

2. Align the SO($2n$) quotient quiver (5.19) against the leg of the target quiver and subtract the ranks of the quotient quiver from those of the target. This deletes the gauge nodes from U(1) up to U($2n-1$) in the maximal chain, leaving only U($2n$). Rebalancing is not required.



(5.21)

3. All edges connected to the U($2n$) gauge node double their non-simply laced-ness – the U($2n$) is the long root.



(5.22)

Note that SO($2n$) quotient quiver subtraction requires a leg of gauge nodes (1)−(2)−$\cdots$−($2n$)−, sourcing (at least) an SU($2n$) factor in the Coulomb branch global symmetry. The SO($2n$) being gauged is embedded in this SU($2n$) with discrete commutant, shown below.

$$[1,0,\cdots,0,1]_{\mathrm{SU}(2n)} \to [0,1,0,\cdots,0]_{\mathrm{SO}(2n)} + [2,0,\cdots,0]_{\mathrm{SO}(2n)} \tag{5.23}$$

In the case that the target quiver has enhanced global symmetry, the SO($2n$) being gauged may be embedded directly into that global symmetry. Nevertheless, it remains sourced by the long leg.

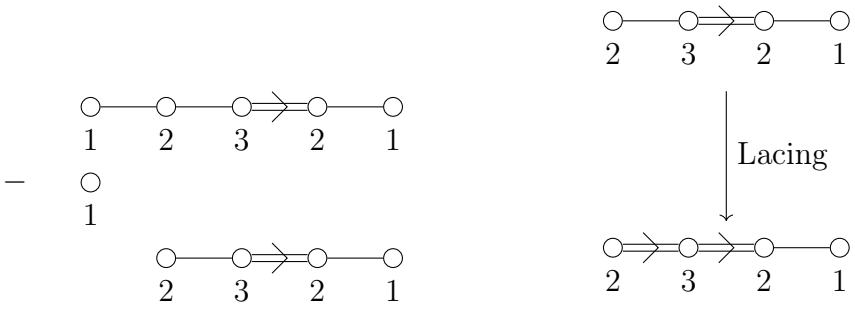
5.3.1 $\overline{min.F_4}///\mathrm{SO}(2)$

The affine $F_4^{(1)}$ quiver has Coulomb branch $\overline{min.F_4}$. It contains a tail of gauge nodes on the long side of the quiver which goes as $(1)-(2)-(3)-$ and is suitable for SO(2) quotient quiver subtraction. This operation is shown in Figure 5.6 and produces $\mathcal{Q}_{5.6}$, with the subtraction of the quotient quiver in Figure 5.6a and the non-simple lacing in Figure 5.6b.

The refined Coulomb branch Hilbert series of Figure 5.6 is cumbersome. However, the unrefined Coulomb branch Hilbert series is

$$\mathrm{HS}\left[\mathcal{C}\left(\mathcal{Q}_{5.6}\right)\right] = \frac{\left(\begin{array}{c} 1+14t^2+168t^4+854t^6+3136t^8+7062t^{10}+11991t^{12}+13708t^{14} \\ +11991t^{16}+7062t^{18}+3136t^{20}+854t^{22}+168t^{24}+14t^{26}+t^{28} \end{array}\right)}{(1-t^2)^7(1-t^4)^7} \tag{5.24}$$

Although this moduli space has no particular name, its Sp(3) symmetry can be confirmed from the refined Hilbert series (not presented here).



(a) (b)

Figure 5.6: SO(2) quotient quiver subtraction on the affine $F_4^{(1)}$ quiver occurs in two steps. The first is shown in 5.6a and involves the subtraction of the SO(2) quotient quiver from the maximal leg. The second step, given in 5.6b, is the non-simple lacing of the edge connecting the left U(2) node to the U(3), producing the resulting quiver $\mathcal{Q}_{5.6}$.

The conclusion is that

$$\overline{min.F_4}///\mathrm{SO}(2) = \mathcal{C}\left(\mathcal{Q}_{5.6}\right) \tag{5.25}$$

which is further verified from an explicit Weyl integration.

The following embedding of $F_4 \hookleftarrow \mathrm{Sp}(3)\times\mathrm{U}(1)$ is employed where the fundamental represen-

tation of F_4 decomposes as

$$(\mu_1)_{F_4} \to \mu_1 (q + 1/q) + \mu_2 \tag{5.26}$$

where the $\mu_{1,2}$ on the right hand side refer to Sp(3) highest weight fugacities and q is a U(1) fugacity.

5.3.2 $\overline{min.E_7}///\mathrm{SO}(4)$

The affine $E_7^{(1)}$ quiver has Coulomb branch $\overline{min.E_7}$. Its two maximal legs of (1)−(2)−(3)−(4)− each support an SO(4) quotient quiver subtraction. One such subtraction, shown explicitly in Figure 5.7, produces $\mathcal{Q}_{5.7}$. Although its refined Coulomb branch Hilbert series is cumbersome, the unrefined expression is

$$\mathrm{HS}\left[\mathcal{C}\left(\mathcal{Q}_{5.7}\right)\right] = \frac{\left(\begin{array}{c} 1 + 7t^2 + 100t^4 + 596t^6 + 3531t^8 + 13712t^{10} + 45536t^{12} + 112650t^{14} \\ + 233881t^{16} + 380039t^{18} + 519199t^{20} + 565768t^{22} + \cdots + t^{44} \end{array}\right)}{(1-t^2)^{11}(1-t^4)^{11}} \tag{5.27}$$

This moduli space, which has no particular name, has SO(6) × SU(2) symmetry, confirmed by the refined Hilbert series.

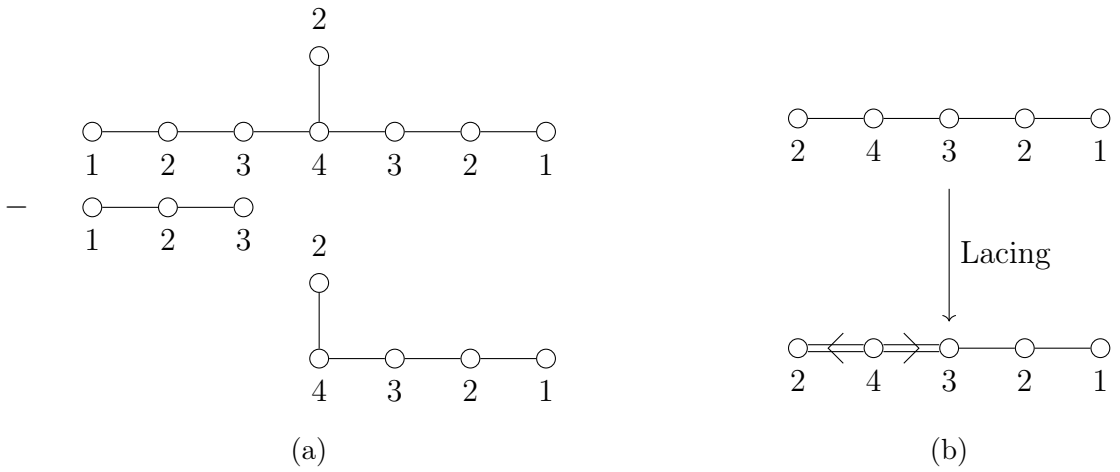


Figure 5.7: SO(4) quotient quiver subtraction on the affine $E_7^{(1)}$ quiver occurs in two steps. The first step, shown in 5.7a, involves the subtraction of the SO(4) quotient quiver from one maximal leg. The second step, in 5.7b, is the non-simple lacing of the two edges emerging from the U(4) node.

The same moduli space arises from Weyl integration and the embedding $E_7 \hookleftarrow \mathrm{SO}(12) \times \mathrm{SU}(2) \hookleftarrow \mathrm{SO}(6)\times\mathrm{SO}(6)\times\mathrm{SU}(2) \hookleftarrow \mathrm{SO}(4)\times\mathrm{SO}(6)\times\mathrm{SU}(2)$ which decomposes the $[0,0,0,0,0,1,0]$ of E_7 as

$$(\mu_6)_{E_7} \to \left(\mu_1 + \nu_1^2 + \nu_2^2\right)\rho + (\mu_2+\mu_3)\,\nu_1\nu_2 \tag{5.28}$$

Note that the μ, ν, and ρ are highest weight fugacities for SO(6), SO(4), and SU(2) respectively. The integration is performed with respect to the SO(4) fugacities.

5.3.3 $\overline{min.E_8}//\mathrm{SO}(4)$

Consider again the affine $E_8^{(1)}$ quiver, whose maximal leg $(1)-(2)-\cdots-(6)-$ admits an SO(4) quotient quiver subtraction. This operation, shown in Figure 5.8, produces $\mathcal{Q}_{5.8}$.

The refined Coulomb branch Hilbert series of Figure 5.8 is cumbersome – its unrefined form is

$$\begin{aligned}\mathrm{HS}\left[\mathcal{C}\left(\mathcal{Q}_{5.8}\right)\right] = \frac{\left(\begin{array}{l} 1 + 22t^2 + 582t^4 + 10360t^6 + 154981t^8 + 1822118t^{10} + 17548922t^{12} \\ + 139175916t^{14} + 925774625t^{16} + 5219073951t^{18} + 25226111030t^{20} \\ + 105435301585t^{22} + 384139161711t^{24} + 1227840826079t^{26} \\ + 3462893979058t^{28} + 8658011097494t^{30} + 19269044472299t^{32} \\ + 38301892953919t^{34} + 68192783223365t^{36} + 108993744295329t^{38} \\ + 156680149569483t^{40} + 202847214133311t^{42} + 236754481344743t^{44} \\ + 249255260007352t^{46} + \cdots + t^{92} \end{array}\right)}{(1-t^2)^{23}(1-t^4)^{23}}\end{aligned} \tag{5.29}$$

This moduli space, which has no particular name as a symplectic singularity, has SO(10) global symmetry.

Weyl integration straightforwardly constructs the same moduli space under the embedding $E_8 \hookleftarrow \mathrm{SO}(16) \hookleftarrow \times\mathrm{SU}(4) \hookleftarrow \mathrm{SO}(10) \hookleftarrow \mathrm{SO}(4)\times\mathrm{SO}(10)$, which decomposes the adjoint of E_8 as

$$(\mu_7)_{E_8} \to \mu_2 + (1+\mu_1)\nu_1^2 + (\mu_4+\mu_5)\nu_1\nu_2 + (1+\mu_1)\nu_2^2 + \nu_1^2\nu_2^2 \tag{5.30}$$

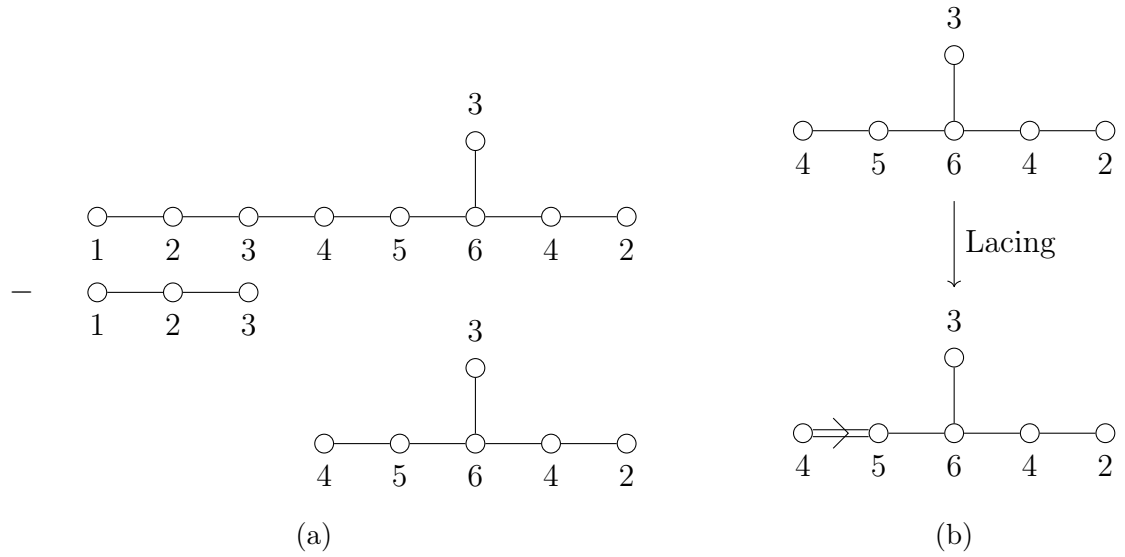
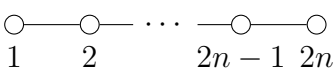


Figure 5.8: SO(4) quotient quiver subtraction on the affine $E_8^{(1)}$ quiver occurs in two steps. The first step is shown in 5.8a and involves the subtraction of the SO(4) quotient quiver from the maximal leg. The second step, shown 5.8b, is the non-simple lacing of the two edges going from the U(4) node producing $\mathcal{Q}_{5.8}$.

The μ and ν are highest weight fugacities for SO(10) and SO(4) respectively and the integration is performed with respect to the SO(4) fugacities.

5.4 SO($2n+1$) Quotient Quivers

The starting point for the analysis is once again the U(N) SQCD with $2N+k$ flavours given in (5.1). Gauging an SO($2n+1$) flavour symmetry subgroup results in the theory $\mathcal{Q}_{5.9a}$ given in Figure 5.9a with Type IIB brane system in Figure 5.9b. The magnetic theory is $\mathcal{Q}_{5.9c}$ given in Figure 5.9c, alongside its brane system in Figure 5.9d. Comparing the magnetic theory of the SQCD before (5.1) and after (Figure 5.9c) gauging identifies the quotient quiver (5.31) and the subtraction prescription, given below. The total rank of gauge nodes in the quotient quiver is $n(2n+1) = \dim(\mathrm{SO}(2n+1))$.

SO($2n+1$) Quotient Quiver 
 (5.31)

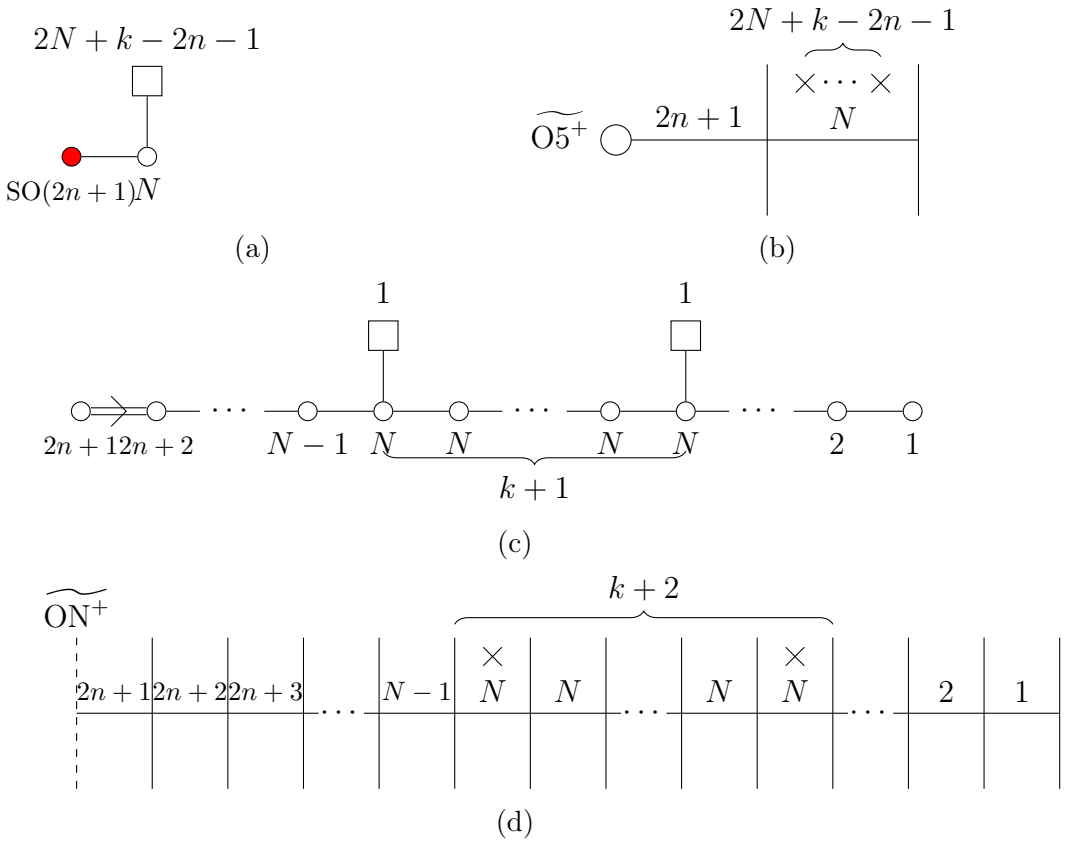
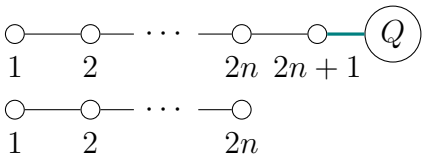


Figure 5.9: Gauging an SO($2n+1$) flavour subgroup of U(N) SQCD with $2N+k$ flavours returns the theory in Figure 5.9a, realised from the brane system in Figure 5.9b. The magnetic theory is conjectured to be Figure 5.9c, associated to the brane system in Figure 5.9d, related to that of Figure 5.9b by brane-creation and S-duality. Comparison to the mirror of the SQCD in (5.1) leads to the conjectural quotient quiver (5.31).

The gauging algorithm, which is almost identical to the SO($2n$) case, is given below for completeness.

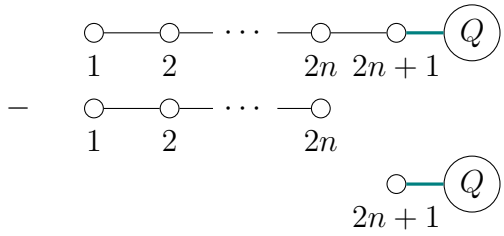
Formal Statement of the Rule

1. Take a target quiver with a long leg of gauge nodes up to at least U($2n+1$). The edge in teal denotes some generic connection to the rest of the quiver $\mathcal{Q}$ – the only restriction is that the long leg must correspond to long roots of the Coulomb branch global symmetry algebra.



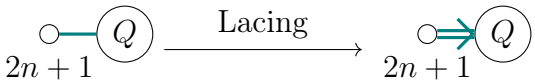
(5.32)

2. Align end of the SO$(2n+1)$ quotient quiver against the leg of the target quiver and subtract the ranks of the quotient quiver from those of the target. This deletes the gauge nodes from U(1) up to U$(2n)$ in the maximal chain, leaving only U$(2n+1)$. Rebalancing is not required.



(5.33)

3. All edges connected to the U$(2n+1)$ gauge node (shown in teal) double their non-simply laced-ness, with the U$(2n+1)$ corresponding to the long root.



(5.34)

Note that SO$(2n+1)$ quotient quiver subtraction requires a $(1)-(2)-\cdots-(2n+1)-$ long leg of gauge nodes, which sources (at least) an SU$(2n+1)$ factor of the Coulomb branch global symmetry. The SO$(2n+1)$ to be gauged is embedded with discrete commutant as follows.

$$[1,0,\cdots,0,1]_{\mathrm{SU}(2n+1)} \to [0,1,0,\cdots,0]_{\mathrm{SO}(2n+1)} + [2,0,\cdots,0]_{\mathrm{SO}(2n+1)} \tag{5.35}$$

This is exactly analogous to the embedding used for SO$(2n)$ quotient quiver subtraction. If the target quiver has enhanced global symmetry, the SO$(2n+1)$ being gauged may be embedded directly into that global symmetry. The origin remains in the gauge nodes in the long leg.

It is important to address the various degeneracies inspired by accidental isomorphisms. The $A_1 \cong B_1 \cong C_1$ isomorphism is particularly interesting as it establishes that SU(2) and Sp(1) quotient quiver subtraction are identical operations. Interestingly, SO(3) quotient quiver subtraction, and the B_1 embedding in the global symmetry of the long leg is distinct to that for A_1 and C_1. Explicitly, SO(3) is embedded inside an SU(3) of the long leg whereas SU(2) and Sp(1) are embedded inside SU(2). For similar reasons the $B_2 \cong C_2$ isomorphism does not extend to

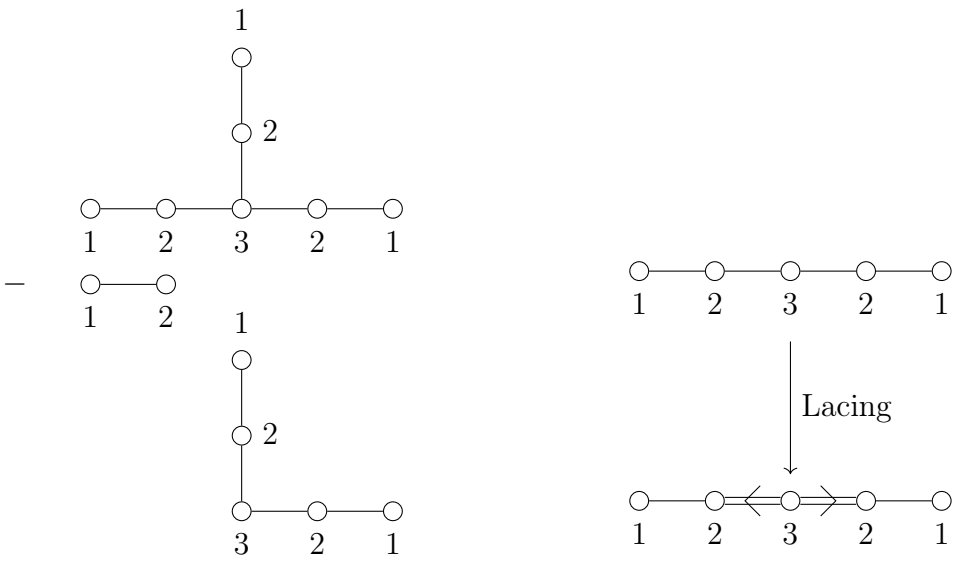
SO(5) and Sp(2) quotient quiver subtraction, both because the resulting quivers are different and because SO(5) is embedded inside SU(5) and Sp(2) is embedded inside SU(4).

5.4.1 $\overline{min.E_6}///\mathrm{SO}(3)$

The affine $E_6^{(1)}$ quiver's (1)−(2)−(3)− long leg is amenable to SO(3) quotient quiver subtraction. This is shown in Figure 5.10 and returns $\mathcal{Q}_{5.10}$. The refined Coulomb branch Hilbert series is unwieldy – the unrefined Coulomb branch Hilbert series is

$$\mathrm{HS}\left[\mathcal{C}\left(\mathcal{Q}_{5.10}\right)\right] = \frac{\left(\begin{array}{c} 1+8t^2+99t^4+479t^6+2095t^8+5355t^{10}+11577t^{12}+16622t^{14}+20072t^{16} \\ +16622t^{18}+11577t^{20}+5355t^{22}+2095t^{24}+479t^{26}+99t^{28}+8t^{30}+t^{32} \end{array}\right)}{(1-t^2)^8(1-t^4)^8} \tag{5.36}$$

This moduli space, which has no particular name as a symplectic singularity, has $\mathrm{SU}(3)\times\mathrm{SU}(3)$ symmetry, confirmed at the level of the refined Hilbert series. The same moduli space may be



(a) (b)

Figure 5.10: SO(3) quotient quiver subtraction on the affine $E_6^{(1)}$ quiver which occurs in two steps. The first step is shown in Figure 5.10a and involves the subtraction of the SO(3) quotient quiver from one maximal leg. The second step, shown in Figure 5.10b, is the non-simple lacing of the two edges going from the U(3) node producing $\mathcal{Q}_{5.10}$.

found through an explicit computation with Weyl integration. This requires the following

embedding of $E_6 \hookleftarrow \mathrm{SU}(3) \times \mathrm{SU}(3) \times \mathrm{SU}(3) \hookleftarrow \mathrm{SU}(3) \times \mathrm{SU}(3) \times \mathrm{SU}(2)$ which decomposes the $[1,0,0,0,0,0]$ of E_6 as

$$(\mu_1)_{E_6} \to \mu_2\nu_2 + (\mu_1 + \nu_1)\rho^2 \tag{5.37}$$

where the μ, ν, and ρ are highest weight fugacities for SU(3), SU(3), and SU(2) respectively. The integration is performed with respect to the SU(2) fugacity.

Notice that $\mathcal{Q}_{5.10}$ looks like two affine $F_4^{(1)}$ quivers which have been "polymerised" together. Indeed $\mathcal{Q}_{5.10}$ is related to the product of two minimal F_4 orbits with a hyper-Kähler quotient, through the action of "quiver polymerisation", a technique discussed in Chapter 6. This yields the following equalities

$$\overline{min.E_6}///\mathrm{SO}(3) = \left(\overline{min.F_4} \times \overline{min.F_4}\right)///\mathrm{SU}(3) = \mathcal{C}\left[\mathcal{Q}_{5.10}\right] \tag{5.38}$$

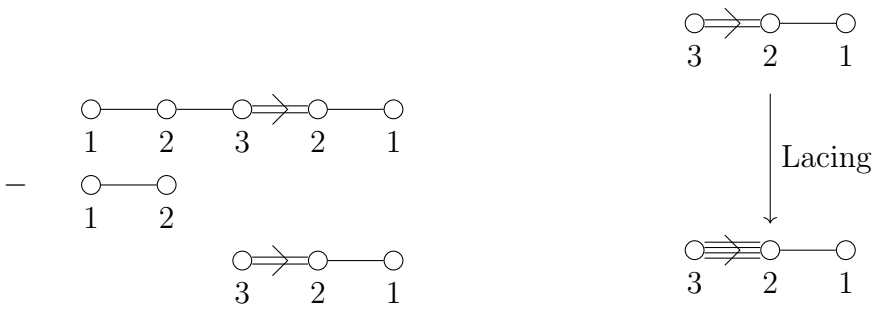
5.4.2 $\overline{min.F_4}///\mathrm{SO}(3)$

The affine $F_4^{(1)}$ quiver's $(1)-(2)-(3)-$ long leg is also amenable to an SO(3) quotient quiver subtraction. This operation is shown in Figure 5.11 and produces $\mathcal{Q}_{5.11}$, with the subtraction of the quotient quiver in Figure 5.11a and the non-simple lacing in Figure 5.11b. It is important in the non-simple lacing step to note that the edge connecting the U(3) and U(2) goes from multiplicity two to multiplicity four.

The refined Coulomb branch Hilbert series of Figure 5.11 is cumbersome to present, however the unrefined Coulomb branch Hilbert series is presented as

$$\mathrm{HS}\left[\mathcal{C}\left(\mathcal{Q}_{5.11}\right)\right] = \frac{1 + 3t^2 + 31t^4 + 55t^6 + 156t^8 + 132t^{10} + 156t^{12} + 55t^{14} + 31t^{16} + 3t^{18} + t^{20}}{(1-t^2)^5(1-t^4)^5} \tag{5.39}$$

This moduli space has no particular name as a symplectic singularity but it does have SU(3) symmetry which can be confirmed from the refined Hilbert series (not presented here). The same moduli space emerges from Weyl integration with the embedding $F_4 \hookleftarrow \mathrm{SU}(3) \times \mathrm{SU}(3) \hookleftarrow$



(a) (b)

Figure 5.11: SO(3) quotient quiver subtraction on the affine $F_4^{(1)}$ quiver occurs in two steps. The first step is shown in Figure 5.11a and involves the subtraction of the SO(3) quotient quiver from one maximal leg. The second step, shown in Figure 5.11b, is the non-simple lacing of the two edges going from the U(3) node producing $\mathcal{Q}_{5.11}$. Note that the non-simply laced-ness of this edge goes from two to four.

SU(3) × SU(2) decomposing the $[1,0,0,0]$ of F_4 as

$$(\mu_1)_{F_4} \to \mu_1\mu_2 + \left(1 + \mu_1^2 + \mu_2^2\right)\nu^2 + \nu^4 \tag{5.40}$$

Note that μ and ν are highest weight fugacities for SU(3) and SU(2) respectively. The integration is performed with respect to the SU(2) fugacity.

This quiver $\mathcal{Q}_{5.11}$ may be thought of as the folding [219] of $\mathcal{Q}_{5.10}$. This is an example of the commutation of quotient quiver subtraction and discrete operations on quivers, first noted in [1].

The quiver $\mathcal{Q}_{5.11}$ is also believed to be a magnetic quiver for the $4d$ $\mathcal{N} = 2$ rank-1 theory with flavour symmetry SU(3). This theory has been conjectured to be derived from the T^2 compactification with $\mathbb{Z}_4$ twist of the $6d$ $\mathcal{N} = (1,0)$ SU(4) gauge theory with 12 flavours and an antisymmetric [220]. The SO(3) quotient quiver subtraction in Figure 5.11 is suggestive of another construction of the Higgs branch of the rank-1 A_2 theory

$$\mathcal{H}(T_3^{\mathbb{Z}_2})///\mathrm{SO}(3) = \overline{min.F_4}///\mathrm{SO}(3) = \mathcal{H}(A_2) \tag{5.41}$$

where the T^3 theory enjoys a $\mathbb{Z}_2$ twist which changes the Higgs branch from $\overline{min.E_6}$ to $\overline{min.F_4}$ [169], seen in the magnetic quiver through folding [219].

5.5 $\mathbf{Sp}(n) + \frac{1}{2}\mathbf{F}$ Quotient Quivers

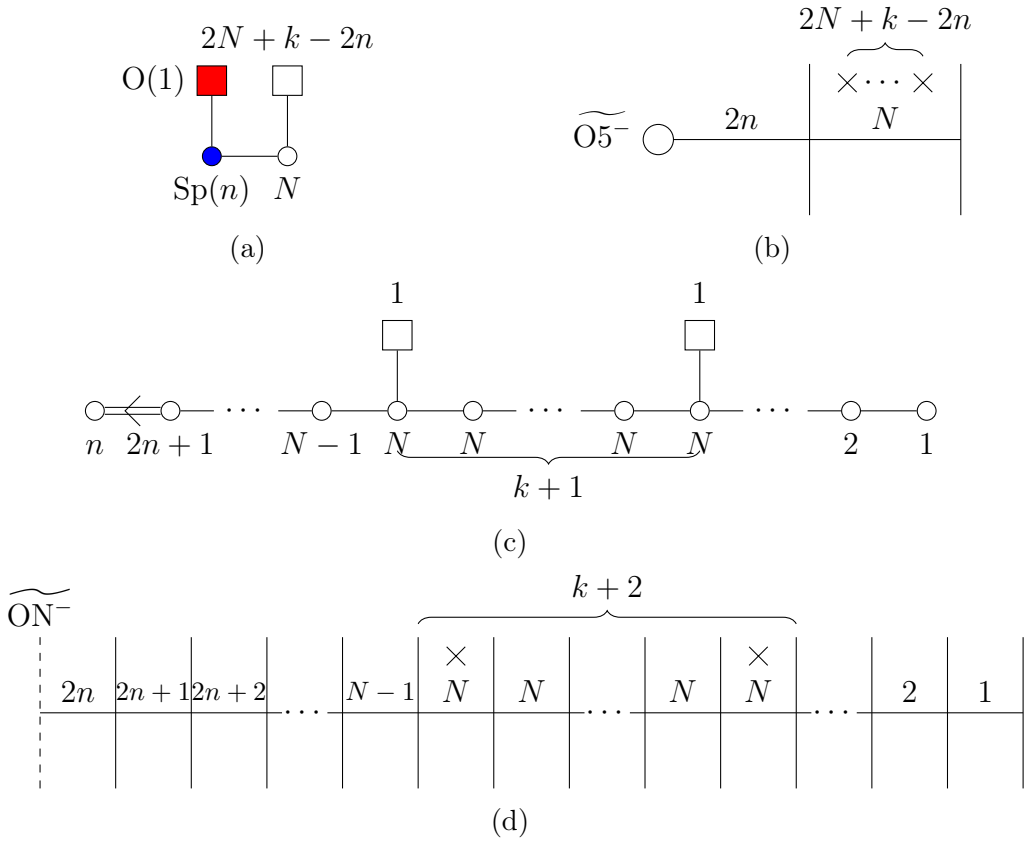
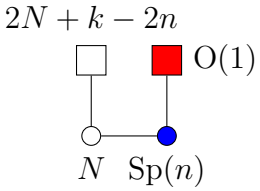


Figure 5.12: Gauging an $\mathrm{Sp}(n)+\frac{1}{2}$ flavour subgroup of $\mathrm{U}(N)$ SQCD with $2N+k$ flavours returns the theory in Figure 5.12a, realised from the brane system in Figure 5.12b. The magnetic theory is conjectured to be Figure 5.12c, associated to the brane system in Figure 5.12d, related to that of Figure 5.12b by brane-creation and S-duality. Comparison to the mirror of the SQCD in (5.1) leads to the conjectural quotient quiver (5.43).

In Sections 5.2, 5.3, and 5.4 a quotient quiver subtraction algorithm was presented to gauge $\mathrm{Sp}(n)$ and $\mathrm{SO}(n)$ subgroups of Coulomb branch global symmetries. Key to these derivations were Type IIB brane systems in the electric phase in the presence of $\mathrm{O5}^{\mp}$ and $\widetilde{\mathrm{O5}}^{+}$.

The final orientifold to complete the quartet is the $\widetilde{\mathrm{O5}}^{-}$. The starting point for the analysis is the $\mathrm{U}(N)$ SQCD with $2N+k$ flavours where k is positive, this parametrisation is for convenience but will not play a role in the resulting quotient quiver subtraction algorithm. Now consider

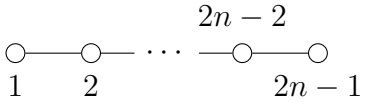
coupling a half-hypermultiplet of Sp(n) and gauge the Sp(n) resulting in



(5.42)

Immediately it is clear that this theory suffers from a Witten anomaly [213] due to the half-hypermultiplet coupled to Sp(n). As an academic exercise, one may consider the effect of this operation of gauging Sp(n) with a half-hyper on the magnetic quiver with the aim of this gauging to construct moduli spaces.

Comparing the magnetic theory of the SQCD before (5.1) and after gauging (Figure 5.12c) identifies the quotient quiver (5.43) and the subtraction prescription. The Sp(n) + $\frac{1}{2}$F quotient quiver is

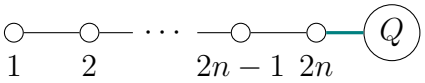


(5.43)

which has total gauge node rank of $n(2n-1)$, which is n short of the expected dimension reduction of gauging Sp(n) and adding a half-hyper, $2n^2$. However one should note that the leftmost gauge node in the quiver shown in Figure 5.12c is U(n) rather than U($2n$), this reduction of the rank by n compensates for the total rank of gauge nodes in the quotient quiver.

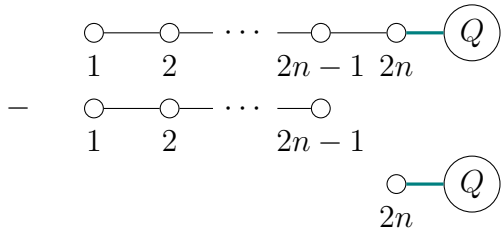
Formal Statement of the Rule

1. Take a target quiver with a long leg of gauge nodes up to at least U($2n$). The edge in teal denotes some generic connection to the rest of the quiver $\mathcal{Q}$ – the only restriction is that the long leg must correspond to long roots of the Coulomb branch global symmetry algebra.



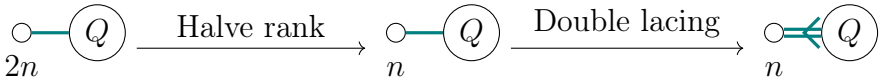
(5.44)

2. Align end of the $\mathrm{Sp}(n) + \frac{1}{2}\mathsf{F}$ quotient quiver against the leg of the target quiver and subtract the ranks of the quotient quiver from those of the target. This deletes the gauge nodes from $\mathrm{U}(1)$ up to $\mathrm{U}(2n-1)$ in the maximal chain, leaving only $\mathrm{U}(2n)$. Rebalancing is not required.



(5.45)

3. The resulting $\mathrm{U}(2n)$ gauge node has its rank halved to become $\mathrm{U}(n)$ and all edges in teal double their non-simply lacedness with the $\mathrm{U}(n)$ node being short.



(5.46)

5.5.1 $\left(\overline{min.E_6} \times \mathbb{H}\right) /\!/\!/ \mathrm{Sp}(1)$

A simple but non-trivial example of the $\mathrm{Sp}(1) + \frac{1}{2}\mathsf{F}$ quotient quiver subtraction is performed on the affine $E_6^{(1)}$ quiver to produce $\mathcal{Q}_{5.13}$ as shown in Figure 5.13.

The Coulomb branch Hilbert series may be computed exactly, but for brevity the unrefined Hilbert series is presented here as

$$\mathrm{HS}\left[\mathcal{C}\left(\mathcal{Q}_{5.13}\right)\right] = \frac{\left(\begin{array}{l} 1 + 17t^2 + 20t^3 + 117t^4 + 180t^5 + 392t^6 + 592t^7 + 701t^8 + 872t^9 \\ \quad + 701t^{10} + 592t^{11} + 392t^{12} + 180t^{13} + 117t^{14} + 20t^{15} + 17t^{16} + t^{18} \end{array}\right)}{(1-t^2)^{18}} \tag{5.47}$$

However the Highest Weight Generating function (HWG), computed from the refined Hilbert series is given as

$$\mathrm{HWG}\left[\mathcal{C}\left(\mathcal{Q}_{5.13}\right)\right] = \mathrm{PE}\left[\mu_1\mu_5 t^2 + \mu_3 t^3 + \mu_2\mu_4 t^4\right] \tag{5.48}$$

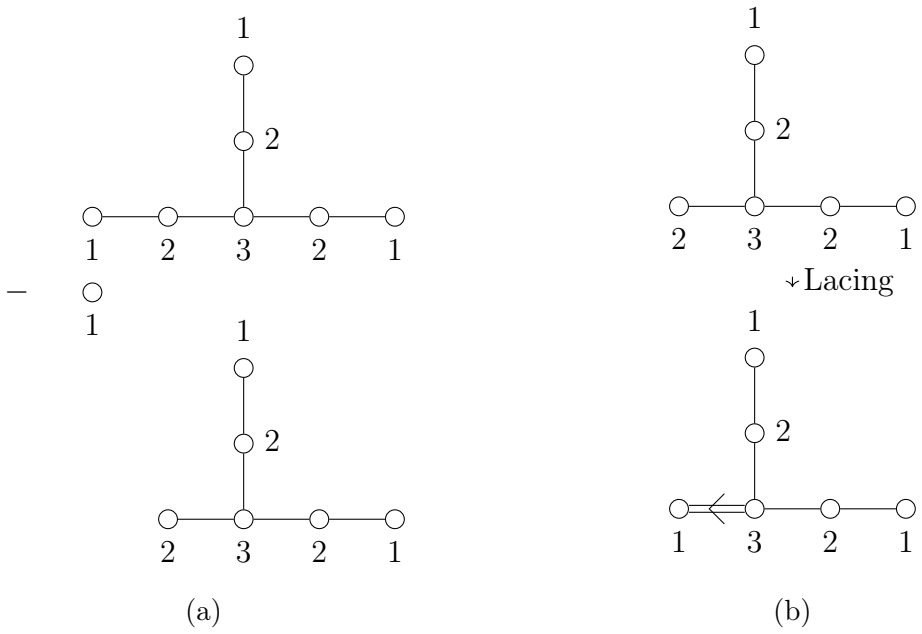
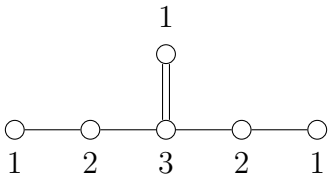


Figure 5.13: $\mathrm{Sp}(1) + \frac{1}{2}\mathsf{F}$ quotient quiver subtraction on the affine $E_6^{(1)}$ quiver which occurs in two steps. The first step is shown in Figure 5.13a and involves the subtraction of the $\mathrm{Sp}(1) + \frac{1}{2}\mathsf{F}$ quotient quiver from one maximal leg. The second step, shown in Figure 5.13b, is the non-simple lacing of the U(2) gauge node producing $\mathcal{Q}_{5.13}$.

identifies the moduli space as a Slodowy slice in the E_6 nilcone

$$\mathcal{C}\left(\mathcal{Q}_{5.13}\right) = \mathcal{S}^{E_6}_{3A_1,A_1} = \mathbb{Z}_2 \text{ Cover } \overline{\mathcal{O}}^{A_5}_{[0,0,2,0,0]} \tag{5.49}$$

The $\mathbb{Z}_2$ cover is apparent in the magnetic quiver $\mathcal{Q}_{5.13}$ since the difference between this quiver and the magnetic quiver for $\overline{\mathcal{O}}^{A_5}_{[0,0,2,0,0]}$, drawn in (5.50), is the non-simply laced edge of multiplicity two [136].



(5.50)

This result is verified with Weyl integration with the embedding of Sp(1) inside E_6 with commutant SU(6) decomposing the adjoint of E_6 as

$$(\mu_6)_{E_6} \to \mu_1\mu_5 + \nu^2 + \mu_3\nu \tag{5.51}$$

where the μ_i refer to SU(6) highest weights fugacity and ν refers to the Sp(1) highest weight fugacity. If an additional fugacity, a, for the O(1) is included, the HWG of the hyper-Kähler quotient is given as

$$\text{HWG}\left[\left(\overline{min.E_6}\times\mathbb{H}\right)///\text{Sp}(1)\right]=\text{PE}\left[\mu_1\mu_5t^2+a\mu_3t^3+\mu_2\mu_4t^4\right] \tag{5.52}$$

which explicitly gives the construction

$$\left(\overline{min.E_6}\times\mathbb{H}\right)///\text{Sp}(1)=\mathcal{C}\left(\mathcal{Q}_{5.13}\right)=\mathcal{S}^{E_6}_{3A_1,A_1}=\mathbb{Z}_2\text{ Cover }\overline{\mathcal{O}}^{A_5}_{[0,0,2,0,0]} \tag{5.53}$$

and as discrete quotients and hyper-Kähler quotients tend to commute, a simple corollary by gauging the $\mathbb{Z}_2$ in $\mathbb{H}$ [221]

$$\left(\overline{min.E_6}\times\mathbb{C}^2/\mathbb{Z}_2\right)///\text{Sp}(1)=\mathcal{S}^{E_6}_{3A_1,A_1}/\mathbb{Z}_2=\overline{\mathcal{O}}^{A_5}_{[0,0,2,0,0]} \tag{5.54}$$

which is related to the duality between the Sp(1) gauging of the rank-1 E_6 theory coupled to two free hypermultiplets and SU(3) with six flavours [215, 1].

Chapter 6

Quiver Polymerisation

6.1 Introduction

In this Chapter the gauging of subgroups of the Coulomb branch isometry of a $3d$ $\mathcal{N} = 4$ quiver gauge theory with unitary gauge groups is further explored. The methods introduced so far, in Chapters 4 and 5 make use of quotient quivers which seem to be related to one- and two-punctured spheres (the two-punctured case is commonly known as a cylinder) in class $\mathcal{S}$. The techniques introduced in this Chapter combine multiple $3d$ $\mathcal{N} = 4$ quivers together or introduce loops. This is closely related to gauging flavour symmetries in class $\mathcal{S}$ theories through their magnetic quivers [222, 223]. From the class $\mathcal{S}$ perspective, the quiver operation realises a gluing of two "maximal" or "full" punctures. This can be done to connect two different Riemann surfaces or to increase the genus of a given Riemann surface by one using cylinders. The effect is of gauging a diagonal flavour symmetry of the $4d$ $\mathcal{N} = 2$ theory which is associated to the maximal punctures. The action on the magnetic quiver is gauging the Coulomb branch global symmetry. In general, the possible (partial) gluings of class $\mathcal{S}$ theories have been well studied, such as through the "Tinkertoys" programme [218, 224–230] and in [231, 168, 232–236, 51, 66, 237, 238, 71, 239, 90, 240, 59], however, these do not have a realisation as operations on quivers in general.

The techniques described in this Chapter, called "chain polymerisation" and "cyclic polymerisa-

tion" on quivers, are inspired by and build on the technique established in [223]. This generalises the gauging of diagonal SU/U(n) subgroups of the Coulomb branch global symmetry of a wide range of $3d$ $\mathcal{N}=4$ theories. The action on the Coulomb branch can again be understood analytically in terms of hyper-Kähler quotients. The action on the Higgs branch is not precisely known, however the Higgs branch dimension increases by rank SU/U(n).

The quivers that can be subjected to polymerisation need to satisfy certain conditions. Importantly, polymerisation requires at least two quiver "legs" of the form $(1)-\cdots-(n)-\cdots$.

One use of chain and cyclic polymerisation on magnetic quivers pertains to finding new and non-trivial relationships between free field theories, nilpotent orbit closures [183, 184], Slodowy slices [133] and Slodowy intersections [134].

A different application of chain polymerisation is to study the Higgs branch of the worldvolume $6d$ $\mathcal{N}=(1,0)$ gauge theory of two fractional $\frac{1}{2}$ M5 branes [168] probing a Klein E_6 singularity. The fractionation effect is similar to that of NS5 branes splitting on an orientifold plane. Magnetic quivers have been instrumental in studying the Higgs branches of six dimensional worldvolume theories of (fractional) M5 branes probing ADE Klein singularities. In the cases where M5 branes probe AD Klein singularities it is possible to reduce M-theory to Type IIA and read off the electric and magnetic quiver from the brane system [241, 46, 155]. For the case of $E_{6,7,8}$ Klein singularity this is not possible and so other approaches such as through a dual description from F-theory constrains the form of the electric gauge theory [149, 168]. The case of interest here is one M5 brane on an E_6 Klein singularity; there may be fractionation to at most four $\frac{1}{4}$ M5 branes. If pairs of these $\frac{1}{4}$ M5 branes have zero separation, resulting in two separated $\frac{1}{2}$ M5 branes, the gauge theory description is as two rank-1 E-strings coupled to an SU(3) gauge group with finite coupling. This is constructed from the collapse of a (-3)-curve supporting SU(3) gauge symmetry. Therefore, the Higgs branch of this theory has a realisation through magnetic quivers as SU(3) chain polymerisation of two affine E_8 quivers. Similar techniques were used in [86, 90] to find magnetic quivers for certain $6d$ $\mathcal{N}=(1,0)$ theories.

Another application of cyclic polymerisation is to give a new construction of the moduli space of

k SU(N) instantons on $\mathbb{C}^2/\mathbb{Z}_l$. The first construction of instanton solutions for classical gauge groups on $\mathbb{C}^2$ was done by Atiyah-Drinfeld-Hitchin-Manin (ADHM) [24]. An interpretation of the ADHM solutions was found in Type IIA string theory [242] whose low energy effective theories are the ADHM quivers. The moduli space of instantons is the Higgs branch of the ADHM quivers. By definition this is a hyper-Kähler quotient construction on the Higgs branch. A later development by Kronheimer-Nakajima generalised the ADHM construction to find instanton solutions for k SU(N) instantons on $\mathbb{C}^2/\mathbb{Z}_l$ [26]. A result from this work in the context of supersymmetric gauge theories was the Kronheimer-Nakajima quiver which gave a Higgs branch construction for these moduli spaces. The Kronheimer-Nakajima quivers were then interpreted in Type IIA and in Type IIB string theory [42, 243, 128, 244]. This gave Higgs branch and Coulomb branch constructions for these moduli spaces through *electric* and *magnetic* quivers respectively. However, the Coulomb branch construction coming from magnetic quivers was as a moduli space of dressed monopole operators and not as a hyper-Kähler quotient.

Importantly for this Chapter, the A-type Kronheimer-Nakajima quivers for the moduli space of k SU(N) instantons on $\mathbb{C}^2/\mathbb{Z}_l$ consist of gauge nodes forming an affine A-type Dynkin diagram (a "necklace" of gauge nodes) with flavours attached to the gauge nodes. Therefore a natural application of cyclic polymerisation is to construct these Kronheimer-Nakajima quivers from quivers without loops. This gives a Coulomb branch hyper-Kähler quotient construction for these moduli spaces which is different to the known Coulomb branch construction. In fact, this construction is dual under $3d$ mirror symmetry to the Higgs branch hyper-Kähler quotient construction of these moduli spaces.

Organisation of the Chapter In Section 6.2, the diagrammatic prescription for chain and cyclic polymerisation is presented. For the corresponding Hilbert series analysis, the relevant embeddings into the Coulomb branch global symmetry and Weyl integration are also discussed. The properties of modified Hall-Littlewood functions are discussed to provide an analytical account of the equivalence between polymerisation and hyper-Kähler quotients over T[SU(n)] theories. Then, a discussion of the connection of polymerisation to class $\mathcal{S}$ theories is presented. Finally, a brief overview of the Kronheimer-Nakajima quiver and the moduli space of k SU(N)

instantons on $\mathbb{C}^2/\mathbb{Z}_l$ is presented.

In Section 6.3, the method of chain polymerisation is demonstrated. Examples are drawn upon magnetic quivers for moduli spaces of free fields and nilpotent orbits. Some of the resulting quivers take the form of Dynkin diagrams for Kac-Moody algebras.

In Section 6.4, the method of cyclic polymerisation is applied to construct the Kronheimer-Nakajima quivers for the moduli spaces of k SU(N) instantons on $\mathbb{C}^2/\mathbb{Z}_l$. Firstly, for specific choices of k, N, and l, then generically.

In Section 6.5, cyclic polymerisation is applied to quivers which are of finite and affine ADE type. A new magnetic quiver for a height 4 nilpotent orbit of SO(7) is found as well as magnetic quivers for slices in exceptional nilcones.

6.2 Chain and Cyclic Polymerisation

6.2.1 Diagrammatic methods

The diagrammatic techniques of chain polymerisation and cyclic polymerisation are shown schematically in Figure 6.1 and Figure 6.2 respectively. For simplicity all the quivers are taken to be unframed. These techniques realise the gauging of a subgroup of the Coulomb branch global symmetry of a $3d$ $\mathcal{N} = 4$ quiver theory. The action on the Coulomb branch is a hyper-Kähler quotient, as will be shown. The geometric action on the Higgs branch is not systematically known, but the Higgs branch dimension increases by the rank of the subgroup of the Coulomb branch global symmetry being gauged, as will be shown.

The first technique is chain polymerisation, shown in Figure 6.1, which gauges an SU(n) subgroup of the Coulomb branch global symmetry. Chain polymerisation requires two computable quivers (in the sense of monopole formula) $\mathcal{Q}_1$ and $\mathcal{Q}_2$, each containing a leg of $(1) - (2) - \cdots - (n)-$ which supports at least SU(n) symmetry. Each quiver also contains a background quiver, Q_1 and Q_2 respectively. These background quivers can be quite general

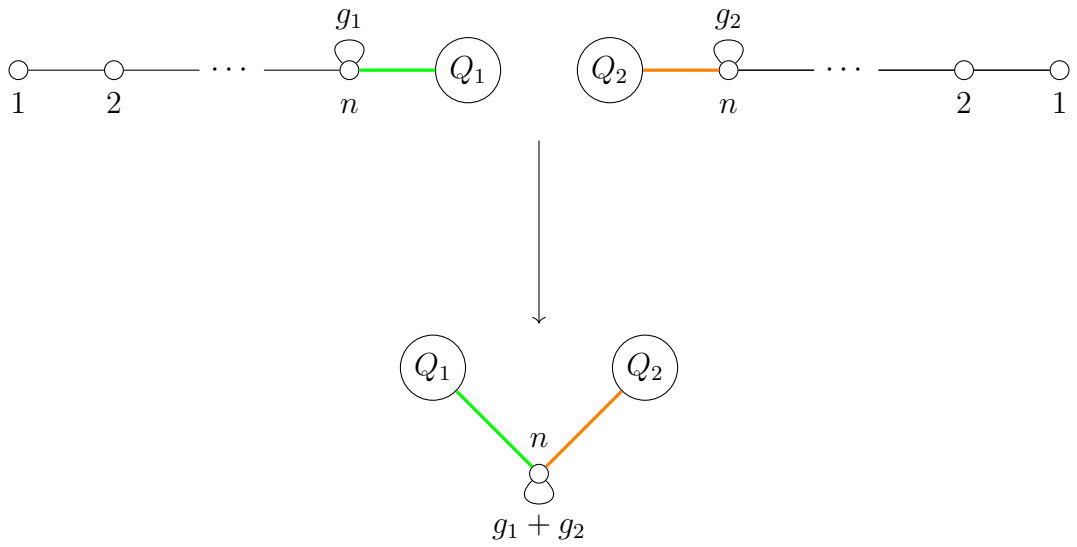


Figure 6.1: Schematic showing the chain polymerisation of two unframed quivers (assumed to be computable) with a node of U(n) on a leg to give a single unframed quiver.

and may have a multiplicity of links to the U(n) nodes. The background quivers may even be disconnected as long as each part is attached to the node of U(n). The gauge node of U(n) in each leg may also carry any number of adjoint hypermultiplet loops. The polymerisation action on the quivers superimposes the U(n) nodes and amputates the other nodes of the two legs. The resulting unframed quiver $\mathcal{Q}_3$ contains a single U(n) node connected to the background quivers Q_1 and Q_2, along with any adjoint hypermultiplet loops on each of the U(n) nodes. The action on the Coulomb branch is an SU(n) hyper-Kähler quotient of the product theory. The rank of the gauge group reduces by $n^2 - 1$ which is consistent with the reduction in Coulomb branch dimension after polymerisation being dim SU(n) $= n^2 - 1$. From counting Higgs branch dimensions, it is clear that the polymerised theory Q_3 has a Higgs branch that is greater in dimension by rank SU(n) $= n - 1$ compared to the unpolymerised product theory $\mathcal{Q}_1 \times \mathcal{Q}_2$. The only contribution to the difference in Higgs branch dimension comes from the amputation of $(1) - \cdots - (n-1)-$:

$$\begin{aligned}\dim\left[\mathcal{H}(\mathcal{Q}_3)\right] - \left(\dim\left[\mathcal{H}(\mathcal{Q}_1)\right] + \dim\left[\mathcal{H}(\mathcal{Q}_2)\right]\right) &= \left(0 - n^2 + 1\right) - 2\left(\sum_{i=1}^{n-1} i(i+1) - \sum_{i=1}^{n} i^2 + 1\right) \\ &= n - 1 \\ &= \text{rank SU}(n). \end{aligned} \tag{6.1}$$

In special cases where both of the starting quivers are $3d$ mirrors of class $\mathcal{S}$ theories, chain polymerisation at the central node reproduces the action of gluing two Riemann surfaces via maximal punctures.

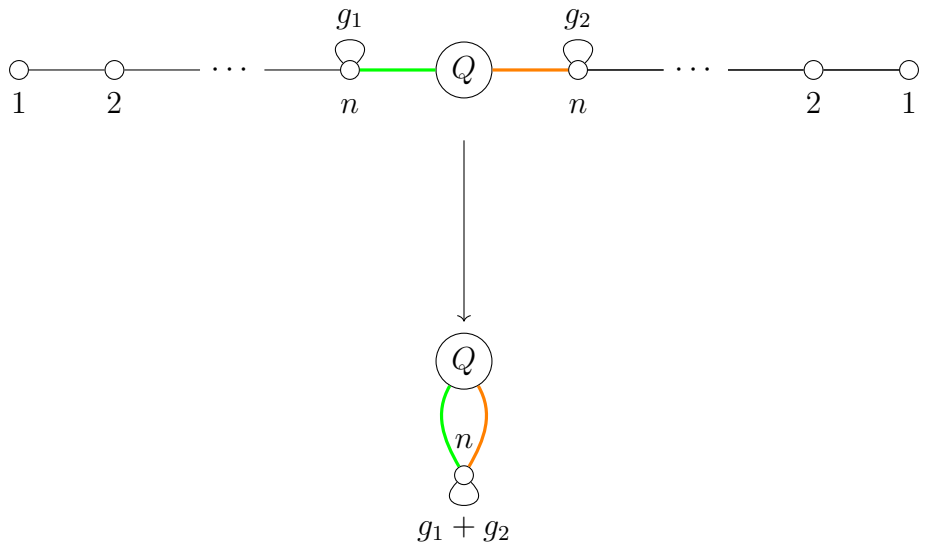


Figure 6.2: Schematic showing the cyclic polymerisation of some generic quiver (assumed good or ugly) with two external legs of $(1) - \cdots - (n) -$.

Cyclic polymerisation, shown in Figure 6.2, is similar to chain polymerisation in that two distinct legs are involved. However, in this case, the background quiver Q is common, so that the polymerisation acts on a single connected quiver $\mathcal{Q}$ (although the links from Q to the two $\mathrm{U}(n)$ nodes may differ). As before, each of the $\mathrm{U}(n)$ nodes may have adjoint hypermultiplet loops. The polymerisation action on the quivers superimposes the $\mathrm{U}(n)$ nodes in each leg and removes the other nodes in these legs. The net effect this time is a gauging of a $\mathrm{U}(n)$ subgroup of the Coulomb branch global symmetry, which corresponds to a $\mathrm{U}(n)$ hyper-Kähler quotient on the Coulomb branch. This is consistent with the rank of the gauge group being reduced by $\dim \mathrm{U}(n) = n^2$. The polymerised theory $\mathcal{Q}'$ has a Higgs branch that is greater in dimension by $\mathrm{rank}\, \mathrm{U}(n) = n$ compared to the unpolymerised theory $\mathcal{Q}$. Again, the difference in the Higgs branch dimension comes from the amputated legs:

$$\begin{aligned}\dim\left[\mathcal{H}(\mathcal{Q}')\right] - \dim\left[\mathcal{H}(\mathcal{Q})\right] &= \left(0 - n^2 + 1\right) - \left(2\sum_{i=1}^{n-1} i(i+1) - 2\sum_{i=1}^{n} i^2 + 1\right) \\ &= n\end{aligned}$$

$$= \text{rank U}(n). \tag{6.2}$$

In the special case of U(1) cyclic polymerisation the U(1) hyper-Kähler quotient of the Higgs branch of the polymerised theory is the Higgs branch of the unpolymerised theory. This special case exists because dim U(1) = rank U(1) = 1. There is no such special case for chain polymerisation as there is no non-trivial choice of n for which dim SU(n) = rank SU(n).

6.3 Chain Polymerisation Examples

The trivial case of chain polymerisation arises when two star shaped quivers are combined on their central nodes. The Literature already contains many examples [218, 109]. Here, the focus is on quivers that are not necessarily star-shaped, and on cases where the nodes being superimposed under the polymerisation are not generally central nodes. This in turn leads to the chaining of quivers. The examples presented below yield magnetic quivers for nilpotent orbit closures or slices in nilcones. Some of the quivers that are constructed take the form of Dynkin diagrams for some Kac-Moody algebras. This includes the construction for unitary quivers with B and D type endings at two ends that were first studied from brane systems with orientifold planes [130]. The string theory construction of [130] is reviewed in Section 2.7. These quivers take the form of affine or twisted affine Dynkin diagrams.

Quivers that take the form of finite Dynkin diagrams are labelled by the corresponding algebra and rank. Following the notation of [245], affine Dynkin diagrams are denoted with a superscript (1), as before, and twisted affine Dynkin diagrams are denoted with a superscript (2). Additionally, Dynkin diagrams which correspond to generalised Cartan matrices which admit *additive* functions[1] [246] are denoted with a preceding $\frac{1}{2}$ in the label also following the notation of [245]. This type of Dynkin diagram involves loops on the nodes. The gauge nodes for quivers that take the form of affine, twisted affine, or "additive" Dynkin diagrams are specified by the dual Coxeter labels unless otherwise stated.

[1] This means that the cokernel of the Cartan matrix is non-trivial, i.e. one is able to define non-trivial Coxeter labels for this Cartan matrix.

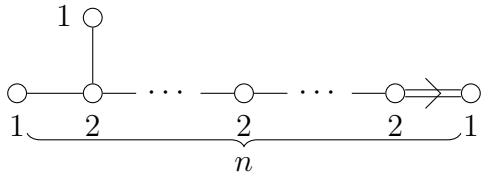
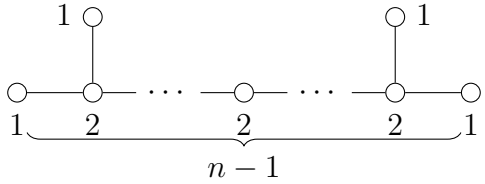
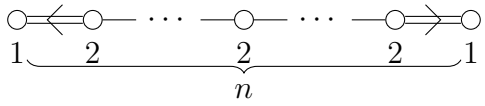
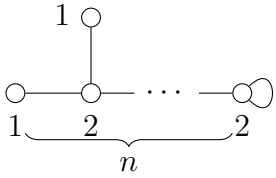
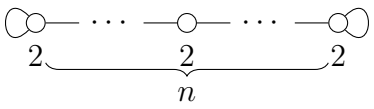
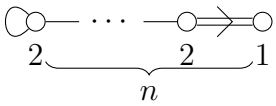
Label	Quiver	Coulomb Branch	Higgs Branch
$B_n^{(1)}$ $n \geq 2$		$\overline{min.B_n}$	–
$D_n^{(1)}$ $n \geq 3$		$\overline{min.D_n}$	D_n
$D_n^{(2)}$ $n \geq 3$		$\overline{min.D_n}$	–
$\frac{1}{2}D_{2n+1}^{(1)}$ $n \geq 3$		$\overline{n.min.B_n}$	$\mathcal{S}^{C_n}_{\mathcal{N},(2n-2,1^2)} \times \mathbb{H}$
$\frac{1}{2}A_{2n-1}^{(1)}$ $n \geq 1$		$\mathcal{S}^{C_{2n}}_{(4,2^{2n-2}),(2^{2n})}$	$\mathbb{H}^2 \times \mathcal{S}^{C_{2n}}_{((2n)^2),((2n-1)^2,1^2)}$
$\frac{1}{2}D_{2n+1}^{(2)}$ $n \geq 2$		$\overline{\mathcal{O}}^{D_n}_{(3,1^{2n-3})}$	–

Table 6.1: Some quivers which take the form of affine, twisted affine, or generalised Dynkin diagrams. The gauge nodes are specified by the dual Coxeter labels, except for $\frac{1}{2}A_{2n-1}^{(1)}$ where twice the dual Coxeter labels are used. The Coulomb branch and Higgs branch are identified where possible.

6.3.1 Affine $D_{k+p}^{(1)}$

A magnetic quiver for the product space of $\mathbb{H}^{2k} \times \mathbb{H}^{2p}$ may be given as a product of the finite D_{k+2} and D_{p+2} quivers. An SU(2) chain polymerisation, shown in Figure 6.3, produces the affine $D_{k+p}^{(1)}$ quiver. The resulting action on the Coulomb branch is:

$$\left(\mathbb{H}^{2k} \times \mathbb{H}^{2p}\right) /\!/\!/ \mathrm{SU}(2) = \overline{min.D_{k+p}}. \tag{6.3}$$

This is an alternative construction to the one using SU(2) quotient quiver subtraction in Section 4.3.

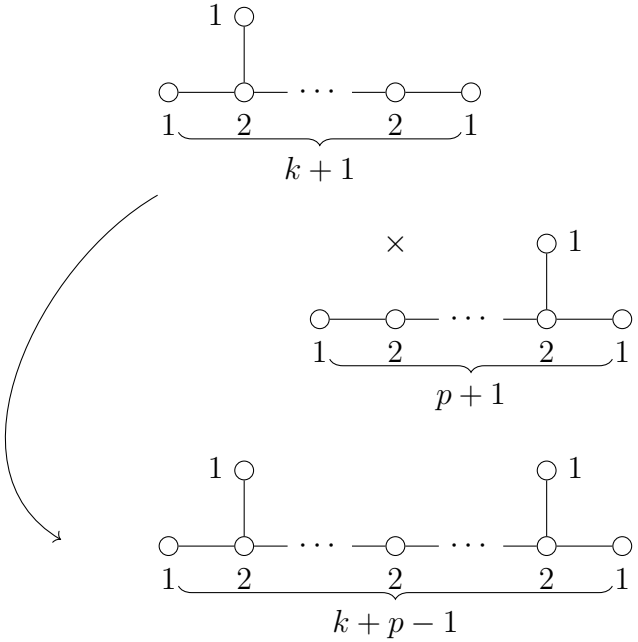


Figure 6.3: SU(2) chain polymerisation of the finite D_{k+2} and D_{p+2} quivers to produce the affine $D^{(1)}_{k+p}$ quiver.

Turning to the action of SU(2) chain polymerisation on the Higgs branches of these theories; the D_{k+2} and D_{p+2} quivers have trivial Higgs branches and the Higgs branch of the $D^{(1)}_{k+p}$ quiver is the Kleinian D_{k+p} singularity which is of dimension 1. There is an increase in the Higgs branch dimension by rank SU(2) = 1 as expected.

6.3.2 Affine $B^{(1)}_{k+p-1}$

The product moduli space $\mathbb{H}^{2k} \times \mathbb{H}^{2p-1}$ has a Coulomb branch construction as the product of the finite D_{k+2} and B_{p+1} quivers. The SU(2) chain polymerisation is performed in Figure 6.4 to produce the affine $B^{(1)}_{k+p-1}$ quiver.

The action on the Coulomb branch is:

$$\left(\mathbb{H}^{2k} \times \mathbb{H}^{2p-1}\right) /\!/\!/ \mathrm{SU}(2) = \overline{min.B_{k+p-1}}. \tag{6.4}$$

This is also an alternative construction to the one using SU(2) quotient quiver subtraction in Section 4.3.

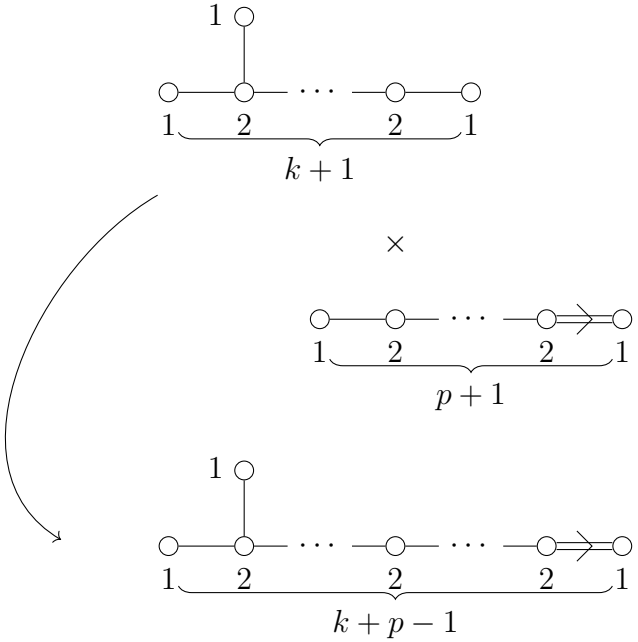


Figure 6.4: SU(2) chain polymerisation of the finite D_{k+2} and B_{p+1} quivers to produce the affine $B^{(1)}_{k+p-1}$ quiver.

No statement about the Higgs branch can be made as it is unknown how to compute Higgs branches of non-simply laced quivers.

6.3.3 Twisted affine $D^{(2)}_{k+p-1}$

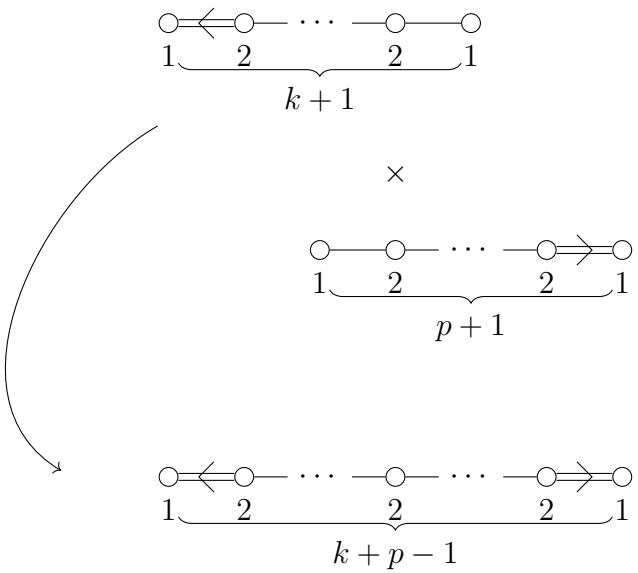


Figure 6.5: SU(2) chain polymerisation of the finite B_{k+1} and B_{p+1} quivers to produce the twisted affine $D^{(2)}_{k+p-1}$ quiver.

The product moduli space $\mathbb{H}^{2k-1} \times \mathbb{H}^{2p-1}$ has a Coulomb branch construction as the product of the finite B_{k+1} and B_{p+1} quivers. The SU(2) chain polymerisation is performed in Figure 6.5 to produce the twisted affine $D^{(2)}_{k+p-1}$ quiver.

The action on the Coulomb branch is:

$$\left(\mathbb{H}^{2k-1} \times \mathbb{H}^{2p-1}\right) ///\mathrm{SU}(2) = \overline{min.D_{k+p-1}}. \tag{6.5}$$

Although the result as an action on moduli spaces has been seen a few times now, it is derived from different quivers.

No statement about the Higgs branch can be made as it is unknown how to compute Higgs branches of non-simply laced quivers.

6.3.4 Additive $\frac{1}{2}D^{(1)}_{2k+2p-1}$

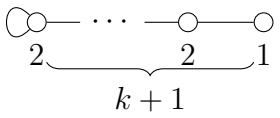


Figure 6.6: Unframed magnetic quiver $\mathcal{Q}_{6.6}$ for $\mathbb{C}^2/\mathbb{Z}_2 \times \mathbb{H}^{2k-1}$.

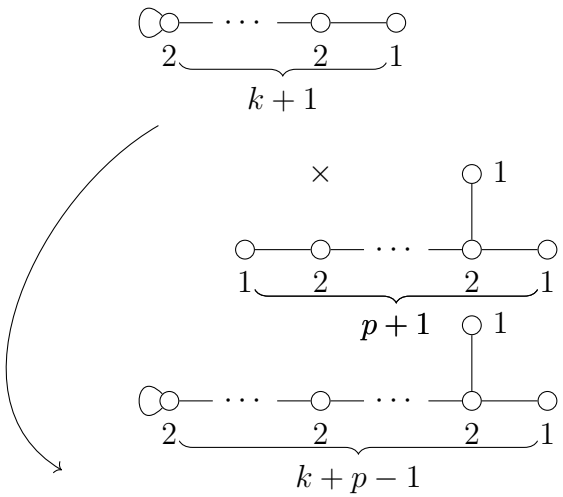


Figure 6.7: SU(2) chain polymerisation of $\mathcal{Q}_{6.6}$ with the finite D_{p+2} quiver to give the additive $\frac{1}{2}D^{(1)}_{2k+2p-1}$ quiver, $\mathcal{Q}_{6.7}$.

The Coulomb branch of $\mathcal{Q}_{6.6}$ is $\mathbb{C}^2/\mathbb{Z}_2 \times \mathbb{H}^{2k-1}$, which can be seen from explicit computation of the Hilbert series. This quiver is of the form of a Dynkin diagram for a generalised Cartan matrix which admits *subadditive* but not *additive functions*[2].

The product may be taken with the D_{p+2} quiver, whose Coulomb branch is $\mathbb{H}^{2p}$. When followed by an SU(2) chain polymerisation, as shown in Figure 6.7, this produces another magnetic quiver $\mathcal{Q}_{6.7}$ for $\overline{n.min.B_{k+p-1}}$. This quiver takes the form of the additive quiver $\frac{1}{2}D^{(1)}_{2k+2p-1}$. The conclusion on the Coulomb branch is that:

$$\left(\left(\mathbb{C}^2/\mathbb{Z}_2 \times \mathbb{H}^{2k-1}\right) \times \mathbb{H}^{2p}\right) /\!/\!/ \mathrm{SU}(2) = \overline{n.min.B_{k+p-1}}. \tag{6.6}$$

The Higgs branch Hilbert series for quiver $\mathcal{Q}_{6.6}$ is easily computed as:

$$\mathrm{HS}\left[\mathcal{H}(\mathcal{Q}_{6.6})\right] = \mathrm{PE}\left[[1]_{\mathrm{SU}(2)}t + [2]_{\mathrm{SU}(2)}t^2 - t^4\right]. \tag{6.7}$$

This identifies the Higgs branch as $\mathcal{H}(\mathcal{Q}_{6.6}) = \mathbb{C}^2/\mathbb{Z}_2 \times \mathbb{H}$, which is of dimension 2 and is independent of the number of nodes.

The Higgs branch Hilbert series for the quiver $\mathcal{Q}_{6.7}$ is also computed as:

$$\mathrm{HS}\left[\mathcal{H}(\mathcal{Q}_{6.7})\right] = \mathrm{PE}\left[[1]_{\mathrm{SU}(2)}t + [2]_{\mathrm{SU}(2)}t^2 + [1]_{\mathrm{SU}(2)}t^{2(k+p-1)-1} - t^{4(k+p-1)}\right]. \tag{6.8}$$

This indicates the Higgs branch is a complete intersection and of dimension 3 [247, 248]. In fact this Higgs branch can be identified as the product of a Slodowy slice of the GNO dual group, with a free field, $\mathcal{H}(\mathcal{Q}_{6.7}) = \mathcal{S}^{C_{k+p-1}}_{\mathcal{N},(2(k+p-2),1^2)} \times \mathbb{H}$. The SU(2) chain polymerisation gives the expected increase of Higgs branch dimension by rank SU(2) = 1.

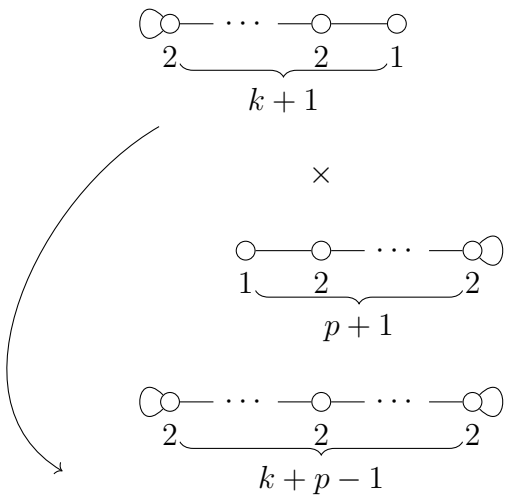


Figure 6.8: SU(2) chain polymerisation of $\mathcal{Q}_{6.6}$ with itself to give the additive $\frac{1}{2}A^{(1)}_{2k+2p-3}$ quiver, $\mathcal{Q}_{6.8}$.

6.3.5 Additive $\frac{1}{2}A^{(1)}_{2k+2p-3}$

The quiver type $\mathcal{Q}_{6.6}$, whose Coulomb branch is $\mathbb{C}^2/\mathbb{Z}_2\times\mathbb{H}^{2k-1}$, may be SU(2) chain polymerised with itself as shown in Figure 6.8. This produces an additive quiver $\frac{1}{2}A^{(1)}_{2k+2p-3}$, $\mathcal{Q}_{6.8}$. In this case the gauge nodes are specified by twice the dual Coxeter labels. This quiver is a magnetic quiver for $\mathcal{S}^{C_{2k+2p-2}}_{(4,2^{2k+2p-4}),(2^{2k+2p-4})}$. There are insufficient fugacities to give refined expressions for the Coulomb branch Hilbert series. However, there is agreement at the level of the unrefined Hilbert series. The conclusion on the Coulomb branch is that:

$$\left(\left(\mathbb{C}^2/\mathbb{Z}_2\times\mathbb{H}^{2k-1}\right)\times\left(\mathbb{C}^2/\mathbb{Z}_2\times\mathbb{H}^{2p-1}\right)\right)///\mathrm{SU}(2) = \mathcal{S}^{C_{2k+2p-2}}_{(4,2^{2k+2p-4}),(2^{2k+2p-2})}. \tag{6.9}$$

Note also that $\mathcal{C}(\mathcal{Q}_{6.8}) = \overline{min.D_{k+p}}/(\mathbb{Z}_2\times\mathbb{Z}_2)$, which can be seen from discrete gauging [241, 156, 219, 5]. The Higgs branch Hilbert series for $\mathcal{Q}_{6.8}$ is also easily computed. These do not have a simple expression as a PE and so the final result is quoted as

$$\mathcal{H}(\mathcal{Q}_{6.8}) = \mathbb{H}^2\times\mathcal{S}^{C_{2k+2p-2}}_{((2k+2p-2)^2),((2k+2p-3)^2,1^2)}. \tag{6.10}$$

[2]If the Cartan matrix admits subadditive functions that are not additive, one cannot define Coxeter labels by definition. For this reason the labelling of the gauge nodes of $\mathcal{Q}_{6.6}$ is judicious to find additive quivers whose gauge nodes are labelled by dual Coxeter labels.

This Higgs branch is of dimension 5 which is consistent with the increase in the Higgs branch dimension by rank SU(2) = 1.

A particularly interesting point is that the Coulomb branch and the (non-trivial part of) the Higgs branch of $\mathcal{Q}_{6.8}$ are not dual under the Barbasch-Vogan map. In fact, the Higgs and Coulomb branch are slices in the same nilcone of a C-type algebra[3]. This is an example of the *metaplectic* Lusztig-Spaltenstein duality [249, 250, 194].

6.3.6 Additive $\frac{1}{2}D^{(2)}_{2k+2p-1}$

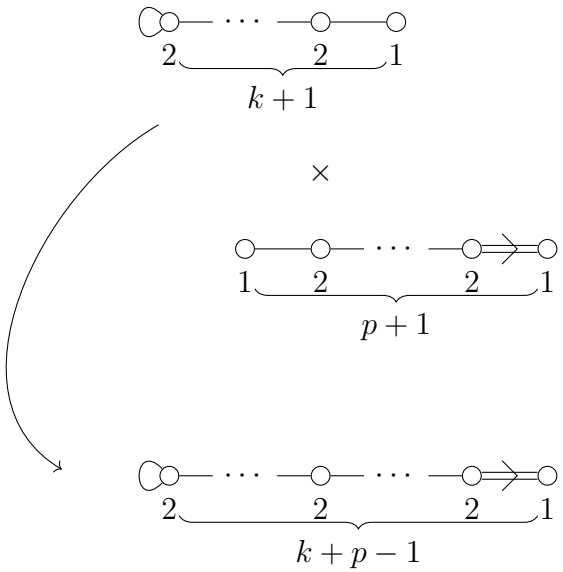


Figure 6.9: SU(2) chain polymerisation of $\mathcal{Q}_{6.6}$ with the finite B_{p+1} quiver to give the additive $\frac{1}{2}D^{(2)}_{2k+2p-1}$ quiver, $\mathcal{Q}_{6.9}$.

The quiver $\mathcal{Q}_{6.6}$, whose Coulomb branch is $\mathbb{C}^2/\mathbb{Z}_2 \times \mathbb{H}^{2k-1}$, may be SU(2) chain polymerised with the finite B_{p+1} quiver as shown in Figure 6.9; this produces another quiver $\mathcal{Q}_{6.9}$, which is the additive quiver $\frac{1}{2}D^{(2)}_{2k+2p-1}$. This quiver is a magnetic quiver for $\overline{\mathcal{O}}^{D_{k+p-1}}_{(3,1^{2k+2p-5})}$. There are insufficient fugacities to give refined expressions for the Coulomb branch Hilbert series. However, there is agreement at the level of the unrefined Hilbert series. The conclusion on the

[3]The partitions in this case are dual under the metaplectic Lusztig-Spaltenstein map, which is the usual Barbasch-Vogan map with an additional − collapse.

Coulomb branch is that:

$$\left(\left(\mathbb{C}^2/\mathbb{Z}_2 \times \mathbb{H}^{2k-1}\right) \times \mathbb{H}^{2p-1}\right) /\!/\!/ \mathrm{SU}(2) = \overline{\mathcal{O}}^{D_{k+p-1}}_{(3,1^{2k+2p-5})}. \tag{6.11}$$

The Higgs branch Hilbert series for $\mathcal{Q}_{6.9}$ cannot be computed due to the non-simply laced edge so no comment can be made about the Higgs branch.

6.3.7 Two $\frac{1}{2}$ M5 branes probing E_6 Klein Singularity

Now the topic is switched to demonstrate a different application of chain polymerisation in the context of $6d$ theories.

Consider an M-theory background with two $\frac{1}{2}$ M5 branes, spanning the directions $x^{0,1,2,3,4,5}$ and separated along the x^6 direction on an E_6 Klein singularity which spans the directions $x^{0,1,2,3,4,5,6}$. Each $\frac{1}{2}$ M5 brane comes from two $\frac{1}{4}$ M5 branes with zero separation along the x^6 direction. The F-theory dual description of four separated $\frac{1}{4}$ M5 branes consists of three curves with self-intersection numbers -1, -3, -1 where the (-1)-curves support an Sp(0) gauge group and the (-3)-curve supports an SU(3) gauge group [149, 168, 251]. The meaning of the Sp(0) gauge group is that there is no vector multiplet but there is a dynamical tensor multiplet. The F-theory description of the two separated $\frac{1}{2}$ M5 branes is derived from collapsing both the left and right (-1)-curves. In doing so the central (-3)-curve becomes a (-1)-curve, with a tensor multiplet, which still supports SU(3) gauge symmetry. The gauge coupling for the two Sp(0) becomes infinite. The gauge coupling for the SU(3) is finite as there is still non-trivial separation between the two $\frac{1}{2}$ M5 branes. However now there is coupling of two copies of the rank-1 E-string theory to SU(3). The brane system and electric quiver are summarised in Figure 6.10.

The Higgs branch of this theory can also be realised through magnetic quivers. The magnetic quiver for the rank-1 E-string theory is the $E_8^{(1)}$ quiver. The collapse of a (-3)-curve implies the gauging of a continuous subgroup of the Higgs branch global symmetry [72]. For this example, the operation on magnetic quivers is the SU(3) chain polymerisation of two $E_8^{(1)}$

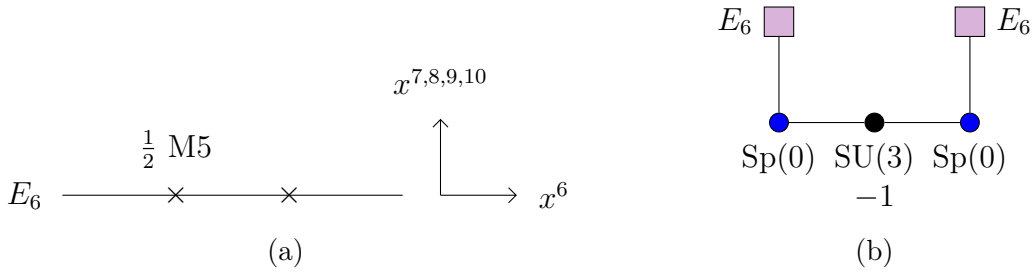


Figure 6.10: Two $\frac{1}{2}$ M5 branes probing an E_6 Klein singularity. The directions $x^{0,1,2,3,4,5}$ are suppressed. The corresponding electric quiver $\mathcal{Q}_{6.10b}$ comes from the F-theory dual description.

quivers, as shown in Figure 6.11. This results in the quiver $\mathcal{Q}_{6.11}$ which is a magnetic quiver for $6d$ $\mathcal{N} = (1,0)$ theory coming from two separated $\frac{1}{2}$ M5 branes probing E_6 Klein singularity. This magnetic quiver has been known in the physics community for some time but has not been documented before.

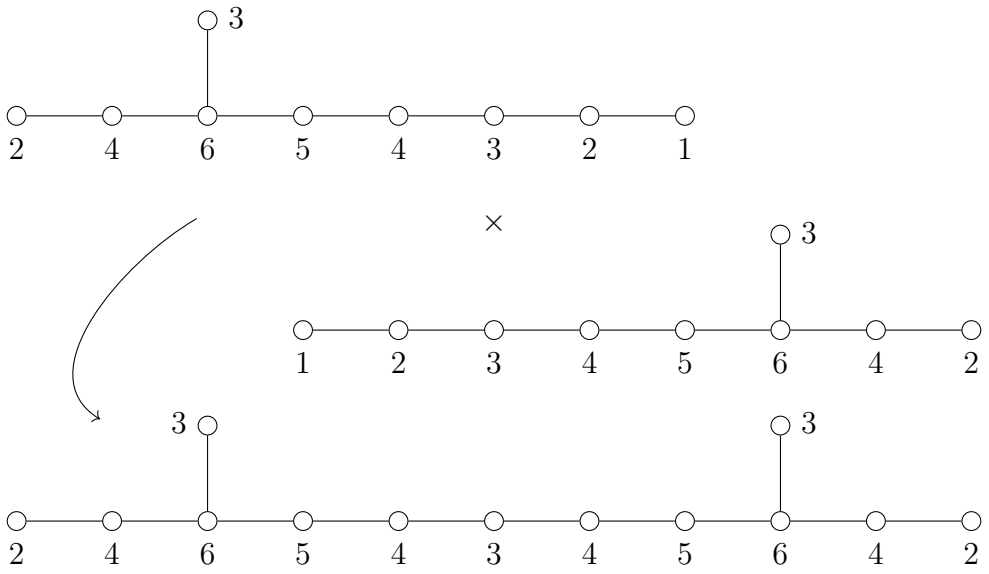


Figure 6.11: SU(3) chain polymerisation of two $E_8^{(1)}$ quivers to produce $\mathcal{Q}_{6.11}$. This quiver is a magnetic quiver for $6d$ $\mathcal{N} = (1,0)$ theory for two separated $\frac{1}{2}$ M5 branes probing Klein E_6 singularity.

The dimension of the moduli space is fifty which is too large to compute exact Hilbert series with the capabilities of a typical computer. For this reason the unrefined perturbative Hilbert series and the PL of the HWG are given up to order t^{10},

$$\mathrm{HS}\left[\mathcal{C}(\mathcal{Q}_{6.11})\right] = 1 + 156t^2 + 13859t^4 + 893669t^6 + 45609733t^8 + 1923636761t^{10} + O(t^{11}) \tag{6.12}$$

$$\mathrm{PL}\left[\mathrm{HS}\left[\mathcal{C}(\mathcal{Q}_{6.11})\right]\right] = 156t^2 + 1613t^4 - 2915t^6 - 627017t^8 - 1911458t^{10} + O(t^{11}) \tag{6.13}$$

$$\mathrm{PL}\left[\mathrm{HWG}\left[\mathcal{C}(\mathcal{Q}_{6.11})\right]\right] = (\mu_6 + \mu_6')t^2 + (1 + \mu_1\mu_5 + \mu_6 + \mu_1\mu_1' + \mu_5\mu_5' + \mu_1'\mu_5' + \mu_6')t^4 + O(t^6), \tag{6.14}$$

where the μ_i and μ_i' are highest weight fugacities for the two different factors of E_6.

It is not clear how to take the SU(3) in the $6d$ theory to infinite coupling in the magnetic quiver $\mathcal{Q}_{6.11}$, neither does it imply a reasonable Type IIA brane construction. The naïve brane system, drawn in Figure 6.12, appears to be a Type I′ background except for the fact that there are only 10 D8 branes in the interval instead of the required 16 for anomaly cancellation. Additionally the two O8$^-$ planes indicate that there is a scale in the problem that one cannot get rid of which is in contrast with the gauge theory which has a phase where there are no scales. This theory will be studied further in Chapter 7.

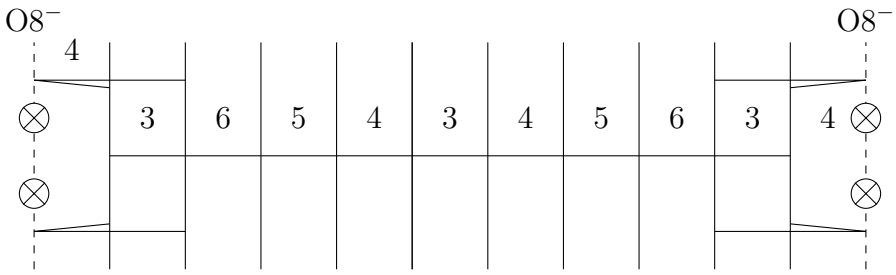


Figure 6.12: Naïve Type IIA brane system for $\mathcal{Q}_{6.11}$. The two O8$^-$ planes are indicative of a Type I′ brane system with 16 D8 branes in the interval, this brane system only has 10.

6.4 Cyclic Polymerisation for SU(N) instanton Moduli Spaces on $\mathbb{C}^2/\mathbb{Z}_l$

The CFHM and Kronheimer-Nakajima quivers, reviewed in Appendix E, are quivers which take the form of a "necklace" of unitary gauge nodes with some flavours. Here, these quivers are constructed (in their unframed form) from cyclic polymerisations of various starting quivers. These starting quivers are drawn from magnetic quivers for the moduli spaces of free fields, nilpotent orbit closures and slices in the affine Grassmannian of type A.

In turn, this provides geometric constructions for the moduli spaces of instantons with special unitary gauge group on A-type singularities as hyper-Kähler quotients of Coulomb branches.

6.4.1 1 SU(N) instanton on $\mathbb{C}^2$

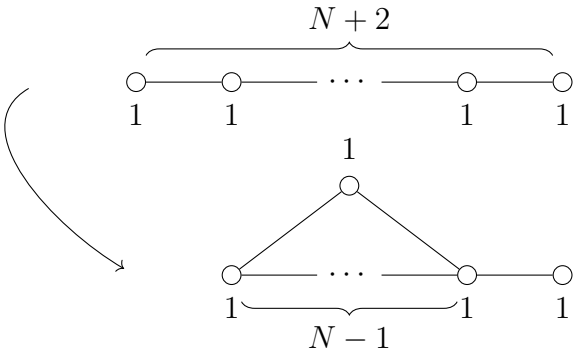


Figure 6.13: U(1) cyclic polymerisation of the finite A_{N+2} quiver to produce the CFHM quiver $\mathcal{Q}_{6.13}$.

The starting point is the finite A_{N+2} quiver, whose Coulomb branch is $\mathbb{H}^{N+1}$. A U(1) cyclic polymerisation is performed by superimposing a U(1) at one end with the penultimate U(1) at the other end. This is shown in Figure 6.13 and produces quiver $\mathcal{Q}_{6.13}$, which is a CFHM quiver (being a special case of the KN quiver).

In terms of the Coulomb branch one finds the following result:

$$\left(\mathbb{H}\times\mathbb{H}^N\right)///\mathrm{U}(1)=\mathcal{M}^{\mathbb{C}^2}_{1,\mathrm{SU}(N)}, \tag{6.15}$$

where the left-hand-side is written in a way which makes the SU(N) symmetry apparent.

In addition, this result (6.15), can be viewed as the ADHM construction [24] for the moduli space of 1 SU(N) instanton on $\mathbb{C}^2$.

The Higgs branch of the finite A_{N+2} quiver is trivial and is of dimension 0. The Higgs branch of $\mathcal{Q}_{6.13}$ is $\mathbb{C}^2/\mathbb{Z}_N$ and is of dimension 1. The conclusion on the Higgs branch is:

$$\mathbb{C}^2/\mathbb{Z}_N///\mathrm{U}(1)=\{0\}, \tag{6.16}$$

which is confirmed from Weyl integration.

6.4.2 2 SU(N) instantons on $\mathbb{C}^2$

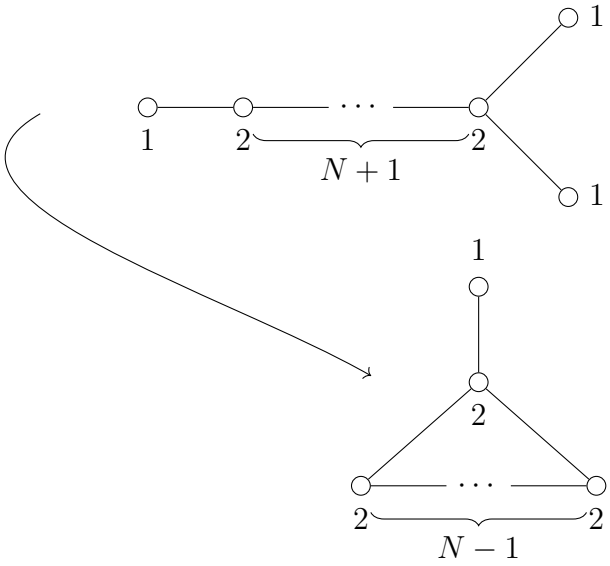
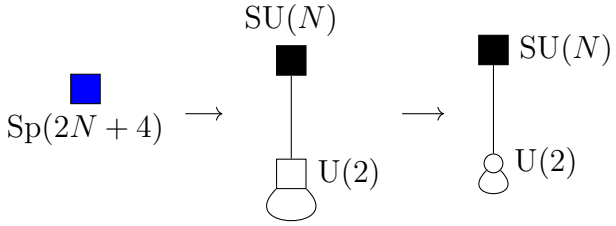


Figure 6.14: U(2) cyclic polymerisation of the finite D_{N+4} quiver to produce $\mathcal{Q}_{6.14}$ for $N \geq 1$.

The starting point is the finite D_{N+4} quiver, whose Coulomb branch is $\mathbb{H}^{2N+4}$ for $N \geq 0$. The cases for $N \geq 1$ are amenable to a cyclic polymerisation for a U(2) hyper-Kähler quotient. Doing the U(2) cyclic polymerisation, as shown in Figure 6.14, produces quiver $\mathcal{Q}_{6.14}$, which is also well known from the CFHM construction [244]. The conclusion on the Coulomb branch is that:

$$\mathbb{H}^{2N+4}///\mathrm{U}(2) = \begin{cases} \mathcal{M}^{\mathbb{C}^2}_{2,\mathrm{SU}(N)}, & N > 1 \\ \mathrm{Sym}^2\left(\mathbb{C}^2\right), & N = 1. \end{cases} \tag{6.17}$$

The result (6.17) is confirmed by Weyl integration. It can be viewed as the $3d$ mirror of the ADHM construction [24] for the moduli space of 2 SU(N) instantons on $\mathbb{C}^2$, which is given below



(6.18)

The Higgs branch of the finite D_{N+4} quiver is trivial and of dimension 0. The Higgs branch of the CFHM quiver $\mathcal{Q}_{6.14}$ is $\text{Sym}^2\left(\mathbb{C}^2/\mathbb{Z}_N\right)$, which is of dimension 2. There is the expected increase of the Higgs branch dimension after polymerisation by rank U(2) = 2.

6.4.3 2 SU(N) instantons on $\mathbb{C}^2/\mathbb{Z}_2$

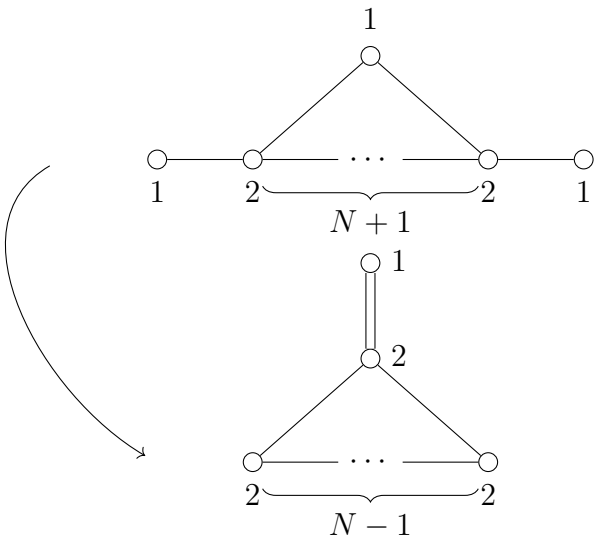


Figure 6.15: U(2) cyclic polymerisation of the unframed magnetic quiver $\mathcal{Q}_M\left(\overline{n.min.A_{N+3}}\right)$ for $N \geq 1$ to produce $\mathcal{Q}_{6.15}$.

The starting point is the magnetic quiver, $\mathcal{Q}_M\left(\overline{n.min.A_{N+3}}\right)$, for $\overline{n.min.A_{N+3}}$ for $N \geq 1$. The U(2) cyclic polymerisation of $\overline{n.min.A_{N+3}}$ for $N \geq 1$ is shown in Figure 6.15 to produce quiver $\mathcal{Q}_{6.15}$. This is a Kronheimer-Nakajima quiver whose Coulomb branch is $\mathcal{M}^{\mathbb{C}^2/\mathbb{Z}_2}_{2,\text{SU}(N)}$. The conclusion is that,

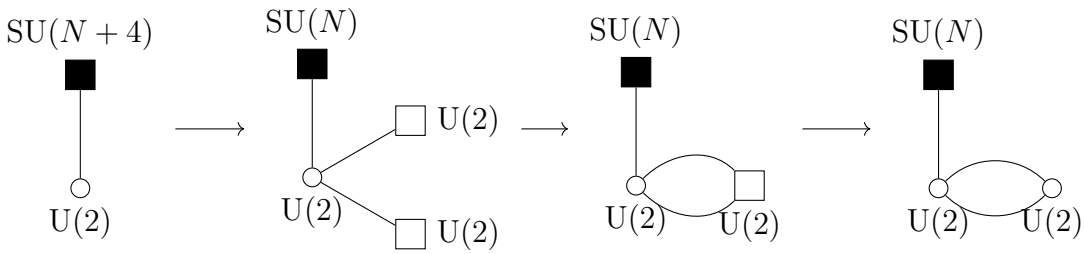
$$\overline{n.min.A_N}///\text{U}(2) = \mathcal{M}^{\mathbb{C}^2/\mathbb{Z}_2}_{2,\text{SU}(N)}, \quad N \geq 1. \tag{6.19}$$

The result (6.19) has been verified with Weyl integration up to $N = 4$.

From Lusztig-Spaltenstein duality the Higgs branch of the quiver at the top of Figure 6.15 is $\mathcal{S}^{A_{N+3}}_{\mathcal{N},(N+2,2)}$, which is of dimension 2. The Higgs branch of the quiver $\mathcal{Q}_{6.15}$ is $\mathcal{M}^{\mathbb{C}^2/\mathbb{Z}_N}_{2,\text{SU}(2)}$ which is of dimension 4. There is the expected increase of the Higgs branch dimension after polymerisation by rank U(2) = 2.

This entire construction also be seen by gauging flavour symmetries from the 3d mirror quiver

for $\mathcal{Q}_M$ $\left(\overline{n.min.A_{N+3}}\right)$ which is U(2) with $N+4$ flavours. Two U(2) factors of the flavour symmetry are separated leaving a commutant of SU(N). These U(2) factors are taken to be diagonal, which is then gauged. The resulting quiver is also a Kronheimer-Nakajima quiver and is $3d$ mirror to $\mathcal{Q}_{6.15}$, which can be seen through the exchange of the number of flavour symmetries and the number of gauge groups in the two quivers.



(6.20)

6.4.4 k SU(N) instantons on $\mathbb{C}^2/\mathbb{Z}_l$

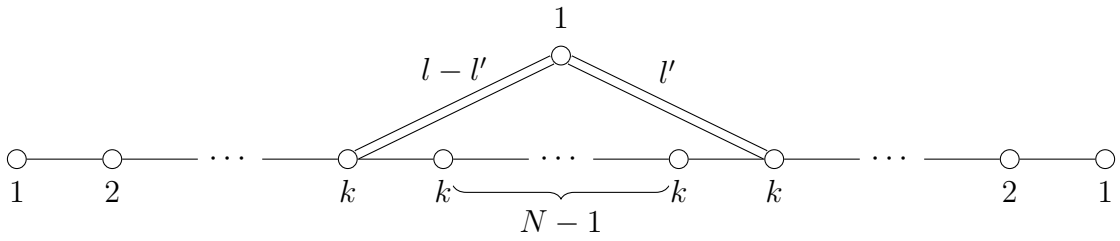


Figure 6.16: Magnetic quiver $\mathcal{Q}_{6.16}$ for $\overline{\left[\mathcal{W}_{A_{2k+N-1}}\right]}^{[0^{k-1},l-l',0^{N-1},l',0^{k-1}]}_{[0^{k-1},l-l'-1,0^{N-1},l'-1,0^{k-1}]}$ for $N \geq 1$ and $l > l' \geq 1$.

Following the construction of the moduli space of 2 SU(N) instanton on $\mathbb{C}^2/\mathbb{Z}_2$ in Section 6.4.3, this construction is generalised for the moduli space of k SU(N) instantons on $\mathbb{C}^2/\mathbb{Z}_l$. In this case, the embedding of $\mathbb{Z}_l$ into the gauge group SU(N) preserves the gauge group.

The starting quiver is $\mathcal{Q}_{6.16}$. The Coulomb branch of $\mathcal{Q}_{6.16}$ depends on various choices of l, l', and N. Firstly, $N \geq 1$ otherwise one cannot perform U(k) cyclic polymerisation. If $l = 1$ and $l' = 0$ the Coulomb branch is $\mathbb{H}^{k^2+Nk}$ due to the underbalanced U(k) node on the right. If $l > 1$ and $l' = 0$ then the Coulomb branch is $\overline{\left[\mathcal{W}_{A_{2k-1}}\right]}^{[0^{k-1},l,0^{k-1}]}_{[0^{k-1},l-2,0^{k-1}]} \times \mathbb{H}^{Nk}$. The appearance of the free part can be seen from application of the dualisation algorithm on $\mathcal{Q}_{6.17a}$;

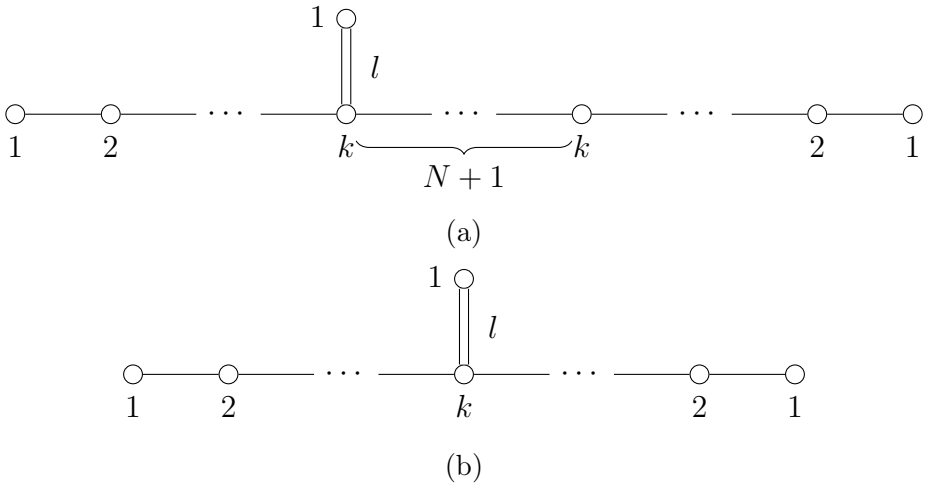


Figure 6.17: Magnetic quiver $\mathcal{Q}_{6.17a}$ for $\overline{[\mathcal{W}_{A_{2k-1}}]}^{[0^{k-1},l,0^{k-1}]}_{[0^{k-1},l-2,0^{k-1}]} \times \mathbb{H}^{Nk}$ for $N \geq 1$. This quiver specialises $\mathcal{Q}_{6.16}$ to the case $l' = 0$. The node of rank k filled in black is "ugly", with balance -1, all other nodes are "good", with non-negative balance. Application of the dualisation algorithm to $\mathcal{Q}_{6.17a}$ yields $\mathcal{Q}_{6.17b}$, which is a magnetic quiver for $\overline{[\mathcal{W}_{A_{2k-1}}]}^{[0^{k-1},l,0^{k-1}]}_{[0^{k-1},l-2,0^{k-1}]}$.

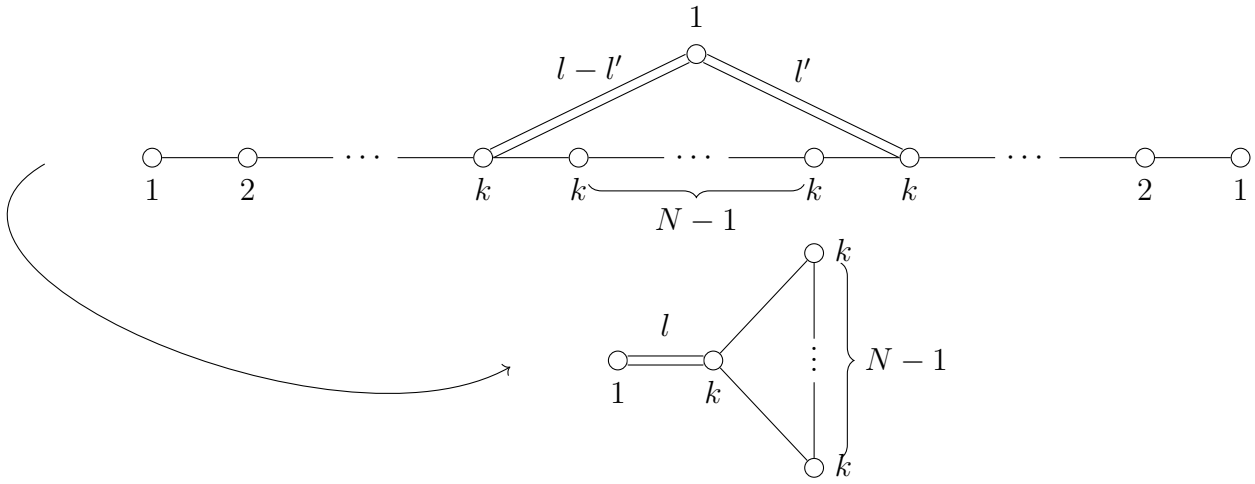


Figure 6.18: U(k) cyclic polymerisation of $\mathcal{Q}_{6.16}$ to produce quiver $\mathcal{Q}_{6.18}$.

with $l \geq 2$ there is a non-trivial part to the moduli space which is given by the Coulomb branch of $\mathcal{Q}_{6.17b}$, $\overline{[\mathcal{W}_{A_{2k-1}}]}^{[0^{k-1},l,0^{k-1}]}_{[0^{k-1},l-2,0^{k-1}]}$[202][4]. Finally for $l > l' \geq 1$ the Coulomb branch is $\overline{[\mathcal{W}_{A_{2k+N-1}}]}^{[0^{k-1},l-l',0^{N-1},l',0^{k-1}]}_{[0^{k-1},l-l'-1,0^{N-1},l'-1,0^{k-1}]}$.

The U(k) cyclic polymerisation on $\mathcal{Q}_{6.16}$ produces $\mathcal{Q}_{6.18}$, as shown in Figure 6.18. This quiver $\mathcal{Q}_{6.18}$ is a Kronheimer-Nakajima quiver [26]. The Coulomb branch is the moduli space of k SU(N) instantons on $\mathbb{C}^2/\mathbb{Z}_l$, $\mathcal{M}^{\mathbb{C}^2/\mathbb{Z}_l}_{k,\mathrm{SU}(N)}$. From the different choices of l and l' the following

[4]To see this, frame $\mathcal{Q}_{6.17b}$ on the top node of U(1). Then remember that the gauge nodes form the finite Dynkin diagram of A_{2k-1} and that the top coweight is given by the flavours on each gauge node and the bottom by the balance of each gauge node.

conclusions on the Coulomb branch are:

$$\overline{\left[\mathcal{W}_{A_{2k+N-1}}\right]}^{[0^{k-1},l-l',0^{N-1},l',0^{k-1}]}_{[0^{k-1},l-l'-1,0^{N-1},l'-1,0^{k-1}]}///\mathrm{U}(k) = \mathcal{M}^{\mathbb{C}^2/\mathbb{Z}_l}_{k,\mathrm{SU}(N)}, \quad l > l' \geq 1 \tag{6.21}$$

$$\overline{\left[\mathcal{W}_{A_{2k-1}}\right]}^{[0^{k-1},l,0^{k-1}]}_{[0^{k-1},l-2,0^{k-1}]} \times \mathbb{H}^{Nk}///\mathrm{U}(k) = \mathcal{M}^{\mathbb{C}^2/\mathbb{Z}_l}_{k,\mathrm{SU}(N)}, \quad l > 1, l' = 0. \tag{6.22}$$

Conclusions about the Higgs branch of $\mathcal{Q}_{6.17a}$ and $\mathcal{Q}_{6.16}$ are also made. Firstly, since $\mathcal{Q}_{6.17a}$ can be dualised to $\mathcal{Q}_{6.17b}$ the Higgs branch of $\mathcal{Q}_{6.17b}$ is also the Higgs branch of $\mathcal{Q}_{6.17a}$. This complication does not arise for $\mathcal{Q}_{6.16}$ for $l > l' \geq 1$. As $\mathcal{Q}_{6.17b}$ and $\mathcal{Q}_{6.16}$ are magnetic quivers for affine Grassmannian slices, the Higgs branch cannot be found from an order inverting duality as was possible for magnetic quivers for slices in nilcones. Instead, the Coulomb branch of the $3d$ mirror quiver can be found, which is constructed from the type IIB brane system with a series of brane moves and S-duality [31]. The $3d$ mirrors of $\mathcal{Q}_{6.17b}$ and $\mathcal{Q}_{6.16}$ are $\mathcal{Q}_{6.19a}$ and $\mathcal{Q}_{6.16}$ respectively, show in Figure 6.19. The Coulomb branch of $\mathcal{Q}_{6.19a}$ is $\overline{\left[\mathcal{W}_{A_{l-1}}\right]}^{[k,0^{l-3},k]}_{[0^{l-1}]}$ and the Coulomb branch of $\mathcal{Q}_{6.19b}$ is $\overline{\left[\mathcal{W}_{A_{l-1}}\right]}^{[k,0^{l-l'-2},N,0^{l'-2},k]}_{[0^{l-l'-1},N,0^{l'-1}]}$. In summary,

$$\mathcal{H}(\mathcal{Q}_{6.17a}) = \mathcal{H}(\mathcal{Q}_{6.17b}) = \mathcal{C}(\mathcal{Q}_{6.19a}) = \overline{\left[\mathcal{W}_{A_{l-1}}\right]}^{[k,0^{l-3},k]}_{[0^{l-1}]}, \tag{6.23}$$

$$\mathcal{H}(\mathcal{Q}_{6.16}) = \mathcal{C}(\mathcal{Q}_{6.19b}) = \overline{\left[\mathcal{W}_{A_{l-1}}\right]}^{[k,0^{l-l'-2},N,0^{l'-2},k]}_{[0^{l-l'-1},N,0^{l'-1}]}. \tag{6.24}$$

These moduli spaces are both of dimension $k(l-1)$ and the Higgs branch of $\mathcal{Q}_{6.18}$ is of dimension kl and so the Higgs branch dimension has increased by rank $\mathrm{U}(k) = k$ after polymerisation as expected.

6.4.5 Generic Kronheimer-Nakajima Quivers

Having constructed specific cases of the Kronheimer-Nakajima quivers, a generic construction from cyclic polymerisation for any computable Kronheimer-Nakajima quiver is presented.

The starting quiver $\mathcal{Q}_{6.20}$, drawn in Figure 6.20, consists of two legs of gauge nodes up to $\mathrm{U}(k_1)$ with the middle of the quiver containing other unitary gauge nodes. All of the gauge nodes in the middle are connected to the U(1) gauge node at the top with some multiplicity of edges.

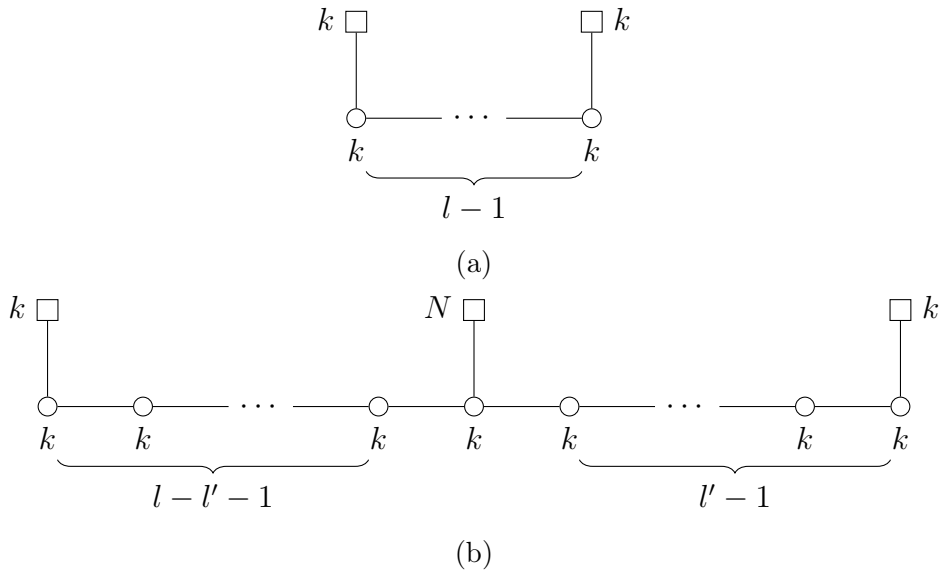


Figure 6.19: (a) Magnetic quiver $\mathcal{Q}_{6.19a}$ for $\overline{[\mathcal{W}_{A_{l-1}}]}^{[k,0^{l-3},k]}_{[0^{l-1}]}$. This quiver is $3d$ mirror to $\mathcal{Q}_{6.17b}$. (b) Magnetic quiver $\mathcal{Q}_{6.19b}$ for $\overline{[\mathcal{W}_{A_{l-1}}]}^{[k,0^{l-l'-2},N,0^{l'-2},k]}_{[0^{l-l'-1},N,0^{l'-1}]}$. This quiver is $3d$ mirror to $\mathcal{Q}_{6.16}$.

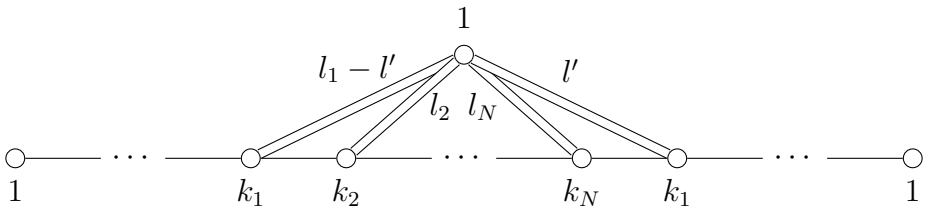


Figure 6.20: Unframed linear quiver $\mathcal{Q}_{6.20}$.

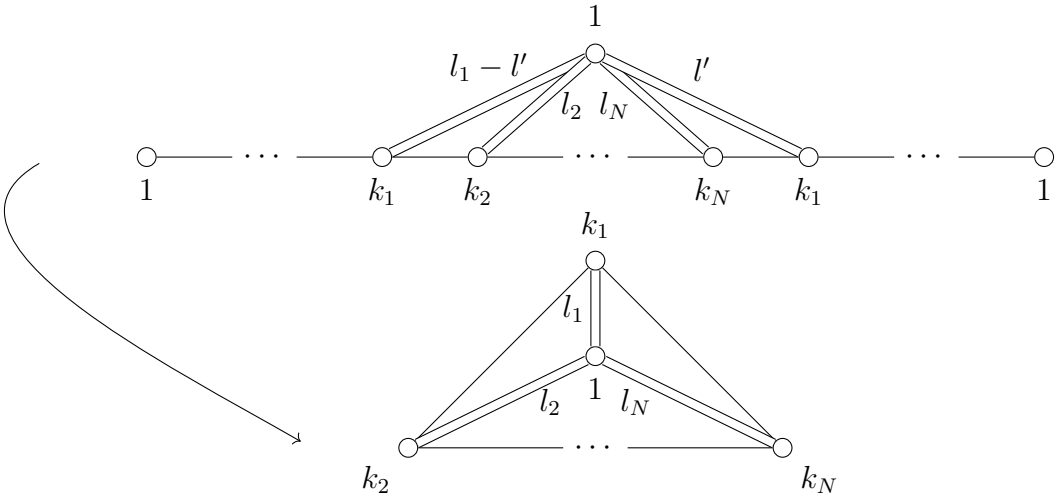


Figure 6.21: Construction of a generic Kronheimer-Nakajima quiver from U(k_1) cyclic polymerisation.

When framed at the U(1) at the top this quiver becomes linear with flavours on top. The Coulomb branch of this quiver depends on the particular values of U(k_i) and l_i for $i = 1, \cdots, N$

so it is difficult to give a generic name to this moduli space.

However, suppose that the k_i and l_i are chosen so that $\mathcal{Q}_{6.20}$ is computable, then the Coulomb branch is an affine Grassmannian slice of A_{2k_1+N-1}. The coweights corresponding to the flavours and balance are easily computed but not presented here for brevity. If $\mathcal{Q}_{6.20}$ is has a gauge node with excess -1, then most likely the moduli space consists of a slice in the affine Grassmannian of A_r for $r < 2k_1 + N - 1$ with a free part.

In either case, U(k_1) cyclic polymerisation may be performed as shown in Figure 6.21 to give the most generic unitary Kronheimer-Nakajima quiver $\mathcal{Q}_{E.2}$,(when framed on the central U(1) gauge node). The conclusion is that:

$$\mathcal{C}\left(\mathcal{Q}_{6.20}\right)///\mathrm{U}(k_1) = \mathcal{M}^{\mathbb{C}^2/\mathbb{Z}_l}_{(k'_1,\cdots,k'_l),(l'_1,\cdots,l'_l)}, \quad l = \sum_{i=1}^{N} l_i. \tag{6.25}$$

This schematic construction generalises to all unitary Kronheimer-Nakajima quivers and hence gives the construction of all SU instantons on $\mathbb{C}^2/\mathbb{Z}_l$ (where $l = \sum_i l_i$), for any data specifying the instanton bundle as a hyper-Kähler quotient on the Coulomb branch.

This should be viewed as the Coulomb branch dual construction to the original ADHM and Kronheimer-Nakajima constructions on Higgs branches. An additional advantage of the Coulomb branch construction is in the explication of the relationship between the moduli space of instantons and other geometric objects, such as affine Grassmannian slices, under hyper-Kähler quotient.

6.5 Cyclic polymerisation of ADE-shaped Quivers

6.5.1 U(1) cyclic polymerisation of A_N for $N \geq 2$

The U(1) cyclic polymerisation of the finite A-type quiver, discussed in Section 6.4.1, is not the only way to perform U(1) cyclic polymerisation. The most general U(1) cyclic polymerisation

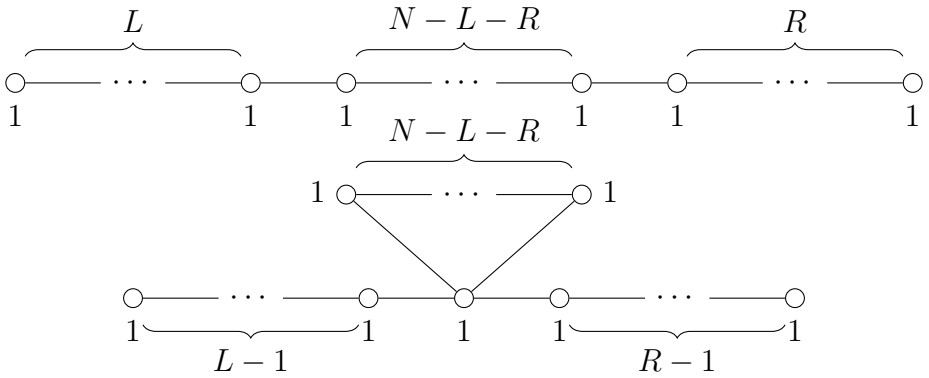


Figure 6.22: U(1) cyclic polymerisation of the finite A_{N+2} quiver to produce $\mathcal{Q}_{6.22}$.

of the finite A_N quiver involves taking the L^{th} U(1) gauge node from the left and the R^{th} U(1) gauge node from the right and superimposing them. This shown in Figure 6.22, and produces $\mathcal{Q}_{6.22}$, which depends on the choice of N, L, and R. The quiver $\mathcal{Q}_{6.22}$ is unframed, and if the U(1) is ungauged at the superimposed nodes, the Coulomb branch is easily read as $\overline{min.A_{N-L-R}} \times \mathbb{H}^{L+R-2}$. The conclusion is that:

$$\mathbb{H}^{N-1}///\mathrm{U}(1) = \overline{min.A_{N-L-R}} \times \mathbb{H}^{L+R-2}, \quad 1 \leq L, R \leq \lceil N/2 \rceil. \tag{6.26}$$

For certain choices of L and R the framings that can be applied to $\mathcal{Q}_{6.22}$ give equivalent but different interpretations of the final moduli space.

For $L = R = 1$, $\mathcal{Q}_{6.22}$ takes the form of the affine $A^{(1)}_{N-2}$ Dynkin diagram and the Coulomb branch is $\overline{min.A_{N-2}}$. This case is encompassed by (6.26). For the case, $L = 1$ and $R = 2$ (or vice versa, but taking the case as given), $\mathcal{Q}_{6.22}$ takes the form of an affine $A^{(1)}_{N-2}$ Dynkin diagram with an extension of a U(1) gauge node. This is a known CFHM quiver [244] for the moduli space of 1 SU$(N-1)$ instanton on $\mathbb{C}^2$ and was studied in Section 6.4.1. For $L = 1$ and $R \geq 3$ (or vice versa), framing $\mathcal{Q}_{6.22}$ at the superimposed U(1), or adjacent to the superimposed U(1), gives two interpretations of the same moduli space. These are:

$$\mathbb{H}^{N-1}///\mathrm{U}(1) = \overline{min.A_{N-1-R}} \times \mathbb{H}^{R-1} = \mathcal{M}^{\mathbb{C}^2}_{1,\mathrm{SU}(N-R)} \times \mathbb{H}^{R-2}, \quad 2 \leq R \leq N-2. \tag{6.27}$$

The Higgs branch of the finite A_N quiver is trivial and of dimension 0. In all cases, the Higgs

branch of the polymerised quiver is the A_{N-L-R} singularity, which is of dimension 1. The relationship on the Higgs branch is:

$$A_{N-L-R}///\mathrm{U}(1) = \{0\}, \tag{6.28}$$

which can be verified with Weyl integration for all valid choices of L and R.

6.5.2 U(1) cyclic polymerisation of $E_6^{(1)}$

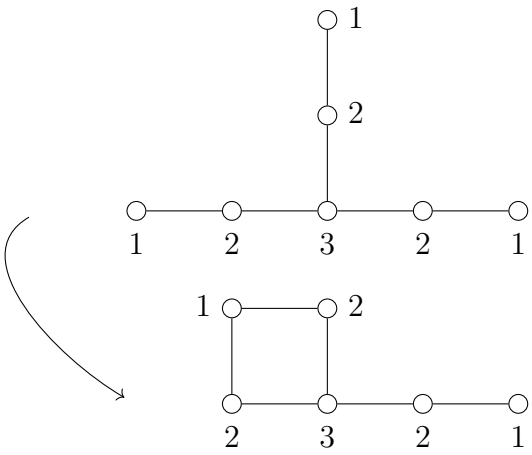


Figure 6.23: U(1) cyclic polymerisation of the affine $E_6^{(1)}$ quiver to produce $\mathcal{Q}_{6.23}$.

The U(1) cyclic polymerisation of the affine $E_6^{(1)}$ quiver, whose Coulomb branch is $\overline{min.E_6}$, produces quiver $\mathcal{Q}_{6.23}$ as shown in Figure 6.23. This is an unframed magnetic quiver for the height two nilpotent orbit closure $\overline{\mathcal{O}}^{D_5}_{(2^4,1^2)}$ [183]. The conclusion on the Coulomb branch is that:

$$\overline{min.E_6}///\mathrm{U}(1) = \overline{\mathcal{O}}^{D_5}_{(2^4,1^2)}. \tag{6.29}$$

The Higgs branch of the affine $E_6^{(1)}$ quiver is the Kleinian singularity E_6, which is of dimension 1. The Higgs branch Hilbert series of $\mathcal{Q}_{6.23}$ is:

$$\mathrm{HS}[\mathcal{H}(\mathcal{Q}_{6.23})] = \mathrm{PE}\left[t^2 + (q+q^{-1})t^4 + t^6 + (q+q^{-1})t^8 - t^{12} - t^{16}\right], \tag{6.30}$$

where q is a fugacity for U(1). The Hilbert series above identifies the moduli space as the

Slodowy slice $\mathcal{S}^{D_5}_{\mathcal{N},(5^2)}$, which is a complete intersection of dimension 2. The relationship between orbits and slices of D_5 is that of Lusztig-Spaltenstein duality, since the D partitions (5^2) and $(2^4,1^2)$ are dual to each other under the Barbasch-Vogan map.

The relationship on the Higgs branch of $\mathcal{Q}_{6.23}$ is that:

$$\mathcal{S}^{D_5}_{\mathcal{N},(5^2)}///\mathrm{U}(1) = E_6. \tag{6.31}$$

This is verified from Weyl integration and is also identifiable from the Hilbert series 6.30.

6.5.3 U(2) cyclic polymerisation of $E_6^{(1)}$

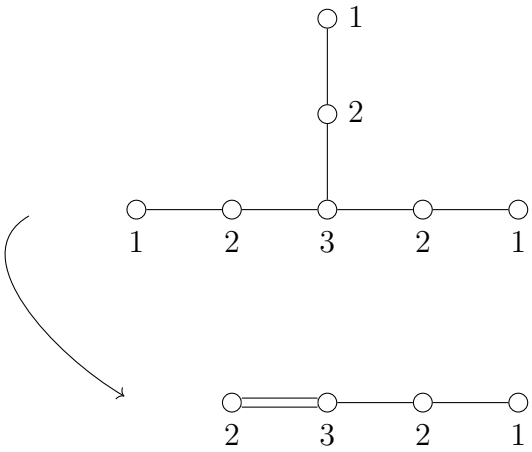


Figure 6.24: U(2) cyclic polymerisation of the affine $E_6^{(1)}$ quiver to produce $\mathcal{Q}_{6.24}$.

The U(2) cyclic polymerisation of the affine $E_6^{(1)}$ quiver, whose Coulomb branch is $\overline{min.E_6}$, produces quiver $\mathcal{Q}_{6.24}$, as shown in Figure 6.24. From the consideration of the balance of the gauge nodes, the Coulomb branch global symmetry appears to be SU(4). However, there is an enhancement of the global symmetry to SO(7) [64].

Applying the monopole formula to $\mathcal{Q}_{6.24}$ and projecting the resulting Coulomb branch Hilbert series onto highest weight fugacities of SO(7), yields the following HWG:

$$\mathrm{HWG}\left[\mathcal{C}\left(\mathcal{Q}_{6.24}\right)\right] = \mathrm{PE}\left[\mu_2 t^2 + (\mu_1^2+\mu_3^2)t^4 + \mu_1\mu_3^2 t^6 + \mu_2^2 t^8 + \mu_1\mu_2\mu_3^2 t^{10} - \mu_1^2\mu_2^2\mu_3^4 t^{20}\right]. \tag{6.32}$$

This is the HWG for the 7-dimensional orbit of B_3, $\overline{\mathcal{O}}^{B_3}_{(3^2,1)}$ [183].

A direct embedding is used to verify (6.32) from Weyl integration. This embedding is $E_6 \hookleftarrow \mathrm{SO}(10)\times\mathrm{U}(1) \hookleftarrow \mathrm{SO}(7)\times\mathrm{SU}(2)\times\mathrm{U}(1)$ which decomposes the adjoint as

$$\mu_6 \to \mu_2 + \nu^2 + \mu_1\nu^2 + \mu_3(\nu/q + \nu q) + 1, \tag{6.33}$$

where the μ_6 on the left hand side is for E_6, the $\mu_{1,2,3}$ on the right hand side are for SO(7), the ν is for SU(2) and the U(1) fugacity is q. There is agreement with (6.32) if the Weyl integration is done w.r.t the $\mathrm{SU}(2)\times\mathrm{U}(1)$.

The conclusion on the Coulomb branch is that,

$$\overline{min.E_6}///\mathrm{U}(2) = \overline{\mathcal{O}}^{B_3}_{(3^2,1)}. \tag{6.34}$$

It is worth noting that this orbit is of height 4 and that $\mathcal{Q}_{6.24}$ is a magnetic quiver for it that was previously unknown.

This quiver $\mathcal{Q}_{6.24}$ is another example of a magnetic quiver whose nodes do not form a balanced Dynkin diagram, but which nevertheless has a global symmetry enhanced to that of a simple group and a Coulomb branch which forms an orbit.

The Higgs branch of the affine $E_6^{(1)}$ quiver is the Kleinian singularity E_6, which is of dimension 1. The Hilbert series of the Higgs branch of $\mathcal{Q}_{6.24}$ is computed as:

$$\mathrm{HS}[\mathcal{H}(\mathcal{Q}_{6.24})] = \mathrm{PE}\left[[2]_{\mathrm{SU}(2)}t^2 + [4]_{\mathrm{SU}(2)}t^4 - t^8 - t^{12}\right]. \tag{6.35}$$

This is a complete intersection of dimension 3 and is the Hilbert series for the Slodowy slice $\mathcal{H}(\mathcal{Q}_{6.24}) = \mathcal{S}^{C_3}_{\mathcal{N},(2^3)}$, as tabulated in [133]. The result is another example of Lusztig-Spaltenstein duality, since the C_3 partition (2^3) is dual to the B_3 partition $(3^2,1)$ under the Barbasch-Vogan map. There is the expected increase in Higgs branch dimension by rank $\mathrm{U}(2) = 2$.

6.5.4 U(1) cyclic polymerisation of $E_7^{(1)}$

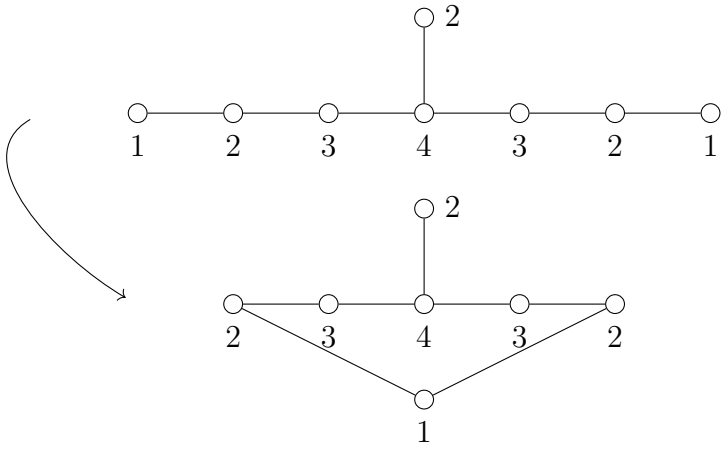


Figure 6.25: U(1) cyclic polymerisation of the $E_7^{(1)}$ quiver to produce $\mathcal{Q}_{6.25}$.

The U(1) cyclic polymerisation of the $E_7^{(1)}$ affine quiver, whose Coulomb branch is $\overline{min.E_7}$, produces quiver $\mathcal{Q}_{6.25}$, as shown in Figure 6.25. This is a magnetic quiver for the height two nilpotent orbit closure $\overline{n.min.E_6}$.

The conclusion on the Coulomb branch is that,

$$\overline{min.E_7}///\mathrm{U}(1) = \overline{n.min.E_6}. \tag{6.36}$$

The Higgs branch of the $E_7^{(1)}$ quiver is the E_7 singularity which is of dimension 1. The Higgs branch Hilbert series of $\mathcal{Q}_{6.25}$ is:

$$\mathrm{HS}[\mathcal{H}(\mathcal{Q}_{6.25})] = \mathrm{PE}\left[t^2 + (q+q^{-1})t^6 + t^8 + (q+q^{-1})t^{12} - t^{18} - t^{24}\right], \tag{6.37}$$

where q is a U(1) charge. The above Hilbert series identifies the moduli space as the Slodowy slice $\mathcal{S}^{E_6}_{\mathcal{N},D_5}$ which is a complete intersection of dimension 2. This is as expected from Lusztig-Spaltenstein duality since this E_6 orbit and slice are dual to each other [252]. The relationship on the Higgs branch is that:

$$\mathcal{S}^{E_6}_{\mathcal{N},D_5}///\mathrm{U}(1) = E_7. \tag{6.38}$$

This is verified from Weyl integration and is also identifiable from the above Hilbert series.

6.5.5 U(3) cyclic polymerisation of $E_7^{(1)}$

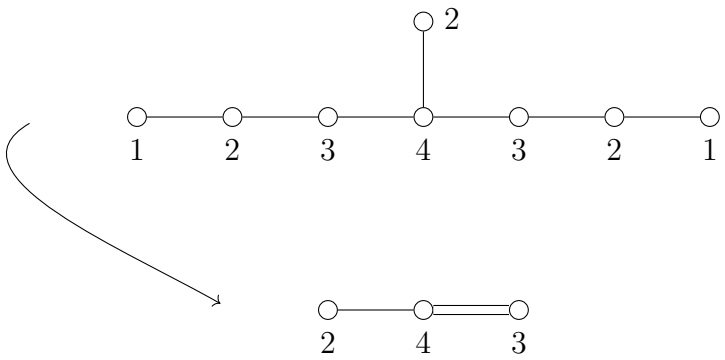


Figure 6.26: U(3) cyclic polymerisation of the $E_7^{(1)}$ quiver to produce $\mathcal{Q}_{6.26}$.

The U(3) cyclic polymerisation of the affine $E_7^{(1)}$ is shown in Figure 6.26. This produces quiver $\mathcal{Q}_{6.26}$. From consideration of the balance of gauge nodes, it would appear that the Coulomb branch global symmetry is SU(3), however yet again there is an enhancement of the global symmetry, this time to G_2 [64]. This can be verified from the Hilbert series. However only the unrefined Hilbert series is presented for brevity:

$$\mathrm{HS}\left[\mathcal{C}\left(\mathcal{Q}_{6.26}\right)\right] = \frac{\left(\begin{array}{l} 1+6t^2+40t^4+149t^6+470t^8+1048t^{10} \\ \quad +1927t^{12}+2668t^{14}+3048t^{16}+\cdots+t^{32} \end{array}\right)}{(1-t^2)^8(1-t^4)^8}, \tag{6.39}$$

and the coefficient of the t^2 term matches the dimension of the G_2 adjoint representation.

This Coulomb branch can be identified as the Slodowy intersection $\mathcal{S}^{E_7}_{A_3+A_2+A_1,A_2+3A_1}$. To do this, either the Hilbert series of the Slodowy intersection can be computed using the formula in [134, Appendix B] to obtain agreement with (6.39).

The conclusion on the Coulomb branch is,

$$\overline{min.E_7}///\mathrm{U}(3) = \mathcal{S}^{E_7}_{A_3+A_2+A_1,A_2+3A_1}. \tag{6.40}$$

The above result is verified using Weyl integration employing the direct embedding of $E_7 \hookleftarrow$

$E_6 \times \mathrm{U}(1) \hookleftarrow G_2 \times \mathrm{SU}(3) \times \mathrm{U}(1)$. This decomposes the fundamental of E_7 as,

$$\mu_6 \to \mu_2\nu_1 q^{-1} + \mu_2\nu_2 q + \nu_1^2 q + \nu_2^2 q^{-1} + q^3 + q^{-3}, \tag{6.41}$$

where on the right hand side the μ_i and ν_i are highest weight fugacities for G_2 and SU(3) respectively, and q is a U(1) charge. The Weyl integration is performed w.r.t $\mathrm{SU}(3) \times \mathrm{U}(1)$.

The Higgs branch of the $E_7^{(1)}$ quiver is the E_7 singularity, which is of dimension 1. The Higgs branch Hilbert series of $\mathcal{Q}_{6.26}$ has been computed, but for brevity only the unrefined Hilbert series is presented:

$$\mathrm{HS}[\mathcal{H}(\mathcal{Q}_{6.26})] = \frac{(1-t^{12})\begin{pmatrix} 1+3t^2+6t^4+13t^6+24t^8 \\ \quad +29t^{10}+29t^{12}+\cdots+t^{24} \end{pmatrix}}{(1-t^4)^5(1-t^6)^4}. \tag{6.42}$$

The Higgs branch is of dimension 4 but is not a complete intersection. In fact, using Lusztig-Spaltenstein duality the Higgs branch can be identified as the Slodowy intersection within the E_7 nilcone, $\mathcal{H}(\mathcal{Q}_{6.26}) = \mathcal{S}^{E_7}_{A_6,A_4+A_2}$, which is dual to the intersection on the Coulomb branch [252]. This can be confirmed from the refined Hilbert series. The Higgs branch dimension increases by rank $\mathrm{U}(3) = 3$ as expected.

Chapter 7

Unframed Orthosymplectic Quotient Quiver Subtraction

7.1 Introduction

In this Chapter, a *quotient quiver subtraction* algorithm for orthosymplectic quivers is presented. The methods are inspired once again by $6d$ $\mathcal{N} = (1,0)$ gauge theories, and *orthosymplectic quotient quiver subtraction* is developed for gauging SU(2), SU(3), G_2, and SO(7) subgroups of the Coulomb branch global symmetry of unframed orthosymplectic $3d$ $\mathcal{N} = 4$ quivers (*i.e.* containing only orthogonal and symplectic nodes). These are found by comparing the magnetic quiver for Sp(k) gauge theory in six dimensions at infinite coupling with SO($4k + 16$) flavour symmetry[1] before and after gauging SU(3), G_2, SO(7) subgroups of the flavour symmetry, for $k = 0, 1, 2$ respectively. This is exactly the same methodology used to derive the quotient quiver subtraction in the unitary case for SU(3) in Chapter 4, where there is a unitary magnetic quiver for the Sp(0) theory before and after gauging. The orthosymplectic quotient quiver subtraction for SU(2) is derived slightly differently but follows from the Higgsing pattern SO(7) $\to G_2 \to$ SU(3) $\to$ SU(2). The quivers studied here are restricted to unframed orthosymplectic quivers containing only SO($2n$) and Sp(n) gauge nodes.

[1] Except for the case $k = 0$ where there is enhancement SO(16) $\to E_8$

Orthosymplectic quotient quiver subtraction shares much in common with its unitary counterpart. In particular, since the orthosymplectic quotient quivers for SU(2), SU(3), G_2, and SO(7) contain gauge nodes with negative balance, their Coulomb branches are potentially smooth. Another similarity is the possibility of unions of moduli spaces arising from an 'overshoot' at a 'junction' of the starting quiver. There are also notable differences, which will be expanded upon in Section 7.3. Briefly, the prescription for rebalancing gauge nodes after subtraction differs between the orthosymplectic and unitary cases. This prescription may explicitly break the alternating SO − Sp gauge node pattern in some cases.

One successful outcome of unitary quotient quiver subtraction was in its use to derive new mathematical relationships between nilpotent orbit closures under hyper-Kähler quotients, examples of this were seen in the previous Chapters. Following this, orthosymplectic quotient quiver subtraction is also applied to $3d$ $\mathcal{N} = 4$ quivers whose Coulomb branches are nilpotent orbit closures. In doing so, previously established relationships found through unitary quotient quiver subtraction and through polymerisation are realised again using orthosymplectic quivers, providing a check of orthosymplectic quotient quiver subtraction. Additionally, new orthosymplectic doppelgängers to known unitary quivers are found. These quivers are doppelgängers in the sense that their Coulomb branches and Higgs branches are the same, but also appear similar in terms of the graph. New relationships between nilpotent orbit closures can be found using the orthosymplectic quotient quiver subtraction for which a unitary construction is not yet known.

Benefiting from the physical implications of this algorithm, orthosymplectic quotient quiver subtraction is also applied to understand certain $6d$ $\mathcal{N} = (1, 0)$ Higgs branches. Magnetic quivers were originally conceived as auxiliary descriptions of $6d$ $\mathcal{N} = (1, 0)$ Higgs branches of the worldvolume gauge theories arising from M5-branes on AD Klein singularities [46, 155], for which the dual Type IIA configuration is crucial. Extension to the case of $E_{6,7,8}$ Klein singularities has been a longstanding challenge, not least for the fact that there is no known dual Type IIA description. However, there do exist descriptions in F-theory [149, 168] from which an electric quiver may be found in both the finite and infinite coupling limits, although there is currently no systematic approach. There also exist descriptions of the $6d$ $\mathcal{N} = (1, 0)$

worldvolume gauge theory of one and two M5 branes on Klein E_6 singularity as a class $\mathcal{S}$ theory, which was derived from compactification on T^2 both without [251, 253] and with magnetic fluxes [220].

Focusing on the case of a single M5 brane on an E_6 Klein singularity, orthosymplectic quotient quiver subtraction is used to provide an orthosymplectic magnetic quiver for two phases of the $6d$ $\mathcal{N} = (1,0)$ gauge theory. The first phase is the $6d$ $\mathcal{N} = (1,0)$ worldvolume theory of two $\frac{1}{2}$M5 branes on a Klein E_6 singularity. This theory is not conformal as there is a scale from the non-trivial vev of the tensor multiplet which is also the (finite) gauge coupling in this case. The orthosymplectic magnetic quiver is consistent with its unitary doppelgänger derived in Chapter 6.3.7, however only the orthosymplectic magnetic quiver admits a suitable description from a Type IIA brane system. The second phase is the infinite coupling limit of this $6d$ $\mathcal{N} = (1,0)$ theory also known as minimal (E_6, E_6) conformal matter[2]. This is believed to be a strongly coupled SCFT. The (E_6, E_6) conformal matter phase is related to the finite coupling phase by a small E_8 instanton transition [45, 154]. The orthosymplectic magnetic quiver conjectured for $6d$ $\mathcal{N} = (1,0)$ (E_6, E_6) conformal matter is the first of its kind and also admits a description from a Type IIA brane system.

Organisation of the Chapter The derivation of the SU(3), G_2, SO(7) orthosymplectic quotient quivers and arguments for the SU(2) quotient quiver and why the methodology is not able to provide more quotient quivers is given in Section 7.2.

The specific rules of the orthosymplectic quotient quiver subtraction algorithm are given in Section 7.3.

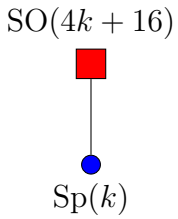
Explicit examples of SU(2), SU(3), G_2, and SO(7) orthosymplectic quotient quiver subtraction are given in Sections 7.4, 7.5, 7.6, and 7.7 respectively, mainly drawing upon nilpotent orbit closures.

The derivation of magnetic quivers for two phases of the worldvolume theory of one M5 brane on Klein E_6 singularity is given in Section 7.8.

[2]Hereafter dropping "minimal".

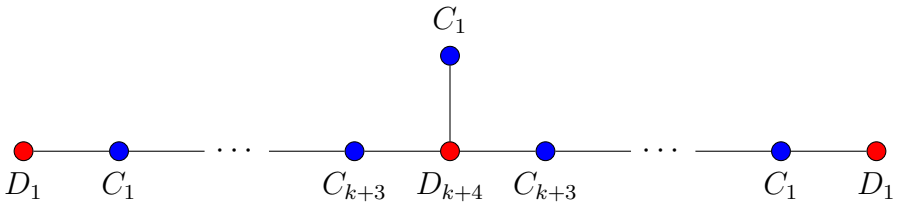
7.2 Derivation of Orthosymplectic Quotient Quivers

The starting point for the analysis is the following electric $6d$ $\mathcal{N}=(1,0)$ gauge theory



(7.1)

at infinite coupling, whose corresponding magnetic quiver,



(7.2)

gives a construction of the Higgs branch $\mathcal{H}_\infty(\mathcal{Q}_{7.1})$ of $\mathcal{Q}_{7.1}$ as a moduli space of dressed monopole operators [155].[3] The Highest Weight Generating function (HWG) for the moduli space is reproduced again as

$$\text{HWG}\left[\mathcal{H}_\infty((7.1))\right] = \text{PE}\left[\sum_{i=1}^{k+3}\mu_{2i}t^{2i} + t^4 + \mu_{2k+8}\left(t^{k+2}+t^{k+4}\right)\right], \tag{7.3}$$

where each of the μ_i are highest weight fugacities for $\text{SO}(4k+16)$.

The objective is now to gauge a subgroup of the flavour symmetry of the electric theory (7.1) and find its associated magnetic quiver. The magnetic quiver for the gauged theory can be compared to that of the pregauged theory (7.2) in order to isolate the particular operation on the magnetic quiver corresponding to the gauging. As $6d$ $\mathcal{N}=(1,0)$ theories are heavily constrained by anomalies there are typically very few permissible gaugings which in turn determines the action on the magnetic quiver precisely.

Anomaly cancellation conditions in six-dimensions leave only a small set of $\text{SO}(4k+16)$ flavour

[3] Note that the $\text{SO}(4k+16)$ global symmetry of $\mathcal{H}_\infty(7.1)$ undergoes enhancement to E_8 at $k=0$.

subgroups that admit a consistent gauging, each corresponding to a different value of k. For $k = 0, 1, 2$ the possible gaugings are of SU(3), G_2, and SO(7) respectively, with SU(2) a special case discussed in Section 7.2.4.

Although gauging a flavour subgroup is relatively straightforward in the electric theory, the derivation of a corresponding magnetic quiver requires the introduction of a Type IIA brane system. $6d$ $\mathcal{N} = (1, 0)$ theories arise as worldvolume theories of D6-branes suspended between NS5-branes on an orientifold plane with flavour D8-branes. In fact, all such gauge theories which admit a formal description in Type IIA string theory – including systems with negatively charged branes – were classified in [166], and explicit brane constructions following this were given in [72] with exploration of finite and infinite coupling phases. The magnetic phase of such brane systems involves suspending the D6-branes between D8-branes through a series of brane moves [31, 129]. Then to find the magnetic quiver of the electric theory at infinite coupling, one simply merges $\frac{1}{2}$NS5-branes pairwise and moves them off the orientifold plane.

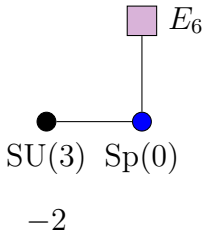
In [72], a set of Type IIA brane configurations involving negatively-charged D6-branes were studied alongside their corresponding electric and magnetic theories [166, 31, 129] – the following section will derive from these the quotient quivers associated to the gauging of flavour subgroups.

These six dimensional theories also have a construction in F-theory. However, it is not known to date how to extract the magnetic quiver from this. It is useful to make connection to the F-theory construction due to the specific effects on the Higgs branch that are seen from collapsing various curves of self-intersection.

7.2.1 Gauging SU(3)

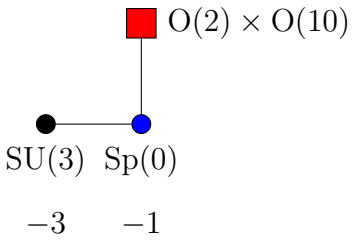
Consider first the electric Sp(0) theory, (7.1) with $k = 0$. Although in other dimensions an Sp(0) gauge theory is trivial, in six dimensions there is still a dynamical tensor multiplet. The case $k = 0$ is special since the expected SO(16) flavour symmetry of (7.1) is enhanced SO(16) $\to E_8$ at infinite gauge coupling, however the HWG (7.3) still holds with the appropriate embedding.

Gauging an SU(3) subgroup of the E_8 flavour symmetry gives (7.4), where the Sp(0) remains at infinite coupling and the SU(3) is at finite coupling supported on a (-2)-curve.



(7.4)

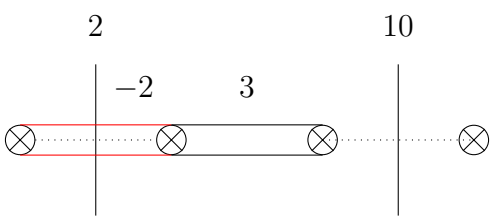
To derive the magnetic quiver, first consider an alternative presentation of (7.4) from F-theory which is amenable to a description in Type IIA. Start with the electric $\mathrm{SU}(3) \times \mathrm{Sp}(0)$ anomaly-free theory with both gauge groups at finite coupling, given in (7.5).



(7.5)

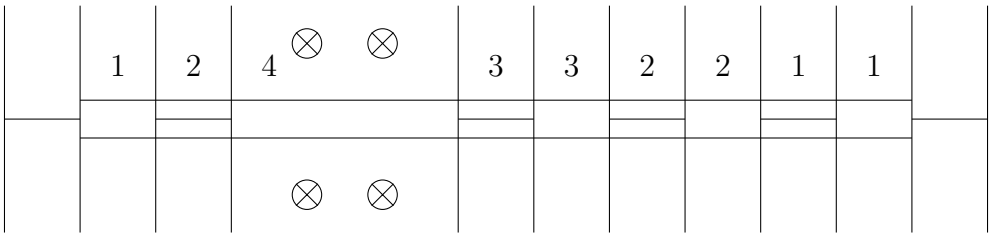
The SU(3) gauge group is supported on a (-3)-curve and the Sp(0) on a (-1)-curve. Collapsing the (-1)-curve corresponds to a small E_8-instanton transition and tunes the Sp(0) gauge coupling to infinity, leaving the rank-1 E-string coupled to SU(3). The self-intersection number of the (-3)-curve also changes to -2.

This change in the Higgs branch can also be seen through brane systems in Type IIA and from magnetic quivers. The quiver (7.5) at finite coupling is the D6 brane worldvolume theory of the following Type IIA brane system



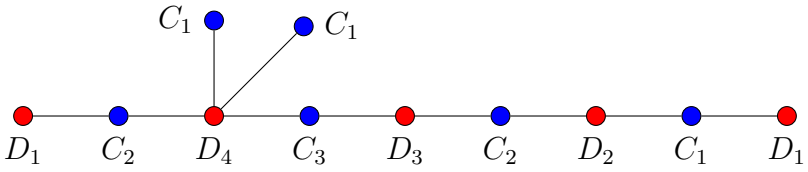
(7.6)

The collapse of the (-1)-curve, which tunes the gauge coupling of Sp(0) to infinity is realised in the magnetic phase of the brane system by firstly suspending D6 between D8 branes and then bringing all four $\frac{1}{2}$-NS5 branes together pairwise and lifting them off the orientifold plane. Doing this results in the following brane system



(7.7)

from which one is able to read off the following magnetic quiver for the Higgs branch of (7.4)



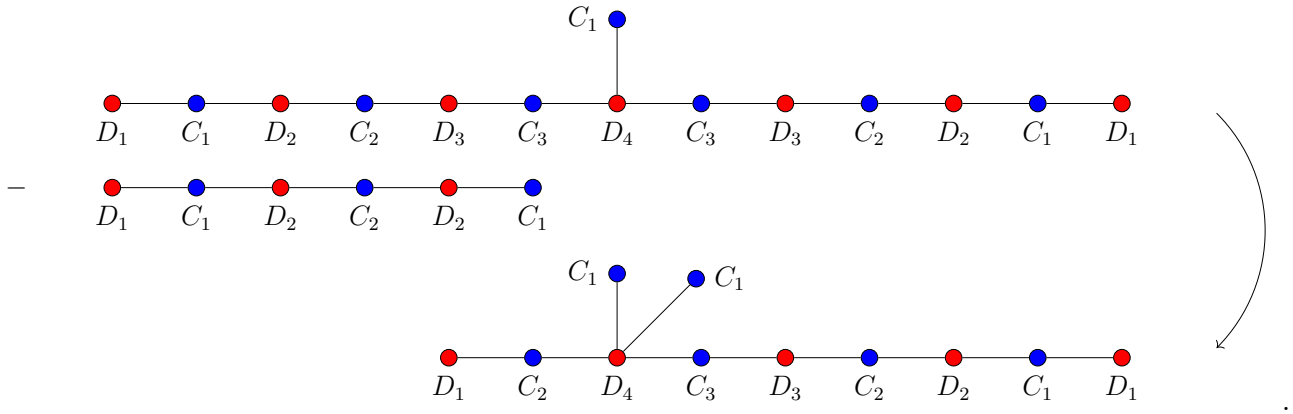
(7.8)

as was done in [72]. The bouquet of two C_1 gauge nodes attached to the D_4 gauge node is indicative of SU(3) being finitely coupled.

As the $6d$ theory (7.4) comes from gauging an SU(3) subgroup of the flavour symmetry of (7.1) (for $k = 0$), comparing their magnetic quivers (7.8) and (7.2) will realise gauging SU(3) subgroups of Coulomb branch global symmetries.

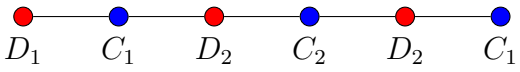
The key observation that translates the notion of gauging flavour symmetries in six-dimensions to the magnetic quiver is a simple and combinatorial one. The two magnetic quivers are related

by the following *quiver subtraction*



(7.9)

The following quiver

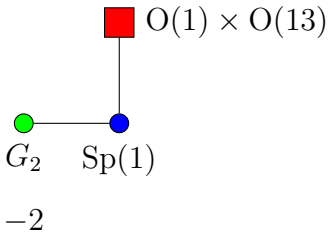


(7.10)

is hence proposed as the SU(3) orthosymplectic quotient quiver. In particular one should note that the C_2 gauge node and the C_1 gauge node on the right have negative balance [123] and hence the Coulomb branch is smooth and its Hilbert series is not computable with the monopole formula [108].

7.2.2 Gauging G_2

A similar set of considerations apply to the G_2 case. In order to gauge a G_2 subgroup of the flavour symmetry of (7.1), the choice $k = 1$ must be made to cancel anomalies. The resulting gauge theory is

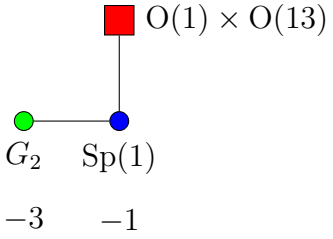


(7.11)

where again the Sp(1) is tuned to infinite coupling and the G_2 is at finite coupling.

As before, the magnetic quiver may be found from a slightly different derivation of (7.11). Take

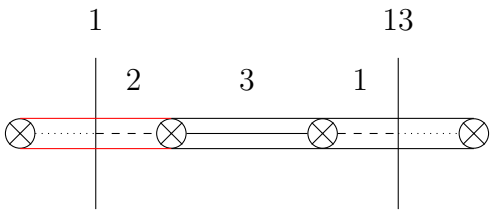
the non-anomalous $G_2 \times \mathrm{Sp}(1)$ gauge theory with both gauge groups at finite coupling. The quiver is



(7.12)

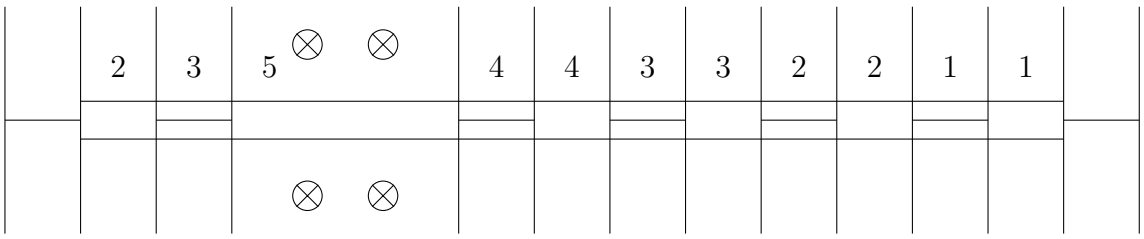
which is similar to (7.11) except that in F-theory the Sp(1) is supported on a (-1)-curve and the G_2 is supported on a (-3)-curve. There are two tensor multiplets associated to each gauge group. The (-1)-curve may be collapsed which tunes the gauge coupling of Sp(1) to infinity. There is also a small E_8 instanton transition as the tensor multiplet associated to the Sp(1) is lost. The electric theory is again (7.11). Compared to the case of gauging SU(3), which involved an Sp(0) gauge node, there is non-trivial matter which is coupled.

The Type IIA brane system which gives (7.12) as the D6 brane worldvolume theory is



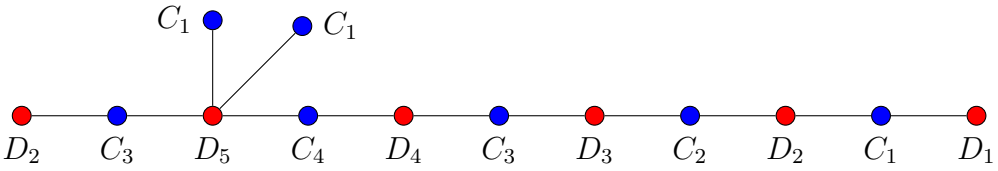
(7.13)

Then the collapse of the (-1)-curve, which tunes the coupling of Sp(1) to infinity, is seen by moving to the magnetic phase by first suspending D6 branes between D8 and then merging all four $\frac{1}{2}$-NS5 branes pairwise and lifting them off the orientifold plane. The resulting brane system is



(7.14)

from which one is able to read off the following magnetic quiver

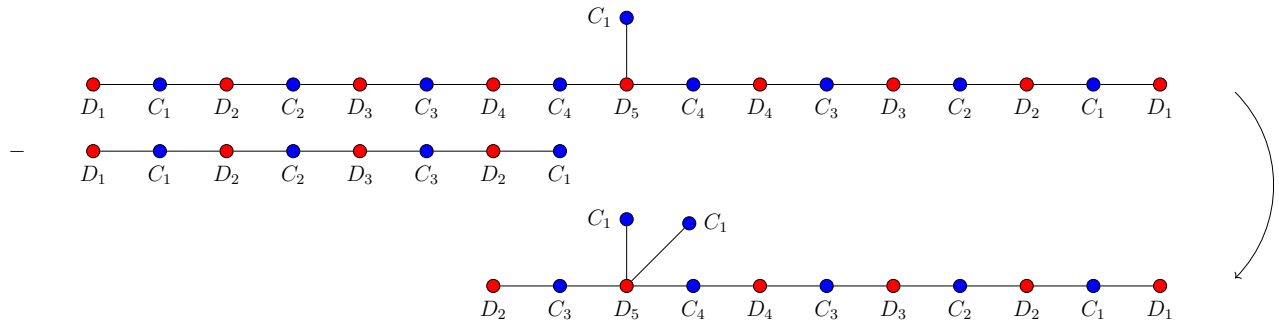


(7.15)

for the Higgs branch of (7.11). The bouquet of C_1 gauge nodes attached to the D_5 gauge node is indicative that the G_2 gauge node in (7.11) is at finite coupling.

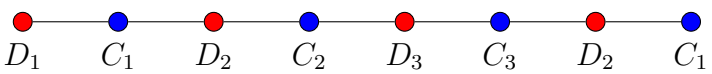
As the $6d$ theory (7.11) comes from gauging a G_2 subgroup of the flavour symmetry of (7.1) (for $k = 1$), comparing their magnetic quivers (7.15) and (7.2) will realise gauging G_2 subgroups of Coulomb branch global symmetries.

The two magnetic quivers are related by the following quiver subtraction



(7.16)

The following quiver

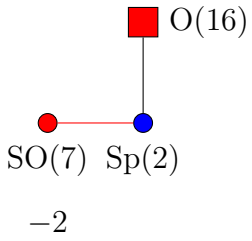


(7.17)

is hence proposed as the G_2 orthosymplectic quotient quiver. This quiver also contains gauge nodes with negative balance [123], the C_3 gauge node and the C_1 gauge node on the right. The Coulomb branch is smooth and its Hilbert series is not computable with the monopole formula [108] and remains a challenge.

7.2.3 Gauging SO(7)

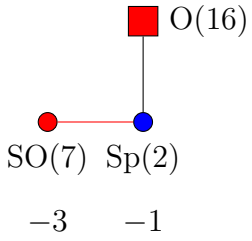
A similar set of considerations apply once again to the SO(7) case. In order to gauge a SO(7) subgroup of the flavour symmetry of (7.1), the choice $k = 2$ must be made to cancel anomalies. The resulting gauge theory is



(7.18)

where the Sp(2) is tuned to infinite coupling and the SO(7) is at finite coupling. The red edge indicates that the hypermultiplet transforms in the bispinor representation when Sp(2) is treated as Spin(5).

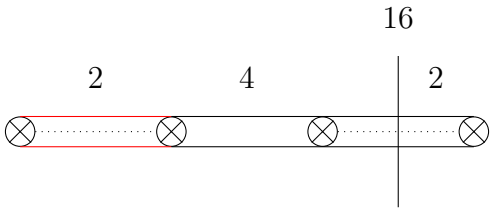
As before, the magnetic quiver may be found from a slightly different derivation of (7.18). Take the non-anomalous $\mathrm{SO}(7) \times \mathrm{Sp}(2)$ gauge theory with both gauge groups at finite coupling. The quiver is



(7.19)

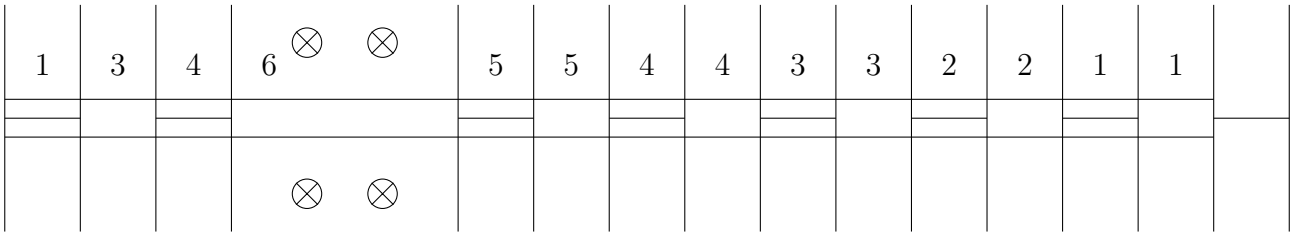
which is similar to (7.18) except that in F-theory the Sp(2) is supported on a (-1)-curve and the SO(7) is supported on a (-3)-curve. There are two tensor multiplets associated to each gauge group. The (-1)-curve may be collapsed which tunes the gauge coupling of Sp(2) to infinity. There is also a small E_8 instanton transition as the tensor multiplet associated to the Sp(2) is lost. The electric theory is again (7.18).

The Type IIA brane system which gives (7.19) as the D6 brane worldvolume theory is



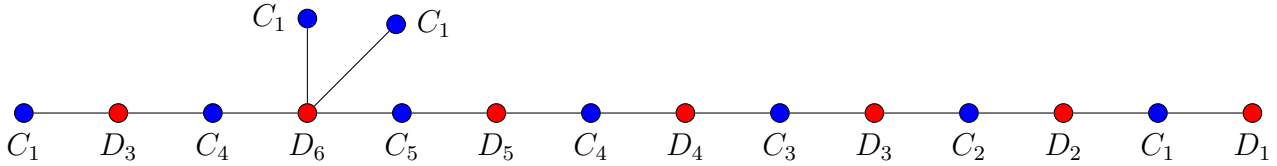
(7.20)

The collapse of the (-1)-curve which tunes the coupling of Sp(2) to infinity is seen in the brane system by moving to the magnetic phase. This is done by first suspending D6 branes between D8 and then merging all four $\frac{1}{2}$-NS5 branes pairwise and lifting them off the orientifold plane. The resulting brane system is



(7.21)

from which one is able to read off the following magnetic quiver

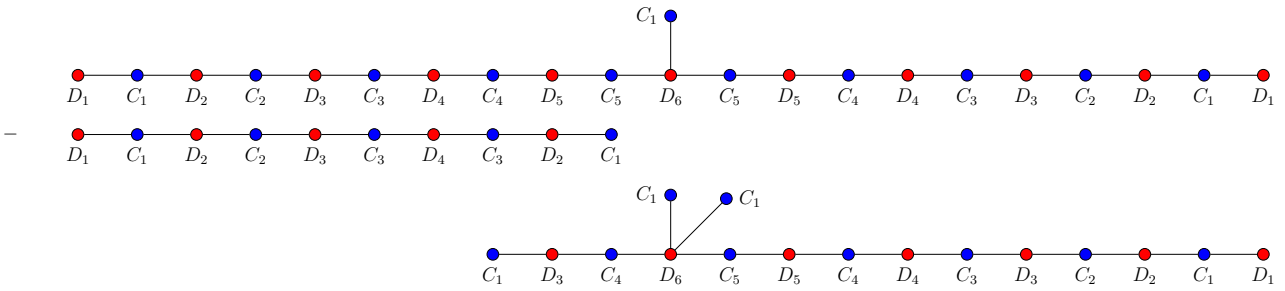


(7.22)

for the Higgs branch of the $6d$ theory (7.18). The bouquet of C_1 gauge nodes attached to the D_6 gauge node is indicative of the SO(7) gauge node in (7.18) being at finite coupling.

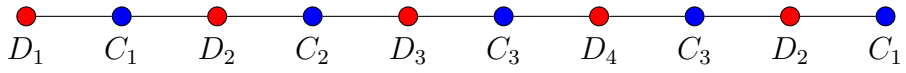
As the $6d$ theory (7.18) comes from gauging an SO(7) subgroup of the flavour symmetry of (7.1) (for $k = 2$), comparing their magnetic quivers (7.22) and (7.2) will realise gauging SO(7) subgroups of Coulomb branch global symmetries.

The two magnetic quivers are related by the quiver subtraction shown below



(7.23)

The following quiver

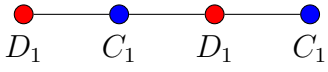


(7.24)

is hence proposed as the SO(7) orthosymplectic quotient quiver. This quiver also contains gauge nodes with negative balance [123], the D_4 gauge node and the C_1 gauge node on the right. The Coulomb branch is smooth and its Hilbert series is not computable with the monopole formula [108] and remains a challenge.

7.2.4 Gauging SU(2)

The SU(2) case differs from the other three in that it is not motivated directly from a six dimensional theory, but rather by the Higgsing pattern observed between the gauge groups introduced thus far. After Higgsing SO(7) $\to G_2 \to$ SU(3), the next gauge group to be broken to is SU(2), and applying the intuition gathered from the previous set of examples leads to the following candidate SU(2) orthosymplectic quotient quiver



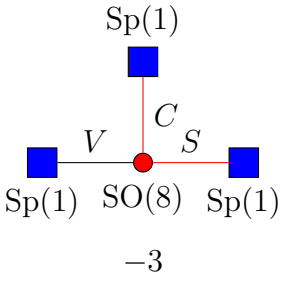
(7.25)

Both C_1 gauge nodes in this quiver have negative balance [123]. The Coulomb branch is smooth and its Hilbert series is not computable with the monopole formula [108].

7.2.5 A comment on other groups

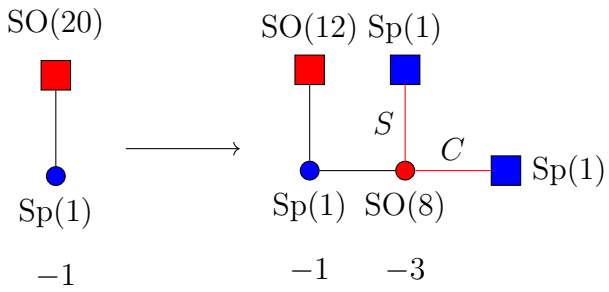
Despite its successes for SU(2), SU(3), G_2, and SO(7), the above analysis does not determine orthosymplectic quotient quivers for any other group. As aforementioned, this is principally a consequence of the anomaly cancellation conditions in six dimensions, which do not ensure graph linearity of the $6d$ quivers. Non-linear quivers also cannot be described by Type IIA brane systems. The most problematic issue with non-linear quivers for this analysis, is that one needs to couple additional matter, this is non-trivial to do on magnetic quivers and no prescription currently exists.

Let this point be illustrated with a specific example of a $6d$ $\mathcal{N} = (1,0)$ SO(8) gauge theory on a (-3)-curve. This non-anomalous SO(8) gauge theory enjoys a triality so the gauge node is coupled to hypermultiplets in the vector, spinor, and co-spinor representations, given in the following quiver (7.26)



(7.26)

Suppose one starts with the non-anomalous Sp(1) gauge theory (7.1) and attempts to gauge an SO(8) subgroup of the SO(20) flavour symmetry. In order to ensure that the SO(8) gauge group is anomaly free, additional matter must be coupled before/after the action of gauging SO(8).



(7.27)

The obstruction of the analysis used in the previous cases of SU(3), G_2, and SO(7) to the above case of SO(8) is that it is not clear how to realise the coupling of additional matter to magnetic quivers in general. This is essential in the treatment of non-linear $6d$ quivers.

Non-linearity similarly afflicts all SO(n) gauge theories for $n \geq 8$, and as such the techniques used in this work cannot derive the associated SO(n) quotient quivers.

Quotient quivers for the groups SU(n) for $n \geq 4$, Sp(n) for $n \geq 2$, and the other exceptional groups remain a challenge due to a lack of constructions of the $6d$ theories from branes or other means and hence there are a lack of magnetic quivers.

7.3 Method of Orthosymplectic Quotient Quiver Subtraction

In this Section, the method for orthosymplectic quotient quiver subtraction is explicitly described. The orthosymplectic quotient quiver subtraction is similar in spirit to the unitary quotient quiver subtraction in Chapter 4. In fact some quirks of the unitary quotient quiver subtraction are shared with the orthosymplectic quotient quiver subtraction.

Consider the subtraction of a quotient quiver from some target quiver. The method proceeds as:

1. Align the quotient quiver against a maximal leg of the target quiver, permitting the quotient quiver to go one node beyond a junction. Ensure that D-type nodes are aligned and C-type nodes are aligned.

2. Subtract the ranks of the nodes of the quotient quiver from the target quiver, ensuring that all nodes have positive rank and have positive (or zero) imbalance.

3. Rebalance only the nodes which do not participate in the subtraction with a gauge node of C_1.

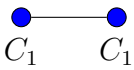
4. If the quotient quiver has gone one node past a junction, the result is the union of all of the possible alignments.

Although there is much similarity with the unitary and orthosymplectic quotient quiver subtraction, there are some differences. In the unitary case, all gauge nodes retain their balance after subtraction, however in the orthosymplectic case, only the gauge nodes not participating in the subtraction retain their balance. In particular, the balance of each of the remaining gauge nodes in the maximal leg of the target quiver generally changes after subtraction.

Another difference is that the orthosymplectic quotient quivers can only be subtracted from maximal legs on the target quiver. In the unitary case, only a leg of $(1)-\cdots-(n)-$ is required to subtract a unitary SU(n) quotient quiver.

In the unitary case, rebalancing can be done with a U(1) gauge node. In the orthosymplectic case, even though there are D-type and C-type nodes, rebalancing is always done with a C_1 gauge node. This may explicitly break the alternating pattern of D-type and C-type gauge nodes in the quiver.

When the result of the quotient quiver subtraction gives a union, the intersection may easily be found through the Kraft-Procesi transition quiver subtraction [254, 255, 110]. To date there is no systematic method of realising the Kraft-Procesi transition on orthosymplectic magnetic quivers. In the cases where a union arises, the typical slice to the intersection is an A_1 transition which corresponds to Kraft-Procesi subtraction of the following quiver



(7.28)

where the edge represents a full hypermultiplet. The Coulomb branch Hilbert series of this quiver is not computable with the monopole formula.

The gauge nodes not participating in the Kraft-Procesi subtraction are again rebalanced with a C_1 gauge node.

7.4 Examples of SU(2) Orthosymplectic Quotient Quiver Subtraction

7.4.1 $\overline{min.E_7}///\mathrm{SU}(2)$

The orthosymplectic quiver with Coulomb branch $\overline{min.E_7}$, given at the top of Figure 7.1, presents one of the simplest examples on which to test SU(2) orthosymplectic quotient quiver subtraction. This example is chosen first as the moduli space of $\overline{min.E_7}$ is well understood and additionally, the orthosymplectic magnetic quiver is star-shaped and constructed using fixtures of D_3. There is a unitary counter-part due to the Lie algebra isomorphism $D_3 \simeq A_3$ and hence there can be comparison to the unitary case.

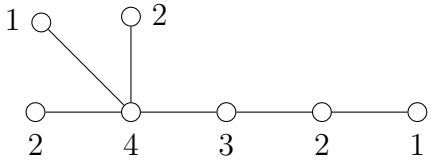
Performing the SU(2) quotient quiver subtraction as in Figure 7.1 results in $\mathcal{Q}_{7.1}$, whose Coulomb branch Hilbert series is

$$\mathrm{HS}\left[\mathcal{C}\left(\mathcal{Q}_{7.1}\right)\right] = \frac{(1+t^2)^2\left(\begin{array}{c}1+36t^2+590t^4+4853t^6+21516t^8+52933t^{10}+71802t^{12}\\+52933t^{14}+21516t^{16}+4853t^{18}+590t^{20}+36t^{22}+t^{24}\end{array}\right)}{(1-t^2)^{28}}. \tag{7.29}$$

This is the same Hilbert series as for $\overline{n.n.min.D_6}$. Hence the conclusion is that

$$\overline{min.E_7}///\mathrm{SU}(2) = \overline{n.n.min.D_6}. \tag{7.30}$$

This result is in fact already known from the unitary quotient quiver subtraction studied in Section 4.4.1, which gives (7.31) as the resulting unitary magnetic quiver for $\overline{n.n.min.D_6}$.



(7.31)

Both the unitary and orthosymplectic magnetic quiver for $\overline{n.n.min.D_6}$ are star-shaped quivers,

and consist of slices in SU(4), or equivalently, SO(6) glued together. The isomorphism $A_3 \simeq D_3$ maps the partition data as in Table 7.1, which gives a further check between the orthosymplectic and unitary quotient quiver subtraction.

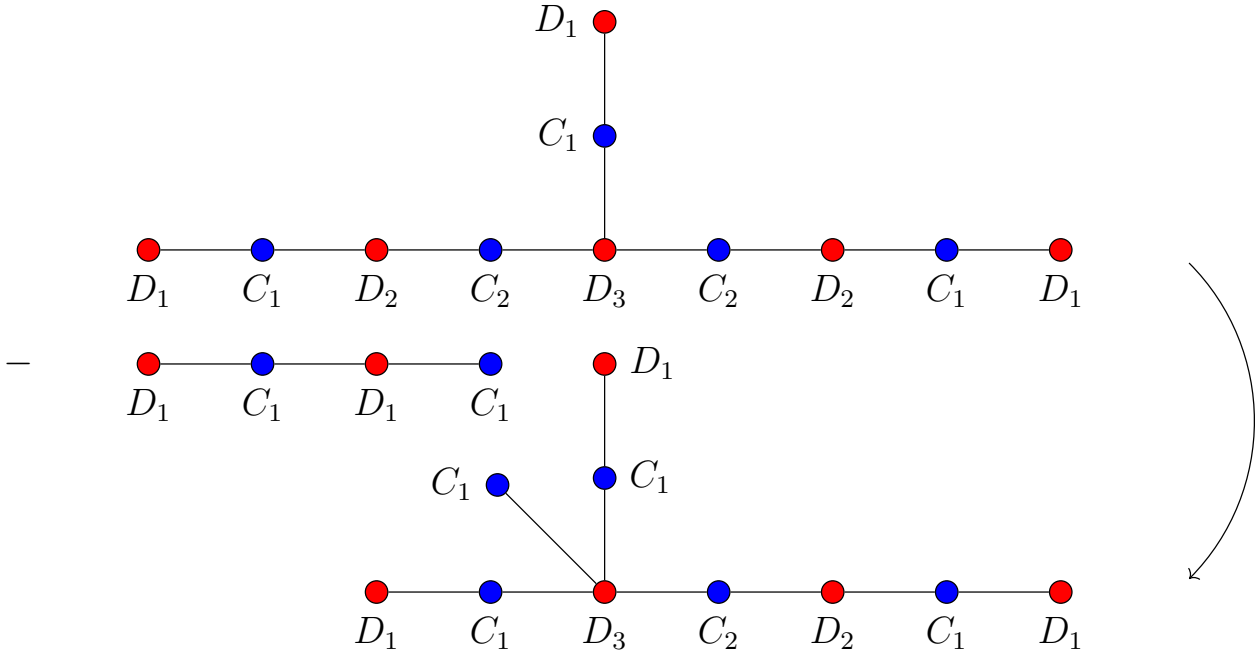


Figure 7.1: Subtraction of the SU(2) orthosymplectic quotient quiver from the orthosymplectic magnetic quiver for $\overline{min.E_7}$ to produce $\mathcal{Q}_{7.1}$.

Orthosymplectic Fixture	Partition of 6	Unitary Fixture	Partition of 4
$C_1 - [D_3]$	$(2^2, 1^2)$	$(1) - [4]$	$(2, 1^2)$
$D_1 - C_1 - [D_3]$	$(3, 1^3)$	$(2) - [4]$	(2^2)
$D_1 - C_2 - [D_3]$	(3^2)	$(1) - (2) - [4]$	$(3, 1)$
$D_1 - C_1 - D_2 - C_2 - [D_3]$	$(5, 1)$	$(1) - (2) - (3) - [4]$	(4)

Table 7.1: The orthosymplectic fixtures of SO(6) alongside the corresponding fixture for SU(4).

The SU(2) orthosymplectic quotient quiver subtraction shown in Figure 7.1 provides another realisation of the Higgs branch side of the $4d$ $\mathcal{N} = 2$ duality proposed in [214]. This duality says that Sp(2) with 6 flavours at infinite coupling is dual to the SU(2) flavour symmetry gauging of the rank 1 E_7 SCFT.

This is the second time this result has been realised using quotient quiver subtraction; the first

with unitary quivers, Section 4.4.1, and the second with orthosymplectic quivers in Figure 7.1.

Due to the isomorphism $A_3 \simeq D_3$, the Higgs branch of $\mathcal{Q}_{7.1}$ is $\mathcal{S}^{D_6}_{\mathcal{N},(7,5)}$ which is the Spaltenstein dual to $\overline{n.n.min.D_6}$. This is seen with the computation of the Higgs branch Hilbert series

$$\text{HS}\left[\mathcal{H}(\mathcal{Q}_{7.1})\right] = \text{PE}\left[2t^4 + t^6 + 2t^8 + t^{10} - t^{16} - t^{20}\right], \tag{7.32}$$

which matches the Hilbert series of $\mathcal{S}^{D_6}_{\mathcal{N},(7,5)}$.

7.4.2 $\overline{min.E_6}///\text{SU}(2)$

The next simplest example is the SU(2) quotient quiver subtraction on the magnetic quiver for $\overline{min.E_6}$. This is shown in Figure 7.2 to produce $\mathcal{Q}_{7.2}$, where rebalancing the gauge nodes introduces a loop into $\mathcal{Q}_{7.2}$. The Higgs branch dimension increases by rank SU(2) = 1 after SU(2) quotient quiver subtraction as expected.

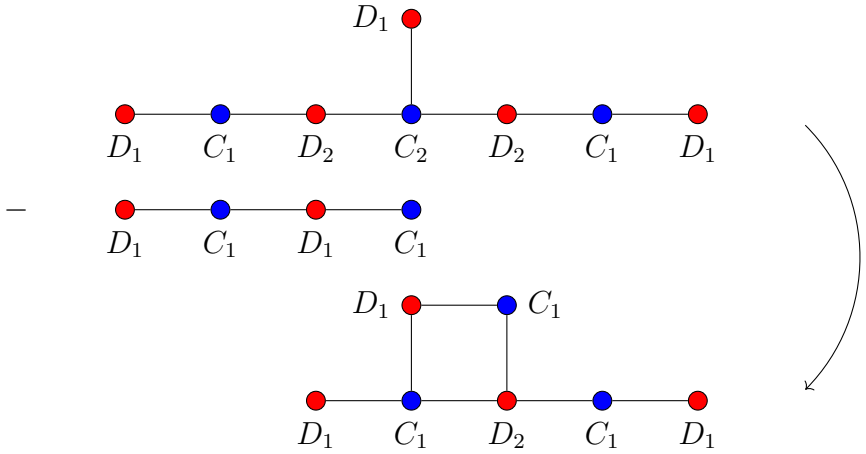


Figure 7.2: Subtraction of the SU(2) orthosymplectic quotient quiver from the orthosymplectic magnetic quiver for $\overline{min.E_6}$ to produce $\mathcal{Q}_{7.2}$.

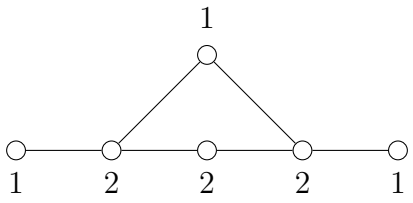
The Coulomb branch Hilbert series is

$$\text{HS}\left[\mathcal{C}\left(\mathcal{Q}_{7.2}\right)\right] = \frac{(1+t^2)^2(1+17t^2+119t^4+251t^6+119t^8+17t^{10}+t^{12})}{(1-t^2)^{16}} \tag{7.33}$$

which exactly matches that of $\overline{n.min.A_5}$, and verifies that

$$\overline{min.E_6}///\mathrm{SU}(2) = \overline{n.min.A_5}. \tag{7.34}$$

The above result is also known from the unitary quotient quiver subtraction in Section 4.4.1 which gives (7.35) as the resulting unitary magnetic quiver for $\overline{n.min.A_5}$



(7.35)

In fact, the Higgs branch Hilbert series of $\mathcal{Q}_{7.2}$ is computed as

$$\mathrm{HS}\left[\mathcal{H}\left(\mathcal{Q}_{7.2}\right)\right] = \frac{1+t^4+t^6+t^8+t^{12}}{(1-t^2)(1-t^4)^2(1-t^6)} \tag{7.36}$$

which is the same Hilbert series as for $\mathcal{S}^{A_5}_{\mathcal{N},(4,2)}$ which is the Spaltenstein dual to $\overline{n.min.A_5}$. The Higgs branch dimension increases by rank $\mathrm{SU}(2) = 1$ after $\mathrm{SU}(2)$ quotient quiver subtraction as expected.

The orthosymplectic $\mathrm{SU}(2)$ quotient quiver subtraction in Figure 7.2 thus gives a novel orthosymplectic quiver with a gauge node loop which is a doppelgänger to the unitary quiver (7.35). This is because they have the same Coulomb branch and the same Higgs branch.

7.4.3 $\overline{n.min.A_5}///\mathrm{SU}(2)$

The quiver $\mathcal{Q}_{7.2}$, the magnetic quiver for $\overline{n.min.A_5}$, resulting from an orthosymplectic $\mathrm{SU}(2)$ quotient quiver subtraction on $\overline{min.E_6}$ may itself be the starting point for a further orthosymplectic $\mathrm{SU}(2)$ quotient quiver subtraction. In this case, there are two alignments of the $\mathrm{SU}(2)$ quotient quiver along the long leg of $\mathcal{Q}_{7.2}$ shown in Figure 7.3a and Figure 7.3b resulting in

$\mathcal{Q}_{7.3a}$ and $\mathcal{Q}_{7.3b}$ respectively. Their intersection is $\mathcal{Q}_{7.3c}$, where the rule of subtracting (7.28) (not shown) discussed in Section 7.3 is used.

The Coulomb branch Hilbert series of $\mathcal{Q}_{7.3a}$ is

$$\mathrm{HS}[\mathcal{C}(\mathcal{Q}_{7.3a})] = \frac{1 + 5t^2 + 14t^4 + 14t^6 + 5t^8 + t^{10}}{(1-t^2)^{10}}, \tag{7.37}$$

from which the Coulomb branch is identified as $\mathcal{C}(\mathcal{Q}_{7.3a}) = \overline{\mathcal{O}}^{A_3}_{(3,1)}$. For $\mathcal{Q}_{7.3b}$, the Coulomb branch Hilbert series is

$$\mathrm{HS}[\mathcal{C}(\mathcal{Q}_{7.3b})] = \frac{1 + 11t^2 + 57t^4 + 170t^6 + 324t^8 + 398t^{10} + \cdots + t^{20}}{(1-t^2)^5(1-t^4)^5}, \tag{7.38}$$

from which the Coulomb branch can be identified as $\mathcal{C}(\mathcal{Q}_{7.3b}) = \overline{[\mathcal{W}_{D_4}]}^{[0,1,0,2]}_{[0,0,0,2]}$. The intersection of $\mathcal{Q}_{7.3a}$ and $\mathcal{Q}_{7.3b}$ is conjectured to be $\mathcal{Q}_{7.3c}$. There is no established method of quiver subtraction for Kraft-Procesi transitions therefore $\mathcal{Q}_{7.3c}$ was found by subtracting (7.28). The Coulomb branch Hilbert series for $\mathcal{Q}_{7.3c}$ is

$$\mathrm{HS}[\mathcal{C}(\mathcal{Q}_{7.3c})] = \frac{(1+t^2)^2(1+5t^2+t^4)}{(1-t^2)^8}, \tag{7.39}$$

which identifies the Coulomb branch as $\mathcal{C}(\mathcal{Q}_{7.3c}) = \overline{\mathcal{O}}^{A_2}_{(2^2)}$.

Therefore the conclusion is that

$$\overline{n.min.A_5}///\mathrm{SU}(2) = \overline{\mathcal{O}}^{A_3}_{(3,1)} \cup \overline{[\mathcal{W}_{D_4}]}^{[0,1,0,2]}_{[0,0,0,2]}, \tag{7.40}$$

In particular the unitary doppelgängers to $\mathcal{Q}_{7.3a}$, $\mathcal{Q}_{7.3b}$, and $\mathcal{Q}_{7.3c}$ are (7.41), (7.42), and (7.43) respectively. The orthosymplectic doppelgänger $\mathcal{Q}_{7.3c}$ to (7.43) follows from the Lie algebra isomorphism $\mathrm{U}(1) \simeq D_1$ and $\mathrm{SU}(2) \simeq \mathrm{Sp}(1)$, however the orthosymplectic doppelgängers $\mathcal{Q}_{7.3a}$ and $\mathcal{Q}_{7.3b}$ to (7.41) and (7.42) are non-trivial.

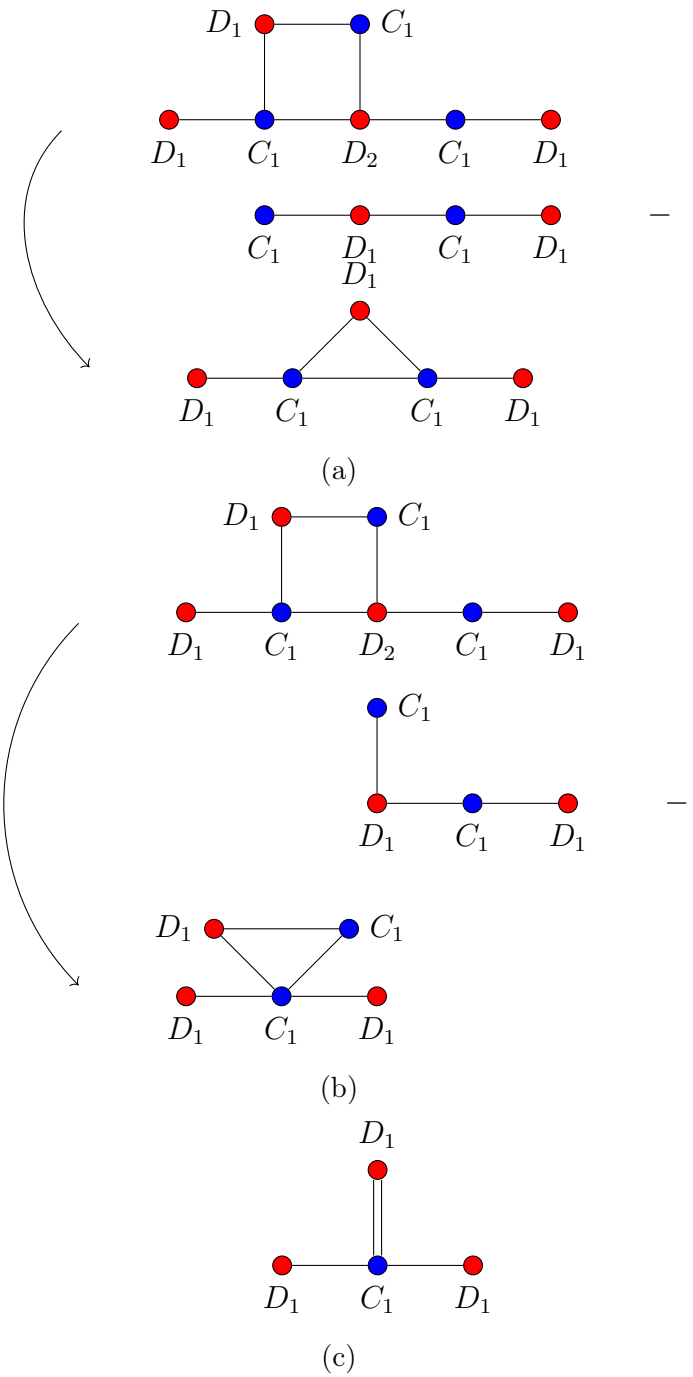
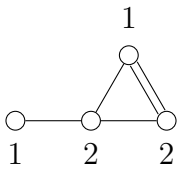
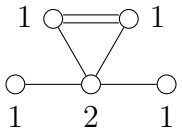


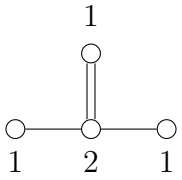
Figure 7.3: Both alignments of the SU(2) quotient quiver against $\mathcal{Q}_{7.2}$ to produce $\mathcal{Q}_{7.3a}$ and $\mathcal{Q}_{7.3b}$. Their intersection is $\mathcal{Q}_{7.3c}$.



(7.41)



(7.42)



(7.43)

This can be verified with computation of the Higgs branch Hilbert series for each quiver. Unlike the Coulomb branch Hilbert series, the Higgs branch Hilbert series admits partial refinement since each quiver has a pair of bifundamental hypers between two gauge nodes, contributing a factor of Sp(1) to the global symmetry. Additionally, the quivers $\mathcal{Q}_{7.3a}$ and $\mathcal{Q}_{7.3b}$ contain a larger loop of gauge nodes and therefore there is an invariant associated to them which contributes an additional factor of U(1) to the global symmetry. It is unknown how to give a fugacity to this U(1). Firstly for $\mathcal{Q}_{7.3a}$,

$$\mathrm{HS}[\mathcal{H}(\mathcal{Q}_{7.3a})] = \mathrm{PE}\left[\left([2]_{\mathrm{Sp}(1)}+1\right)t^2 + 2[1]_{\mathrm{Sp}(1)}t^3 - t^6 - t^8\right], \tag{7.44}$$

where the Dynkin label is a shorthand for the character of the given Sp(1) representation. With guidance from Spaltenstein duality, the Hilbert series for $\mathcal{S}^{A_3}_{\mathcal{N},(2,1^2)}$ – the Spaltenstein dual of $\overline{\mathcal{O}}^{A_3}_{(3,1)}$ – is

$$\mathrm{HS}\left[\mathcal{S}^{A_3}_{\mathcal{N},(2,1^2)}\right] = \mathrm{PE}\left[\left([2]_{\mathrm{Sp}(1)}+1\right)t^2 + (q+1/q)[1]_{\mathrm{Sp}(1)}t^3 - t^6 - t^8\right], \tag{7.45}$$

where q is a U(1) fugacity. This produces the same Hilbert series as $\mathcal{H}(\mathcal{Q}_{7.3a})$ in the limit $q \to 1$.

The Higgs branch Hilbert series of $\mathcal{Q}_{7.3b}$ may also be partially refined although the resulting

Hilbert series is not a complete intersection. The unrefined Hilbert series is given as

$$\mathrm{HS}[\mathcal{H}(\mathcal{Q}_{7.3b})] = \frac{\left(\begin{array}{l} 1+3t^2+2t^3+6t^4+4t^5+10t^6+6t^7+9t^8 \\ \quad +6t^9+10t^{10}+4t^{11}+6t^{12}+2t^{13}+3t^{14}+t^{16} \end{array}\right)}{(1-t^2)(1-t^3)^2(1-t^4)(1-t^5)^2} \tag{7.46}$$

There is no simple analogue of Spaltenstein duality for slices in the affine Grassmannian, however it is simple to check that the Higgs branch Hilbert series of (7.42) matches.

Finally, for $\mathcal{Q}_{7.3c}$ the Higgs branch Hilbert series is computed as

$$\mathrm{HS}\left[\mathcal{S}^{A_3}_{\mathcal{N},(2,1^2)}\right] = \mathrm{PE}\left[[2]_{\mathrm{Sp}(1)}t^2 + [2]_{\mathrm{Sp}(1)}t^4 - t^6 - t^8\right], \tag{7.47}$$

which is the same Hilbert series as for $\mathcal{S}^{A_3}_{(2^2)}$, the Spaltenstein dual of $\overline{\mathcal{O}}^{A_3}_{(2^2)}$. The Higgs branch dimension increases by rank $\mathrm{SU}(2) = 1$ after $\mathrm{SU}(2)$ quotient quiver subtraction as expected.

The novelty of the $\mathrm{SU}(2)$ orthosymplectic quotient quiver subtraction in Figure 7.3 is in the discovery of orthosymplectic doppelgängers to (7.41), (7.42), and (7.43) which are $\mathcal{Q}_{7.3a}$, $\mathcal{Q}_{7.3b}$, and $\mathcal{Q}_{7.3c}$ respectively. It is also interesting to note that the alternating SO/Sp gauge node structure typical of orthosymplectic quivers is not present in $\mathcal{Q}_{7.3a}$ and $\mathcal{Q}_{7.3b}$.

7.4.4 $\overline{min.E_8}//\mathrm{SU}(2)$

The $\mathrm{SU}(2)$ orthosymplectic quotient quiver may be subtracted from the orthosymplectic magnetic quiver for $\overline{min.E_8}$, as shown in Figure 7.4, to produce $\mathcal{Q}_{7.4}$.

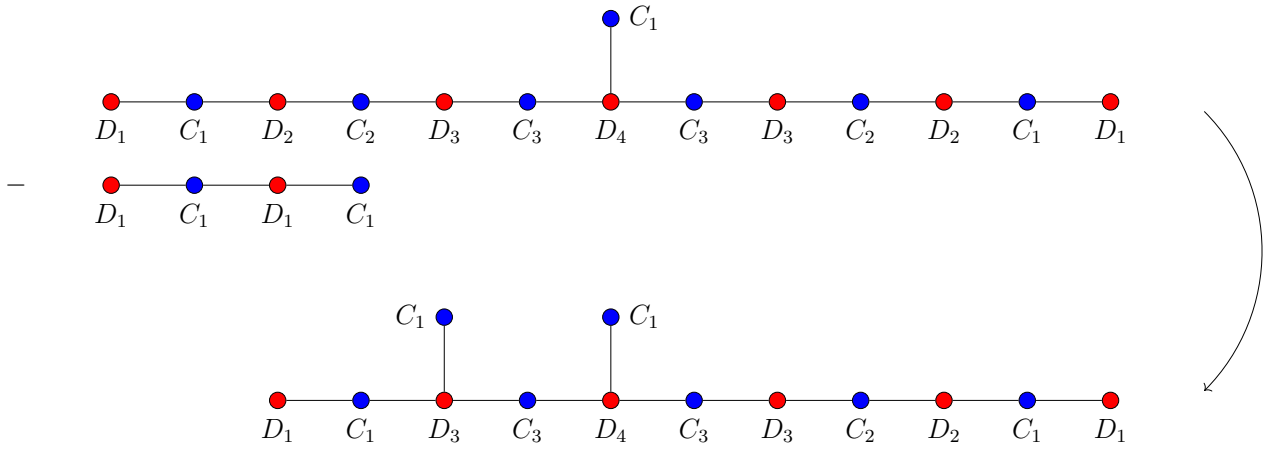


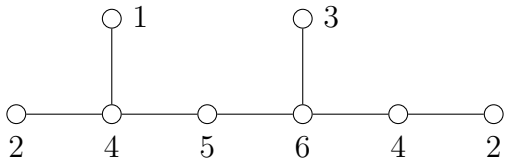
Figure 7.4: Subtraction of the SU(2) orthosymplectic quotient quiver from the orthosymplectic magnetic quiver for $\overline{min.E_8}$ to produce $\mathcal{Q}_{7.4}$.

The Coulomb branch Hilbert series is

$$\text{HS}\left[\mathcal{C}\left(\mathcal{Q}_{7.4}\right)\right] = \frac{(1+t^2)^2\left(\begin{array}{l}1+79t^2+3161t^4+75291t^6+1158376t^8+12099785t^{10}\\ \quad +88650725t^{12}+465895118t^{14}+1783653576t^{16}+5026645901t^{18}\\ \quad +10497603729t^{20}+16309233956t^{22}+18885794304t^{24}+\cdots+t^{48}\end{array}\right)}{(1-t^2)^{52}} \tag{7.48}$$

which confirms the Coulomb branch as $\overline{n.min.E_7}$.

This is again consistent with the unitary quotient quiver subtraction studied in Section 4.4.1 which gives the following unitary magnetic quiver for $\overline{n.min.E_7}$



(7.49)

The Higgs branch Hilbert series of $\mathcal{Q}_{7.4}$ is computed as

$$\text{HS}\left[\mathcal{H}\left(\mathcal{Q}_{7.4}\right)\right] = \text{PE}\left[t^4+t^8+t^{10}+t^{12}+t^{16}+t^{18}-t^{28}-t^{36}\right] \tag{7.50}$$

which is the same Hilbert series as $\mathcal{S}^{E_7}_{\mathcal{N},[2,2,0,2,0,2,2]}$ (Bala-Carter label $E_7(a_2)$) which is Spaltenstein

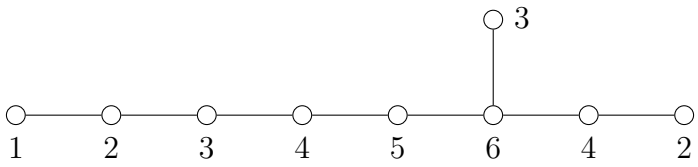
dual to $\overline{n.min.E_7}$.

The orthosymplectic quotient quiver subtraction hence gives a new orthosymplectic doppelgänger to (7.49).

7.4.5 $\overline{min.E_8}/\!/\!/ \left(\mathrm{SU}(2) \times \mathrm{SU}(2)\right)$

All of the examples so far have recovered known results from either Type IIA string theory, class $\mathcal{S}$ theories, and in particular from unitary quotient quiver subtraction. It is now time to explore the differences between unitary and orthosymplectic magnetic quivers. In doing so, results which can be obtained from orthosymplectic quivers, but not from unitary quivers (at present), are discussed.

The unitary and orthosymplectic minimal E-type quivers share the same Coulomb and Higgs branches but they are far from identical. Take for example the affine $E_8^{(1)}$ quiver (7.51), which is the unitary magnetic quiver for $\overline{min.E_8}$.



(7.51)

This has one long leg of gauge nodes of the form $(1) - (2) - \cdots - (6) -$, making it amenable to one subtraction of either an SU(2), SU(3), or SU(4) unitary quotient quiver. In contrast, the orthosymplectic magnetic quiver for $\overline{min.E_8}$ has two long legs exchanged under an S_2 outer automorphism symmetry, and is hence amenable to the subtraction of an SU(2) or SU(3) orthosymplectic quotient quiver on either long leg. The action on the Coulomb branch is the hyper-Kähler quotient by $G \times G'$ where G and G' are either SU(2) or SU(3).

The discussion below will focus on $\overline{min.E_8}/\!/\!/ \left(\mathrm{SU}(2) \times \mathrm{SU}(2)\right)$ for now with gaugings involving SU(3) studied in the next Section. The subtraction of two SU(2) orthosymplectic quotient quivers from each leg of the orthosymplectic magnetic quiver for $\overline{min.E_8}$ is shown in Figure 7.5 to produce quiver $\mathcal{Q}_{7.5}$. From counting the ranks of the gauge nodes, the Coulomb branch of $\mathcal{Q}_{7.5}$

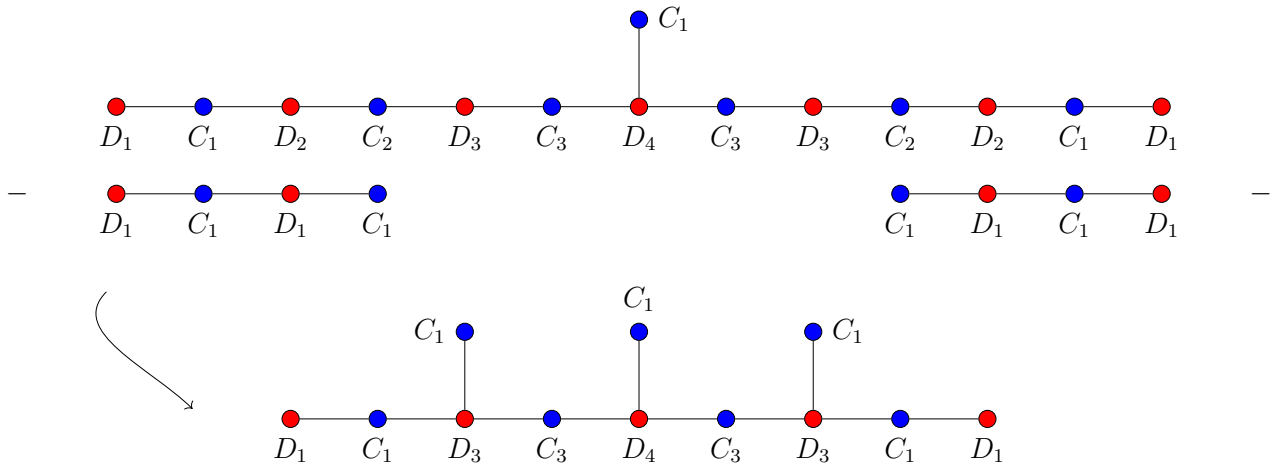


Figure 7.5: Subtraction of two SU(2) orthosymplectic quotient quivers from each long leg of the orthosymplectic magnetic quiver for $\overline{min.E_8}$. The result is quiver $\mathcal{Q}_{7.5}$.

has dimension 23 which precludes an exact computation of its Coulomb branch Hilbert series. Nevertheless, the unrefined perturbative Hilbert series may be computed and is presented here up to order t^{10} together with its PL.

$$\mathrm{HS}\left[\mathcal{C}(\mathcal{Q}_{7.5})\right] = 1 + 66t^2 + 2706t^4 + 79651t^6 + 1810160t^8 + 33147464t^{10} + O\left(t^{11}\right) \quad (7.52)$$

$$\mathrm{PL}\left[\mathrm{HS}\left[\mathcal{C}(\mathcal{Q}_{7.5})\right]\right] = 66t^2 + 495t^4 - 3135t^6 - 64636t^8 + 884156t^{10} + O\left(t^{11}\right) \quad (7.53)$$

The t^2 term is 66 is indicative of an SO(12) global symmetry. The only other generator, at order t^4, appears to transform in the $\wedge^4\left([1,0,0,0,0,0]_{D_6}\right)$ indicating that the moduli space is not a slice in the affine Grassmannian. But otherwise it is difficult to identify the moduli space exactly.

To compare, the unrefined Hilbert series for $\overline{min.E_8}/\!/\!/\left(\mathrm{SU}(2)\times\mathrm{SU}(2)\right)$ can be computed exactly and is evaluated as

$$\mathrm{HS}\left[\overline{min.E_8}/\!/\!/\left(\mathrm{SU}(2)\times\mathrm{SU}(2)\right)\right]$$

$$= \frac{\left(\begin{array}{l} 1+43t^2+1418t^4+31351t^6+521884t^8+6691001t^{10}+68405360t^{12}+569379869t^{14} \\ +3933117266t^{16}+22876102070t^{18}+113436359067t^{20}+484431480383t^{22} \\ +1797063507391t^{24}+5832469898724t^{26}+16662719682327t^{28}+42117041766495t^{30} \\ +94593877569560t^{32}+189460950668991t^{34}+339409608683291t^{36}+545161969037398t^{38} \\ +786610379435045t^{40}+1021071962986483t^{42}+1193603944481102t^{44} \\ +1257280044576400t^{46}+\cdots+t^{92} \end{array}\right)}{(1-t^2)^{23}(1-t^4)^{23}} \tag{7.54}$$

$$= 1+66t^2+2706t^4+79651t^6+1810160t^8+33147464t^{10}+O\left(t^{11}\right), \tag{7.55}$$

which matches the Coulomb branch Hilbert series of $\mathcal{Q}_{7.5}$ up to order t^{10}.

The Hilbert series (7.54) was evaluated using the embedding of $E_8 \hookleftarrow \mathrm{SO}(12)\times\mathrm{SU}(2)\times\mathrm{SU}(2)$ which decomposes the fundamental as

$$(\mu_7)_{E_8} \to \mu_2+\nu^2+\rho^2+\mu_5\nu+\mu_6\rho+\mu_1\nu\rho, \tag{7.56}$$

where on the right-hand side the μ_i, ν, and ρ are highest weight fugacities for $\mathrm{SO}(12), \mathrm{SU}(2)$, and $\mathrm{SU}(2)$ respectively.

This verifies that

$$\mathcal{C}\left(\mathcal{Q}_{7.5}\right) = \overline{min.E_8}/\!/\!/\left(\mathrm{SU}(2)\times\mathrm{SU}(2)\right), \tag{7.57}$$

where it is worth reiterating that such a result has not been seen using unitary quivers.

7.5 Examples of SU(3) Orthosymplectic Quotient Quiver Subtraction

7.5.1 $\overline{min.E_7}///\mathrm{SU}(3)$

Similar to the SU(2) quotient quiver subtraction, the orthosymplectic magnetic quiver for $\overline{min.E_7}$ also admits an SU(3) quotient quiver subtraction with two alignments, as shown in Figure 7.6. The resulting quivers are $\mathcal{Q}_{7.6a}$ and $\mathcal{Q}_{7.6b}$, whose intersection is $\mathcal{Q}_{7.6c}$, which is the same as $\mathcal{Q}_{7.2}$, whose Coulomb branch is $\overline{n.min.A_5}$.

The Coulomb branch Hilbert series for $\mathcal{Q}_{7.6a}$ is given in (7.58), which identifies $\mathcal{C}(\mathcal{Q}_{7.6a}) = \overline{\mathcal{O}}^{A_5}_{(2^3)}$.

$$\mathrm{HS}\left[\mathcal{C}\left(\mathcal{Q}_{7.6a}\right)\right] = \frac{(1+t^2)^3(1+14t^2+72t^4+133t^6+72t^8+14t^{10}+t^{12})}{(1-t^2)^{18}} \tag{7.58}$$

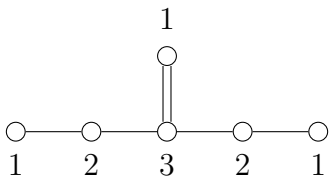
For $\mathcal{Q}_{7.6b}$, the Coulomb branch Hilbert series in (7.59) similarly identifies $\mathcal{C}(\mathcal{Q}_{7.6b}) = \overline{\mathcal{O}}^{A_5}_{(3,1^3)}$.

$$\mathrm{HS}\left[\mathcal{C}\left(\mathcal{Q}_{7.6b}\right)\right] = \frac{(1+t^2)(1+16t^2+136t^4+416t^6+626t^8+416t^{10}+136t^{12}+16t^{14}+t^{16})}{(1-t^2)^{18}} \tag{7.59}$$

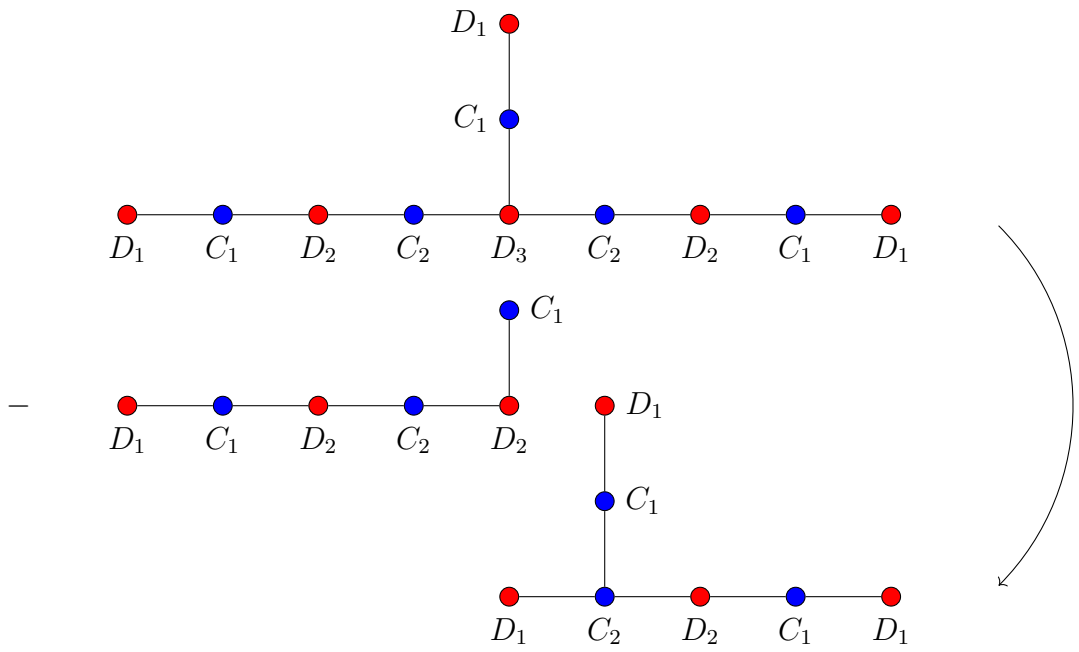
Taking the intersection of $\mathcal{C}(\mathcal{Q}_{7.6b})$ and $\mathcal{C}(\mathcal{Q}_{7.6a})$ hence leads to (7.60), which is consistent with the result from the unitary quotient quiver subtraction in Section 4.4.2.

$$\overline{min.E_7}///\mathrm{SU}(3) = \overline{\mathcal{O}}^{A_5}_{(2^3)} \cup \overline{\mathcal{O}}^{A_5}_{(3,1^3)} \tag{7.60}$$

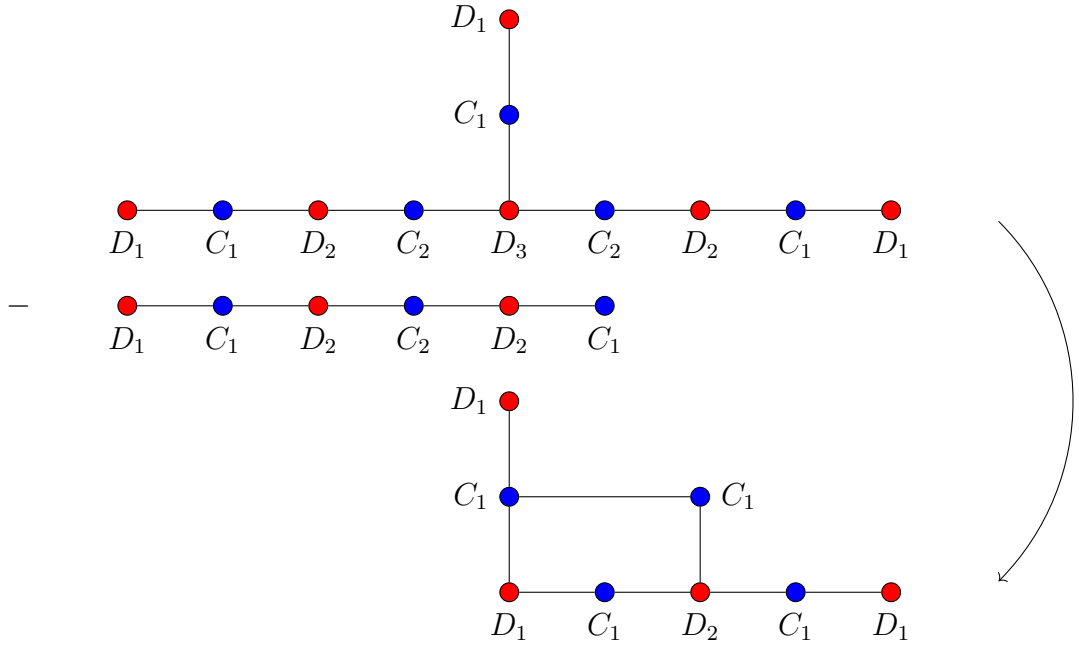
In particular, the unitary doppelgängers to $\mathcal{Q}_{7.6a}$ and $\mathcal{Q}_{7.6b}$ are (7.61) and (7.62) respectively.



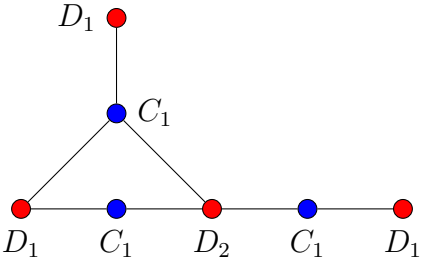
(7.61)



(a)

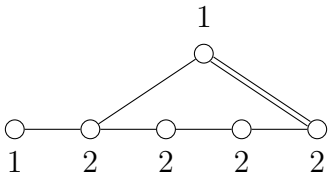


(b)



(c)

Figure 7.6: Two alignments of the SU(3) quotient quiver against the magnetic orthosymplectic quiver for $\overline{min.E_7}$ producing $\mathcal{Q}_{7.6a}$ and $\mathcal{Q}_{7.6b}$. Their intersection is $\mathcal{Q}_{7.6c}$.



(7.62)

Computations of the Higgs branch Hilbert series give further evidence for this claim. The Higgs branch Hilbert series of $\mathcal{Q}_{7.6a}$ can be computed with refinement of the Sp(1) rotating the two bifundamental hypermultiplets between the C_1 and C_2 gauge nodes. This gives

$$\mathrm{HS}\left[\mathcal{H}(\mathcal{Q}_{7.6a})\right] = \mathrm{PE}\left[[2]_{\mathrm{Sp}(1)}t^2 + [2]_{\mathrm{Sp}(1)}t^4 + [2]_{\mathrm{Sp}(1)}t^6 - t^8 - t^{10} - t^{12}\right] \tag{7.63}$$

where the Dynkin label is a shorthand for the character of the given representation. This is the same Hilbert series as for $\mathcal{S}^{A_5}_{\mathcal{N},(3^2)}$ which is the Spaltenstein dual to $\overline{\mathcal{O}}^{A_5}_{(3^2)}$.

The Higgs branch Hilbert series of $\mathcal{Q}_{7.6b}$ may also be computed with refinement of the Sp(1) symmetry rotating the two bifundamental hypermultiplets between the C_1 gauge nodes. This gives

$$\mathrm{HS}\left[\mathcal{H}(\mathcal{Q}_{7.6b})\right] = \mathrm{PE}\left[[2]_{\mathrm{Sp}(1)}t^2 + 2[1]_{\mathrm{Sp}(1)}t^5 - t^{10} - t^{12}\right] \tag{7.64}$$

The Hilbert series of $\mathcal{S}^{A_5}_{\mathcal{N},(4,1^2)}$, the Spaltenstein dual to $\overline{\mathcal{O}}^{A_5}_{(3,1^3)}$, is given as

$$\mathrm{HS}\left[\mathcal{S}^{A_5}_{\mathcal{N},(3,1^3)}\right] = \mathrm{PE}\left[[2]_{\mathrm{Sp}(1)}t^2 + (q+1/q)\,[1]_{\mathrm{Sp}(1)}t^5 - t^{10} - t^{12}\right], \tag{7.65}$$

where q is a U(1) fugacity. This Hilbert series in the limit $q \to 1$ matches that of the Higgs branch of $\mathcal{Q}_{7.6b}$. The Higgs branch dimension increases by rank SU(3) = 2 after SU(3) quotient quiver subtraction as expected.

The SU(3) quotient quiver subtraction in Figure 7.6 hence provides new constructions for $\overline{\mathcal{O}}^{A_5}_{(2^3)}$ and $\overline{\mathcal{O}}^{A_5}_{(3,1^3)}$ from the orthosymplectic magnetic quivers $\mathcal{Q}_{7.6a}$ and $\mathcal{Q}_{7.6b}$ respectively. It is interesting to note that neither of these quivers preserve the alternating SO − Sp pattern of gauge nodes typical of orthosymplectic theories.

7.5.2 $\overline{min.E_8}///\mathrm{SU}(3)$ and $\overline{min.E_8}///(\mathrm{SU}(3)\times\mathrm{SU}(3))$

The subtraction of the SU(3) orthosymplectic quotient quiver against the orthosymplectic magnetic quiver for $\overline{min.E_8}$ to produce quiver $\mathcal{Q}_{7.7}$ is shown in Figure 7.7. This is confirmed in [72].

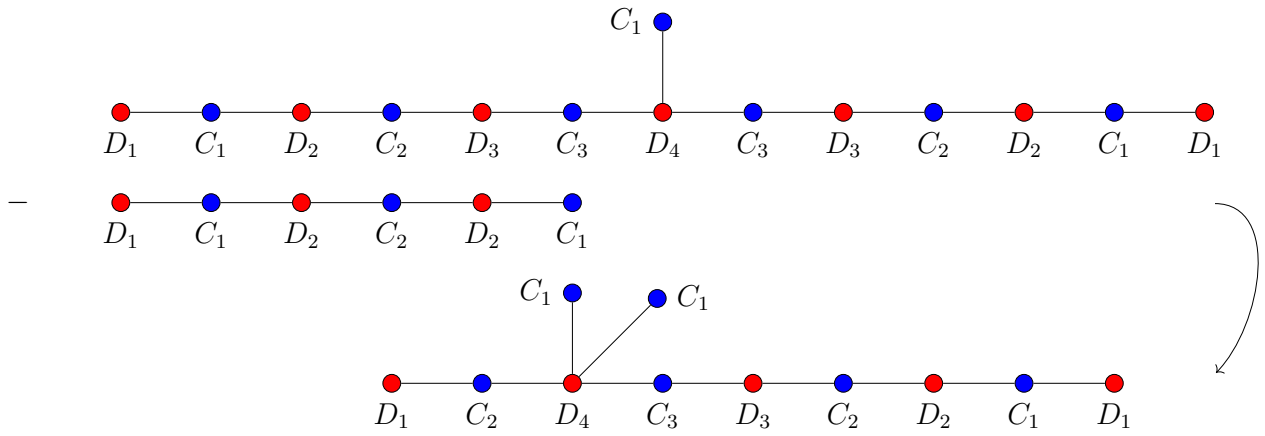


Figure 7.7: Subtraction of the SU(3) orthosymplectic quotient quiver from the orthosymplectic magnetic quiver for $\overline{min.E_8}$.

As mentioned in Section 7.4.5, since the orthosymplectic magnetic quiver for $\overline{min.E_8}$ contains two long legs, a further SU(2) or SU(3) quotient quiver subtraction can be done.

For the case of doing a further SU(3) quotient quiver subtraction, the result is shown in Figure 7.8 producing $\mathcal{Q}_{7.8}$.

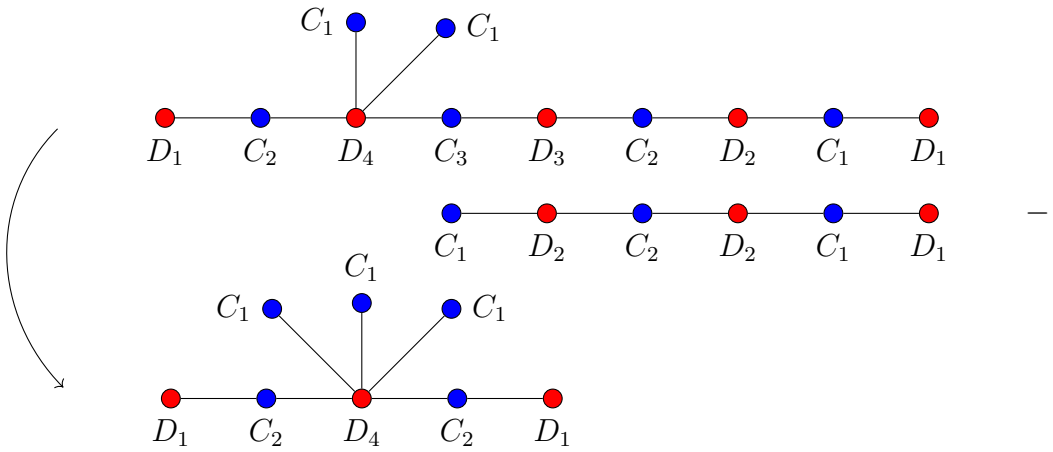


Figure 7.8: Subtraction of the SU(3) orthosymplectic quotient quiver from the orthosymplectic magnetic quiver for $\overline{min.E_8}///\mathrm{SU}(3)$. This gives $\overline{min.E_8}///\mathrm{SU}(3)\times\mathrm{SU}(3)$ as a moduli space of dressed monopole operators.

The Coulomb branch Hilbert series for both $\mathcal{Q}_{7.7}$ and $\mathcal{Q}_{7.8}$ are given in [72] with further discussion of the appearance of these quivers as magnetic quivers for six dimensional theories.

Here the Higgs branch Hilbert series of $\mathcal{Q}_{7.7}$ is presented. One subtlety to address in the magnetic quivers is the appearance of $\wedge^2\left([1]_{\mathrm{Sp}(1)}\right)$ hypermultiplets on the C_1 gauge nodes in the bouquet. In the Type IIA brane system these hypermultiplets come from D4 branes ending on the same NS5. These hypermultiplets are typically suppressed since they do not contribute to the monopole formula and the Coulomb branch Hilbert series. In the Higgs branch Hilbert series each $\wedge^2\left([1]_{\mathrm{Sp}(1)}\right)$ contributes a factor of $\mathbb{H}$. These will be ignored in the following computations.

The Higgs branch Hilbert series of $\mathcal{Q}_{7.7}$ is computed as

$$\mathrm{HS}\left[\mathcal{H}\left(\mathcal{Q}_{7.7}\right)\right]=\left(1+3t^{12}+2t^{14}+2t^{24}+3t^{26}+t^{38}\right)\mathrm{PE}\left[2t^4+t^6+t^8+t^{10}+t^{12}\right] \tag{7.66}$$

This Hilbert series does not elucidate the moduli space. However, it is known that the Coulomb branch of $\mathcal{Q}_{7.7}$ is the double cover of $\overline{\mathcal{O}}^{E_6}_{[0,0,0,0,0,2]}$ (Bala-Carter label A_2) [72]. One may expect that the Higgs branch is related to the dual slice to this orbit which is $\mathcal{S}^{E_6}_{\mathcal{N},[2,0,2,0,2,0]}$ (Bala-Carter label $E_6(a_3)$) whose Hilbert series is

$$\mathrm{HS}\left[\mathcal{S}^{E_6}_{\mathcal{N},[2,0,2,0,2,0]}\right]=\mathrm{PE}\left[2t^4+3t^6+2t^8+t^{10}+t^{12}-t^{16}-t^{18}-t^{24}\right] \tag{7.67}$$

The volumes of the moduli spaces may be compared as

$$\frac{\mathrm{Vol}\left[\mathcal{H}\left(\mathcal{Q}_{7.7}\right)\right]}{\mathrm{Vol}\left[\mathcal{S}^{E_6}_{\mathcal{N},[2,0,2,0,2,0]}\right]}=\lim_{t\to 1}\frac{\mathrm{HS}\left[\mathcal{H}\left(\mathcal{Q}_{7.7}\right)\right]}{\mathrm{HS}\left[\mathcal{S}^{E_6}_{\mathcal{N},[2,0,2,0,2,0]}\right]}=\frac{1}{2} \tag{7.68}$$

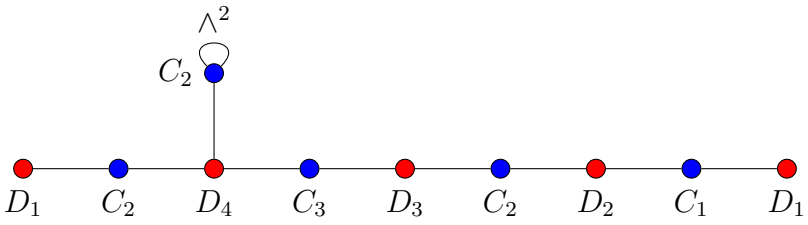
which suggests that $\mathcal{H}\left(\mathcal{Q}_{7.7}\right)=\mathcal{S}^{E_6}_{\mathcal{N},[2,0,2,0,2,0]}/\mathbb{Z}_2$. This suggests that the Hilbert series (7.66) can be written as the $\mathbb{Z}_2$ group average of (7.67). The even contribution to this average is (7.67) itself whereas the odd contribution to the group average is

$$\mathrm{HS}\left[\mathcal{S}^{E_6}_{\mathcal{N},[2,0,2,0,2,0]}\right]^{-}=\mathrm{PE}\left[2t^4-t^6+t^{10}+3t^{12}+t^{18}-t^{24}-t^{36}\right] \tag{7.69}$$

The above Hilbert series has negative terms in the expansion which is allowed since it should

not be thought of as a standalone object.

The two C_1 gauge nodes in the bouquet of $\mathcal{Q}_{7.7}$ may be discretely gauged and gives the following quiver



(7.70)

whose Coulomb branch is $\overline{\mathcal{O}}^{E_6}_{[0,0,0,0,0,2]}$. The Higgs branch is of dimension 4 so it is not the $\mathcal{S}^{E_6}_{\mathcal{N},[2,0,2,0,2,0]}$ which is of dimension 3. Instead, the Higgs branch should be related to the $\mathcal{S}^{E_6}_{\mathcal{N},[2,1,0,1,2,1]}$ (Bala-Carter label A_5) which is a slice from a non-special orbit whose Hasse diagram contains the special piece $\mathcal{S}^{E_6}_{\mathcal{N},[2,0,2,0,2,0]}$ on top.

The Higgs branch Hilbert series is presented as

$$\begin{aligned}\mathrm{HS}\left[\mathcal{H}\left((7.70)\right)\right] = &\left(1+t^{12}+[1]_{\mathrm{Sp}(1)}t^{13}-[1]_{\mathrm{Sp}(1)}t^{27}-t^{28}-t^{40}\right)\\ &\times \mathrm{PE}\left[[2]_{\mathrm{Sp}(1)}t^2+[1]_{\mathrm{Sp}(1)}t^5+t^8+[1]_{\mathrm{Sp}(1)}t^{11}+[2]_{\mathrm{Sp}(1)}t^{14}-t^{16}-t^{24}\right]\end{aligned} \tag{7.71}$$

where the Dynkin labels are shorthand for the character of the Sp(1) representation. The Hilbert series for $\mathcal{S}^{E_6}_{\mathcal{N},[2,0,2,0,2,0]}$ is computed as

$$\mathrm{HS}\left[\mathcal{S}^{E_6}_{\mathcal{N},[2,0,2,0,2,0]}\right] = \mathrm{PE}\left[[2]_{\mathrm{Sp}(1)}t^2+[1]_{\mathrm{Sp}(1)}t^5+t^6+[1]_{\mathrm{Sp}(1)}t^7+t^8+[1]_{\mathrm{Sp}(1)}t^{11}-t^{16}-t^{18}-t^{24}\right] \tag{7.72}$$

Comparison of the volumes of the moduli space gives

$$\frac{\mathrm{Vol}\left[\mathcal{H}\left((7.70)\right)\right]}{\mathrm{Vol}\left[\mathcal{S}^{E_6}_{\mathcal{N},[2,1,0,1,2,1]}\right]} = \lim_{t\to 1,\, x\to 1}\frac{\mathrm{HS}\left[\mathcal{H}\left(\mathcal{Q}_{7.7}\right)\right]}{\mathrm{HS}\left[\mathcal{S}^{E_6}_{\mathcal{N},[2,1,0,1,2,1]}\right]} = \frac{1}{2} \tag{7.73}$$

where x is a fugacity for the Sp(1). This suggests that $\mathcal{H}\left((7.70)\right) = \mathcal{S}^{E_6}_{\mathcal{N},[2,1,0,1,2,1]}/\mathbb{Z}_2$. Although the $\mathbb{Z}_2$ group average may in principle be performed through the HWG [219], the particular form of the HWG is cumbersome to present.

Instead the odd contribution to the HS is presented as

$$\mathrm{HS}\left[\mathcal{S}^{E_6}_{\mathcal{N},[2,0,2,0,2,0]}\right]^{-} = \mathrm{PE}\left[\begin{array}{l}[2]_{\mathrm{Sp}(1)}t^2+[1]_{\mathrm{Sp}(1)}t^5-t^6-[1]_{\mathrm{Sp}(1)}t^7+t^8+[1]_{\mathrm{Sp}(1)}t^{11}+t^{12}\\ +\left([2]_{\mathrm{Sp}(1)}-1\right)t^{14}-t^{16}+t^{18}-t^{24}-t^{36}\end{array}\right] \tag{7.74}$$

7.6 Examples of G_2 Orthosymplectic Quotient Quiver Subtraction

7.6.1 $\overline{min.E_8}///G_2$

Hyper-Kähler quotients of larger groups naturally find application to magnetic quivers describing moduli spaces of higher dimension – for G_2 quotient quiver subtraction, the most straightforward variety to begin with is $\overline{min.E_8}$.

Shown in Figure 7.9, the G_2 quotient quiver has two possible alignments against the orthosymplectic quiver for $\overline{min.E_8}$, giving two quivers $\mathcal{Q}_{7.9a}$ and $\mathcal{Q}_{7.9b}$.

The Hilbert series for the Coulomb branch of $\mathcal{Q}_{7.9a}$ is

$$\mathrm{HS}\left[\mathcal{Q}_{7.9a}\right] = \frac{(1+t^2)\left(\begin{array}{l}1+21t^2+231t^4+1498t^6+6219t^8+16834t^{10}\\ +30420t^{12}+36972t^{14}+\cdots+t^{28}\end{array}\right)}{(1-t^2)^{30}}, \tag{7.75}$$

from which the Coulomb branch can be identified as $\mathcal{C}(\mathcal{Q}_{7.9a}) = \overline{\mathcal{O}}^{F_4}_{[2,0,0,0]}$ (Bala-Carter label A_2). The Hilbert series for the Coulomb branch of $\mathcal{Q}_{7.9b}$ is computed as

$$\mathrm{HS}\left[\mathcal{Q}_{7.9b}\right] = \frac{(1+t^2)\left(\begin{array}{l}1+21t^2+257t^4+2018t^6+9573t^8+28261t^{10}\\ +53781t^{12}+66651t^{14}+\cdots+t^{28}\end{array}\right)}{(1-t^2)^{30}}, \tag{7.76}$$

from which the Coulomb branch can be identified as $\mathcal{C}(\mathcal{Q}_{7.9b}) = \text{Normalisation}\left[\overline{\mathcal{O}}^{F_4}_{[0,0,0,2]}\right]$ (Bala-Carter label $\tilde{A}_2$), where the normalisation of the nilpotent orbit closure is computed by the

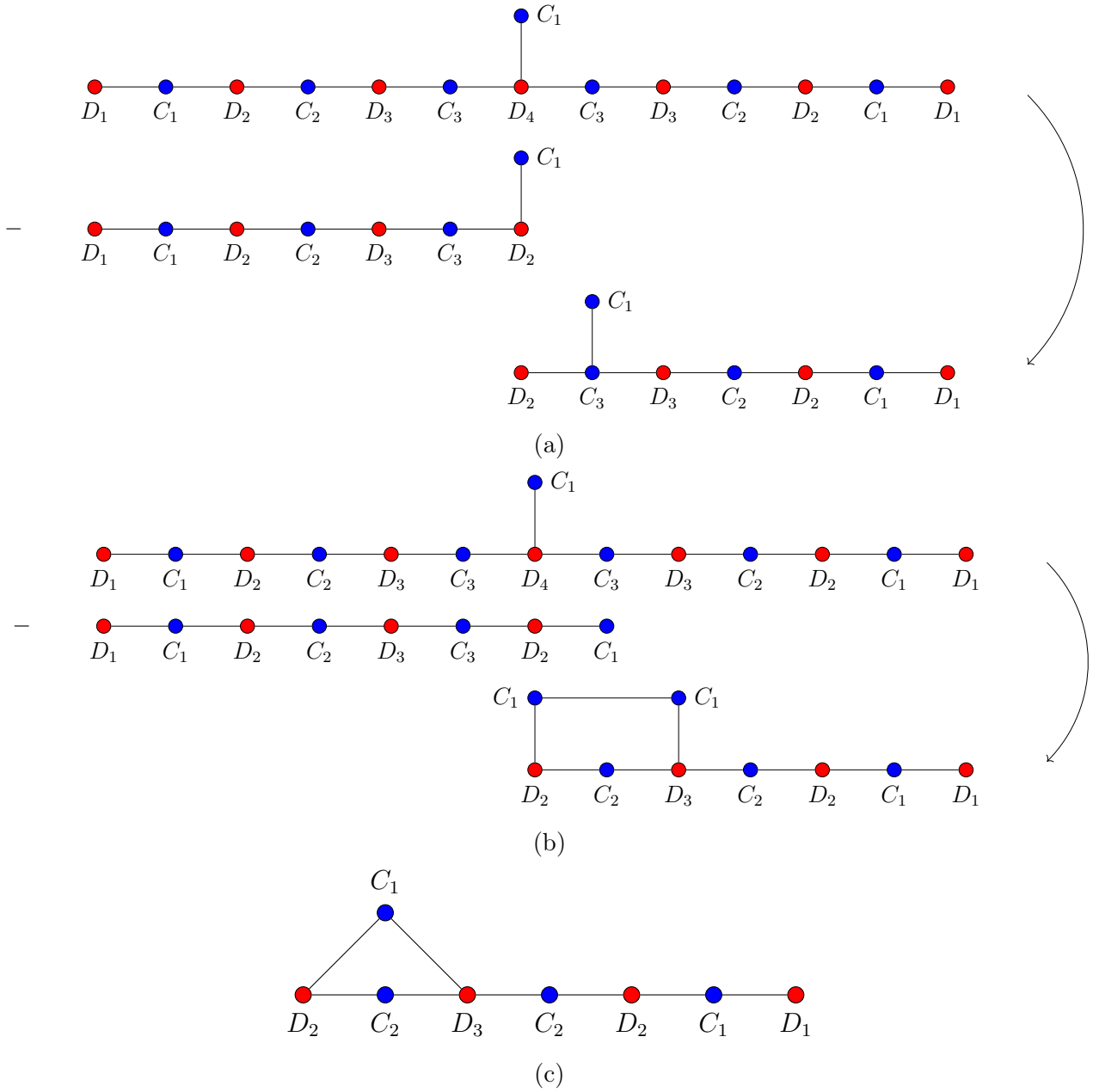


Figure 7.9: Two alignments of the G_2 quotient quiver against the orthosymplectic quiver for $\overline{min.E_8}$ producing $\mathcal{Q}_{7.9a}$ and $\mathcal{Q}_{7.9b}$. Their intersection is $\mathcal{Q}_{7.9c}$.

localisation formula [184].

The proposed intersection of the quivers $\mathcal{Q}_{7.9a}$ and $\mathcal{Q}_{7.9b}$ is $\mathcal{Q}_{7.9c}$, with Coulomb branch Hilbert series

$$\mathrm{HS}\left[\mathcal{Q}_{7.9c}\right] = \frac{(1+t^2)\left(\begin{array}{c}1+22t^2+254t^4+1773t^6+7171t^8\\ +16619t^{10}+22030t^{12}+\cdots+t^{24}\end{array}\right)}{(1-t^2)^{28}}, \tag{7.77}$$

from which there is the identification $\mathcal{C}(\mathcal{Q}_{7.9c}) = \overline{\mathcal{O}}^{F_4}_{[0,1,0,0]}$ (Bala-Carter label $A_1 + \tilde{A}_1$).

The conclusion is hence that

$$\overline{min.E_8}///G_2 = \overline{\mathcal{O}}^{F_4}_{[2,0,0,0]} \cup \text{Normalisation}\left[\overline{\mathcal{O}}^{F_4}_{[0,0,0,2]}\right], \tag{7.78}$$

with the following Hilbert series

$$\begin{aligned}\text{HS}\left[\overline{min.E_8}///G_2\right] &= \frac{\left(\begin{array}{l}1+22t^2+278t^4+2275t^6+12644t^8+47792t^{10}+121354t^{12}\\ \quad +202670t^{14}+217542t^{16}+144142t^{18}+52945t^{20}+6213t^{22}\\ \quad -2660t^{24}-1199t^{26}-208t^{28}-20t^{30}-t^{32}\end{array}\right)}{(1-t^2)^{30}} \qquad (7.79)\\ &= \text{HS}\left[\mathcal{Q}_{7.9a}\right]+\text{HS}\left[\mathcal{Q}_{7.9b}\right]-\text{HS}\left[\mathcal{Q}_{7.9c}\right] \qquad (7.80)\end{aligned}$$

This is verified using Weyl integration and the embedding $E_8 \hookleftarrow F_4 \times G_2$, in which the fundamental of E_8 decomposes as

$$(\mu_7)_{E_8} \hookleftarrow \mu_1+\nu_1+\mu_4\nu_2, \tag{7.81}$$

where μ_i and ν_i are highest weight fugacities for F_4 and G_2 respectively.

It is challenging to find constructions of nilpotent orbit closures of height three or more either as a Higgs branch or a Coulomb branch from unitary or orthosymplectic quivers. The nilpotent orbits of F_4 with characteristics $[2,0,0,0]$ and $[0,0,0,2]$ are of height 4 and the orbit with characteristic $[0,1,0,0]$ is of height three. It is non-trivial to have found the quivers $\mathcal{Q}_{7.9a}$, $\mathcal{Q}_{7.9b}$, and $\mathcal{Q}_{7.9c}$ whose Coulomb branches are (normalisations of) these nilpotent orbits and are the first of their kind.

It is also straightforward to compute the Higgs branch Hilbert series of these quivers with refinement of the global symmetry. The Higgs branch Hilbert series of $\mathcal{Q}_{7.9a}$ is computed, with refinement of the Sp(1) rotating the hypermultiplet between the C_1 and C_3 gauge node, as

$$\text{HS}\left[\mathcal{H}(\mathcal{Q}_{7.9a})\right] = \text{PE}\left[[2]_{\text{Sp}(1)}t^2+[4]_{\text{Sp}(1)}t^8-t^{16}-t^{24}\right] \tag{7.82}$$

where the Dynkin label is short-hand for the character of the given Sp(1) representation. This

is the same Hilbert series as for $\mathcal{S}^{F_4}_{\mathcal{N},[2,2,0,0]}$ (Bala-Carter label B_3) which is the Spaltenstein dual to $\overline{\mathcal{O}}^{F_4}_{[2,0,0,0]}$.

The Higgs branch Hilbert series of $\mathcal{Q}_{7.9b}$ is computed with refinement of the two bifundamental hypermultiplets between the two C_1 gauge nodes.

$$\mathrm{HS}\left[\mathcal{H}(\mathcal{Q}_{7.9b})\right] = \mathrm{PE}\left[[2]_{\mathrm{Sp}(1)}t^2 + [1]_{\mathrm{Sp}(1)}t^5 + t^8 + [1]_{\mathrm{Sp}(1)}t^{11} - t^{16} - t^{24}\right] \tag{7.83}$$

This Hilbert series is the same as for $\mathcal{S}^{F_4}_{\mathcal{N},[1,0,1,2]}$ (Bala-Carter label C_3) which is the Spaltenstein dual to $\overline{\mathcal{O}}^{F_4}_{[0,0,0,2]}$.

The Higgs branch Hilbert series of $\mathcal{Q}_{7.9c}$ is computed without refinement.

$$\mathrm{HS}\left[\mathcal{H}(\mathcal{Q}_{7.9c})\right] = \mathrm{PE}\left[2t^4 + t^6 + t^8 + t^{10} + t^{12} - t^{16} - t^{24}\right] \tag{7.84}$$

This Hilbert series is the same as for $\mathcal{S}^{F_4}_{\mathcal{N},[0,2,0,2]}$ (Bala-Carter label $F_4(a_2)$) which is the Spaltenstein dual to $\overline{\mathcal{O}}^{F_4}_{[0,1,0,0]}$.

There are no known unitary doppelgängers to these three quivers and remains a challenge to find them.

7.6.2 $(\overline{min.E_7} \times \overline{min.E_7})///G_2$

The magnetic quiver for $\overline{min.E_7} \times \overline{min.E_7}$ admits subtraction of the G_2 quotient quiver from the maximal leg. This is shown in Figure 7.10 to produce $\mathcal{Q}_{7.10}$.

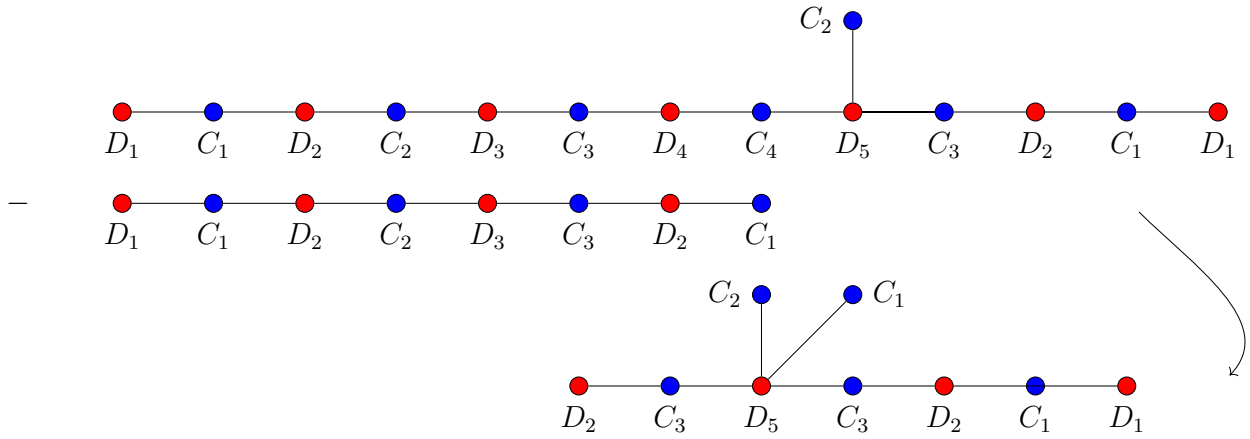


Figure 7.10: Subtraction of the G_2 orthosymplectic quotient quiver from the orthosymplectic magnetic quiver for $\overline{min.E_7} \times \overline{min.E_7}$.

The Coulomb branch Hilbert series is computed perturbatively up to order t^{10} together with its PL.

$$\mathrm{HS}[\mathcal{C}(\mathcal{Q}_{7.10})] = 1 + 42t^2 + 1098t^4 + 21238t^6 + 329230t^8 + 4255866t^{10} + 47097064t^{12} + O\left(t^{13}\right) \tag{7.85}$$

$$\mathrm{PL}\left[\mathrm{HS}[\mathcal{C}(\mathcal{Q}_{7.10})]\right] = 42t^2 + 195t^4 - 196t^6 - 6728t^8 - 2304t^{10} + 460312t^{12} + O\left(t^{13}\right) \tag{7.86}$$

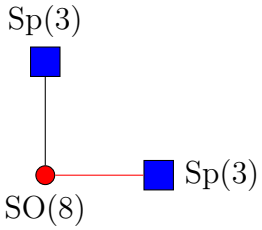
The t^2 coefficient indicates a $\mathrm{Sp}(3) \times \mathrm{Sp}(3)$ global symmetry. This is verified with Weyl integration using the following embedding of $E_7 \times E_7 \hookleftarrow \mathrm{Sp}(3) \times \mathrm{Sp}(3) \times G_2$ which decomposes the fundamental as

$$\mu_{1\,E_7} + \mu'_{1\,E_7} \to \mu_1^2 + \mu_1'^2 + 2\nu_1 + (\mu_2 + \mu'_2)\nu_2 \tag{7.87}$$

where the μ_i and μ'_i are highest weight fugacities for the two $\mathrm{Sp}(3)$ and the ν_i are highest weight fugacities for the G_2 being gauged.

This quiver $\mathcal{Q}_{7.10}$ may also be interpreted as a magnetic quiver for the class $\mathcal{S}$ theory specified by algebra $\mathrm{SO}(10)$ on a four punctured sphere with puncture data $\{(3^3,1),(2^2,1^6),(2^4,1^2),(5,2^2,1)\}$. This quiver may also be a magnetic quiver for the Higgs branch of the diagonal G_2 flavour symmetry gauging of two $4d$ $\mathcal{N}=2$ rank-1 E_7 SCFTs [224]. In [215, Table 2 Ex. 11] the diagonal G_2 flavour symmetry gauging of two rank-1 E_7 theories is proposed to be dual to

the following theory



(7.88)

Computation of the Higgs branch Hilbert series of $\mathcal{Q}_{7.88}$ matches the Hilbert series of the magnetic quiver in (7.85) to the same order in t.

7.7 Example of SO(7) Orthosymplectic Quotient Quiver Subtraction

7.7.1 $(\overline{min.E_7} \times \overline{min.E_7})///\mathrm{SO}(7)$

The orthosymplectic magnetic quiver for $\overline{min.E_7} \times \overline{min.E_7}$ admits two possible alignments of the SO(7) orthosymplectic quotient quiver. These are shown in Figure 7.11a and Figure 7.11b to give $\mathcal{Q}_{7.11a}$ and $\mathcal{Q}_{7.11b}$ respectively.

The Coulomb branch Hilbert series of $\mathcal{Q}_{7.11a}$ is computed perturbatively up to order t^{10} as

$$\mathrm{HS}\left[\mathcal{C}\left(\mathcal{Q}_{7.11a}\right)\right] = 1 + 26t^2 + 438t^4 + 5385t^6 + 52704t^8 + 427872t^{10} + O(t^{11}) \tag{7.89}$$

$$\mathrm{PL}\left[\mathrm{HS}\left[\mathcal{C}\left(\mathcal{Q}_{7.11a}\right)\right]\right] = 26t^2 + 87t^4 - 153t^6 - 1434t^8 + 5124t^{10} + O(t^{11}) \tag{7.90}$$

The Coulomb branch Hilbert series of $\mathcal{Q}_{7.11b}$ is also computed perturbatively up to order t^{20} as

$$\mathrm{HS}\left[\mathcal{C}\left(\mathcal{Q}_{7.11b}\right)\right] = 1 + 26t^2 + 439t^4 + 5505t^6 + 55520t^8 + 466241t^{10} + 3347718t^{12} + O(t^{13}) \tag{7.91}$$

$$\mathrm{PL}\left[\mathrm{HS}\left[\mathcal{C}\left(\mathcal{Q}_{7.11b}\right)\right]\right] = 26t^2 + 88t^4 - 59t^6 - 1501t^8 - 1442t^{10} + 52349t^{12} + O(t^{13}) \tag{7.92}$$

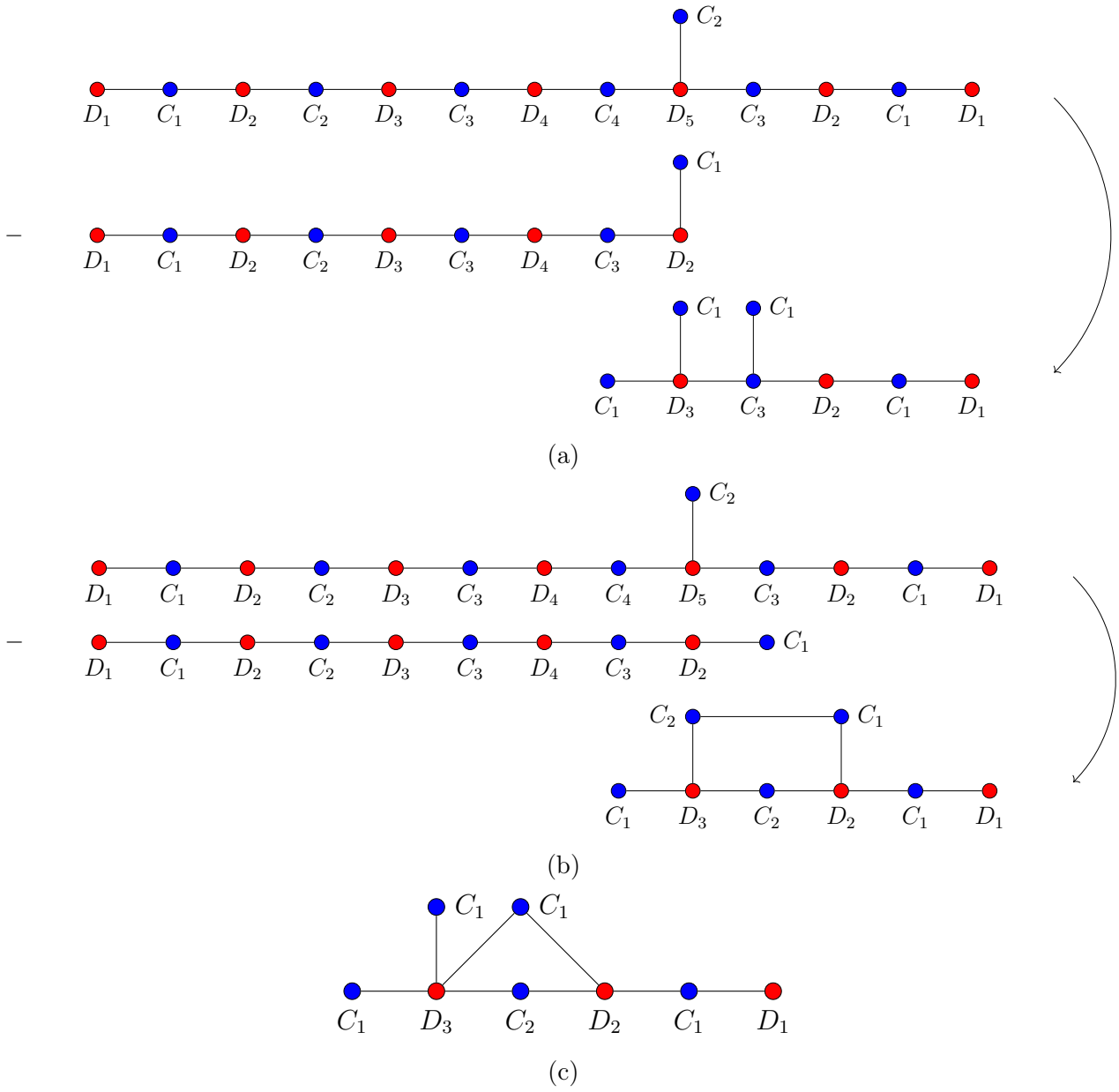


Figure 7.11: Two alignments of the SO(7) quotient quiver against the orthosymplectic magnetic quiver for $\overline{min.E_7} \times \overline{min.E_7}$ producing $\mathcal{Q}_{7.11a}$ and $\mathcal{Q}_{7.11b}$. Their intersection is $\mathcal{Q}_{7.11c}$.

The Coulomb branch Hilbert series of $\mathcal{Q}_{7.11c}$, which is the intersection of $\mathcal{Q}_{7.11a}$ and $\mathcal{Q}_{7.11b}$, is also computed perturbatively up to order t^{20} as

$$\mathrm{HS}\left[\mathcal{C}\left(\mathcal{Q}_{7.11c}\right)\right] = 1 + 26t^2 + 438t^4 + 5385t^6 + 52505t^8 + 421837t^{10} + O(t^{11}) \tag{7.93}$$

$$\mathrm{PL}\left[\mathrm{HS}\left[\mathcal{C}\left(\mathcal{Q}_{7.11c}\right)\right]\right] = 26t^2 + 87t^4 - 153t^6 - 1633t^8 + 4263t^{10} + O(t^{11}) \tag{7.94}$$

The Hilbert series of the union of Coulomb branches is computed as

$$\begin{aligned}\mathrm{HS}\left[\mathcal{C}\left(\mathcal{Q}_{7.11a}\right) \cup C\left(\mathcal{Q}_{7.11b}\right)\right] &= \mathrm{HS}\left[\mathcal{C}\left(\mathcal{Q}_{7.11a}\right)\right] + \mathrm{HS}\left[\mathcal{C}\left(\mathcal{Q}_{7.11b}\right)\right] - \mathrm{HS}\left[\mathcal{C}\left(\mathcal{Q}_{7.11c}\right)\right] \\ &= 1 + 26t^2 + 439t^4 + 5505t^6 + 55719t^8 + 472276t^{10} + 3441602t^{12} \\ &\quad + O(t^{13})\end{aligned} \tag{7.95}$$

$$\mathrm{PL}\left[\mathrm{HS}\left[\mathcal{C}\left(\mathcal{Q}_{7.11a}\right) \cup C\left(\mathcal{Q}_{7.11b}\right)\right]\right] = 26t^2 + 88t^4 - 59t^6 - 1302t^8 - 581t^{10} + 36486t^{12} + O(t^{13}) \tag{7.96}$$

The result from the unions of the Coulomb branches has an $\mathrm{SO}(5)^2 \times \mathrm{SU}(2)^2$ global symmetry as indicated from the t^2 coefficient of the Hilbert series. This is confirmed with Weyl integration which uses the following embedding of $E_7 \times E_7 \hookleftarrow \mathrm{SO}(5)^2 \times \mathrm{SU}(2)^2 \times \mathrm{SO}(7)$ which decomposes the bifundamental as

$$\mu_{1\,E_7} + \mu'_{1\,E_7} \to \nu^2 + \nu'^2 + \mu_2^2 + \mu_2^{2\prime} + \mu_1\rho_1 + \mu'_1\rho_1 + 2\rho_2 + \nu\mu_2\rho_3 + \nu'\mu'_2\rho_3 \tag{7.97}$$

where the μ_i and μ'_i are highest weight fugacities for the two $\mathrm{SO}(5)$, ν and ν' are highest weight fugacities for each $\mathrm{SU}(2)$, and the ρ_i are highest weight fugacities for the $\mathrm{SO}(7)$ which is gauged.

This result may be viewed as the diagonal flavour symmetry gauging of $\mathrm{SO}(7)$ from two $4d$ $\mathcal{N} = 1$ rank-1 E_7 SCFTs realised through magnetic quivers [224].

7.8 Magnetic Quivers for one M5-brane on E_6 Klein Singularity

When an M5-brane probes an E_6 Klein singularity there is fractionation to at most four $\frac{1}{4}$M5 branes along the direction the singularity extends [168], as shown in Figure 7.12. The fraction refers to the three-form flux each fractional M5 brane carries.

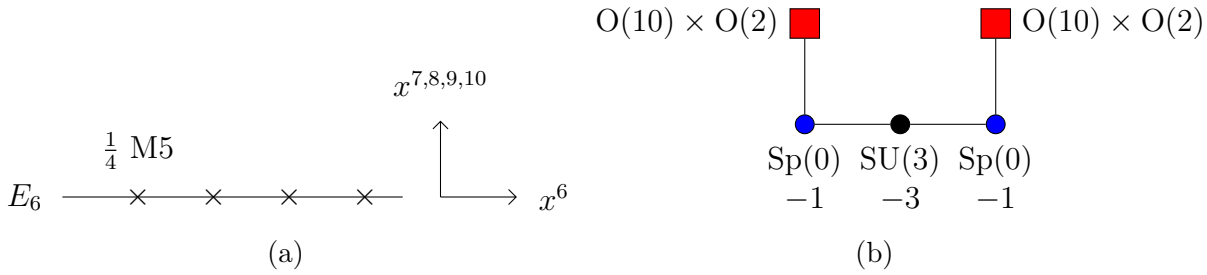


Figure 7.12: Four $\frac{1}{4}$M5-branes on an E_6 Klein singularity. The directions $x^{0,1,2,3,4,5}$ are suppressed. The corresponding electric quiver $\mathcal{Q}_{7.12b}$ comes from the F-theory dual description.

In general, the light spectrum of the low energy $6d$ $\mathcal{N} = (1,0)$ field theory changes with the separation between the fractional M5-branes; as in the case for unitary 6d quivers [241, 75]. In particular, the Higgs branch of the field theory changes dramatically between finite and infinite gauge coupling. This is a reflection of the presence of tensionless strings in the spectrum which changes the Higgs branch. This effect is difficult to see in general. However one can study this physics through a Type IIA brane system and magnetic quiver. Both of which are perturbative descriptions and moreover the magnetic quiver is a Lagrangian description.

Unlike the case of M5-branes on A/D Klein singularities, there is no perturbative Type IIA description for the M-theory background on Klein singularities of E-type. Instead, F-theory translates the notion of bringing together fractional M5-branes to the collapse of curves of negative self-intersection [149, 168]. The following section will propose a pair of orthosymplectic magnetic quivers – and the corresponding Type IIA brane system – whose Coulomb branches are conjectured to be the Higgs branches of the worldvolume $6d$ $\mathcal{N} = (1,0)$ theories of two $\frac{1}{2}$M5-branes and one M5-brane on a Klein E_6 singularity respectively. The latter is referred to in the Literature as $6d$ $\mathcal{N} = (1,0)$ (E_6, E_6) conformal matter and is believed to be a strongly interacting SCFT [168].

7.8.1 Two $\frac{1}{2}$M5-branes on E_6 Klein singularity

First consider the phase in which the four $\frac{1}{4}$M5-branes on the E_6 Klein singularity coincide pairwise to become two $\frac{1}{2}$M5-branes, represented by the brane system and electric quiver of Figure 7.13.

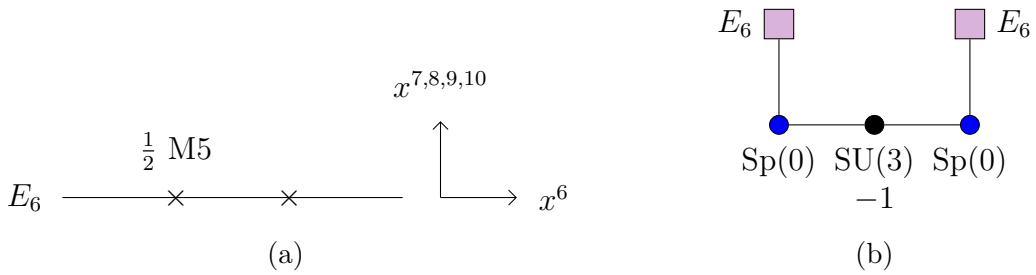


Figure 7.13: Two $\frac{1}{2}$ M5 branes on an E_6 Klein singularity. The directions $x^{0,1,2,3,4,5}$ are suppressed. The corresponding electric quiver $\mathcal{Q}_{7.13b}$ comes from the F-theory dual description.

This transition removes two of the tensor multiplets and tunes the coupling of both Sp(0) to infinite coupling, increasing the dimension of the Higgs branch due to tensionless strings arising. The gauge coupling of the SU(3) in $\mathcal{Q}_{7.13b}$ remains finite. The corresponding operation in F-theory collapses both (-1)-curves and simultaneously collapses the (-3)-curve supporting the SU(3) gauge symmetry to a (-1)-curve. Moreover, the F-theory picture suggests that the theory is described by two rank-1 E-strings (each with Higgs branch $\overline{min.E_8}$) coupled to a diagonal SU(3) gauge symmetry which remains at finite coupling. From this argument, the Higgs branch of $\mathcal{Q}_{7.13b}$ is thus predicted to be $\left(\overline{min.E_8} \times \overline{min.E_8}\right) /\!/\!/ \mathrm{SU}(3)$.

The construction of a suitable magnetic quiver for the Higgs branch of $\mathcal{Q}_{7.13b}$ begins with the $\overline{min.E_8} \times \overline{min.E_8}$ theory of [67], which matches the $E_8 \times E_8$ global symmetry supported by the two (-1)-curves, and then performing SU(3) quotient quiver subtraction which is illustrated in Figure 7.14 to give $\mathcal{Q}_{7.14}$.

Although the high rank of the resulting theory $\mathcal{Q}_{7.14}$ makes computation of an exact Hilbert series challenging, a calculation to order t^{10} can be made, shown in (7.98), and its PL (7.99). From this, a conjecture of which representations the generators and relations transform in are given in (7.100) up to order t^6 as well as the PL of the HWG (7.101).

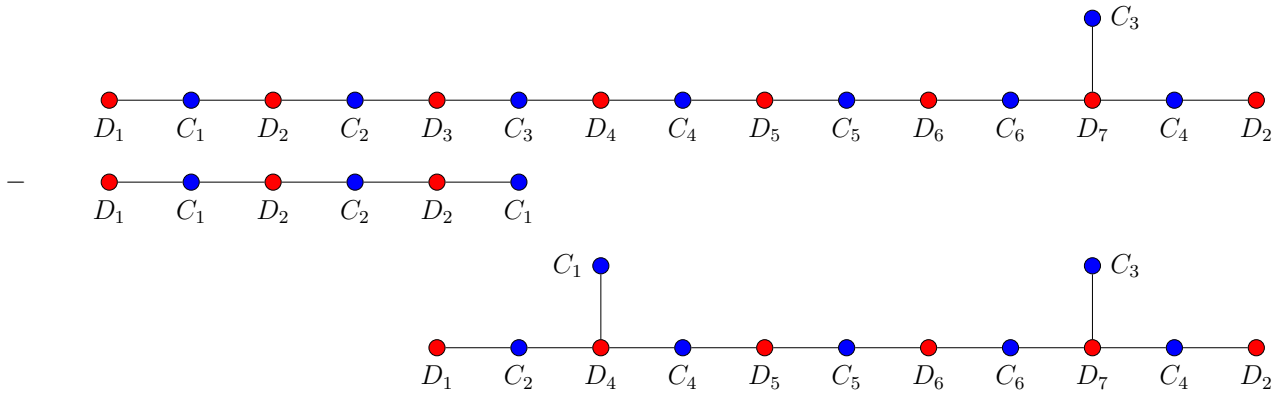


Figure 7.14: The subtraction of the SU(3) quotient quiver on the orthosymplectic quiver for $\overline{min.E_8} \times \overline{min.E_8}$ to give $\mathcal{Q}_{7.14}$. This is a magnetic quiver for the $6d$ $\mathcal{N} = (1,0)$ worldvolume theory of two separated $\frac{1}{2}$M5 branes on E_6 Klein singularity.

$$\text{HS}\left[\mathcal{C}(\mathcal{Q}_{7.14})\right] = 1 + 156t^2 + 13859t^4 + 893669t^6 + 45609733t^8 + 1923636761t^{10} + O(t^{11}) \tag{7.98}$$

$$\text{PL}\left[\text{HS}\left[\mathcal{C}(\mathcal{Q}_{7.14})\right]\right] = 156t^2 + 1613t^4 - 2915t^6 - 627017t^8 - 1911458t^{10} + O(t^{11}) \tag{7.99}$$

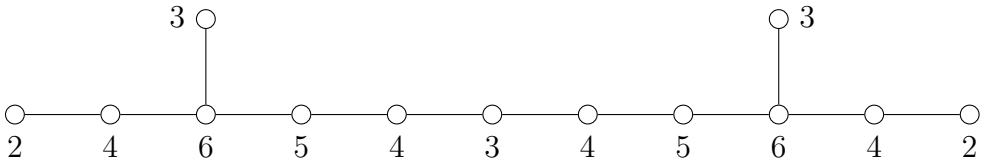
$$\begin{aligned}\text{PL}\left[\text{HS}\left[\mathcal{C}(\mathcal{Q}_{7.14})\right]\right] &= (\nu_6 + \nu_6')\, t^2 + (\nu_1\nu_5' + \nu_5\nu_1' + \nu_6 + \nu_6' - 1)\, t^4 \\ &\quad - (\nu_1\nu_5' + \nu_5\nu_1' + \nu_6 + \nu_6' + \nu_1\nu_5 + \nu_1'\nu_5' + 1)\, t^6 + O(t^8)\end{aligned} \tag{7.100}$$

$$\begin{aligned}\text{PL}\left[\text{HWG}\left[\mathcal{C}(\mathcal{Q}_{7.14})\right]\right] &= (\mu_6 + \mu_6')\, t^2 + (1 + \mu_1\mu_5 + \mu_1'\mu_5 + \mu_1\mu_5' + \mu_1'\mu_5' + \mu_6 + \mu_6')t^4 \\ &\quad + \big(1 + \mu_1'\mu_2 + \mu_1\mu_2' + 2\mu_3 + 2\mu_3' + \mu_1\mu_5 + \mu_1'\mu_5 + \mu_4'\mu_5 + \mu_1\mu_5' + \mu_1'\mu_5' \\ &\quad + \mu_4\mu_5' + \mu_6 + \mu_6'\big)t^6 + O(t^8)\end{aligned} \tag{7.101}$$

The ν_i and ν_i' in (7.100) are highest weight fugacities for each factor of E_6 and are shorthand for the character of the corresponding representation in the PL of the HS. The μ_i and μ_i' are also highest weight fugacities for each factor of E_6 and appear in the PL of the HWG (7.101).

The t^2 term in (7.99) shows that there is a generator transforming in the adjoint of $E_6 \times E_6$ which correctly identifies an $E_6 \times E_6$ global symmetry. The t^4 term suggests that there is a generator in the bifundamental as well as another generator in the adjoint. The relation at t^4 sets the second Casimir of each E_6 the same. At order t^6 relations appear which transform in the bifundamental, adjoint, singlet, and $\nu_1\nu_5 + \nu_1'\nu_5'$.

This matches the Coulomb branch Hilbert series of the unitary doppelgänger which is constructed through the SU(3) chain polymerisation of two unitary affine $E_8^{(1)}$ quivers, derived in Section 6.3.7. The result is reproduced in (7.102).



(7.102)

It is particularly interesting to note that although the orthosymplectic quiver $\mathcal{Q}_{7.14}$ and its unitary doppelgänger take the same shape, the unitary quiver has a clear S_2 outer automorphism symmetry whereas the orthosymplectic quiver does not.

One must emphasise that a significant challenge with studying the physics of strongly interacting M5 brane on Klein $E_{6,7,8}$ singularities is the lack of a perturbative description as a magnetic quiver or in Type IIA. The problem of finding a magnetic quiver has been addressed with the derivation of $\mathcal{Q}_{7.14}$ and (7.102). It is challenging to find a consistent brane construction of (7.102) as was discussed in Section 6.3.7. However, it is straightforward to give a Type IIA brane system from $\mathcal{Q}_{7.14}$ as shown in Figure 7.15. This time, there is only one O8$^-$ plane, and so even though the brane system only has six full D8 branes, any additional D8 branes for anomaly cancellation can be thought of as placed at infinity. Importantly, the C_1 gauge node in $\mathcal{Q}_{7.14}$ is interpreted as arising from a D4 brane ending between the NS5 and D6.

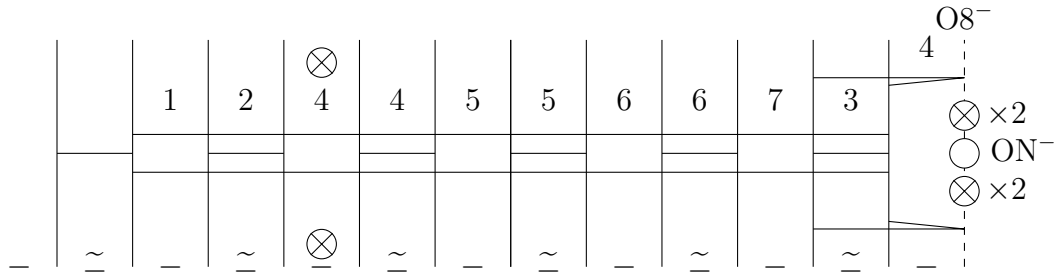


Figure 7.15: The Type IIA brane system for the magnetic quiver $\mathcal{Q}_{7.14}$. This is a magnetic quiver for the $6d$ $\mathcal{N}=(1,0)$ worldvolume theory of two $\frac{1}{2}$M5 branes on a Klein E_6 singularity.

7.8.2 One M5 brane on E_6 Klein Singularity – $6d$ $\mathcal{N} = (1,0)$ (E_6, E_6) Conformal Matter

When all four $\frac{1}{4}$M5 brane fractions are taken to be coincident, as shown in Figure 7.16a, the resulting gauge theory, termed $6d$ $\mathcal{N} = (1,0)$ (E_6, E_6) *conformal matter*, is believed to be a strongly coupled $6d$ $\mathcal{N} = (1,0)$ SCFT described by the electric quiver $\mathcal{Q}_{7.16b}$ [168].

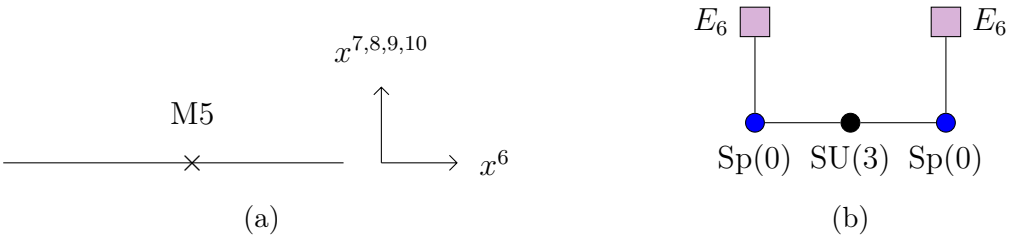


Figure 7.16: One M5 brane on an E_6 Klein singularity. The directions $x^{0,1,2,3,4,5}$ are suppressed. The corresponding electric quiver $\mathcal{Q}_{7.16b}$ comes from the F-theory dual description.

Although the two electric quivers $\mathcal{Q}_{7.13b}$ and $\mathcal{Q}_{7.16b}$ may look similar, the latter results from shrinking the (-1)-curve in the former to zero size, which in field theory corresponds to tuning the gauge coupling associated to the SU(3) to infinity. This is known to give a small E_8 instanton transition [45]. In the Type IIA brane system, this is seen by taking an NS5-brane onto the $O8^-$-plane [154] accounting for any brane creation [31]. The small E_8 instanton transition can also be seen through the magnetic quiver by "sliding off" a C_1 gauge node and adding an affine $E_8^{(1)}$ shaped orthosymplectic quiver with node ranks given by the dual Coxeter numbers of $E_8^{(1)}$ [154]. The resulting brane system is shown in the magnetic phase in Figure 7.17, in the electric phase in Figure 7.18 and the corresponding magnetic quiver $\mathcal{Q}_{7.19}$ is shown in Figure 7.19. In particular, $\mathcal{Q}_{7.19}$ is conjectured to be the magnetic quiver for $6d$ $\mathcal{N} = (1,0)$ (E_6, E_6) conformal matter.

Several pieces of evidence support this conjecture. The most basic is the dimension of the moduli space, which is easily read from $\mathcal{Q}_{7.19}$ to be dim $E_6 + 1 = 79$, as expected. The high dimension makes it difficult for exact calculation of the Hilbert series under current techniques. However the first three terms of the HS, can be computed as (7.103) and the PL (7.104). It is then simple to conjecture representations the generators and relations transform in up to order t^6, which is given in (7.105) and also conjecture a HWG whose PL is given in (7.106). Due to

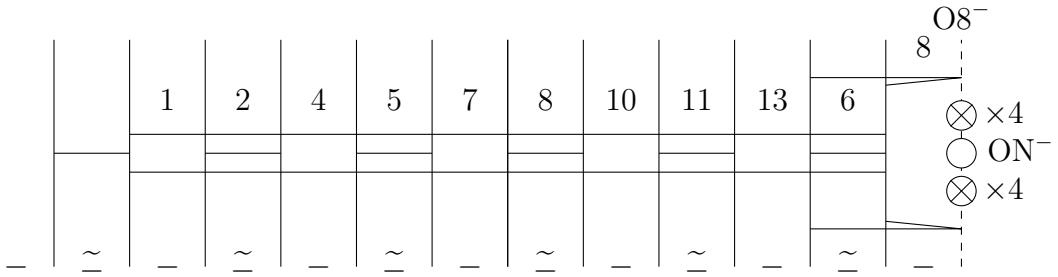


Figure 7.17: The Type IIA brane system from which the magnetic quiver $\mathcal{Q}_{7.19}$ is read. This is a magnetic quiver for $6d$ $\mathcal{N}=(1,0)$ (E_6,E_6) conformal matter. This configuration can be obtained from that of Figure 7.15 by moving the NS5-brane onto the $O8^-$-plane.

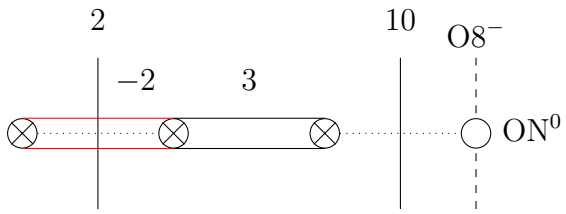


Figure 7.18: The electric phase of the magnetic Type IIA brane system shown in Figure 7.17 from which $\mathcal{Q}_{7.19}$ is read.

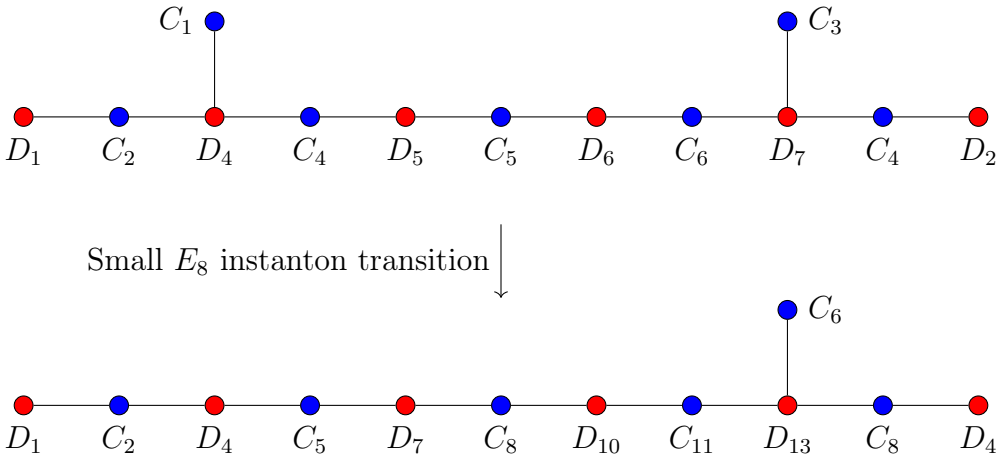


Figure 7.19: The effect of a small E_8-instanton transition on the magnetic quiver $\mathcal{Q}_{7.14}$ associated to the brane system in Figure 7.15 as the NS5-brane is taken onto the $O8^-$-plane. The resulting quiver $\mathcal{Q}_{7.19}$ is the magnetic quiver for $6d$ $\mathcal{N}=(1,0)$ (E_6,E_6) conformal matter.

the balance of the nodes the next term in the Hilbert series is expected to show up at order t^8.

$$\mathrm{HS}\left[\mathcal{C}(\mathcal{Q}_{7.19})\right] = 1 + 156t^2 + 13703t^4 + 876875t^6 + O(t^8) \tag{7.103}$$

$$\mathrm{PL}\left[\mathrm{HS}\left[\mathcal{C}(\mathcal{Q}_{7.19})\right]\right] = 156t^2 + 1457t^4 + 4627t^6 + O(t^8). \tag{7.104}$$

$$\text{PL}\left[\text{HS}\left[\mathcal{C}(\mathcal{Q}_{7.19})\right]\right] = (\nu_6+\nu_6')\,t^2 + (\nu_1\nu_5' + \nu_5\nu_1' - 1)\,t^4 + (\nu_6\nu_6' + 1 - \nu_1\nu_5' - \nu_5\nu_1') + O(t^8) \tag{7.105}$$

$$\begin{aligned}\text{PL}\left[\text{HWG}\left[\mathcal{C}(\mathcal{Q}_{7.19})\right]\right] = {} & (\mu_6+\mu_6')\,t^2 + (1+\mu_1\mu_5 + \mu_1'\mu_5 + \mu_1\mu_5' + \mu_1'\mu_5')\,t^4 \\ & + \big(1+\mu_1\mu_2' + \mu_2\mu_1' + \mu_3 + \mu_3' + \mu_1\mu_5 + \mu_1'\mu_5' + \mu_1\mu_5' + \mu_5\mu_1' \\ & + \mu_4\mu_5' + \mu_5\mu_4' + \mu_6\mu_6'\big)t^6 + O(t^8)\end{aligned} \tag{7.106}$$

The ν_i and ν_i' in (7.105) are highest weight fugacities for each E_6 and are shorthand for the character of the given representation. The μ_i and μ_i' are also highest weight fugacities for each E_6 and appear in the PL of the HWG in (7.106).

The specific representations that appear in (7.105) have simple physical interpretations. The t^2 term identifies a generator transforming in the adjoint of $E_6 \times E_6$ indicating an $E_6 \times E_6$ global symmetry. The t^4 term is interpreted as a generator transforming in the bifundamental representation of $E_6 \times E_6$ with a relation. This relation expresses the equality of the second Casimir of each E_6. At order t^6 there are generators transforming in the biadjoint and singlet. The relations at this order transform in the bifundamental and come from the fact that the tensor product representation of the adjoint and bifundamental of $E_6 \times E_6$ produce two identical bifundamentals (among other representations).

It is interesting to note that the magnetic quiver $\mathcal{Q}_{7.19}$ for $6d$ $\mathcal{N} = (1,0)$ (E_6, E_6) conformal matter is star-shaped. Therefore this quiver $\mathcal{Q}_{7.19}$ is also a magnetic quiver for the Higgs branch of the class $\mathcal{S}$ theory specified by algebra SO(26) on a three-punctured sphere with puncture data given by the following list of partitions of 26, $\{(3^8, 1^2), (9^2, 7, 1), (13^2)\}$. This class $\mathcal{S}$ theory is apparently different to the T^2 compactification of $6d$ $\mathcal{N} = (1,0)$ (E_6, E_6) conformal matter [251] which is also specified by a three-punctured sphere but with algebra E_6 and two maximal and one minimal puncture.

Chapter 8

Conclusion

The gauging of global symmetries is a ubiquitous procedure in the study of quantum field theories. This thesis provides advances in the systematisation of gauging Coulomb branch global symmetries of $3d$ $\mathcal{N} = 4$ quiver gauge theories. Lagrangian descriptions are inadequate to analyse the gauging of these symmetries and so quiver combinatorics comes to the rescue, replacing the notion of gauging with simple diagrammatic procedures. These techniques extend beyond the remit of $3d$ $\mathcal{N} = 4$ theories and can be applied to study the gauging of flavour symmetries of theories with eight supercharges in four, five, and six dimensions and the corresponding action on their Higgs branches, through the programme of magnetic quivers. In many cases, the magnetic quiver also captures non-perturbative effects which correct the classical Higgs branch.

The action of gauging either a Coulomb branch global symmetry of a $3d$ $\mathcal{N} = 4$ theory or a flavour symmetry subgroup of a theory with eight supercharges, corresponds to a hyper-Kähler quotient by that subgroup on the Coulomb branch or Higgs branch respectively. This gives a geometric result relating the moduli spaces of theories before and after gauging.

This thesis focuses on four such combinatorial techniques:

1. SU(n) quotient quiver subtraction

2. Sp(n), SO(n), and Sp(n) + $\frac{1}{2}\mathsf{F}$ quotient quiver subtraction

3. Quiver polymerisation

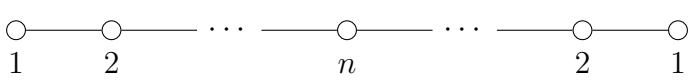
4. Unframed orthosymplectic quotient quiver subtraction

The first three techniques apply to quivers with unitary gauge groups, whereas the last technique applies to only unframed orthosymplectic quivers. Although, it was not considered in this thesis, there is also a quotient quiver subtraction on framed orthosymplectic quivers, formulated for SO(n) and Sp(n) Coulomb branch global symmetry subgroups [7].

Each of the techniques in this thesis has been applied to either derive new results in the topic of Higgs branches of theories with eight supercharges and symplectic singularities, or provides novel ways of thinking about established results. These applications, aside from being results in their own right, are at least a proof-of-concept that gauging Coulomb branch symmetries of magnetic quivers are a fruitful way to gain insight into the complexities of theories with eight supercharges. One can hope that the techniques developed both in this thesis and in related works not covered here will be useful for physicists as another tool in the magnetic quiver toolbox.

The organisation of the rest of this Chapter takes each of the four techniques in turn and summarises results derived with the technique and then proposals for future directions are made.

In Chapter 4 the technique of SU(n) quotient quiver subtraction was presented, which gauges SU(n) Coulomb branch isometry subgroups of all magnetic quivers with unitary gauge nodes that respect the selection rules presented in Section 4.2. The procedure involves the subtraction of the following SU(n) quotient quiver



(8.1)

from a target quiver which has been unframed w.r.t. an overall U(1).

For cases where there are multiple permissible alignments of the quotient quiver against the target quiver, the subtraction generates the hyper-Kähler quotient as the union of the Coulomb

branches of the alternative resulting quivers. Unions of cones have appeared as Higgs branches [112, 80] although identifying the constituent cones requires a little more work. Quotient quiver subtraction gives a direct identification of the corresponding magnetic quiver(s) for the constituent cones.

The SU(n) quotient quiver subtraction was applied to some moduli spaces of free fields, Section 4.3, which is summarised in Table 8.1. These establish relationships between $\mathbb{H}^n$ for $n \geq 4$ and the minimal nilpotent orbits of type B and D for odd and even n respectively. This is in accordance with [180].

Target Moduli Space	SU(2) hyper-Kähler quotient	Rank
$\mathbb{H}^{2k}$	$\overline{min.D_k}$	$k \geq 2$
$\mathbb{H}^{2k+1}$	$\overline{min.B_k}$	$k \geq 2$

Table 8.1: The moduli spaces $\mathbb{H}^n$ and their SU(2) hyper-Kähler quotients. These fall into two families for even and odd n. These families are labelled by an integer k, with the appropriate limits on k shown.

Target Moduli Space	SU(2) hyper-Kähler quotient
$\overline{min.F_4}$	$\overline{n.min.C_3}$
$\overline{min.E_6}$	$\overline{n.min.A_5}$
$\overline{min.E_7}$	$\overline{n.n.min.D_6}$
$\overline{min.E_8}$	$\overline{n.min.E_7}$

Table 8.2: Some classical and exceptional nilpotent orbits and their SU(2) hyper-Kähler quotients. For families of orbits, labelled by their rank k, the limits on k are shown.

Target Moduli Space	SU(3) hyper-Kähler quotient
$\overline{min.E_7}$	$\overline{\mathcal{O}}^{A_5}_{(2^3)} \cup \overline{\mathcal{O}}^{A_5}_{(3,1^3)}$
$\overline{min.E_8}$	$\left[\overline{\mathcal{W}_{E_6}}\right]^{[0,0,1,0,0,0]}_{[0,0,0,0,0,0]}$

Table 8.3: Some classical and exceptional nilpotent orbits and their SU(3) hyper-Kähler quotients. For families of orbits, labelled by their rank k, the limits on k are shown.

Target Moduli Space	SU(4) hyper-Kähler quotient
$\overline{min.E_8}$	$\left[\overline{\mathcal{W}_{D_5}}\right]^{[0,2,0,0,0]}_{[0,0,0,0,0]} \cup \left[\overline{\mathcal{W}_{D_5}}\right]^{[1,0,0,2,0]}_{[0,0,0,0,0]}$

Table 8.4: Exceptional nilpotent orbits and their SU(4) hyper-Kähler quotients.

The technique of SU(n) quotient quiver subtraction was also applied to magnetic quivers for

exceptional nilpotent orbits, Section 4.4, with the results summarised in Tables 8.2, 8.3, and 8.4. These establish interesting relationships between classical and exceptional nilpotent orbits under SU(n) hyper-Kähler quotient and other orbits or affine Grassmannian slices, and include many results that have not been found in the literature, extending the work of Kobak-Swann [210].

In Chapter 5 prescriptions for the gauging of Sp(n) (possibly coupled to a half hypermultiplet) and SO(n) Coulomb branch global symmetry subgroups for $3d$ $\mathcal{N}=4$ quivers with unitary gauge nodes, were introduced. This completes the family of prescriptions to gauging classical Coulomb branch global symmetry subgroups in unitary quivers as a quiver subtraction.

The quotient quivers roughly take the form of one "half" of the SU($2n$) quotient quivers for gauging Sp(n), SO($2n+1$), Sp(n) + $\frac{1}{2}$F and one "half" of the SU($2n-1$) quotient quiver for gauging SO($2n$). In addition to a quiver subtraction, there is also a changing of the graph type of the quiver to; type D for gauging Sp(n), type C for gauging SO($2n$) or SO($2n+1$), type B for gauging Sp(n) + $\frac{1}{2}$F. The Coulomb branch global symmetries correspond to the four types of O5 planes and the graph-types correspond to the respective S-dual ON plane.

The methods in this Chapter were used to provide new descriptions of Higgs branches of certain $4d$ $\mathcal{N}=2$ theories as magnetic quivers and verified relationships between some $4d$ $\mathcal{N}=2$ theories under gauging [215], while also conjecturing a new family of dualities based on the analysis done here.

In Chapter 6 the two related diagrammatic techniques of chain polymerisation and cyclic polymerisation on unitary $3d$ $\mathcal{N}=4$ quivers are introduced. They are summarised in Figure 6.1 and Figure 6.2 respectively.

In both cases, there is a gauging of a diagonal subgroup of either SU(n) or U(n) of the Coulomb branch global symmetry sourced by two distinct legs of $(1)-(2)-\cdots-(n)-$.

Both types of polymerisation are generalisations of examples in [223], which approach these gaugings from a class $\mathcal{S}$ perspective and their $3d$ mirrors. Alternatively, the techniques of chain and cyclic polymerisation can be thought of as Coulomb branch global symmetry analogues of

gauging diagonal flavour symmetries.

In Section 6.3, examples of chain polymerisation were presented. One set of examples is in the construction of affine Dynkin diagram shaped quivers, or generalised Dynkin diagram quivers through quiver polymerisation. The results are summarised in Table 8.5 (with slightly different parametrisation).

Initial Quivers	Chained Quiver	Initial Coulomb	Initial Higgs	Chained Coulomb	Chained Higgs
$D_{k+2} \times D_{n-k+2}$	$D_n^{(1)}$	$\mathbb{H}^{2n}$	Trivial	$\overline{min.D_n}$	D_n
$D_{k+2} \times B_{n-k+1}$	$B_{n-1}^{(1)}$	$\mathbb{H}^{2n-1}$	–	$\overline{min.B_{n-1}}$	–
$B_{k+1} \times B_{n-k+1}$	$D_{n-1}^{(2)}$	$\mathbb{H}^{2n-2}$	–	$\overline{min.D_{n-1}}$	–
$\mathcal{Q}_{6.6} \times D_{n-k+2}$	$\frac{1}{2}D_{2n-1}^{(1)}$	$\mathbb{C}^2/\mathbb{Z}_2 \times \mathbb{H}^{2n-1}$	$\mathbb{C}^2/\mathbb{Z}_2$	$\overline{n.min.B_{n-1}}$	$\mathcal{S}^{C_{n-1}}_{\mathcal{N},(2(n-2),1^2)}$
$\mathcal{Q}_{6.6} \times \mathcal{Q}_{6.6}$	$\frac{1}{2}A_{2n-1}^{(1)}$	$(\mathbb{C}^2/\mathbb{Z}_2)^2 \times \mathbb{H}^{2n}$	$(\mathbb{C}^2/\mathbb{Z}_2)^2 \times \mathbb{H}^2$	$\mathcal{S}^{C_{2n}}_{(4,2^{2n-2}),(2^{2n})}$	$\mathbb{H}^2 \times \mathcal{S}^{C_{2n}}_{((2n)^2),((2n-1)^2,1^2)}$
$\mathcal{Q}_{6.6} \times B_{n-k+1}$	$\frac{1}{2}D_{2n-1}^{(2)}$	$\mathbb{C}^2/\mathbb{Z}_2 \times \mathbb{H}^{2n-1}$	–	$\overline{\mathcal{O}}^{D_{n-1}}_{(3,1^{2n-5})}$	–

Table 8.5: SU(2) chain polymerisation of finite D and B type and related quivers. Initial and chained Coulomb and Higgs branches are shown if known.

chain polymerisation was also applied to find a unitary magnetic quiver for the $6d$ $\mathcal{N} = (1, 0)$ theory coming from two separated $\frac{1}{2}$ M5 branes on an E_6 Klein singularity. This came from the SU(3) chain polymerisation of two $E_8^{(1)}$ quivers, which was originally motivated from the F-theory description. This resulting unitary magnetic quiver does not admit a sensible Type IIA brane description, neither is the implementation of the small E_8 instanton transition in the magnetic quiver easy to see.

A significant application of cyclic polymerisation, in Section 6.4, is in the construction of the moduli space of SU(N) instantons on $\mathbb{C}^2$ and on $\mathbb{C}^2/\mathbb{Z}_l$, as a Coulomb branch hyper-Kähler quotient. Both the ADHM and Kronheimer-Nakajima constructions of these moduli spaces can be realised from polymerised quivers.

Additionally, non-trivial relationships between free moduli spaces, nilpotent orbits, affine Grassmannian slices and moduli spaces of instantons were found in this study. Some of these are tabulated in Table 8.6.

The most general construction was discussed in Section 6.4.5 and provides a counterpart to the Higgs branch hyper-Kähler quotient construction of the moduli space of SU instantons on

Initial Quiver	Cyclic Poly.	Final Quiver	Initial Coulomb	Initial Higgs	Final Coulomb	Final Higgs
A_{N+2}	U(1)	$\mathcal{Q}_{6.13}$	$\mathbb{H}^{N+1}$	Trivial	$\mathcal{M}^{\mathbb{C}^2}_{1,\mathrm{SU}(N)}$	$\mathbb{C}^2/\mathbb{Z}_N$
D_{N+4}	U(2)	$\mathcal{Q}_{6.14}$	$\mathbb{H}^{2N+4}$	Trivial	$\mathcal{M}^{\mathbb{C}^2}_{2,\mathrm{SU}(N)}$	$\mathrm{Sym}^2(\mathbb{C}^2/\mathbb{Z}_N)$
$\mathcal{Q}_M\left(\overline{\mathcal{O}}^{A_{N+3}}_{(2^2,1^N)}\right)$	U(2)	$\mathcal{Q}_{6.15}$	$\overline{\mathcal{O}}^{A_{N+3}}_{(2^2,1^N)}$	$\mathcal{S}^{A_{N+3}}_{\mathcal{N},(N+2,2)}$	$\mathcal{M}^{\mathbb{C}^2/\mathbb{Z}_2}_{2,\mathrm{SU}(N)}$	$\mathcal{M}^{\mathbb{C}^2/\mathbb{Z}_N}_{2,\mathrm{SU}(2)}$
$\mathcal{Q}_{6.16}$	U(k)	$\mathcal{Q}_{6.18}$	See text	See text	$\mathcal{M}^{\mathbb{C}^2/\mathbb{Z}_l}_{k,\mathrm{SU}(N)}$	$\mathcal{M}^{\mathbb{C}^2/\mathbb{Z}_N}_{k,\mathrm{SU}(l)}$

Table 8.6: Table of cyclic polymerisations to produce Kronheimer-Nakajima quivers.

Klein A singularities.

In Section 6.5 cyclic polymerisations were carried out on some finite and affine ADE quivers to generate quivers with loops or multiple links. These illustrate a variety of relationships between free fields, nilpotent orbit closures and the moduli spaces of instantons. These are summarised in Table 8.7 and Table 8.8 respectively.

Initial Quiver	Cyclic Poly.	Final Quiver	Initial Coulomb	Initial Higgs	Final Coulomb	Final Higgs
A_N	U(1)	$\mathcal{Q}_{6.22}$	$\mathbb{H}^{N-1}$	Trivial	$\overline{min.A_{N-L-R}} \times \mathbb{H}^{L+R-2}$	A_{N-L-R}
D_{N+4}	U(2)	$\mathcal{Q}_{6.14}$	$\mathbb{H}^{2N+4}$	Trivial	$\mathcal{M}^{\mathbb{C}^2}_{2,\mathrm{SU}(N)}$	$\mathrm{Sym}^2(\mathbb{C}^2/\mathbb{Z}_N)$

Table 8.7: Table of cyclic polymerisations of finite A_N and D_{N+4} quivers.

Initial Quiver	Cyclic Poly.	Final Quiver	Initial Coulomb	Initial Higgs	Final Coulomb	Final Higgs
$E_6^{(1)}$	U(1)	$\mathcal{Q}_{6.23}$	$\overline{min.E_6}$	E_6	$\overline{\mathcal{O}}^{D_5}_{(2^4,1^2)}$	$\mathcal{S}^{D_5}_{\mathcal{N},(5^2)}$
$E_6^{(1)}$	U(2)	$\mathcal{Q}_{6.24}$	$\overline{min.E_6}$	E_6	$\overline{\mathcal{O}}^{B_3}_{(3^2,1)}$	$\mathcal{S}^{C_3}_{\mathcal{N},(2^3)}$
$E_7^{(1)}$	U(1)	$\mathcal{Q}_{6.25}$	$\overline{min.E_7}$	E_7	$\overline{n.min.E_6}$	$\mathcal{S}^{E_6}_{\mathcal{N},D_5}$
$E_7^{(1)}$	U(3)	$\mathcal{Q}_{6.26}$	$\overline{min.E_7}$	E_7	$\mathcal{S}^{E_7}_{A_3+A_2+A_1,A_2+3A_1}$	$\mathcal{S}^{E_7}_{A_6,A_4+A_2}$

Table 8.8: Table of cyclic polymerisations of affine $D_{N+4}^{(1)}$, $E_6^{(1)}$, and $E_7^{(1)}$ quivers.

In Chapter 7 the method of orthosymplectic quotient quiver subtraction is introduced. This is an operation on orthosymplectic magnetic quivers which has the effect of gauging either a SU(2), SU(3), G_2, or SO(7) subgroup of the Coulomb branch global symmetry. The effect on the Coulomb branch is a hyper-Kähler quotient by the corresponding group. The technique involves the subtraction of certain orthosymplectic quivers with negatively balanced nodes called the orthosymplectic quotient quivers which are tabulated in Table 8.9.

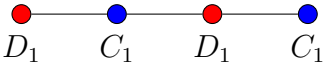
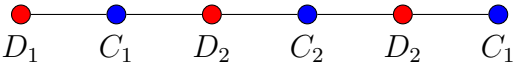
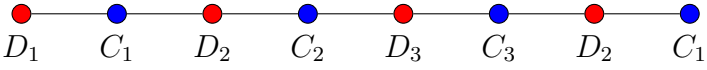
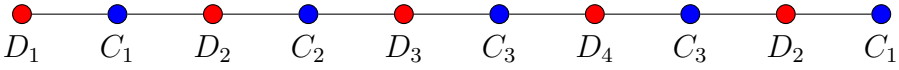
G	Unframed Quotient Quiver
SU(2)	
SU(3)	
G_2	
SO(7)	

Table 8.9: The set of orthosymplectic quotient quivers introduced in Chapter 7.

The full explanation of the algorithm is in Section 7.3 but it shares much in common with the SU(n) quotient quiver subtraction in Chapter 4. They both involve subtraction of quotient quivers which contain gauge nodes of negative balance. Similarly, if the quotient quiver goes past a junction then the result is a union of the Coulomb branches coming from the different alignments. In the orthosymplectic case rebalancing of gauge nodes is done with a C_1 gauge node, this breaks the alternating SO − Sp pattern of gauge nodes typically seen in orthosymplectic quivers. In all cases studied here, the resulting intersection is found through an A_1 Kraft-Procesi (KP) transition [179, 180].

In contrast to the unitary quotient quiver subtraction, where quotient quivers are known for the entire SU(n) family, identification of orthosymplectic quotient quivers has thus-far resisted attempts at generalisation beyond the four cases considered here. This is because they were derived from studying the various flavour symmetry gaugings of the non-anomalous $6d$ $\mathcal{N} = (1, 0)$ Sp(k) electric gauge theory at infinite coupling. The consideration of anomaly cancellation and requirement of linearity of the electric $6d$ theory narrows down the possible flavour symmetry subgroups that can be gauged. In Section 7.2, the orthosymplectic quotient quivers for SU(3), G_2, and SO(7) were derived from comparing magnetic quivers for these electric theories before and after gauging those flavour symmetry subgroups. The SU(2) orthosymplectic quotient quiver was conjectured through the natural Higgsing pattern of SO(7) → G_2 → SU(3) → SU(2) observed in $6d$.

The method of orthosymplectic quotient quiver subtraction was applied to magnetic quivers

for nilpotent orbit closures in Sections 7.4, 7.5, 7.6, and 7.7. In many cases the result from orthosymplectic quotient quiver subtraction either matched unitary quotient quiver subtraction or from quiver polymerisation. This gave orthosymplectic doppelgängers to some known unitary quivers, with both the Coulomb branch and Higgs branch matching. The doppelgängers which are explicitly checked are summarised in Tables 8.10 and 8.11. Many other unitary doppelgängers were proposed but were not completely checked either due to the large dimension of the moduli space or because one or both quivers contained non-simply laced edges. New orthosymplectic quiver constructions for some nilpotent orbits were also found for which there is no known unitary doppelgänger.

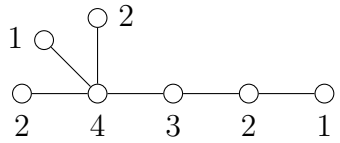
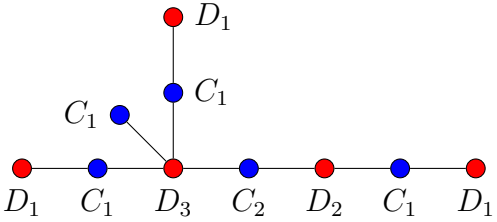
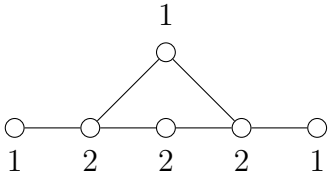
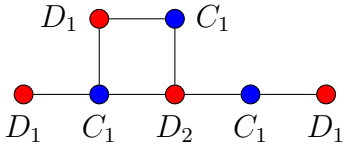
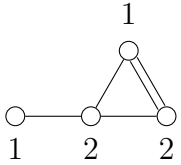
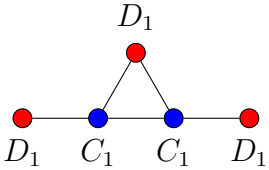
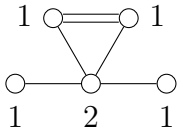
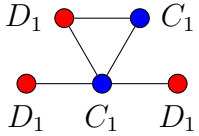
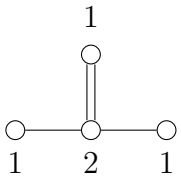
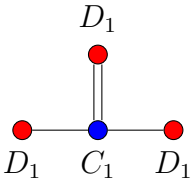
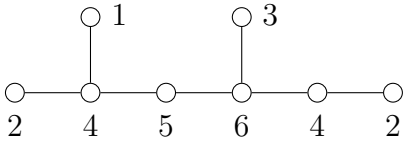
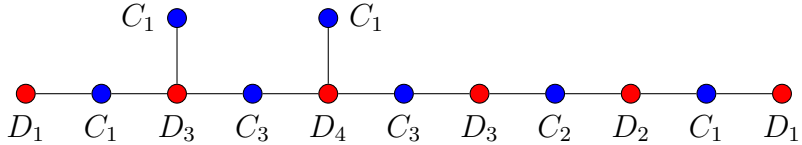
Unitary Quiver	Orthosymplectic Quiver	Coulomb Branch	Higgs Branch
		$\overline{n.n.min.D_6}$	$\mathcal{S}^{D_6}_{\mathcal{N},(7,5)}$
		$\overline{n.min.A_5}$	$\mathcal{S}^{A_5}_{\mathcal{N},(4,2)}$
		$\overline{\mathcal{O}}^{A_3}_{(3,1)}$	$\mathcal{S}^{A_3}_{\mathcal{N},(2,1^2)}$
		$\overline{[\mathcal{W}_{D_4}]}^{[0,1,0,2]}_{[0,0,0,2]}$	No particular name
		$\overline{\mathcal{O}}^{A_2}_{(2^2)}$	$\mathcal{S}^{A_2}_{\mathcal{N},(2^2)}$
		$\overline{n.min.E_7}$	$\mathcal{S}^{E_7}_{\mathcal{N},[2,2,0,2,0,2,2]}$

Table 8.10: Some unitary quivers and their orthosymplectic doppelgängers.

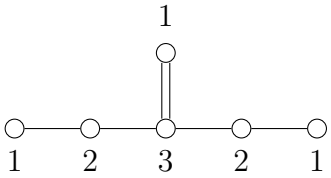
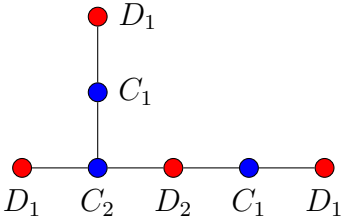
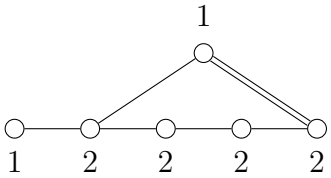
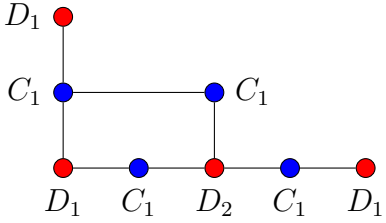
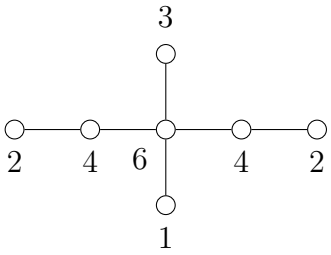
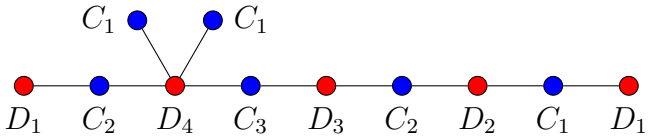
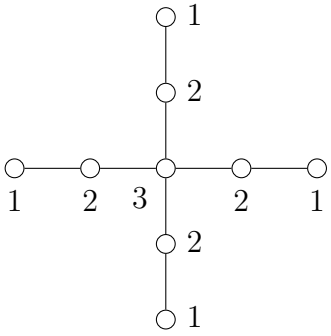
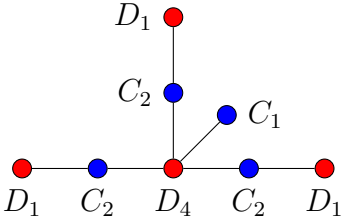
Unitary Quiver	Orthosymplectic Quiver	Coulomb Branch	Higgs Branch
		$\overline{\mathcal{O}}^{A_5}_{(2^3)}$	$\mathcal{S}^{A_5}_{\mathcal{N},(3^2)}$
		$\overline{\mathcal{O}}^{A_5}_{(3,1^3)}$	$\mathcal{S}^{A_5}_{(4,1^2)}$
		$\overline{\mathcal{O}}^{E_6}_{[0,0,0,0,0,2]}$ Double Cover	$\mathcal{S}^{E_6}_{\mathcal{N},[2,0,2,0,2,0]}/\mathbb{Z}_2$
		No particular name	No particular name

Table 8.11: Table 8.10 continued.

The longstanding problem of finding a magnetic quiver for the $6d$ $\mathcal{N}=(1,0)$ (E_6,E_6) minimal conformal matter theory is solved in Section 7.8. Firstly, an orthosymplectic magnetic quiver for the worldvolume gauge theory of two $\frac{1}{2}$M5 branes on E_6 Klein singularity is found. The F-theory description of this gauge theory is as the diagonal SU(3) gauging of two rank-1 E-strings. Therefore the derivation of the magnetic quiver $\mathcal{Q}_{7.14}$ comes from application of the SU(3) orthosymplectic quotient quiver subtraction on the magnetic quiver for $\overline{min.E_8}\times\overline{min.E_8}$. The Coulomb branch Hilbert series of $\mathcal{Q}_{7.14}$ matches that of the unitary magnetic quiver proposed in Chapter 6. The difference this time is that one can find a suitable Type IIA brane description for the orthosymplectic magnetic quiver. This is drawn in Figure 7.15 based off this magnetic quiver $\mathcal{Q}_{7.14}$. The final step of performing a small E_8 instanton transition is now possible and hence a magnetic quiver for the $6d$ $\mathcal{N}=(1,0)$ (E_6,E_6) can be found and is given in $\mathcal{Q}_{7.19}$. The corresponding brane system in the magnetic and electric phase are in Figure 7.17 and Figure 7.18 respectively.

The unrefined Hilbert series for both theories is also computed, (7.98) for $\mathcal{Q}_{7.14}$ and (7.103) for $\mathcal{Q}_{7.19}$, together with the PL (7.99) and (7.104). From this, a conjecture of which representations the generators transform in was made. The generators up to order t^6 are shown in Table 8.12. Importantly, there is a clear difference in the generators of the Higgs branch between these two theories. This reflects the presence of tensionless strings as the gauge coupling of the SU(3) goes from finite to infinite.

R-charge	Higgs branch generators (Finite Coupling)	Higgs branch generators (Infinite Coupling)
1	$(\mathbf{78},\mathbf{1})$, $(\mathbf{1},\mathbf{78})$	$(\mathbf{78},\mathbf{1})$, $(\mathbf{1},\mathbf{78})$
2	$(\mathbf{27},\overline{\mathbf{27}})$, $(\overline{\mathbf{27}},\mathbf{27})$, $(\mathbf{78},\mathbf{1})$, $(\mathbf{1},\mathbf{78})$	$(\mathbf{27},\overline{\mathbf{27}})$, $(\overline{\mathbf{27}},\mathbf{27})$
3	None	$(\mathbf{78},\mathbf{78})$, $(\mathbf{1},\mathbf{1})$

Table 8.12: The $E_6\times E_6$ representations Higgs branch generators transform in, of the $6d$ $\mathcal{N}=(1,0)$ worldvolume theory of two $\frac{1}{2}$M5 branes (finite coupling) and one M5 brane (infinite coupling) on Klein E_6 singularity.

There are further curiosities to note about $\mathcal{Q}_{7.19}$. Firstly, it is a star-shaped quiver and therefore is a magnetic quiver for the class $\mathcal{S}$ theory [222] specified by an SO(26) algebra and a three punctured sphere specified by partitions $\{(3^8,1^2),(9^2,7,1),(13^2)\}$. This is apparently different to a result in [251] which showed that the compactification of $6d$ $\mathcal{N}=(1,0)$ (E_6,E_6) conformal

matter on T^2 results in the $4d$ $\mathcal{N}=2$ class $\mathcal{S}$ theory defined by an E_6 algebra and a three punctured sphere with two maximal and one minimal puncture. There is no known magnetic quiver for class $\mathcal{S}$ theories specified by exceptional algebras. Could $\mathcal{Q}_{7.19}$ be the magnetic for this class $\mathcal{S}$ theory with E_6 algebra?

The appearance of the SO(26) algebra does not appear to be a coincidence as it is related to E_6 in the following way. There is an embedding of $E_6 \hookleftarrow F_4$ through the folding action and also and embedding of SO(26) $\hookleftarrow F_4$ through the fundamental of F_4 since this representation (like all representations of F_4) is real. It remains a challenge to see if this is a general behaviour and whether magnetic quivers for class $\mathcal{S}$ theories specified by exceptional algebras can be found systematically.

It is worth re-emphasising that the magnetic quiver and Type IIA brane system for $6d$ $\mathcal{N}=(1,0)$ (E_6,E_6) conformal matter conjectured in this paper are the first of their kind, and that a similar set of magnetic quivers may also exist for the case of (E_7,E_7) and (E_8,E_8) but it is not yet clear how to find these.

Having reviewed the four techniques in this thesis for gauging Coulomb branch global symmetries and their applications it is time to suggest future directions.

Future Directions All four of the techniques require legs of a quiver which correspond to "maximal" punctures. These maximal punctures are not the only type of leg in a quiver which supports a non-Abelian Coulomb branch symmetry. An obvious future direction would be to systematise the gauging of non-Abelian Coulomb branch global symmetry subgroups in non-maximal legs.

The selection rules for which quivers are amenable to the diagrammatic methods for gauging restrict to cases where one finds complete Higgsing of the symmetry. This restriction allows for simple checks of the hyper-Kähler quotient through the Hilbert series and Weyl integration since the F-flat space is a complete intersection. In the case of incomplete Higgsing, the F-flat space is generically not a complete intersection and its determination requires the computation of a Gröbner basis which is computationally expensive and technical. It may turn out that the

diagrammatic methods for gauging still produce the "correct" answer or would require a few modifications to do so. A future direction would be to check the diagrammatic methods for cases with incomplete Higgsing. A huge benefit of doing this would be in replacing technical computations with simple combinatorial methods.

As always, when new prescriptions for any procedure is introduced, one is always looking for novel applications. A limited few were considered in this thesis mostly in the study of $4d$ or $6d$ Higgs branches through magnetic quivers or in the discovery of new relationships between symplectic singularities. A future direction would be to find new applications of the techniques developed here.

A challenging direction to look into would be in giving brane interpretations of gauging global symmetries. However, it is not quite clear how this will be formulated precisely. Many other quiver techniques that have been developed so far, such as those used in deriving stratification of the Coulomb branch and Higgs branch, do have interpretations from brane systems and so it would be useful to tie the gauging of global symmetries into brane systems.

Bibliography

[1] A. Hanany, R. Kalveks and G. Kumaran, *Quotient quiver subtraction*, *Nucl. Phys. B* **1009** (2024) 116731 [2308.05853].

[2] A. Hanany, R. Kalveks and G. Kumaran, *Quiver polymerisation*, *JHEP* **11** (2024) 168 [2406.11561].

[3] S. Bennett, A. Hanany and G. Kumaran, *Orthosymplectic quotient quiver subtraction*, *JHEP* **12** (2024) 063 [2409.15419].

[4] S. Bennett, A. Hanany and G. Kumaran, *Quotient Quiver Subtraction – Classical Groups*, 2603.08774.

[5] A. Hanany, G. Kumaran, C. Li, D. Liu and M. Sperling, *Actions on the quiver: discrete quotients on the Coulomb branch*, *JHEP* **05** (2024) 318 [2311.02773].

[6] S. Bennett, A. Hanany, G. Kumaran, C. Li, D. Liu and M. Sperling, *Quiver subtraction on the Higgs branch*, *Nucl. Phys. B* **1016** (2025) 116917 [2409.16356].

[7] S. Bennett, A. Hanany and G. Kumaran, *Orthosymplectic quotient quiver subtraction. Part II. Framed quivers*, *JHEP* **12** (2025) 046 [2503.19954].

[8] S. Bennett, A. Hanany, G. Kumaran and L. Mansi, *Symmetry Mitosis and Hasse Diagram Diamonds: A Note on Brane Configurations with* ON^0 *Planes*, 2601.10826.

[9] E. Noether, *Invariante variationsprobleme*, *Nachrichten von der Gesellschaft der Wissenschaften zu Göttingen, Mathematisch-Physikalische Klasse* **1918** (1918) 235.

[10] S. Coleman and J. Mandula, *All possible symmetries of the s matrix*, *Phys. Rev.* **159** (1967) 1251.

[11] N. Seiberg, *Naturalness versus supersymmetric nonrenormalization theorems*, *Phys. Lett. B* **318** (1993) 469 [hep-ph/9309335].

[12] F. Englert and R. Brout, *Broken Symmetry and the Mass of Gauge Vector Mesons*, *Phys. Rev. Lett.* **13** (1964) 321.

[13] P.W. Higgs, *Broken Symmetries and the Masses of Gauge Bosons*, *Phys. Rev. Lett.* **13** (1964) 508.

[14] G.S. Guralnik, C.R. Hagen and T.W.B. Kibble, *Global Conservation Laws and Massless Particles*, *Phys. Rev. Lett.* **13** (1964) 585.

[15] T.W.B. Kibble, *Symmetry breaking in non-abelian gauge theories*, *Phys. Rev.* **155** (1967) 1554.

[16] E. Cremmer and B. Julia, *The N=8 Supergravity Theory. 1. The Lagrangian*, *Phys. Lett. B* **80** (1978) 48.

[17] E. Cremmer, B. Julia and J. Scherk, *Supergravity Theory in 11 Dimensions*, *Phys. Lett. B* **76** (1978) 409.

[18] E. Cremmer and B. Julia, *The SO(8) Supergravity*, *Nucl. Phys. B* **159** (1979) 141.

[19] M.B. Green and J.H. Schwarz, *Anomaly Cancellation in Supersymmetric D=10 Gauge Theory and Superstring Theory*, *Phys. Lett. B* **149** (1984) 117.

[20] K.S. Narain, *New Heterotic String Theories in Uncompactified Dimensions < 10*, *Phys. Lett. B* **169** (1986) 41.

[21] K.S. Narain, M.H. Sarmadi and E. Witten, *A Note on Toroidal Compactification of Heterotic String Theory*, *Nucl. Phys. B* **279** (1987) 369.

[22] C.M. Hull and P.K. Townsend, *Unity of superstring dualities*, *Nucl. Phys. B* **438** (1995) 109 [hep-th/9410167].

[23] A. Beauville, *Symplectic singularities*, *Inventiones Mathematicae* **139** (2000) 541 [math/9903070].

[24] M.F. Atiyah, N.J. Hitchin, V.G. Drinfeld and Y.I. Manin, *Construction of Instantons*, *Phys. Lett. A* **65** (1978) 185.

[25] N.J. Hitchin, A. Karlhede, U. Lindstrom and M. Rocek, *Hyperkahler Metrics and Supersymmetry*, *Commun. Math. Phys.* **108** (1987) 535.

[26] P.B. Kronheimer and H. Nakajima, *Yang-mills instantons on ale gravitational instantons.*, *Mathematische Annalen* **288** (1990) 263.

[27] H. Nakajima, *Towards a mathematical definition of Coulomb branches of* 3*-dimensional* $\mathcal{N} = 4$ *gauge theories, I*, *Adv. Theor. Math. Phys.* **20** (2016) 595 [1503.03676].

[28] H. Nakajima and A. Weekes, *Coulomb branches of quiver gauge theories with symmetrizers*, *J. Eur. Math. Soc.* **25** (2021) 203.

[29] T. Braden, A. Licata, N. Proudfoot and B. Webster, *Quantizations of conical symplectic resolutions II: category* $\mathcal{O}$ *and symplectic duality*, *arXiv e-prints* (2014) arXiv:1407.0964 [1407.0964].

[30] M.R. Douglas and G.W. Moore, *D-branes, quivers, and ALE instantons*, hep-th/9603167.

[31] A. Hanany and E. Witten, *Type IIB superstrings, BPS monopoles, and three-dimensional gauge dynamics*, *Nucl. Phys. B* **492** (1997) 152 [hep-th/9611230].

[32] A. Hanany and A. Zaffaroni, *Chiral symmetry from type IIA branes*, *Nucl. Phys. B* **509** (1998) 145 [hep-th/9706047].

[33] O. Aharony, A. Hanany and B. Kol, *Webs of (p,q) five-branes, five-dimensional field theories and grid diagrams*, *JHEP* **01** (1998) 002 [hep-th/9710116].

[34] A. Hanany and A. Zaffaroni, *Branes and six-dimensional supersymmetric theories*, *Nucl. Phys. B* **529** (1998) 180 [hep-th/9712145].

[35] I. Affleck, M. Dine and N. Seiberg, *Dynamical Supersymmetry Breaking in Supersymmetric QCD*, *Nucl. Phys. B* **241** (1984) 493.

[36] P.C. Argyres, M.R. Plesser and N. Seiberg, *The Moduli space of vacua of N=2 SUSY QCD and duality in N=1 SUSY QCD*, *Nucl. Phys. B* **471** (1996) 159 [hep-th/9603042].

[37] P.C. Argyres and M.R. Douglas, *New phenomena in SU(3) supersymmetric gauge theory*, *Nucl. Phys. B* **448** (1995) 93 [hep-th/9505062].

[38] P.C. Argyres, M.R. Plesser, N. Seiberg and E. Witten, *New N=2 superconformal field theories in four-dimensions*, *Nucl. Phys. B* **461** (1996) 71 [hep-th/9511154].

[39] N. Seiberg, *Five-dimensional SUSY field theories, nontrivial fixed points and string dynamics*, *Phys. Lett. B* **388** (1996) 753 [hep-th/9608111].

[40] D.R. Morrison and N. Seiberg, *Extremal transitions and five-dimensional supersymmetric field theories*, *Nucl. Phys. B* **483** (1997) 229 [hep-th/9609070].

[41] K.A. Intriligator, D.R. Morrison and N. Seiberg, *Five-dimensional supersymmetric gauge theories and degenerations of Calabi-Yau spaces*, *Nucl. Phys. B* **497** (1997) 56 [hep-th/9702198].

[42] E. Witten, *Small instantons in string theory*, *Nucl. Phys. B* **460** (1996) 541 [hep-th/9511030].

[43] E. Witten, *Some comments on string dynamics*, in *STRINGS 95: Future Perspectives in String Theory*, pp. 501–523, 7, 1995 [hep-th/9507121].

[44] A. Strominger, *Open p-branes*, *Phys. Lett. B* **383** (1996) 44 [hep-th/9512059].

[45] O.J. Ganor and A. Hanany, *Small E(8) instantons and tensionless noncritical strings*, *Nucl. Phys. B* **474** (1996) 122 [hep-th/9602120].

[46] S. Cabrera, A. Hanany and M. Sperling, *Magnetic quivers, Higgs branches, and 6d N=(1,0) theories*, *JHEP* **06** (2019) 071 [1904.12293].

[47] A. Bourget, S. Cabrera, J.F. Grimminger, A. Hanany, M. Sperling, A. Zajac et al., *The Higgs mechanism — Hasse diagrams for symplectic singularities*, *JHEP* **01** (2020) 157 [1908.04245].

[48] A. Bourget, S. Cabrera, J.F. Grimminger, A. Hanany and Z. Zhong, *Brane Webs and Magnetic Quivers for SQCD*, *JHEP* **03** (2020) 176 [1909.00667].

[49] J.F. Grimminger and A. Hanany, *Hasse diagrams for 3d $\mathcal{N} = 4$ quiver gauge theories — Inversion and the full moduli space*, *JHEP* **09** (2020) 159 [2004.01675].

[50] A. Bourget, J.F. Grimminger, A. Hanany, M. Sperling and Z. Zhong, *Magnetic Quivers from Brane Webs with O5 Planes*, *JHEP* **07** (2020) 204 [2004.04082].

[51] A. Bourget, J.F. Grimminger, A. Hanany, M. Sperling, G. Zafrir and Z. Zhong, *Magnetic quivers for rank 1 theories*, *JHEP* **09** (2020) 189 [2006.16994].

[52] A. Bourget, J.F. Grimminger, A. Hanany, R. Kalveks, M. Sperling and Z. Zhong, *Magnetic Lattices for Orthosymplectic Quivers*, *JHEP* **12** (2020) 092 [2007.04667].

[53] E. Beratto, S. Giacomelli, N. Mekareeya and M. Sacchi, *3d mirrors of the circle reduction of twisted A_{2N} theories of class S*, *JHEP* **09** (2020) 161 [2007.05019].

[54] C. Closset, S. Schafer-Nameki and Y.-N. Wang, *Coulomb and Higgs Branches from Canonical Singularities: Part 0*, *JHEP* **02** (2021) 003 [2007.15600].

[55] M. Akhond, F. Carta, S. Dwivedi, H. Hayashi, S.-S. Kim and F. Yagi, *Five-brane webs, Higgs branches and unitary/orthosymplectic magnetic quivers*, *JHEP* **12** (2020) 164 [2008.01027].

[56] M. van Beest, A. Bourget, J. Eckhard and S. Schafer-Nameki, *(Symplectic) Leaves and (5d Higgs) Branches in the Poly(go)nesian Tropical Rain Forest*, *JHEP* **11** (2020) 124 [2008.05577].

[57] A. Bourget, S. Giacomelli, J.F. Grimminger, A. Hanany, M. Sperling and Z. Zhong, *S-fold magnetic quivers*, *JHEP* **02** (2021) 054 [2010.05889].

[58] M. Van Beest, A. Bourget, J. Eckhard and S. Schäfer-Nameki, *(5d RG-flow) Trees in the Tropical Rain Forest*, *JHEP* **03** (2021) 241 [2011.07033].

[59] S. Giacomelli, N. Mekareeya and M. Sacchi, *New aspects of Argyres–Douglas theories and their dimensional reduction*, *JHEP* **03** (2021) 242 [2012.12852].

[60] M. Akhond, F. Carta, S. Dwivedi, H. Hayashi, S.-S. Kim and F. Yagi, *Factorised 3d $\mathcal{N} = 4$ orthosymplectic quivers*, *JHEP* **05** (2021) 269 [2101.12235].

[61] F. Carta, S. Giacomelli, N. Mekareeya and A. Mininno, *Conformal manifolds and 3d mirrors of Argyres-Douglas theories*, *JHEP* **08** (2021) 015 [2105.08064].

[62] G. Arias-Tamargo, A. Bourget and A. Pini, *Discrete gauging and Hasse diagrams*, *SciPost Phys.* **11** (2021) 026 [2105.08755].

[63] A. Bourget, J.F. Grimminger, A. Hanany, R. Kalveks, M. Sperling and Z. Zhong, *Folding orthosymplectic quivers*, *JHEP* **12** (2021) 070 [2107.00754].

[64] K. Gledhill and A. Hanany, *Coulomb branch global symmetry and quiver addition*, *JHEP* **12** (2021) 127 [2109.07237].

[65] M. van Beest and S. Giacomelli, *Connecting 5d Higgs branches via Fayet-Iliopoulos deformations*, *JHEP* **12** (2021) 202 [2110.02872].

[66] F. Carta, S. Giacomelli, N. Mekareeya and A. Mininno, *Conformal manifolds and 3d mirrors of (D_n, D_m) theories*, *JHEP* **02** (2022) 014 [2110.06940].

[67] M. Sperling and Z. Zhong, *Balanced B and D-type orthosymplectic quivers — magnetic quivers for product theories*, *JHEP* **04** (2022) 145 [2111.00026].

[68] S. Nawata, M. Sperling, H.E. Wang and Z. Zhong, *Magnetic quivers and line defects — On a duality between 3d $\mathcal{N} = 4$ unitary and orthosymplectic quivers*, *JHEP* **02** (2022) 174 [2111.02831].

[69] M. Akhond, F. Carta, S. Dwivedi, H. Hayashi, S.-S. Kim and F. Yagi, *Exploring the orthosymplectic zoo*, *JHEP* **05** (2022) 054 [2203.01951].

[70] S. Giacomelli, M. Moleti and R. Savelli, *Probing 7-branes on orbifolds*, *JHEP* **08** (2022) 163 [2205.08578].

[71] M.J. Kang, C. Lawrie, K.-H. Lee, M. Sacchi and J. Song, *Higgs branch, Coulomb branch, and Hall-Littlewood index*, *Phys. Rev. D* **106** (2022) 106021 [2207.05764].

[72] A. Hanany and M. Sperling, *Magnetic quivers and negatively charged branes*, *JHEP* **11** (2022) 010 [2208.07270].

[73] J. Gu, Y. Jiang and M. Sperling, *Rational Q-systems, Higgsing and mirror symmetry*, *SciPost Phys.* **14** (2023) 034 [2208.10047].

[74] M. Fazzi and S. Giri, *Hierarchy of RG flows in 6d (1, 0) orbi-instantons*, *JHEP* **12** (2022) 076 [2208.11703].

[75] A. Bourget and J.F. Grimminger, *Fibrations and Hasse diagrams for 6d SCFTs*, *JHEP* **12** (2022) 159 [2209.15016].

[76] K. Gledhill and A. Hanany, *Poisson brackets for some Coulomb branches*, *JHEP* **03** (2023) 154 [2210.02966].

[77] M. Fazzi, S. Giacomelli and S. Giri, *Hierarchies of RG flows in 6d (1, 0) massive E-strings*, *JHEP* **03** (2023) 089 [2212.14027].

[78] L. Bhardwaj, M. Bullimore, A.E.V. Ferrari and S. Schafer-Nameki, *Generalized Symmetries and Anomalies of 3d N=4 SCFTs*, 2301.02249.

[79] A. Bourget, S. Giacomelli and J.F. Grimminger, *FI-flows of 3d $N = 4$ Theories*, *JHEP* **04** (2023) 015 [2302.03698].

[80] A. Bourget, J.F. Grimminger, A. Hanany, R. Kalveks, M. Sperling and Z. Zhong, *A Tale of N Cones*, 2303.16939.

[81] M. Del Zotto, M. Fazzi and S. Giri, *A new vista on the heterotic moduli space from six and three dimensions*, *Phys. Rev. D* **109** (2024) L021903 [2307.10356].

[82] M. Del Zotto, M. Fazzi and S. Giri, *The Higgs branch of heterotic ALE instantons*, *JHEP* **01** (2024) 167 [2307.11087].

[83] A. Bourget, M. Sperling and Z. Zhong, *Decay and Fission of Magnetic Quivers*, 2312.05304.

[84] C. Lawrie and L. Mansi, *The Higgs Branch of Heterotic LSTs: Hasse Diagrams and Generalized Symmetries*, 2312.05306.

[85] S. Benvenuti, R. Comi and S. Pasquetti, *Mirror dualities with four supercharges*, 2312.07667.

[86] L. Mansi and M. Sperling, *Unravelling T-Duality: Magnetic Quivers in Rank-zero Little String Theories*, 2312.12510.

[87] M. Fazzi, S. Giri and P. Levy, *Proving the 6d a-theorem with the double affine Grassmannian*, 2312.17178.

[88] A. Bourget, M. Sperling and Z. Zhong, *Higgs branch RG-flows via Decay and Fission*, 2401.08757.

[89] S. Giacomelli, R. Savelli and G. Zoccarato, $\mathcal{N} = 2$ *Orbi-S-Folds*, *JHEP* **01** (2025) 059 [2405.00101].

[90] C. Lawrie and L. Mansi, *The Higgs Branch of 6d (1,0) SCFTs & LSTs with DE-type SUSY Enhancement*, 2406.02670.

[91] J. Bao and H.Y. Zhang, *Atomic Higgsings of 6D SCFTs. Part I*, *JHEP* **05** (2025) 124 [2409.17224].

[92] M. Akhond, G. Arias-Tamargo, F. Carta, J.F. Grimminger and A. Hanany, *On brane systems with O^+ planes — 5d and 6d SCFTs*, *JHEP* **03** (2025) 137 [2411.02491].

[93] S. Giacomelli, W. Harding, N. Mekareeya and A. Mininno, *All class $\mathcal{S}$ theories of type-A originate from orbi-instantons*, *JHEP* **02** (2025) 185 [2411.03425].

[94] Z. Zhong, *A Bound on 3d Mirror Pairs*, 2411.14531.

[95] C. Lawrie, L. Mansi, M. Sperling and Z. Zhong, *A Pathway to Decay and Fission of Orthosymplectic Quiver Theories*, 2412.15202.

[96] A. Bourget, Q. Lamouret, S.M. Soysüren and M. Sperling, *Classification of minimal Abelian Coulomb branches*, *Phys. Rev. D* **111** (2025) 125020 [2412.19766].

[97] M. De Marco, M. Del Zotto, J.F. Grimminger and A. Sangiovanni, *Remarks on the Higgs branch of 5d conformal matter*, *JHEP* **10** (2025) 144 [2502.04431].

[98] F. Marino and M. Sperling, *Vacua, symmetries, and Higgsing of Chern-Simons matter theories*, *SciPost Phys.* **18** (2025) 174 [2503.02744].

[99] C. Lawrie, T. Lepper and A. Mininno, *Discrete gauging of 6D SCFTs and wreathed 3D N=4 quivers*, *Phys. Rev. D* **112** (2025) 026035 [2504.03830].

[100] A. Bourget, Q. Lamouret, S. Moura Soysüren and M. Sperling, *Classifying Isolated Symplectic Singularities via 3d $\mathcal{N} = 4$ Coulomb Branches*, 2504.05373.

[101] S. Giacomelli, W. Harding, N. Mekareeya and A. Mininno, *From regular to irregular: a unified origin for Argyres-Douglas theories*, *JHEP* **10** (2025) 155 [2507.13434].

[102] H. Ahmed, F. Baume and P.-K. Oehlmann, *The Weight of $Spin(32)/\mathbb{Z}_2$ Little Strings: T-duality and Hasse Diagrams*, 2510.24842.

[103] J. Bao, N. Mekareeya, G. Zafrir and H.Y. Zhang, *Orbi-Instantons and Class $\mathcal{S}$ Theories of Type D*, 2602.03931.

[104] S. Bennett, A. Hanany and R. Kalveks, *Quiver Maps, Nilpotent Orbits and Special Pieces of Nilcones*, 2603.22433.

[105] A. Hanany and E.V.d. Driessche, *Higgs branch of 5d $\mathcal{N} = 1$ symplectic gauge theories and dressed instanton operators*, 2507.08669.

[106] A. Hanany and E. Van den Driessche, *Chiral ring along the RG flow in 5d $\mathcal{N} = 1$*, 2510.15635.

[107] A. Hanany, A. Tomasiello and E. Van den Driessche, *5d Higgs branch and instanton magnetization*, 2603.29679.

[108] S. Cremonesi, A. Hanany and A. Zaffaroni, *Monopole operators and Hilbert series of Coulomb branches of* $3d$ $\mathcal{N} = 4$ *gauge theories*, *JHEP* **01** (2014) 005 [1309.2657].

[109] A. Gadde, L. Rastelli, S.S. Razamat and W. Yan, *Gauge Theories and Macdonald Polynomials*, *Commun. Math. Phys.* **319** (2013) 147 [1110.3740].

[110] S. Cabrera and A. Hanany, *Quiver Subtractions*, *JHEP* **09** (2018) 008 [1803.11205].

[111] K.A. Intriligator and N. Seiberg, *Mirror symmetry in three-dimensional gauge theories*, *Phys. Lett. B* **387** (1996) 513 [hep-th/9607207].

[112] G. Ferlito and A. Hanany, *A tale of two cones: the Higgs Branch of Sp(n) theories with 2n flavours*, 1609.06724.

[113] B. Feng, A. Hanany and Y.-H. He, *Counting gauge invariants: The Plethystic program*, *JHEP* **03** (2007) 090 [hep-th/0701063].

[114] D. Forcella, A. Hanany, Y.-H. He and A. Zaffaroni, *Mastering the Master Space*, *Lett. Math. Phys.* **85** (2008) 163 [0801.3477].

[115] D. Forcella, A. Hanany, Y.-H. He and A. Zaffaroni, *The Master Space of N=1 Gauge Theories*, *JHEP* **08** (2008) 012 [0801.1585].

[116] D. Forcella, A. Hanany and A. Zaffaroni, *Master Space, Hilbert Series and Seiberg Duality*, *JHEP* **07** (2009) 018 [0810.4519].

[117] A. Hanany and A. Zaffaroni, *The master space of supersymmetric gauge theories*, *Adv. High Energy Phys.* **2010** (2010) 427891.

[118] A.F. Möbius, *Über eine besondere art von umkehrung der reihen*, *J. Reine Angew. Math.* **1832** (1832) 105.

[119] N. Seiberg, *IR dynamics on branes and space-time geometry*, *Phys. Lett. B* **384** (1996) 81 [hep-th/9606017].

[120] N. Seiberg and E. Witten, *Gauge dynamics and compactification to three-dimensions*, in *Conference on the Mathematical Beauty of Physics (In Memory of C. Itzykson)*, pp. 333–366, 6, 1996 [hep-th/9607163].

[121] V. Borokhov, A. Kapustin and X.-k. Wu, *Topological disorder operators in three-dimensional conformal field theory*, *JHEP* **11** (2002) 049 [hep-th/0206054].

[122] G. 't Hooft, *On the phase transition towards permanent quark confinement*, *Nuclear Physics B* **138** (1978) 1.

[123] D. Gaiotto and E. Witten, *S-Duality of Boundary Conditions In N=4 Super Yang-Mills Theory*, *Adv. Theor. Math. Phys.* **13** (2009) 721 [0807.3720].

[124] H. Nakajima, *Questions on provisional Coulomb branches of 3-dimensional $\mathcal{N} = 4$ gauge theories*, *arXiv e-prints* (2015) arXiv:1510.03908 [1510.03908].

[125] A. Braverman, M. Finkelberg and H. Nakajima, *Towards a mathematical definition of Coulomb branches of 3-dimensional $\mathcal{N} = 4$ gauge theories, II*, *Adv. Theor. Math. Phys.* **22** (2018) 1071 [1601.03586].

[126] D. Bashkirov and A. Kapustin, *Supersymmetry enhancement by monopole operators*, *JHEP* **05** (2011) 015 [1007.4861].

[127] M.K. Benna, I.R. Klebanov and T. Klose, *Charges of Monopole Operators in Chern-Simons Yang-Mills Theory*, *JHEP* **01** (2010) 110 [0906.3008].

[128] A. Kapustin, *D(n) quivers from branes*, *JHEP* **12** (1998) 015 [hep-th/9806238].

[129] B. Feng and A. Hanany, *Mirror symmetry by O3 planes*, *JHEP* **11** (2000) 033 [hep-th/0004092].

[130] A. Hanany and J. Troost, *Orientifold planes, affine algebras and magnetic monopoles*, *JHEP* **08** (2001) 021 [hep-th/0107153].

[131] A. Hanany and A. Zaffaroni, *Issues on orientifolds: On the brane construction of gauge theories with SO(2n) global symmetry*, *JHEP* **07** (1999) 009 [hep-th/9903242].

[132] S. Cremonesi, A. Hanany, N. Mekareeya and A. Zaffaroni, *Coulomb branch Hilbert series and Hall-Littlewood polynomials*, *JHEP* **09** (2014) 178 [1403.0585].

[133] S. Cabrera, A. Hanany and R. Kalveks, *Quiver Theories and Formulae for Slodowy Slices of Classical Algebras*, *Nucl. Phys. B* **939** (2019) 308 [1807.02521].

[134] A. Hanany and R. Kalveks, *Quiver Theories and Hilbert Series of Classical Slodowy Intersections*, *Nucl. Phys. B* **952** (2020) 114939 [1909.12793].

[135] A. Hanany and R. Kalveks, *Highest Weight Generating Functions for Hilbert Series*, *JHEP* **10** (2014) 152 [1408.4690].

[136] A. Hanany and A. Zajac, *Ungauging Schemes and Coulomb Branches of Non-simply Laced Quiver Theories*, *JHEP* **09** (2020) 193 [2002.05716].

[137] W. Crawley-Boevey, *Geometry of the Moment Map for Representations of Quivers*, *Compositio Mathematica* **126** (2001) 257.

[138] A. Bourget, J.F. Grimminger, A. Hanany, R. Kalveks, M. Sperling and Z. Zhong, *Magnetic Lattices for Orthosymplectic Quivers*, .

[139] P. Pasti, D.P. Sorokin and M. Tonin, *On Lorentz invariant actions for chiral p forms*, *Phys. Rev. D* **55** (1997) 6292 [hep-th/9611100].

[140] A. Sen, *Covariant Action for Type IIB Supergravity*, *JHEP* **07** (2016) 017 [1511.08220].

[141] K. Mkrtchyan, *On Covariant Actions for Chiral p−Forms*, *JHEP* **12** (2019) 076 [1908.01789].

[142] A. Sen, *Self-dual forms: Action, Hamiltonian and Compactification*, *J. Phys. A* **53** (2020) 084002 [1903.12196].

[143] Z. Avetisyan, O. Evnin and K. Mkrtchyan, *Nonlinear (chiral) p-form electrodynamics*, *JHEP* **08** (2022) 112 [2205.02522].

[144] M. Berkooz, M. Rozali and N. Seiberg, *Matrix description of M theory on T**4 and T**5*, *Phys. Lett. B* **408** (1997) 105 [hep-th/9704089].

[145] N. Seiberg, *New theories in six-dimensions and matrix description of M theory on T**5 and T**5 / Z(2)*, *Phys. Lett. B* **408** (1997) 98 [hep-th/9705221].

[146] A. Losev, G.W. Moore and S.L. Shatashvili, *M & m's*, *Nucl. Phys. B* **522** (1998) 105 [hep-th/9707250].

[147] K. Kodaira, *On compact analytic surfaces: Ii*, *Annals of Mathematics* **77** (1963) 563.

[148] K. Kodaira†, *On compact analytic surfaces, iii*, *Annals of Mathematics* **78** (1963) 1.

[149] P.S. Aspinwall and D.R. Morrison, *Nonsimply connected gauge groups and rational points on elliptic curves*, *JHEP* **07** (1998) 012 [hep-th/9805206].

[150] P.S. Aspinwall and D.R. Morrison, *Point - like instantons on K3 orbifolds*, *Nucl. Phys. B* **503** (1997) 533 [hep-th/9705104].

[151] M. Bershadsky, K.A. Intriligator, S. Kachru, D.R. Morrison, V. Sadov and C. Vafa, *Geometric singularities and enhanced gauge symmetries*, *Nucl. Phys. B* **481** (1996) 215 [hep-th/9605200].

[152] M. Bershadsky and C. Vafa, *Global anomalies and geometric engineering of critical theories in six-dimensions*, hep-th/9703167.

[153] C. Vafa, *Evidence for F theory*, *Nucl. Phys. B* **469** (1996) 403 [hep-th/9602022].

[154] A. Hanany and N. Mekareeya, *The small E_8 instanton and the Kraft Procesi transition*, *JHEP* **07** (2018) 098 [1801.01129].

[155] S. Cabrera, A. Hanany and M. Sperling, *Magnetic quivers, Higgs branches, and 6d $\mathcal{N} = (1, 0)$ theories — orthogonal and symplectic gauge groups*, *JHEP* **02** (2020) 184 [1912.02773].

[156] A. Hanany and A. Zajac, *Discrete Gauging in Coulomb branches of Three Dimensional $\mathcal{N} = 4$ Supersymmetric Gauge Theories*, *JHEP* **08** (2018) 158 [1807.03221].

[157] K. Dasgupta and J. Park, *Brane mapping under (-1)**F(L)*, *Phys. Lett. B* **457** (1999) 47 [hep-th/9903125].

[158] A. Hanany, B. Kol and A. Rajaraman, *Orientifold points in M theory*, *JHEP* **10** (1999) 027 [hep-th/9909028].

[159] A. Sen, *Stable nonBPS bound states of BPS D-branes*, *JHEP* **08** (1998) 010 [hep-th/9805019].

[160] A. Hanany and B. Kol, *On orientifolds, discrete torsion, branes and M theory*, *JHEP* **06** (2000) 013 [hep-th/0003025].

[161] N.J. Evans, C.V. Johnson and A.D. Shapere, *Orientifolds, branes, and duality of 4-D gauge theories*, *Nucl. Phys. B* **505** (1997) 251 [hep-th/9703210].

[162] L.J. Romans, *Massive N=2a Supergravity in Ten-Dimensions*, *Phys. Lett. B* **169** (1986) 374.

[163] I.R. Klebanov and M.J. Strassler, *Supergravity and a confining gauge theory: Duality cascades and chi SB resolution of naked singularities*, *JHEP* **08** (2000) 052 [hep-th/0007191].

[164] S. Kachru, J. Pearson and H.L. Verlinde, *Brane / flux annihilation and the string dual of a nonsupersymmetric field theory*, *JHEP* **06** (2002) 021 [hep-th/0112197].

[165] S. Kachru, R. Kallosh, A.D. Linde and S.P. Trivedi, *De Sitter vacua in string theory*, *Phys. Rev. D* **68** (2003) 046005 [hep-th/0301240].

[166] N. Mekareeya, T. Rudelius and A. Tomasiello, *T-branes, Anomalies and Moduli Spaces in 6D SCFTs*, *JHEP* **10** (2017) 158 [1612.06399].

[167] F. Hassler, J.J. Heckman, T.B. Rochais, T. Rudelius and H.Y. Zhang, *T-Branes, String Junctions, and 6D SCFTs*, *Phys. Rev. D* **101** (2020) 086018 [1907.11230].

[168] M. Del Zotto, J.J. Heckman, A. Tomasiello and C. Vafa, *6d Conformal Matter*, *JHEP* **02** (2015) 054 [1407.6359].

[169] R. Brylinski and B. Kostant, *Nilpotent orbits, normality, and Hamiltonian group actions*, *arXiv Mathematics e-prints* (1992) math/9204227 [math/9204227].

[170] P. Horava and E. Witten, *Heterotic and Type I string dynamics from eleven dimensions*, *Nucl. Phys. B* **460** (1996) 506 [hep-th/9510209].

[171] P. Horava and E. Witten, *Eleven-dimensional supergravity on a manifold with boundary*, *Nucl. Phys. B* **475** (1996) 94 [hep-th/9603142].

[172] A. Weinstein, *The local structure of poisson manifolds*, *J. Differential Geom.* **18** (1983) 523.

[173] Y. Namikawa, *Extension of 2-forms and symplectic varieties*, *arXiv Mathematics e-prints* (2000) math/0010114 [math/0010114].

[174] D. Kaledin, *Symplectic singularities from the Poisson point of view*, *arXiv Mathematics e-prints* (2003) math/0310186 [math/0310186].

[175] D.H. Collingwood and W.M. McGovern, *Nilpotent Orbits in Semisimple Lie Algebras*, Routledge (1993), 10.1201/9780203745809.

[176] N. Jacobson, *Completely Reducible Lie Algebras of Linear Transformations*, *Proceedings of the American Mathematical Society* **2** (1951) 105.

[177] V.V. Morozov, *On a nilpotent element in a semi-simple Lie algebra*, *C. R. (Doklady) Acad. Sci. URSS (N.S.)* **36** (1942) 83.

[178] E. Dynkin, *Semisimple subalgebras of semisimple Lie algebras*, *Trans. Am. Math. Soc. Ser. 2* **6** (1957) 111.

[179] H. Kraft and C. Procesi, *Minimal singularities in GLn*, *Inventiones mathematicae* **62** (1980) 503.

[180] H. Kraft and C. Procesi, *On the geometry of conjugacy classes in classical groups*, *Commentarii Mathematici Helvetici* **57** (1982) 539.

[181] P. Bala and R.W. Carter, *Classes of unipotent elements in simple algebraic groups. i*, *Mathematical Proceedings of the Cambridge Philosophical Society* **79** (1976) 401–425.

[182] P. Bala and R.W. Carter, *Classes of unipotent elements in simple algebraic groups. ii*, *Mathematical Proceedings of the Cambridge Philosophical Society* **80** (1976) 1–18.

[183] A. Hanany and R. Kalveks, *Quiver Theories for Moduli Spaces of Classical Group Nilpotent Orbits*, *JHEP* **06** (2016) 130 [1601.04020].

[184] A. Hanany and R. Kalveks, *Quiver Theories and Formulae for Nilpotent Orbits of Exceptional Algebras*, *JHEP* **11** (2017) 126 [1709.05818].

[185] A. Hanany and R. Kalveks, *Construction and Deconstruction of Single Instanton Hilbert Series*, *JHEP* **12** (2015) 118 [1509.01294].

[186] S. Cremonesi, A. Hanany, N. Mekareeya and A. Zaffaroni, T_ρ^σ *(G) theories and their Hilbert series*, *JHEP* **01** (2015) 150 [1410.1548].

[187] D.I. Panyushev, *Complexity and nilpotent orbits*, *Manuscripta Mathematica* **83** (1994) 223.

[188] B. Fu, D. Juteau, P. Levy and E. Sommers, *Generic singularities of nilpotent orbit closures*, *arXiv e-prints* (2015) arXiv:1502.05770 [1502.05770].

[189] J. Gray, A. Hanany, Y.-H. He, V. Jejjala and N. Mekareeya, *SQCD: A Geometric Apercu*, *JHEP* **05** (2008) 099 [0803.4257].

[190] A. Broer, *Decomposition varieties in semisimple lie algebras*, *Canadian Journal of Mathematics* **50** (1998) 929–971.

[191] P. Slodowy, *Simple Singularities and Simple Algebraic Groups*, Lecture Notes in Mathematics, Springer, Berlin, Germany, 1980 ed. (Aug., 1980).

[192] G. Lusztig and N. Spaltenstein, *Induced unipotent classes*, *Journal of the London Mathematical Society* **s2-19** (1979) 41 [https://londmathsoc.onlinelibrary.wiley.com/doi/pdf/10.1112/jlms/s2-19.1.41].

[193] D. Barbasch and D.A. Vogan, *Unipotent representations of complex semisimple groups*, *Annals of Mathematics* **121** (1985) 41.

[194] D. Barbasch, J.-J. Ma, B. Sun and C.-B. Zhu, *On the notion of metaplectic Barbasch-Vogan duality*, *arXiv e-prints* (2020) arXiv:2010.16089 [2010.16089].

[195] A. Beauville and Y. Laszlo, *Conformal blocks and generalized theta functions*, alg-geom/9309003.

[196] S. Kumar, M.S. Narasimhan and A. Ramanathan, *Infinite grassmannians and moduli spaces ofg-bundles*, *Math. Ann.* **300** (1994) 41.

[197] A. Beauville, Y. Laszio and C. Sorger, *The picard group of the moduli of G-bundles on a curve*, *Compos. Math.* **112** (1998) 183.

[198] A. Malkin, V. Ostrik and M. Vybornov, *The minimal degeneration singularities in the affine grassmannians*, math/0305095.

[199] G. Pappas and M. Rapoport, *Twisted loop groups and their affine flag varieties*, *Adv. Math. (N. Y.)* **219** (2008) 118.

[200] J. Kamnitzer, B. Webster, A. Weekes and O. Yacobi, *Yangians and quantizations of slices in the affine grassmannian*, 1209.0349.

[201] M. Bullimore, T. Dimofte and D. Gaiotto, *The Coulomb Branch of 3d $\mathcal{N} = 4$ Theories*, *Commun. Math. Phys.* **354** (2017) 671 [1503.04817].

[202] A. Bourget, J.F. Grimminger, A. Hanany, M. Sperling and Z. Zhong, *Branes, Quivers, and the Affine Grassmannian*, *Adv. Stud. Pure Math.* **88** (2023) 331 [2102.06190].

[203] D. Muthiah and A. Weekes, *Fundamental Monopole Operators and Embeddings of Kac-Moody Affine Grassmannian Slices*, *Int. Math. Res. Not.* **2024** (2024) 11159 [2211.04788].

[204] M. Finkelberg, *DOUBLE AFFINE GRASSMANNIANS AND COULOMB BRANCHES OF 3d n = 4 QUIVER GAUGE THEORIES*, in *Proceedings of the International Congress of Mathematicians (ICM 2018)*, WORLD SCIENTIFIC, May, 2019.

[205] A. Braverman, M. Finkelberg and D. Gaitsgory, *Uhlenbeck spaces via affine Lie algebras*, *arXiv Mathematics e-prints* (2003) math/0301176 [math/0301176].

[206] K. Dasgupta and S. Mukhi, *F theory at constant coupling*, *Phys. Lett. B* **385** (1996) 125 [hep-th/9606044].

[207] D.R. Morrison and C. Vafa, *Compactifications of F theory on Calabi-Yau threefolds. 1*, *Nucl. Phys. B* **473** (1996) 74 [hep-th/9602114].

[208] D.R. Morrison and C. Vafa, *Compactifications of F theory on Calabi-Yau threefolds. 2.*, *Nucl. Phys. B* **476** (1996) 437 [hep-th/9603161].

[209] J.A. Minahan and D. Nemeschansky, *Superconformal fixed points with E(n) global symmetry*, *Nucl. Phys. B* **489** (1997) 24 [hep-th/9610076].

[210] P.Z. Kobak and A. Swann, *Classical nilpotent orbits as hyperkähler quotients*, *International Journal of Mathematics* **07** (1996) 193.

[211] R. Bielawski and V. Pidstrygach, *Gelfand-Zeitlin actions and rational maps*, *arXiv Mathematics e-prints* (2006) math/0612365 [math/0612365].

[212] A. Braverman, M. Finkelberg and H. Nakajima, *Ring objects in the equivariant derived Satake category arising from Coulomb branches (with an appendix by Gus Lonergan)*, 1706.02112.

[213] E. Witten, *An SU(2) Anomaly*, *Phys. Lett. B* **117** (1982) 324.

[214] P.C. Argyres and N. Seiberg, *S-duality in N=2 supersymmetric gauge theories*, *JHEP* **12** (2007) 088 [0711.0054].

[215] P.C. Argyres and J.R. Wittig, *Infinite coupling duals of N=2 gauge theories and new rank 1 superconformal field theories*, *JHEP* **01** (2008) 074 [0712.2028].

[216] P.N. Achar and A. Henderson, *Geometric Satake, Springer correspondence, and small representations*, *arXiv e-prints* (2011) arXiv:1108.4999 [1108.4999].

[217] A. Bourget, J.F. Grimminger, M. Martone and G. Zafrir, *Magnetic quivers for rank 2 theories*, *JHEP* **03** (2022) 208 [2110.11365].

[218] O. Chacaltana and J. Distler, *Tinkertoys for Gaiotto Duality*, *JHEP* **11** (2010) 099 [1008.5203].

[219] A. Bourget, A. Hanany and D. Miketa, *Quiver origami: discrete gauging and folding*, *JHEP* **01** (2021) 086 [2005.05273].

[220] K. Ohmori, Y. Tachikawa and G. Zafrir, *Compactifications of 6d $N = (1, 0)$ SCFTs with non-trivial Stiefel-Whitney classes*, *JHEP* **04** (2019) 006 [1812.04637].

[221] S. Benvenuti, A. Hanany and N. Mekareeya, *The Hilbert Series of the One Instanton Moduli Space*, *JHEP* **06** (2010) 100 [1005.3026].

[222] D. Gaiotto, *N=2 dualities*, *JHEP* **08** (2012) 034 [0904.2715].

[223] F. Benini, Y. Tachikawa and D. Xie, *Mirrors of 3d Sicilian theories*, *JHEP* **09** (2010) 063 [1007.0992].

[224] O. Chacaltana and J. Distler, *Tinkertoys for the D_N series*, *JHEP* **02** (2013) 110 [1106.5410].

[225] O. Chacaltana, J. Distler and A. Trimm, *Tinkertoys for the Twisted D-Series*, *JHEP* **04** (2015) 173 [1309.2299].

[226] O. Chacaltana, J. Distler and A. Trimm, *Tinkertoys for the E_6 theory*, *JHEP* **09** (2015) 007 [1403.4604].

[227] O. Chacaltana, J. Distler and A. Trimm, *Tinkertoys for the Twisted E_6 Theory*, 1501.00357.

[228] O. Chacaltana, J. Distler and A. Trimm, *Tinkertoys for the Z3-twisted D4 Theory*, 1601.02077.

[229] O. Chacaltana, J. Distler, A. Trimm and Y. Zhu, *Tinkertoys for the E_7 theory*, *JHEP* **05** (2018) 031 [1704.07890].

[230] O. Chacaltana, J. Distler, A. Trimm and Y. Zhu, *Tinkertoys for the E_8 Theory*, 1802.09626.

[231] O. Chacaltana, J. Distler and Y. Tachikawa, *Nilpotent orbits and codimension-two defects of 6d N=(2,0) theories*, *Int. J. Mod. Phys. A* **28** (2013) 1340006 [1203.2930].

[232] P. Agarwal, I. Bah, K. Maruyoshi and J. Song, *Quiver tails and $\mathcal{N} = 1$ SCFTs from M5-branes*, *JHEP* **03** (2015) 049 [1409.1908].

[233] Y. Tachikawa, *A review of the T_N theory and its cousins*, *PTEP* **2015** (2015) 11B102 [1504.01481].

[234] G. Ferlito, A. Hanany, N. Mekareeya and G. Zafrir, *3d Coulomb branch and 5d Higgs branch at infinite coupling*, *JHEP* **07** (2018) 061 [1712.06604].

[235] P. Agarwal, K. Maruyoshi and J. Song, *A "Lagrangian" for the E_7 superconformal theory*, *JHEP* **05** (2018) 193 [1802.05268].

[236] S. Giacomelli, C. Meneghelli and W. Peelaers, *New $\mathcal{N} = 2$ superconformal field theories from $\mathcal{S}$-folds*, *JHEP* **01** (2021) 022 [2007.00647].

[237] F. Baume, M.J. Kang and C. Lawrie, *Two 6D origins of 4D SCFTs: Class S and 6D (1, 0) on a torus*, *Phys. Rev. D* **106** (2022) 086003 [2106.11990].

[238] I.G. Etxebarria, B. Heidenreich, M. Lotito and A.K. Sorout, *Deconfining $\mathcal{N} = 2$ SCFTs or the art of brane bending*, *JHEP* **03** (2022) 140 [2111.08022].

[239] H.-C. Kim and S.S. Razamat, *Star Shaped Quivers in Four Dimensions*, *Phys. Rev. Lett.* **130** (2023) 211601 [2302.05113].

[240] D. Xie, *General Argyres-Douglas Theory*, *JHEP* **01** (2013) 100 [1204.2270].

[241] A. Hanany and G. Zafrir, *Discrete Gauging in Six Dimensions*, *JHEP* **07** (2018) 168 [1804.08857].

[242] M.R. Douglas, *Branes within branes*, *NATO Sci. Ser. C* **520** (1999) 267 [hep-th/9512077].

[243] J. de Boer, K. Hori, H. Ooguri and Y. Oz, *Mirror symmetry in three-dimensional gauge theories, quivers and D-branes*, *Nucl. Phys. B* **493** (1997) 101 [hep-th/9611063].

[244] S. Cremonesi, G. Ferlito, A. Hanany and N. Mekareeya, *Coulomb Branch and The Moduli Space of Instantons*, *JHEP* **12** (2014) 103 [1408.6835].

[245] V.G. Kac, *Infinite Dimensional Lie Algebras*, Birkhäuser, 1 ed. (1983), 10.1007/978-1-4757-1382-4.

[246] J. Fuchs and C. Schweigert, *Symmetries, lie algebras and representations : a graduate course for physicists*, Cambridge monographs on mathematical physics, Cambridge University Press, Cambridge (2003 - 1997).

[247] A. Hanany and N. Mekareeya, *Tri-vertices and SU(2)'s*, *JHEP* **02** (2011) 069 [1012.2119].

[248] M. Finkelberg and E. Goncharov, *Coulomb branch of a multiloop quiver gauge theory*, *arXiv e-prints* (2019) arXiv:1903.05822 [1903.05822].

[249] C. Moeglin, *Sur la classification des séries discrètes des groupes classiques p-adiques: paramètres de langlands et exhaustivité*, *Journal of the European Mathematical Society* **004** (2002) 143.

[250] D. Jiang, B. Liu and G. Savin, *Raising nilpotent orbits in wave-front sets*, *arXiv e-prints* (2014) arXiv:1412.8742 [1412.8742].

[251] K. Ohmori, H. Shimizu, Y. Tachikawa and K. Yonekura, *6d $\mathcal{N} = (1, 0)$ theories on T^2 and class S theories: Part I*, *JHEP* **07** (2015) 014 [1503.06217].

[252] D. Juteau, P. Levy and E. Sommers, *Minimal special degenerations and duality*, *arXiv e-prints* (2023) arXiv:2310.00521 [2310.00521].

[253] K. Ohmori, H. Shimizu, Y. Tachikawa and K. Yonekura, *6d $\mathcal{N} = (1, 0)$ theories on S^1/T^2 and class S theories: part II*, *JHEP* **12** (2015) 131 [1508.00915].

[254] S. Cabrera and A. Hanany, *Branes and the Kraft-Procesi Transition*, *JHEP* **11** (2016) 175 [1609.07798].

[255] S. Cabrera and A. Hanany, *Branes and the Kraft-Procesi transition: classical case*, *JHEP* **04** (2018) 127 [1711.02378].

[256] S.A. Cherkis, *Moduli Spaces of Instantons on the Taub-NUT Space*, *Commun. Math. Phys.* **290** (2009) 719 [0805.1245].

[257] E. Witten, *Branes, Instantons, And Taub-NUT Spaces*, *JHEP* **06** (2009) 067 [0902.0948].

[258] A. Dey, A. Hanany, N. Mekareeya, D. Rodríguez-Gómez and R.-K. Seong, *Hilbert Series for Moduli Spaces of Instantons on C^2/Z_n*, *JHEP* **01** (2014) 182 [1309.0812].

[259] N. Mekareeya, *The moduli space of instantons on an ALE space from 3d $\mathcal{N} = 4$ field theories*, *JHEP* **12** (2015) 174 [1508.06813].

Appendix A

Violation of Quotient Quiver Subtraction Rules

Examples of violating the Junction Rule and External Leg Rule presented in Chapter 4 are considered here. Even though the offending examples result in reasonable quivers, the action on the moduli as a hyper-Kähler quotient involves incomplete Higgsing. These cases require further care as the F-flat moduli space is not a complete intersection. It is possible that a more appropriate analysis, by construction of a Gröbner basis, to deal with incomplete Higgsing appropriately may find that the result from quotient quiver subtraction works even in cases with incomplete Higgsing.

A.1 Violation of the Junction Rule

Here we give an example of the incorrect application of quotient quiver subtraction for SU(n) hyper-Kähler quotient by explicitly breaking the Junction Rule. Recall that this rule prevents quotient quiver subtraction being performed on cases which result in incomplete Higgsing.

For our example we will take the magnetic quiver for $\overline{min.E_6}$ and try and take the SU(3) hyper-Kähler quotient using quotient quiver subtraction. We ignore the Junction Rule and permit

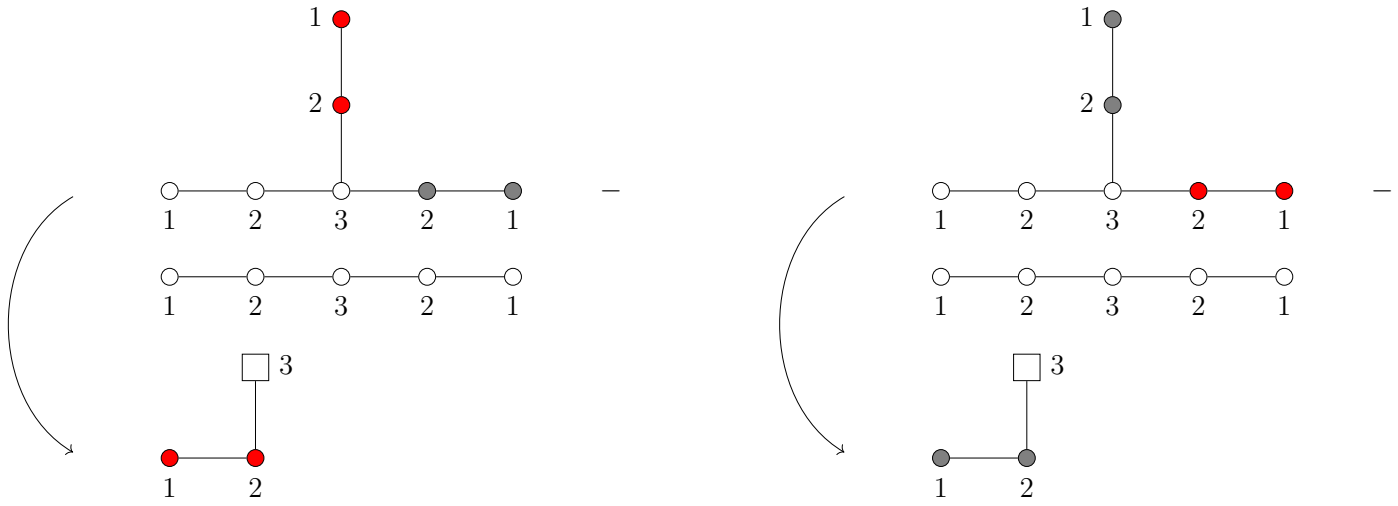


Figure A.1: Both (incorrect) alignments of the SU(3) quotient quiver against the unitary unframed magnetic quiver for $\overline{min.E_6}$ to give quivers $\mathcal{Q}_{A.1a}$ and $\mathcal{Q}_{A.1b}$. Their intersection is trivial.

the junction for the alignment of the SU(3) quotient quiver and target quiver to be located at the central node of rank 3 of the quotient quiver instead of a node of rank 2. There are two alignments of the SU(3) quotient quiver and these are related by an outer automorphism, thus we use colours for each leg of the target quiver to distinguish them. This procedure gives quivers $\mathcal{Q}_{A.1a}$ and $\mathcal{Q}_{A.1b}$ whose Coulomb branch is $\overline{max.A_2}$. The incorrect application of the rules of quiver subtraction leads us to believe

$$\overline{min.E_6}///\mathrm{SU}(3) \stackrel{?}{=} \overline{max.A_2} \cup \overline{max.A_2}. \tag{A.1}$$

It is simple to compute the refined HS and HWG of the union (A.1) however, to show inconsistency between Weyl integration and ignorance of the Junction Rule only the unrefined HS will suffice. We find:

$$\mathrm{HS}\left[\overline{max.A_2} \cup \overline{max.A_2}\right] = 2 \times \frac{1+2t^2+2t^4+t^6}{(1-t^2)^6} - 1 \tag{A.2}$$

$$= \frac{1+10t^2-11t^4+22t^6-15t^8+6t^{10}-t^{12}}{(1-t^2)^6} \tag{A.3}$$

There is an embedding of $\mathrm{SU}(3) \times \mathrm{SU}(3) \times \mathrm{SU}(3)$ into E_6 which decomposes the fundamental

as

$$(\mu_6)_{E_6} \to \mu_1\rho_1 + \nu_1\rho_2 + \mu_2\nu_2 \tag{A.4}$$

where the μ_i, ν_i, and ρ_i refer to highest weight fugacities of the three SU(3) factors.

This embedding is also a Dynkin type embedding. After applying this embedding, Weyl integration can be used to compute the SU(3) hyper-Kähler quotient of $\overline{min.E_6}$ whose HS we find to be

$$\text{HS}\left[\overline{min.E_6}///\text{SU}(3)\right] = \frac{1 + 9t^2 + 43t^4 + 81t^6 + 20t^8 - 89t^{10} + 53t^{12} - 11t^{14} + t^{16}}{(1-t^2)^7}, \tag{A.5}$$

where the quaternionic dimension of the moduli space is 3.5, indicating that incomplete Higgsing has occurred. This does not match the prediction from quotient quiver subtraction if we fail to apply the Junction Rule. We find that the application of the Junction Rule is necessary to avoid such mismatches that result from incomplete Higgsing.

A.2 Violation of the External Leg Rule

The External Leg Rule requires that the SU(n) quotient quiver must be subtracted from nodes of the target quiver corresponding to long roots. Here we give an example where this rule is ignored.

We will attempt to subtract the SU(2) quotient quiver from the family of $\overline{n.min.C_k}$ quivers. In order to prevent violation of the Single Edge Rule we require $k \geq 4$. The "subtraction" is shown in Figure A.2 and produces quivers $\mathcal{Q}_{A.2a}$ and $\mathcal{Q}_{A.2b}$. The respective Coulomb branches are identified as $\overline{n.min.C_{k-2}}$ and $\overline{min.C_{k-2}} \times \overline{min.A_1}$. So we are lead to conjecture that:

$$\overline{min.C_k}///\text{SU}(2) \stackrel{?}{=} \overline{n.min.C_{k-2}} \cup \overline{min.C_{k-2}} \times \overline{min.A_1}, \tag{A.6}$$

where the global symmetry of the union (A.6) is $\text{Sp}(k-2) \times \text{SU}(2)$.

Although it is straightforward to compute the refined HS and HWG of the union (A.6) for

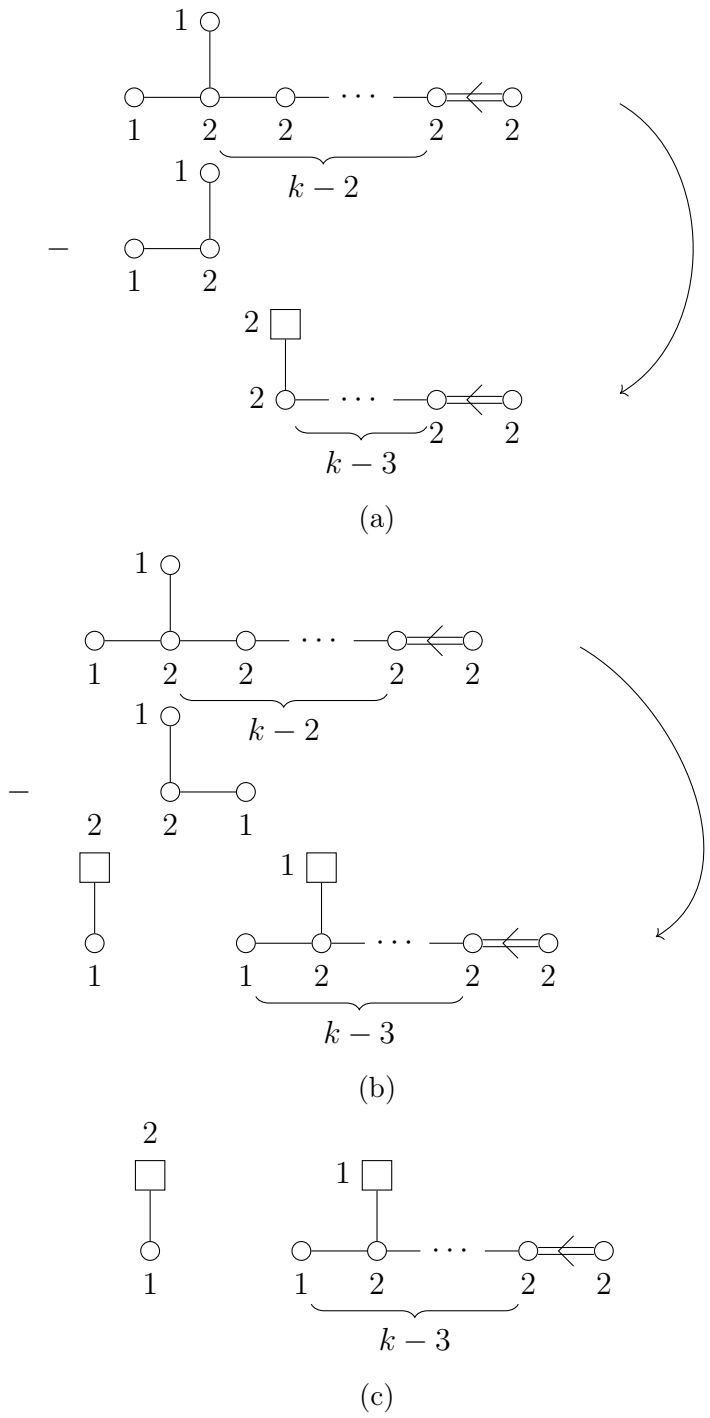


Figure A.2: Both alignments of the SU(2) quotient quiver against the magnetic quiver for $\overline{min.C_k}$ for $k \geq 4$ giving quivers $\mathcal{Q}_{A.2a}$ and $\mathcal{Q}_{A.2b}$. Their intersection, reached via A_1 KP transitions, is quiver $\mathcal{Q}_{A.2c}$.

particular values of $k \geq 4$, calculation of the unrefined HS will suffice to demonstrate the inconsistency with Weyl integration that arises if the External Leg Rule is ignored. We present the calculation using Weyl integration and quiver subtraction for the case $k = 5$, however, we have also computed up to $k = 6$.

We find from quiver subtraction that:

$$\begin{aligned}
&\text{HS}\left[\overline{n.min.C_3} \cup \overline{min.C_3} \times \overline{min.A_1}\right] \\
&= \frac{\left(\begin{array}{l} 1+15t^2+135t^4+625t^6+1725t^8+3048t^{10}+3686t^{12} \\ \quad +3048t^{14}+1725t^{16}+625t^{18}+135t^{20}+15t^{22}+t^{24} \end{array}\right)}{(1-t^2)^{12}(1+t^2)^6} \\
&+ \frac{(1-t^4)}{(1-t^2)^3}\frac{(1+t^2)(1+10t^2+41t^4+10t^6+t^8)}{(1-t^2)^{10}} \\
&- \frac{(1+t^2)(1+10t^2+41t^4+10t^6+t^8)}{(1-t^2)^{10}} \qquad \text{(A.7)} \\
&= \frac{\left(\begin{array}{l} 1+18t^2+185t^4+1004t^6+3219t^8+6457t^{10}+8438t^{12} \\ \quad +7094t^{14}+3653t^{16}+934t^{18}-11t^{20}-66t^{22}-13t^{24}-t^{26} \end{array}\right)}{(1-t^2)^{12}(1+t^2)^6} \qquad \text{(A.8)}
\end{aligned}$$

There is a Dynkin type embedding of $\text{Sp}(k) \hookleftarrow \text{Sp}(k-1) \times \text{Sp}(1)$ which branches the vector of $\text{Sp}(k)$ as:

$$[1,0,\cdots,0]_{\text{Sp}(k)} \to [1,0\cdots,0]_{\text{Sp}(k-1)} + [1]_{\text{Sp}(1)}. \qquad \text{(A.9)}$$

If the embedding (A.9) is chosen for Weyl integration then the expected global symmetries do not match as Weyl integration would give a result with $\text{Sp}(k-1)$ global symmetry as opposed to the union (A.6). A second problem is that this embedding gives incomplete Higgsing as seen from the HS:

$$\text{HS}\left[\overline{n.min.C_5}///\text{SU}(2)\right] = \frac{(1+t^2)(1+22t^2+253t^4+812t^6+1058t^8+392t^{10}+36t^{12})}{(1-t^2)^{13}}. \qquad \text{(A.10)}$$

This is clearly in disagreement with (A.6) which was obtained using SU(2) quotient quiver subtraction but ignoring the External Leg Rule. We find that the application of the External Leg Rule is necessary to avoid such pathological results where incomplete Higgsing occurs.

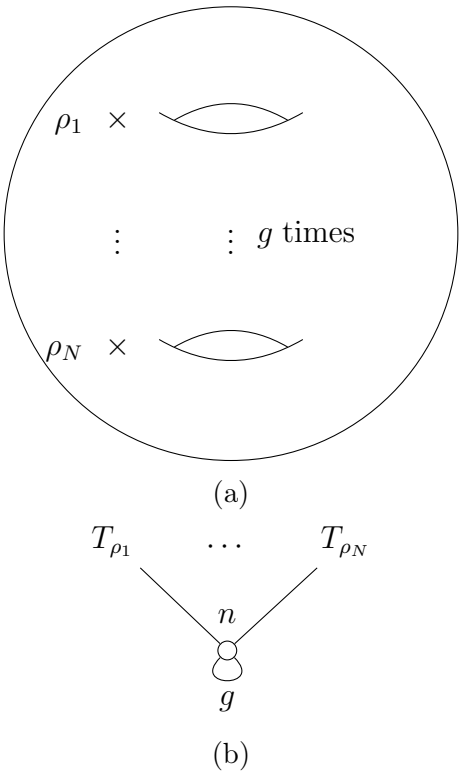
Appendix B

Star-shaped Quivers and Connections to Class $\mathcal{S}$

The chain and cyclic polymerisation techniques introduced in Chapter 6 are related to those presented in [223] and [218] for star-shaped quivers which are magnetic quivers for class $\mathcal{S}$ theories [222] with *regular* punctures. For this reason a brief account of class $\mathcal{S}$ theories and their $3d$ mirrors and their gluing is presented [223]. There is discussion of the incomplete Higgsing in the class $\mathcal{S}$ theories which are not visible in the $3d$ mirror theories.

A class $\mathcal{S}$ theory is a $4d$ $\mathcal{N}=2$ SCFT specified by a genus g Riemann surface $\mathcal{C}_{N,g}$ with n punctures labelled by nilpotent orbits of some ADE Lie algebra $\mathfrak{g}$. This $4d$ $\mathcal{N}=2$ SCFT comes from compactification of a $6d$ $\mathcal{N}=(2,0)$ theory specified by the same ADE algebra $\mathfrak{g}$ on $\mathcal{C}_{N,g}$ with a topological twist.

For the examples herein, the algebra is A_{n-1} with partitions of n labelling the punctures. In terms of notation, ρ_i, $i \in \{1, \cdots, N\}$ denotes a puncture and also the corresponding partition of n labelling that puncture. These partitions are exactly the same as those used to define nilpotent orbits of A_{n-1}. The magnetic quiver for a class $\mathcal{S}$ theory is a star-shaped quiver with each leg corresponding to a $T_{\rho_i}[\mathrm{SU}(n)]$ quiver [186], which is also a magnetic quiver for the Slodowy slice labelled by the very same partition [133]. The common $\mathrm{SU}(n)$ flavour symmetry is gauged leading to a star-shaped quiver with $\mathrm{U}(n)$ gauge group at the centre of the star once



(a)

(b)

Figure B.1: In Figure B.1a is a punctured Riemann surface $\mathcal{C}_{N,g}$ of genus g with n punctures, ρ_i, of type A_{n-1}. In Figure B.1b is the corresponding $3d$ mirror which consists of legs which are the $T_{\rho_i}[\mathrm{SU}(n)]$ glued at the common flavour symmetry. There are g adjoint on the central $\mathrm{U}(n)$ gauge node corresponding to the genus of the Riemann surface.

the overall U(1) is included. Additionally, g adjoint hypermultiplets are added to the central $\mathrm{U}(n)$ gauge node due to the genus g of $\mathcal{C}_{N,g}$. This is illustrated schematically in Figure B.1.

Gluing Maximal Punctures

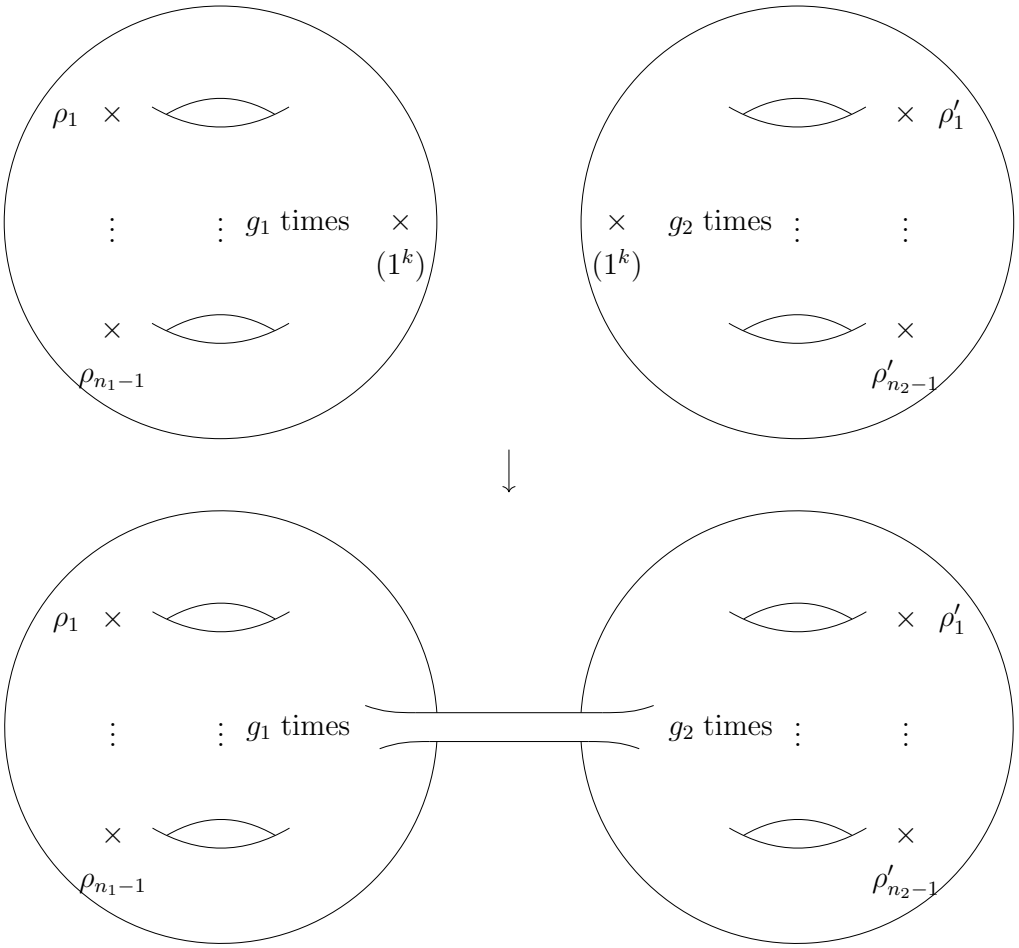
In class $\mathcal{S}$ theories with A_{n-1} Lie algebra, two punctured Riemann surfaces $\mathcal{C}_{N_1,g_1}$ and $\mathcal{C}_{N_2,g_2}$, with at least one maximal puncture each, may be joined by a cylinder to form a new Riemann surface $\mathcal{C}_{N_1+N_2-2,g_1+g_2}$. Without loss of generality let the N_1^{th} and N_2^{th} punctures be the maximal punctures to be joined. The effect on the $4d$ $\mathcal{N}=2$ theory is of gauging the diagonal $\mathrm{SU}(n)$ flavour symmetry. The action on the magnetic quiver is the gauging of a diagonal $\mathrm{SU}(n)$ Coulomb branch global symmetry as discussed in [223] which is the same as chain polymerisation at the central node. This is summarised in Figure B.2. It is possible to also glue together non-maximal punctures, in which case a subgroup of the $\mathrm{SU}(n)$ symmetry is gauged [218] however this does not have a neat formulation in terms of the magnetic quivers to date.

One may also take a Riemann surface $\mathcal{C}_{N+2,g}$ with at least two maximal SU(n) punctures may also be glued to itself with a cylinder. The resulting Riemann surface is $\mathcal{C}_{N,g+1}$. The action on the $3d$ mirror quiver consists of the amputation of these maximal external legs and the addition of an adjoint hypermultiplet at the central node of SU(n). This adjoint hypermultiplet corresponds to a unit increase in the genus of the Riemann surface. This is summarised in Figure B.3. The cyclic polymerisation introduced in this work is not the same as the action in Figure B.3.

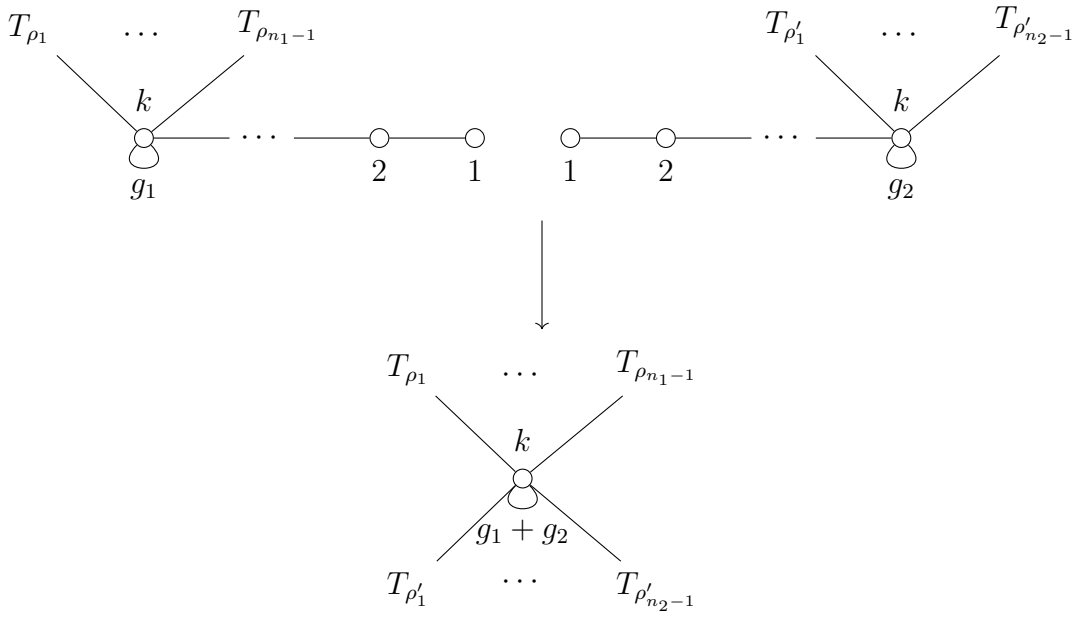
The cyclic polymerisation introduced in this work gauges a SU(n') $\subset$ SU(n) subgroup of the symmetry of the puncture.

It is important to reiterate that although for the $4d$ $\mathcal{N} = 2$ SCFT gauging SU(n') $\subset$ SU(n) subgroups of the flavour symmetry in general lead to IR free theories[1], the focus of this study is on $3d$ $\mathcal{N} = 4$ theories.

[1]We thank Gabi Zafrir for discussion about this point.



(a)



(b)

Figure B.2: In (Figure B.2a) is the gluing of maximal punctures on the Riemann surfaces. In (Figure B.2b) is the perspective on the $3d$ mirror quiver, this is the same as chain polymerisation at the node of $\mathrm{U}(n)$.

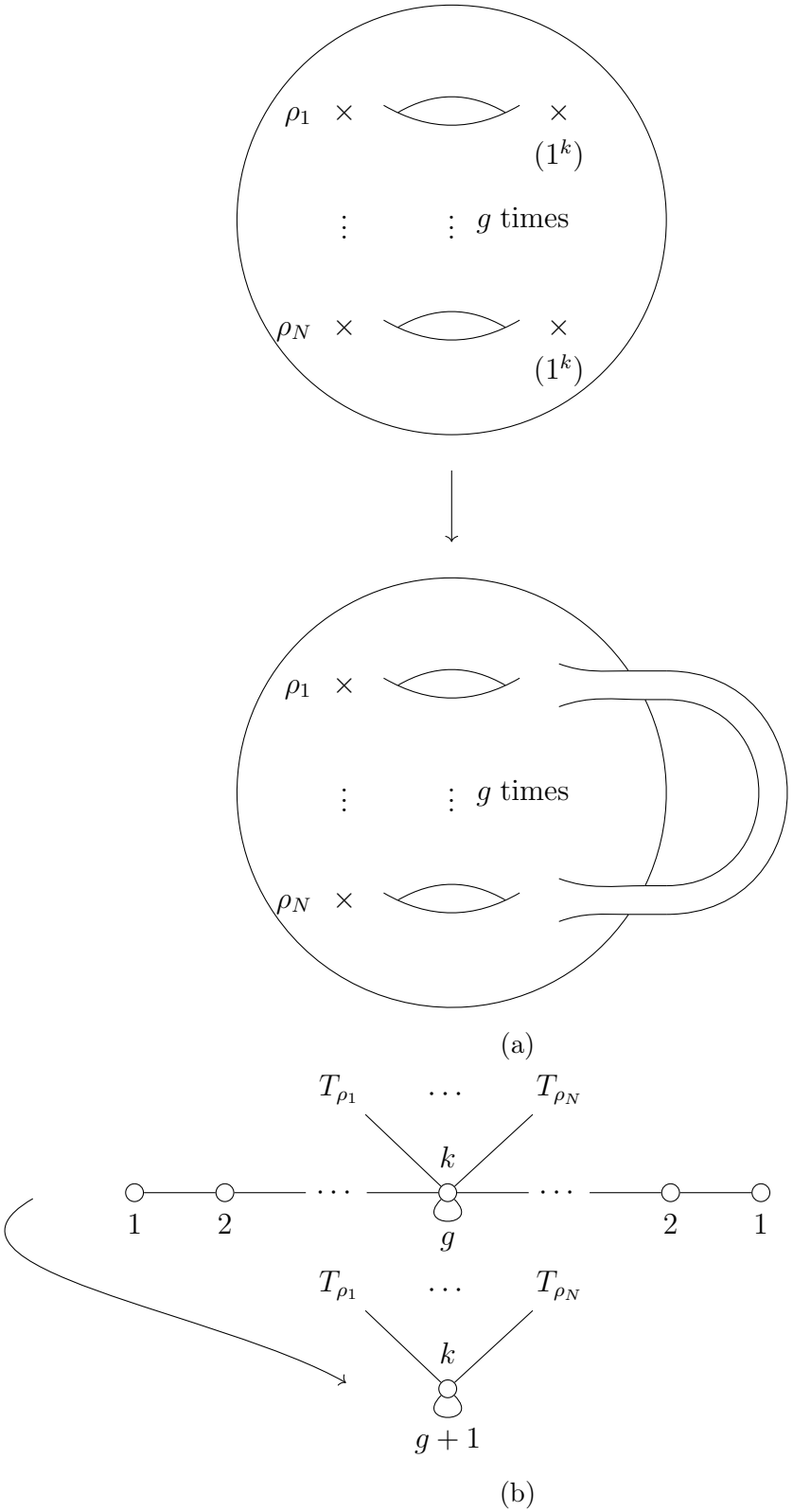


Figure B.3: In Figure B.3a is the gluing of two maximal punctures on the same Riemann surface. In Figure B.3b is the corresponding action on the $3d$ mirror quivers, this differs from cyclic polymerisation.

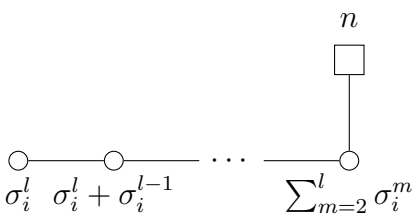
Appendix C

Gluing Hilbert Series and Hall-Littlewood Polynomials

The method of gluing Coulomb branch Hilbert series gives a significant computational advantage when studying quivers that are star-shaped or approximately star-shaped. This Section will mostly follow notation and conventions from [133, 134, 52, 2].

Consider a star-shaped quiver with a central gauge node of G, with possibly g adjoint hypermultiplets and with N legs labelled by partitions $\rho_i = (\sigma_i^1, \cdots, \sigma_i^l)$, with $\sigma_i^1 \geq \cdots \geq \sigma_i^l > 0 \; \forall i, l$. This is a description of a class $\mathcal{S}$ theory on $\mathcal{C}_{N,g}$ with algebra G as described in Section B.

The building block for the magnetic quiver involves a family of theories called the $T_\rho[G]$ theories. For a given partition $\rho_i = (\sigma_i^1, \cdots, \sigma_i^l)$ one can formulate the ranks of gauge nodes from ρ. If $G = \mathrm{SU}(n)$ then

$T_{\rho_i}[\mathrm{SU}(n)] =$ 

(C.1)

For a generic G its Higgs branch and Coulomb branch are

$$\mathcal{H}\left(T_{\rho_i}[G]\right) = \overline{\mathcal{O}}^{G}_{\rho_i^\vee}, \quad \mathcal{C}\left(T_{\rho_i}[\mathrm{SU}(n)]\right) = \mathcal{S}^{G^\vee}_{\mathcal{N},\rho_i^\vee} \tag{C.2}$$

where $G^\vee$ is the GNO dual to G and $\rho_i^\vee$ is the dual partition under the Barbasch-Vogan map [193].

And so the Coulomb branch of the magnetic quiver for the class $\mathcal{S}$ theory with algebra G, can be computed by taking a product of Hilbert series for Slodowy slices corresponding to the partitions ρ and summing over the magnetic lattice for G.

$$\mathrm{HS}_{\mathcal{C}}\left(\mathcal{Q}_{B.1b}\right)(t,\{\mathbf{x_i}\}) = \sum_{\lambda} \underbrace{P^G_\lambda(t)\, t^{2\Delta(\lambda)}}_{\text{central node}} \underbrace{\left(t^{-2\Delta(\lambda)}\right)^g}_{\text{adjoint loops}} \underbrace{\prod_{i=1}^{N} \mathrm{HS}\left[\mathcal{S}^{G^\vee}_{\mathcal{N},\rho_i^\vee}\right](t,\mathbf{x_i},\lambda)}_{\text{legs}} \tag{C.3}$$

The notation is as follows: λ defines the partition of magnetic charges for the node of G according to the Dirac quantisation condition, $P^G_\lambda(t)$ is the dressing function, $\Delta(\lambda)$ refers to the contribution to the conformal dimension from matter that transforms in the adjoint representation of G [52]. The Hilbert series for each Slodowy slice labelled by partition ρ_i may also contain fugacities $\mathbf{x_i}$ for the global symmetry of the slice.

A useful reformulation of the gluing formula turns the sum over the magnetic lattice λ into a sum over Dynkin labels of G, which will be denoted $[\mathbf{n}]$. The partitions λ, which are partitions for the magnetic charges of G, are in one-to-one correspondence with irreps of G. Therefore λ may be replaced by a collection of Dynkin labels $[\mathbf{n}]$ for G, with the sum now being over Dynkin labels of G instead. This change of $\lambda \to [\mathbf{n}]$ will be mostly implicit. However it is useful for pedagogical purposes to show how the $\Delta(\lambda)$ become explicit functions of the $[\mathbf{n}]$ for the specific case of $G = \mathrm{SU}(n)$. Let $\mathbf{A}$ be the Cartan matrix of $\mathrm{SU}(n)$, then $\Delta(\lambda[\mathbf{n}]) \equiv \Delta[\mathbf{n}] = -[\mathbf{n}]\cdot\mathbf{A}^{-1}\cdot\mathbf{2}$. Alternatively, drawing on the Characteristics and weight maps ω of nilpotent orbits, $\Delta[\mathbf{n}]$ can be found simply from the weight map of the regular orbit as, $\Delta[\mathbf{n}] = -[\mathbf{n}]\cdot\omega(\text{reg.})$ [183, 184]. The advantage of doing this is that the Hilbert series become Hall-Littlewood polynomials which enjoy orthogonality that can be leveraged in computations. Much of this change in basis

will be done implicitly, except for the conversion of the Hilbert series of the legs which is given by

$$\mathrm{HS}\left[\mathcal{S}^{G^\vee}_{\mathcal{N},\rho_i^\vee}\right](t,\mathbf{x_i},[\mathbf{n}]) = \mathrm{HS}\left[\mathcal{S}^{\mathbf{G}^\vee}_{\mathcal{N},\rho_\mathbf{i}^\vee}\right](\mathbf{t},\mathbf{x_i},\lambda)\frac{\mathrm{HL}^{\mathbf{G}^\vee}(\mathbf{t},\mathbf{x_i},[\mathbf{n}])}{\mathrm{HL}^{\mathbf{G}^\vee}(\mathbf{t},\mathbf{x_i},[\mathbf{0}])} \tag{C.4}$$

where the HL refer to the Hall-Littlewood polynomials.

The Coulomb branch Hilbert series formula then takes the form

$$\mathrm{HS}_{\mathcal{C}}\left(\mathcal{Q}_{B.1b}\right)(t,\{\mathbf{x_i}\}) = \sum_{[\mathbf{n}]} \underbrace{P^G_{[\mathbf{n}]}(t)\; t^{2\Delta[\mathbf{n}]}}_{\text{central node}} \underbrace{\left(t^{-2\Delta[\mathbf{n}]}\right)^g}_{\text{adjoint loops}} \underbrace{\prod_{i=1}^{N} t^{-2\Delta[\mathbf{n}]}\mathrm{HS}\left[\mathcal{S}^{G^\vee}_{\mathcal{N},\rho_i^\vee}\right](t,\mathbf{x_i},[\mathbf{n}])}_{\text{legs}} \tag{C.5}$$

Quivers which are almost star-shaped can also be computed using a similar technique. Instead of using $T_\rho[G]$ theories and gluing together Slodowy slices one deals with generic shapes of quiver for the leg. The Hilbert series of this generic leg can be computed with the monopole formula, keeping in the dependency of the magnetic charges of the central node of G. This dependency on the magnetic charges may also be replaced into a dependency on Dynkin labels through the localisation formula of [186, 134].

Appendix D

Justification of Quiver Polymerisation

Now that the diagrammatic techniques of chain and cyclic polymerisation have been presented in Chapter 6, and the relevant embeddings for Weyl integration have been discussed, it remains to justify the polymerisation techniques. Ultimately, the polymerisation techniques follow from the orthogonality of modified Hall-Littlewood functions. The formulation is quite general and will be presented for a group G where G is $\mathrm{SU}(n)/\mathrm{U}(n)$ for chain and cyclic polymerisation respectively.

Although the focus in this work is on unitary quivers, the formulation of the arguments easily generalises to orthosymplectic quivers as well.

D.1 Justifying Chain Polymerisation – Unitary Case

The starting point is the pair of quivers $\mathcal{Q}_1$ and $\mathcal{Q}_2$ shown in Figure 6.1. Each quiver in the pair contains a leg which takes the form of $(1)-\cdots-(n)-$. Each leg may have g_1 (resp. g_2) adjoint hypermultiplet loops on the $\mathrm{U}(n)$ node. The leg is also attached to some background quiver Q_1 (resp. Q_2).

The quiver $\mathcal{Q}_1$ can be thought of as the theory that results from gauging a diagonal $G=\mathrm{SU}(n)$ flavour symmetry of a $T_{(1^n)}[G]$ theory, Q_1, and g_1 free G adjoint hypermultiplets. The Hilbert

series takes a form similar to that in (C.5) where one uses the fact that $\mathrm{HS}\left[\mathcal{S}^{G^\vee}_{\mathcal{N},(1^n)}\right](t,\mathbf{y},[\mathbf{n}]) = \mathrm{mHL}^G_{[\mathbf{n}]}(t,\mathbf{y})$ where mHL is a *modified Hall-Littlewood* function. A full account of mHL and the notations used herein are found in [185].

$$\mathrm{HS}_{\mathcal{C}}\left[\mathcal{Q}_1\right](t,\mathbf{y},\mathbf{q}_1) = \sum_{[\mathbf{n}]} P^G_{[\mathbf{n}]}(t)\; t^{\Delta[\mathbf{n}](1-2g_1)}\; \mathrm{HS}_{\mathcal{C}}\left[Q_1\right](t,\mathbf{q}_1,[\mathbf{n}])\; \mathrm{mHL}^G_{[\mathbf{n}]}(t,\mathbf{y}) \tag{D.1}$$

The Coulomb branch Hilbert series takes the form of The Coulomb branch Hilbert series for $\mathcal{Q}_2$ is found by simply exchanging $1 \leftrightarrow 2$ and $\mathbf{y} \leftrightarrow \mathbf{y}^*$.

Chain polymerisation of $\mathcal{Q}_1$ and $\mathcal{Q}_2$ produces a new quiver $\mathcal{Q}_3$. The action on the Coulomb branch is a hyper-Kähler quotient by the diagonal G in each leg of $\mathcal{Q}_1$ and $\mathcal{Q}_2$; this gives the Coulomb branch of $\mathcal{Q}_3$. A key assumption is that the hyper-Kähler quotient involves complete Higgsing of the Coulomb branch global symmetry. With this assumption, the hyper-Kähler quotient is evaluated using the Weyl integration formula:

Recall the key orthogonality relations between the mHL functions:

$$\oint_G d\mu^G_{\mathrm{mHL}}(\mathbf{y})\; \mathrm{mHL}^G_{[\mathbf{m}]}(\mathbf{y}^*,t)\; \mathrm{mHL}^G_{[\mathbf{n}]}(\mathbf{y},t) = \frac{\delta_{[\mathbf{m}][\mathbf{n}]}}{(1-t^2)^{\mathrm{rank}\,G} P^G_{[\mathbf{n}]}(t)}, \tag{D.2}$$

where $d\mu^G_{\mathrm{mHL}}$ is the modified Hall-Littlewood Haar measure,

$$d\mu^G_{\mathrm{mHL}}(\mathbf{y}) \equiv d\mu^G(\mathbf{y})\; \mathrm{PE}\left[\left(\mathrm{rank}\; G - \chi^G_{\mathrm{adj}}(\mathbf{y})\right) t^2\right]. \tag{D.3}$$

Substituting (D.2) into (D.3) gives the convenient result:

$$\oint_G d\mu^G\; \mathrm{PE}\left[-\chi^G_{\mathrm{adjoint}} t^2\right]\; \mathrm{mHL}^G_{[\mathbf{m}]}(\mathbf{y}^*,t)\; \mathrm{mHL}^G_{[\mathbf{n}]}(\mathbf{y},t) = \frac{\delta_{[\mathbf{m}][\mathbf{n}]}}{P^G_{[\mathbf{n}]}(t)}. \tag{D.4}$$

Now, the explicit form of the Coulomb branch Hilbert series for $\mathcal{Q}_1$ (D.1), and similarly for $\mathcal{Q}_2$, may be substituted into the Weyl integration formula. Upon performing the integration and using the orthogonality property of the modified Hall-Littlewood functions (D.4), the Coulomb

branch Hilbert series for $\mathcal{Q}_3$ is computed as

$$\mathrm{HS}_{\mathcal{C}}\left[\mathcal{Q}_3\right](t,\mathbf{q}_1,\mathbf{q}_2)=\sum_{[\mathbf{n}]}P^G_{[\mathbf{n}]}(t)\;t^{2\Delta[\mathbf{n}](1-(g_1+g_2))}\;\mathrm{HS}_{\mathcal{C}}\left[Q_1\right](t,\mathbf{q}_1,[\mathbf{n}])\;\mathrm{HS}_{\mathcal{C}}\left[Q_2\right](t,\mathbf{q}_2,[\mathbf{n}]). \quad \text{(D.5)}$$

It is clear that the Coulomb branch Hilbert series of $\mathcal{Q}_3$ shown in (D.5) is that of the Coulomb branch of the resulting quiver in Figure 6.1.

D.2 Justifying Cyclic Polymerisation – Unitary Case

Much of the above analysis carries over to the case of cyclic polymerisation, except with some minor differences.

The starting point is the quiver $\mathcal{Q}$ shown in Figure 6.2. This quiver contains two legs of the form $(1)-\cdots-(n)-$ with g_1 and g_2 adjoint hypermultiplets on each $\mathrm{U}(n)$. These legs are connected, perhaps in different ways, to some background quiver Q.

The Coulomb branch Hilbert series of $\mathcal{Q}$ may be computed by gluing the two legs to the background quiver Q. The embedding requires that the symmetry in each leg is broken to $\mathrm{SU}(n)\times\mathrm{U}(1)$. Each leg carries a diagonal $G=\mathrm{U}(n)$ symmetry with the remaining $\mathrm{U}(1)$ dependence being absorbed into the background quiver Q. The background quiver Q has fugacities $\mathbf{q}$, which include this remaining $\mathrm{U}(1)$ from the legs. Each leg carries conjugate G fugacities as before. Therefore, the Coulomb branch Hilbert series of $\mathcal{Q}$ is computed as:

$$\begin{aligned}\mathrm{HS}_{\mathcal{C}}\left[\mathcal{Q}\right](t,\mathbf{y},\mathbf{q})=&\sum_{\lambda,\lambda'}P^G_{\lambda}(t)\;P^G_{\lambda'}(t)\;t^{2\Delta(\lambda)(1-g_1)}\;t^{2\Delta(\lambda')(1-g_2)}\\&\times\mathrm{HS}_{\mathcal{C}}\left[Q\right](t,\mathbf{q},\lambda,\lambda')\;\mathrm{HS}_{\mathcal{C}}\left[T[G]_{(1^n)}\right](t,\mathbf{y},\lambda)\mathrm{HS}_{\mathcal{C}}\left[T[G]_{(1^n)}\right](t,\mathbf{y}^*,\lambda'). \quad \text{(D.6)}\end{aligned}$$

The notation is similar, but as there are two gluings involved this time, there is another set of partitions λ' for G magnetic charges. The sum over partitions λ and λ' may be changed to a

sum over Dynkin labels $[\mathbf{n}]$ and $[\mathbf{m}]$ of G to get to the following, but equivalent, Hilbert series:

$$\begin{aligned}\mathrm{HS}_{\mathcal{C}}\left[\mathcal{Q}\right](t,\mathbf{y},\mathbf{q},q) = \sum_{[\mathbf{n}],[\mathbf{m}]} P^{G}_{[\mathbf{n}]}(t)\ P^{G}_{[\mathbf{m}]}(t)\ t^{\Delta[\mathbf{n}](1-2g_1)}\ t^{\Delta[\mathbf{m}](1-2g_2)} \\ \times \mathrm{HS}_{\mathcal{C}}\left[Q\right](t,\mathbf{q},[\mathbf{n}],[\mathbf{m}])\ \mathrm{mHL}^{G}_{[\mathbf{n}]}(t,\mathbf{y})\ \mathrm{mHL}^{G}_{[\mathbf{m}]}(t,\mathbf{y}^{*}).\end{aligned} \tag{D.7}$$

Cyclic polymerisation takes the quiver $\mathcal{Q}$ and produces a new quiver $\mathcal{Q}'$. The hyper-Kähler quotient action on the Hilbert series is again computed by Weyl integration by G with fugacities $\mathbf{y}$. The assumption that there is complete Higgsing is made again. The Coulomb branch Hilbert series of $\mathcal{Q}'$ is:

$$\mathrm{HS}_{\mathcal{C}}\left[\mathcal{Q}'\right](t,\mathbf{q}) = \oint_{G} d\mu^{G}(\mathbf{y})\mathrm{PE}\left[-\chi^{G}_{\mathrm{adj}}(\mathbf{y})t^{2}\right]\mathrm{HS}_{\mathcal{C}}\left[\mathcal{Q}\right](t,\mathbf{y},\mathbf{q}). \tag{D.8}$$

The integral over G proceeds in a similar fashion to the case of chain polymerisation. The final result is:

$$\mathrm{HS}_{\mathcal{C}}\left[\mathcal{Q}'\right](t,\mathbf{q}) = \sum_{[\mathbf{n}]} P^{G}_{[\mathbf{n}]}(t)\ t^{2\Delta[\mathbf{n}](1-(g_1+g_2))}\ \mathrm{HS}_{\mathcal{C}}[Q](t,\mathbf{q},[\mathbf{n}],[\mathbf{n}]). \tag{D.9}$$

This is the correct form for the Coulomb branch Hilbert series of $\mathcal{Q}'$ as expected from polymerisation and the monopole formula.

Appendix E

Kronheimer-Nakajima Quivers and Moduli Spaces of Instantons

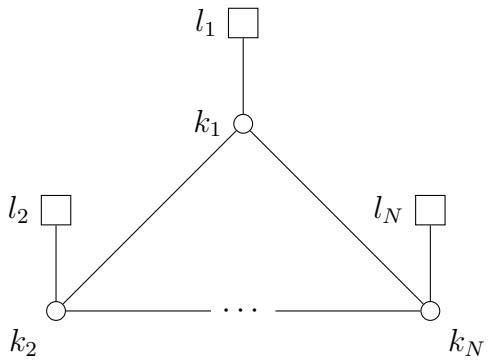


Figure E.1: Most general A-type Kronheimer-Nakajima quiver. The Higgs branch is the moduli space of instantons $\mathcal{M}^{\mathbb{C}^2/\mathbb{Z}_N;\mathrm{SU}(l)}_{(k_1,\cdots,k_N),(l_1,\cdots,l_N)}$, where $l = \sum_{i=1}^{N} l_i$. The Coulomb branch is the moduli space of instantons $\mathcal{M}^{\mathbb{C}^2/\mathbb{Z}_l;\mathrm{SU}(N)}_{(k'_1,\cdots,k'_l),(l'_1,\cdots,l'_l)}$, where the k'_i and l'_i are linear functions of the k_i and l_i respectively.

It will be useful to review the Kronheimer-Nakajima construction for the moduli space of instantons with special unitary gauge group on an A-type Klein singularity [26] which was prevalent in Chapter 6. The construction extends the work of Atiyah-Drinfeld-Hitchin-Manin [24] and results in the Kronheimer-Nakajima quiver shown in Figure E.1. Both the Coulomb and Higgs branches of these quivers are moduli spaces of special unitary gauge instantons on A-type Klein singularity, with the ADHM construction as a particular limit of Figure E.1.

A moduli space of instantons is typically described by the gauge group, the singularity, and

some geometric data of the instanton bundle, such as its rank, the first and second Chern classes, and the monodromy of gauge fields at infinity. All of this data is encoded in the Kronheimer-Nakajima quiver, the precise dictionary between quiver data and instanton bundle data is rather cumbersome, attempts at explicating this dictionary were made in [256–259]. For this reason, it is sufficient to only refer to the quiver data and not the geometric data.

Despite difficulties with a general and precise dictionary between geometric and quiver data, there are broad correspondences between the two. For example, the framing of the quiver determines the monodromy of gauge fields at infinity and the balance determines the monodromy of gauge fields at the origin [257, 256]. Both of these have interpretations in the Type IIB brane system as linking numbers of NS5 branes and D5 branes respectively.

E.1 Brane Realisations

Instantons can be thought of as solitonic codimension 4 objects. In string theory, one of the most well-known string theory constructions of instantons is in Type IIA string theory with D2 branes inside D6 brane worldvolume [242] possibly in the presence of orientifold planes. The low energy effective theories are the ADHM quivers whose Higgs branch is the moduli space of instantons of type SU, SO, and Sp on $\mathbb{C}^2$.

Application of T-duality, transverse to the D2 and in a direction occupied by the D6, followed by S-duality to the Type IIA brane system gives a Type IIB brane system whose Coulomb phase corresponds to the same moduli space of instantons. The low energy effective field theories for moduli spaces of SU, SO, and Sp instantons on $\mathbb{C}^2$ are extended Dynkin quivers as found in [111, 243, 128, 131, 244]. For exceptional gauge groups, which do not have any perturbative open string formulations, the moduli space of instantons of these gauge symmetries on $\mathbb{C}^2$ are also extended Dynkin diagrams [111, 244].

Importantly, the Kronheimer-Nakajima quivers have constructions in Type IIB string theory as a system of NS5 and D5 branes with D3 branes on S^1 [31]. Here, the action of S-duality on

this brane system exchanges NS5 and D5 branes. The effect on the quiver is that the number of gauge nodes and the total number of flavours swaps.

E.2 Special Cases

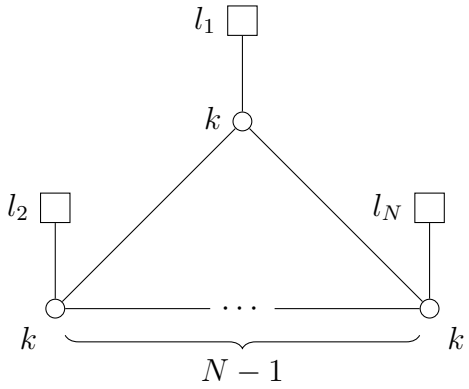


Figure E.2: The Kronheimer-Nakajima quiver with all gauge nodes the same. The Coulomb branch is the moduli space of k SU(N) instantons on $\mathbb{C}^2/\mathbb{Z}_l$ where $l = \sum_{i=1}^{N} l_i$.

A particularly special case of the Kronheimer-Nakajima quiver $\mathcal{Q}_{E.1}$ is to set all of the gauge nodes to be the same U(n), resulting in $\mathcal{Q}_{E.2}$. In particular, the balance of each gauge node is given by its framing. This also corresponds to the vanishing of the first Chern class c_1 of the instanton bundle. The second Chern class is $c_2 = k$ which is the instanton number. Another simplification is in finding the residual gauge group broken by the monodromies of the gauge fields.

In the case where all $l_i > 0$, the monodromy of the gauge fields breaks the flavour symmetry $\mathrm{SU}(l) \to \mathrm{S}\left(\prod_{i=1}^{N} \mathrm{U}(l_i)\right)$. The instantons live on $\mathbb{C}^2/\mathbb{Z}_N$ and the instanton number is k. Thus $\mathcal{H}(\mathcal{Q}_{E.2}) = \mathcal{M}^{\mathbb{C}^2/\mathbb{Z}_N}_{k,\mathrm{S}\left(\prod_{i=1}^{N} \mathrm{U}(l_i)\right)}$, where a simplification of the notation used in Figure E.1 is now possible. The Coulomb branch is easily found from application of S-duality to the brane system for $\mathcal{Q}_{E.2}$, which results in l U(n) gauge nodes in a necklace with framing $(0^{l_1-1}, 1, 0^{l_2-1}, 1 \cdots, 0^{l_N-1}, 1)$. The Coulomb branch of $\mathcal{Q}_{E.2}$ is $\mathcal{C}\left(\mathcal{Q}_{E.2}\right) = \mathcal{M}^{\mathbb{C}^2/\mathbb{Z}_l}_{k,\mathrm{U}(1)^{N-1}}$.

A further simplification can be made if only one of the U(n) gauge nodes has flavours, say l flavours, and the others do not. In this case the full SU(l) symmetry is preserved and the Higgs branch is $\mathcal{H}(\mathcal{Q}_{E.3}) = \mathcal{M}^{\mathbb{C}^2/\mathbb{Z}_N}_{k,\mathrm{SU}(l)}$. In this case, application of S-duality simply swaps the role of

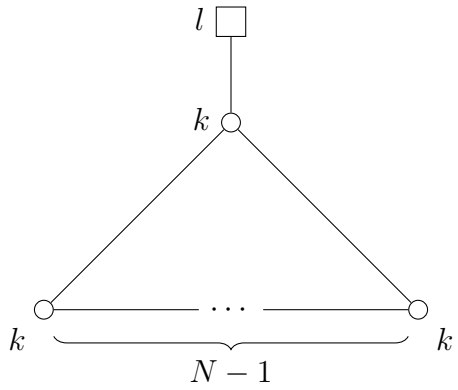


Figure E.3: The Kronheimer-Nakajima quiver with all gauge nodes the same. The Coulomb branch is the moduli space of k SU(N) instantons on $\mathbb{C}^2/\mathbb{Z}_l$ where $l = \sum_{i=1}^{N} l_i$.

NS5 and D5 branes and hence the Coulomb branch is $\mathcal{C}(\mathcal{Q}_{E.3}) = \mathcal{M}^{\mathbb{C}^2/\mathbb{Z}_l}_{k,\mathrm{SU}(N)}$, which simply swaps $N \leftrightarrow l$.

The Kronheimer-Nakajima quivers give Higgs and Coulomb branch constructions of the moduli space of SU instantons on A-type singularities. The Higgs branch construction is as a hyper-Kähler quotient. However, it is important to emphasise that the Coulomb branch construction here is as a moduli space of dressed monopole operators of the theory $\mathcal{Q}_{E.1}$.